Weather Modification Level III Feasibility Study

Laramie Range Siting and Design

Final Report

Frank McDonough, John F. Mejia, Kacie N. Shourd,
Rosemary W. Carroll, Alexandra D. Lutz, Jeff Dean,
Jeese W. Juchtzer, Arlen W. Huggins, Mike L. Kaplan
Desert Research Institute
Reno, Nevada
Ray DeLuna, Cameron Trembath
TREC, Inc
Casper, Wyoming

Table of Contents

1 Scoping and Project Meetings 4

2 Review and Summary of Previous Data 7

2.1 Background 7

2.2 Selected Research and Validation Programs 8

3 Climatology of the Project Area 10

3.1 Introduction 10

3.2 Ten Year Laramie Range Observed Winter Storm Climatology 10

3.2.1 December 3, 2011, Case Overview 11

3.2.2 Results and Observed Climatology 19

3.2.2.1 Scenario 1 Storm Climatology 25

3.2.2.2 Scenario 2 Climatology 31

3.2.3 Summary 37

3.3 WRF Modeling 38

3.3.1 The Regional Climate Model Simulations 38

3.3.2 Model Climatology Results 42

3.3.2.1 Decade-long Mean Cloud Seeding Potential 42

3.3.2.2 Seasonality 47

3.3.2.3 Model Potential Precipitation Augmentation 49

3.3.2.4 Summary 51

3.4 Model Evaluations 52

3.4.1 Upper-Air Regional Climate Model (RCM) Performance 52

3.4.2 Near-surface RCM Performance 58

4 Development of a Preliminary Project Design 66

4.1 Introduction 66

4.2 Cloud Seeding Methods 66

4.3 Project Design 68

5 Model Evaluation of the Preliminary Design 71

5.1 Lagrangian Dispersion Model: Ground-based Siting Considerations 71

5.1.1 The Backward Integrations 71

5.1.2 The Forward Integrations 73

5.1.3 Efficiency of the proposed ground-based siting 78

6 Field Surveys- Proposed AgI Ground Generator and AgI/Liquid Propane Dispenser Locations 80

6.1 Preliminary selection of locations before site visits 80

6.2 Post Visit Site Selection 82

6.3 Summary of Site Visits 85

7 Access/Easements and Environmental Permitting/Reporting 90

8 Establishment of an Operational Criteria 113

8.1 Introduction 113

8.2 Forecasting 114

8.2.1 Satellite 114

8.2.2 Numerical Model 114

8.2.3 Surface Observations 114

8.2.4 Radar Observations 115
8.2.5 Icing Pilot Reports 116
8.3 Suspension of Seeding 117

9 Environmental Considerations 119
9.1 Liquid Propane 119
9.2 Silver Iodide 120
9.3 Downwind "extra-area" Effects 122
9.4 Legal Considerations 123
9.5 Summary 124

10 Evaluation Methodology 125
10.1 Background 125
10.2 Validation Plan 125

11 Potential Benefits/Hydrologic Assessment 127
11.1 Introduction 127
11.2 Review of Approaches to Estimate Streamflow Changes 127
11.3 Linear Approach 128
11.3.1 Muddy Creek Basin 131
11.3.2 Deer Creek Basin 133
11.3.3 Box Elder Creek Basin 134
11.3.4 Laprele Creek Basin 136
11.3.5 Wagonhound Creek and La Bonte Creek Basins 137
11.3.6 Laramie Range 138
11.4 Outline Steps for Hydrologic Model – GSFLOW Approach 139
11.4.1 Collect and synthesize data required – Limited Modeling Approach 145
11.4.2 Precipitation Changes 150
11.4.3 Model Evaluation 152
11.4.4 Results of Limited Model in Deer Creek and Box Elder 154
11.4.5 Comparison 158

12 Cost Estimates 160

13 Preliminary Cost Benefit Estimates 163

14 Reports and Executive Summaries 165

15 Report Presentations 166

16 Climatological Monitoring of the Study Area 167
16.1 Radiometer 167
16.2 Other Data Sets 174

17 References 176

18 Appendix A. Public Hearings and Comments 187

19 Appendix B. Case Studies 201

20 Appendix C. Table of Acronyms 221

1 Scoping and Project Meetings

A series of local meetings was scheduled to familiarize the Wyoming Water Development Commission (WWDC), technical advisory team members, governmental agencies, and local stakeholders about the scope of the Laramie Range Weather Modification Feasibility Study, as well as to obtain input from interested parties. The first meeting took place on the evening of September 30, 2015 at the Converse County Courthouse in Douglas, Wyoming, and the second meeting took place on the afternoon of October 1, 2016 at the Platt Valley Bank in Wheatland, Wyoming (Fig. 1.1).

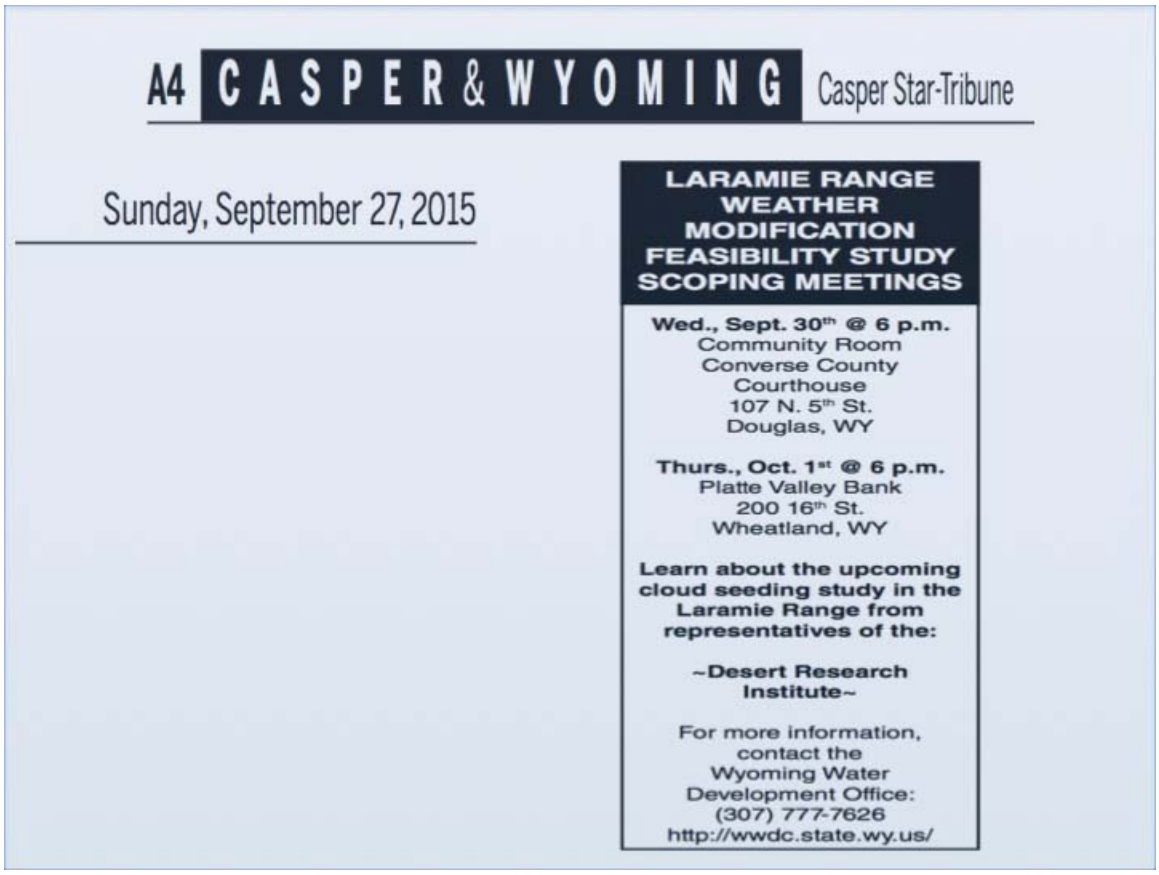
A4 CASPER & WYOMING Casper Star-Tribune

Sunday, September 27, 2015

LARAMIE RANGE WEATHER MODIFICATION FEASIBILITY STUDY SCOPING MEETINGS

Wed., Sept. 30th @ 6 p.m.
Community Room
Converse County
Courthouse
107 N. 5th St.
Douglas, WY

Thurs., Oct. 1st @ 6 p.m.
Platte Valley Bank
200 16th St.
Wheatland, WY

Learn about the upcoming cloud seeding study in the Laramie Range from representatives of the:

~Desert Research Institute~

For more information, contact the Wyoming Water Development Office: (307) 777-7626 http://wwdc.state.wy.us/

Figure 1.1 Newspaper posting for Laramie Range Scoping Meeting.

At these meetings, the ranching community raised concerns about winter weather. The first issue was that the Laramie Range is a "working man's mountain range," with active winter ranching at elevations below 8,000 ft mean sea level (MSL). Stakeholders explained that the impacts of cold and snow during parts of the winter season can significantly impact cattle ranchers' ability to graze and feed cattle, and that an overabundance of additional snowfall was not welcome on the ranches.

The winter impacts to ranching were included in a document presented to the Wyoming Livestock Roundup by University of Wyoming professors Dr. Donal O'Toole and Dr. Meri Raisbeck. Their discussion is as follows:

> *Cattle require extra feed during multi-day periods which are colder than average. The biggest economic impact we see is* ***weak calf syndrome****. This is not a specific diagnosis. It simply means that calves born full-term and alert quickly become weak and dull, and die. Several things are going on here. The calves born to emaciated dams have little body fat to provide insulation. They quickly run down their reserves of brown fat, which is a type of adipose tissue designed to throw out a lot of heat. All calves are born wet. If there is high wind chill, cold temperatures, and little shelter, they rapidly become hypo-thermic. Unlike adult cattle, whose rumens generate a lot of heat, calves are pre-ruminants that lack this internal wood stove to keep them warm. Compounding this is the poor quality of colostrum from malnourished dam. Calves depend on colostrum for energy and fat, and for antibodies to prevent scours and pneumonia. Antibodies are proteins. A starved cow will not be able to make enough for her own needs or her calf. The answer is to ensure that dams are in good enough nutritional condition to take care of themselves and their calf at and immediately after birth.*

A second question raised by the ranching community regarded calf abortions due to ingestion of live pine needles. Again from Dr. Donal O'Toole and Dr. Meri Raisbeck's presentation to the Wyoming Livestock Roundup:

> ***Pine needle abortion*** *is a result of hungry cattle sheltering in stands of pine trees during winter storms, and eating the needles. They rarely eat needles unless they are hungry, although they can become habituated to them and their toxic effects. In cattle that are not habituated, abortion can occur, generally during the last third of gestation. An important complication is retention of the afterbirth, leading to uterine infections.*

Stakeholders also requested that the amounts of additional precipitation over ranch land on the east slopes of the Laramie Range below 8,000 ft MSL be estimated and asked the project team to address how additional snow from cloud seeding may impact cattle feed costs.

Answers to the ranchers' questions:

Cloud seeding does not change temperatures or winds in any significant way. Storms and precipitation are already present when cloud seeding takes place. Cloud seeding changes the cloud particles from small liquid water drops to small snowflakes. These new snowflakes will grow to larger sizes and reach the ground, whereas the unseeded clouds will be less efficient at producing larger snowflakes and produce less snowfall.

The additional contribution of new snow from cloud seeding is less than 10% of the total snowfall produced by a seeded storm (Ritzman et. al. 2015). In addition, only half of the winter storms in the Laramie Range can be seeded at elevations above 8,000 ft MSL, whereas a significantly lower occurrence of seedable conditions develop away from the higher terrain (Fig 1.2). For example, using the Laprele Creek National Resources Conservation Services (NRCS) snow gauge (SNOTEL), sited at 8,375 ft MSL and above the elevations of the ranches, it is estimated that 4.7" of additional snow will be produced on average from cloud seeding. The majority of the active winter ranchland in the Laramie Range is located below 8,000 ft MSL and the climatology of the area (see Chapter 3) show these elevations are expected to receive less than half of the estimated 4.7 inches of additional snow created over the higher terrain. This results in a marginal 2" to 3" of additional snow accumulating during the entire winter at ranching elevations. Although the preliminary project design is not intended to target areas below 8,000 ft MSL, it is expected that minor impacts will occur.

Cloud seeding will not change the wind chill temperature or the presence of clouds and fog. The program will only minimally increase the amount of snowfall accumulating in the winter ranching areas. Because the impact of cloud seeding is well within the realm of natural snowfall variability, the likelihood that cattle will be unable to graze on typical winter feed is very low.

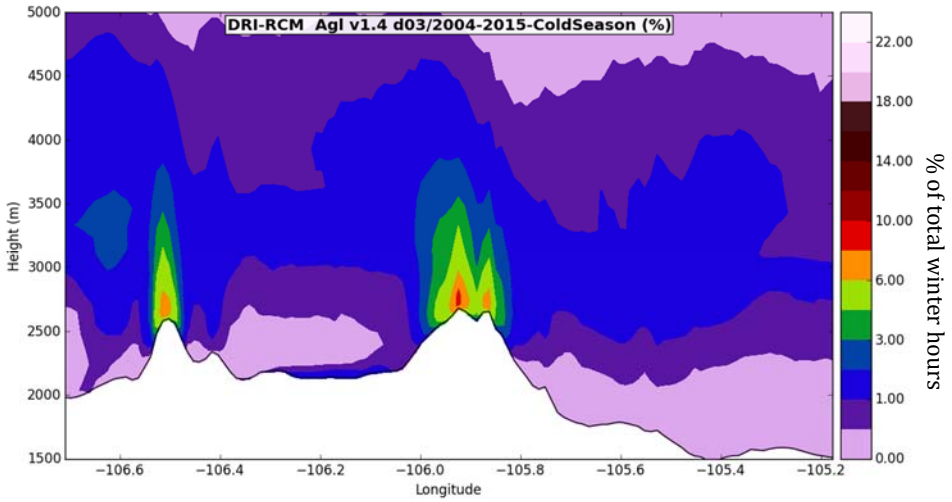

Figure 1.2 West to east vertical cross section of the percent of time that cloud seeding potential is present over the Laramie Range region of Wyoming.

2 Review and Summary of Previous Data

2.1 Background

Glacoigenic cloud seeding promotes production of ice crystals in clouds containing super-cooled (temperatures below freezing) liquid water drops. The theoretical work that summarizes pertinent physical mechanisms in clouds below freezing is known as the Wegener-Bergeron-Findeisen process (Rogers and Yau 1989). This process predicts that clouds containing supercooled cloud drops are supersaturated with respect to ice. Once embryonic ice crystals initially form in these clouds, the crystals can rapidly grow to a size of many tens of micrometers in a matter of minutes (Rogers and Yau 1989). Initial formation of the embryonic ice crystals at temperatures warmer than -40^{o}C requires special, and relatively rare, small aerosol particles (ice nuclei) that serve as a lattice or substrate on which water molecules can collect, and a crystalline configuration that promotes freezing. In natural clouds, this initial freezing often does not start to occur until cloud temperatures cool below -15^{o}C. Clouds warmer than -15^{o}C often have supercooled liquid water, which will freeze when they come in contact with aircraft. Pilot reports of icing are a direct indication that supercooled liquid water is present. As the aircraft collides with the supercooled drops they freeze onto the airframe and form the ice on the aircraft. Bernstein et. al. (2005) show that the majority of these icing reports occur at temperatures warmer than -15^{o}C.

The first cloud seeding experiment occurred by accident. While conducting research on the aircraft icing problem for General Electric in 1946, Vincent Schaffer built a supercooled cloud chamber using a freezer lined with black velvet. He formed supecooled liquid clouds by breathing into the freezer and noted that at temperatures as cold -23^{o}C the clouds failed to produce ice crystals. After the freezer was slow to cool down one day, Schaffer attempted to rapidly cool the freezer, using dry ice (-78^{o}C). After the dry ice cooling he breathed into the freezer and noted many thousands of ice crystals had formed within the light beam of the freezer. The supercooled liquid cloud had produced ice crystals due to homogenous freezing (cooling the cloudy air below -40^{o}C and freezing the cloud drops without the need for ice nuclei) (Rogers and Yau 1989).

Expanding on Schaffer's creation of ice crystals, his colleague Bernard Vonnegut, worked to identify molecules that would serve as ice nuclei (structures that have similar lattice structures as ice) and create ice crystals in supercooled liquid clouds at temperatures warmer than -40^{o}C (Vonnegut 1947). Vonnegut's work led to the finding that a smoke of silver iodide (AgI) could begin to initiate ice formation in supercooled liquid water clouds at temperatures much warmer than -40^{o}C.

The implications that artificial ice nuclei could be introduced into subfreezing liquid water clouds to produce additional precipitation quickly led to operational cloud seeding programs in the 1950s, such as Southern California Edison's Big Creek hydroelectric project.

2.2 Selected Research and Validation Programs

During the past six decades, there have been many projects that have defined and refined the conceptual model of cloud seeding. The conceptual model states that clouds with liquid water at temperatures colder than -6°C can have ice nuclei introduced to form ice crystals. The crystals will grow to precipitation sizes and exit the cloud base increasing the total precipitation. These projects included both basic supercooled cloud physics research and statistical evaluations of the effectiveness of cloud seeding. The design of the statistical evaluations can include comparing precipitation quantities using randomized seeding (one storm is seeded and another is not) or target and control (when a seeded location is compared to an adjacent unseeded location). After a significant number of cases are collected statistics can be computed.

A set of randomized seeding experiments – Climax I (Grant and Mielke 1967) and Climax II (Mielke et al. 1971) – was conducted in the 1960s over the central Colorado Rockies. Analysis of the original experiments suggested significant (100% and 24%) increases in precipitation from seeded clouds. These results were challenged by Hobbs and Rango (1987), who questioned the statistical methods, data quality, and randomization methods. Their reanalysis of the Climax data found precipitation increases of up to 10%.

The Bridger Range Experiment (Super and Heimbach 1983) was conducted in southwestern Montana during three winters (1969–1972). This was a ground-based silver iodide (AgI) experiment that had the cloud-seeding generators sited at higher elevations. At higher elevations the seeding was more effective, avoiding low-level valley inversions. The low-level inversions can inhibit vertical mixing, while the higher altitude generators, above the low-level cold pool, allow the cloud-seeding plume to more effectively reach the cloud bases and deposit increased snowfall in higher terrain. The results of this experiment suggested precipitation increases of up to 15% in the target area. The project also pioneered targeting validation using airborne plume sampling and chemical analysis of silver in the snow.

Over other parts of the western U.S., Griffith et al. (1997) found positive cloud seeding precipitation increases of 9% to 21% from programs at several locations in Utah and precipitation increases of 7% to 9% also were observed over the upper Payette River in southern Idaho. Their methods used a comparison of the cloud seeding target area precipitation to a set of control area precipitation measurements during both seeded and unseeded historical periods. When the seeded target area consistently showed higher snowfall ratios, this was presumed to be evidence of a positive seeding effect.

The Snowy Precipitation Enhancement Research Project was conducted in the Snowy Mountains in New South Wales Australia (Manton and Warren 2011). This project used a 2:1 randomized design. The primary analysis suggested a 7% increase in precipitation at the 24% significance level. The Snowy Mountain ground-based generator project included the release of AgI as the active chemical and indium as a passive tracer. Chemical analysis suggested that AgI was often successfully delivered into the target area. The chemical analysis values were enhanced relative to the indium tracer, suggesting that there was a microphysical impact (change in the cloud particles) from the AgI. A secondary analysis

showed that when there were more than 45 generator hours in an event, the increase in precipitation was 14%. The study also established that a positive seeding impact is further influenced by the amount of SLW available at the start of a seeding event.

The Wyoming Weather Modification Pilot Program (WWMPP) was conducted in the Sierra Madre and Medicine Bow Mountains in southern Wyoming from 2005 to 2014. These mountain ranges are closely adjacent to the Laramie Range. The WWMPP was a randomized, ground-based, cloud-seeding experiment in which winter storms with favorable seeding conditions in one range would be seeded, while the other range was not seeded. Analysis of the initial data set showed a 3% increase in precipitation with a 28% chance that it was a random result (Breed et al 2014). Post analysis of the data collected from the study showed that "cross contamination" had occurred between the two mountain ranges. For example, it was discovered that at times, a randomly selected seeding case targeting the Sierra Madre Range was inadvertently seeding the Medicine Bow control cases. When the cross-contaminated cases were eliminated, the precipitation increases were determined to be between 4 and 9%. Numerical model analysis from the Weather Research and Forecast (WRF) model (Skamarock et al. 2008) of three years of seeded case data showed that when the generator hours (normally 32) were below 27, the plume often didn't reach the target area. Elimination of the seeding cases with less than 27 generator hours resulted in precipitation increases of 5 to 15% per seedable storm. The post analysis also concluded, however, that only 30% of the winter storms in the area were suitable for seeding.

2.3 Current Wyoming Cloud Seeding Projects

There are currently two distinct operational cloud-seeding programs being conducted in the state of Wyoming. First, the Eden Valley Irrigation and Drainage District conducts cloud seeding to target stream flow into the Big Sandy Reservoir. Second, a larger project run by Weather Modification Inc. is conducted over the central Wind River Mountains using remotely controlled, ground-based AgI generators. This project is designed to add water to the Green River and Colorado River system.

3 Climatology of the Project Area

3.1 Introduction

Two climatology compilations have been built to assess the meteorological cloud seeding potential for the Laramie Range. A ten-year observational climatology was constructed to infer the number of storms that have the potential for periods of cloud seeding, using only observed data. In addition, high-resolution numerical model producing hourly output was constructed to compute the simulated cloud seeding potential over eleven-year winters. A set of case studies is presented in Appendix B.

For the observational climatology, storm periods when precipitation was reported in the mountains was used to define a set of storm cases to be evaluated. These cases were analyzed using observational data sets and the number of seedable storms was identified, as well as the potential maximum number of seedable hours. The second climatology used an eleven-year WRF simulation to identify the locations, time periods, and quantity of precipitation accompanying favorable cloud seeding conditions. In this Section, each of these climatologies are described in detail and the potential for cloud seeding weather is assessed.

3.2 Ten Year Laramie Range Observed Winter Storm Climatology

Ten (winter) water years were considered in the assembly of this Laramie Range winter storm climatology. A winter water year is defined for this study as lasting from mid October through the end of April. The 2005-2014 water years were considered for the climatology. Snow water equivalent (SWE) values obtained from the SNOTEL data from the NRCS instruments over the northern Laramie Range were analyzed and storm periods were determined. Statistics from these representative time periods during the storms were used to characterize the storms, build the climatology, and determine the number of storms exhibiting suitable cloud seeding conditions. Although the number of total storm hours can be computed and the number of storms associated with suitable cloud seeding weather conditions can be inferred, determining the total observed number of cloud seeding hours was not possible due to the lack of regularly observed supercooled liquid water (SLW). SLW is not regularly observed by the US meteorological observing network, but following methods such as Bernstein et al. (2005) the presence of SLW can be inferred using observed data such as satellite, surface observations, pilot reports (etc.). Detailed hourly cloud seeding results are presented in the modeled WRF climatology (Section 3.3).

The database for the observed climatology was built using a variety of different archived weather observations. The data sources examined include: Geostationary Operational Environmental Satellite (GOES) imagery, icing pilot reports (PIREPS) from the Aviation Weather Center, Storm Prediction Center (SPC) experimental hourly mesoscale 700 hectoPascal (hPa) and 500 hPa analyses from the operational WRF-Rapid Refresh (RAP) 13-

km numerical model initialization half-hourly surface analyses, nearby meteorological terminal aviation routine weather reports (METARs), stability profiles from Froude numbers calculated using half-hourly, 1-km WRF simulations (Section 3.3) at three different point locations, and SNOTEL SWE values at two point locations.

Specific fields examined in this observational climatology include cloud top temperatures (CTT), cloud base heights (CB). surface winds, storm type, 700 hPa temperatures, wind speed and direction, and geopotential height, 500 hPa wind speed and direction, icing pilot reports (PIREPs), calculated Froude numbers, accumulated SWE, and storm start/end times.

Cases were selected based on daily (SWE) accumulations at one of two possible SNOTEL locations at the highest elevations in the proposed target area. The other two Laramie Range SNOTEL sites were below 8,000 ft MSL and outside the cloud seeding target area. Days when more than 0.2" of SWE was measured at either the Reno Hill (8400 ft.) or Laprele Creek (8375 ft.) SNOTEL locations were considered to be a case. A lower threshold of 0.2" was chosen due to the resolution of the observed data (generally observed to be ±0.1"). Since the SNOTEL data was analyzed daily, snowfall events lasting longer than one day are counted as one case per day, such that a three day storm would be represented as three separate cases in the database. This analysis resulted in the identification of 447 cases. Start and end times for each case were determined by manual observations of the hourly SWE, GOES satellite imagery, and occasional radar composites. Radar coverage of the Laramie Range is limited to elevations above 11,500 ft. MSL, therefore start and end times were largely determined by the amount/type of satellite observed cloud cover impacting the range. Each case was assigned a unique, four digit case number, where the first two digits represent the water year (i.e., 09 or 14), and the second two digits represent the case within a given water year. So case 2 from 2013 will have the four digit case number 1302.

3.2.1 December 3, 2011, Case Overview

To demonstrate the creation of the observational climatology data set an example case is presented. December 3, 2011 (case number 1214) was flagged as a case at both the Reno Hill and the Laprele Creek SNOTEL sites with each location showing an increase in SWE of 0.2" (Figure 3.1).

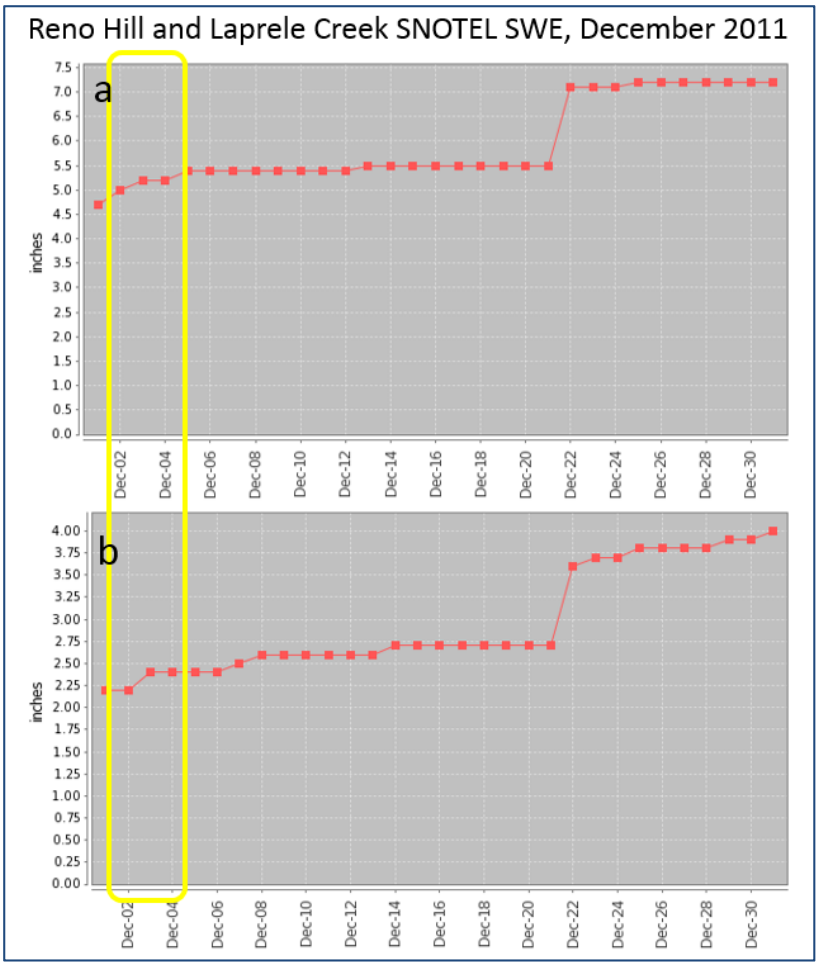

Figure 3.1. a) Reno Hill SNOTEL (station 716) and b) Laprele Hill SNOTEL (station 571) SWE for December 3, 2011. Case 1214, highlighted within the yellow box, with both stations reporting a SWE increase of 0.2" on December 3.

Once a storm period was defined as a case via the SNOTEL SWE analysis, a representative time when the storm low-level SLW may have been maximized was selected. This was done by manually looking at surface observations, hourly SNOTEL SWE, radar composite maps, the GOES infrared (IR) and visible (during daylight) satellite imagery. With the representative time for the storm is selected the closest (in time) observed data sets (within 45 minutes of the representative time) are mapped to the case database. Case analysis suggested that the representative time for the December 3, 2011 case would be 0300 Universal Time Coordinate (UTC), therefore all of the meteorological observations closest to that time period were collected and placed in the database. Figure 3.2 shows the combined surface weather conditions, satellite imagery, and radar composite at the closest available time to 0300 UTC.

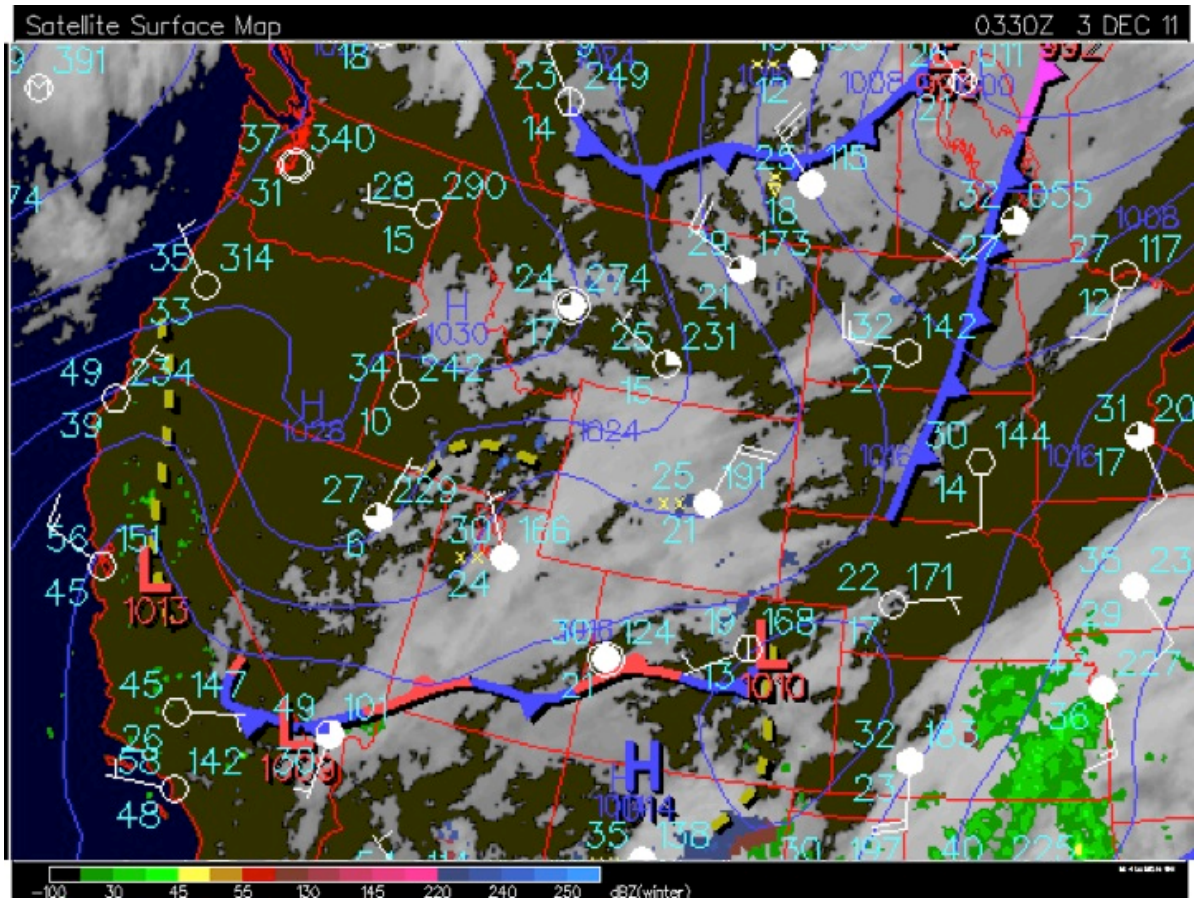

Figure 3.2 0330 UTC December 3, 2011, the satellite-radar-surface analysis composite map from UNISYS. Clouds are visible in the satellite imagery and some very weak radar echos are detected over the Laramie Range. The nearby surface station at the Casper, WY airport (KCPR) was reporting light to moderate snowfall with north-northeast winds.

This case is listed in the database as an all-day storm since clouds covered the Laramie Range for the entire day. Using the GOES satellite image nearest to the representative time, the CTT was determined to be -30°C. (Figure 3.3). The other observational data for this event was collected for the representative 0300 UTC time as well.

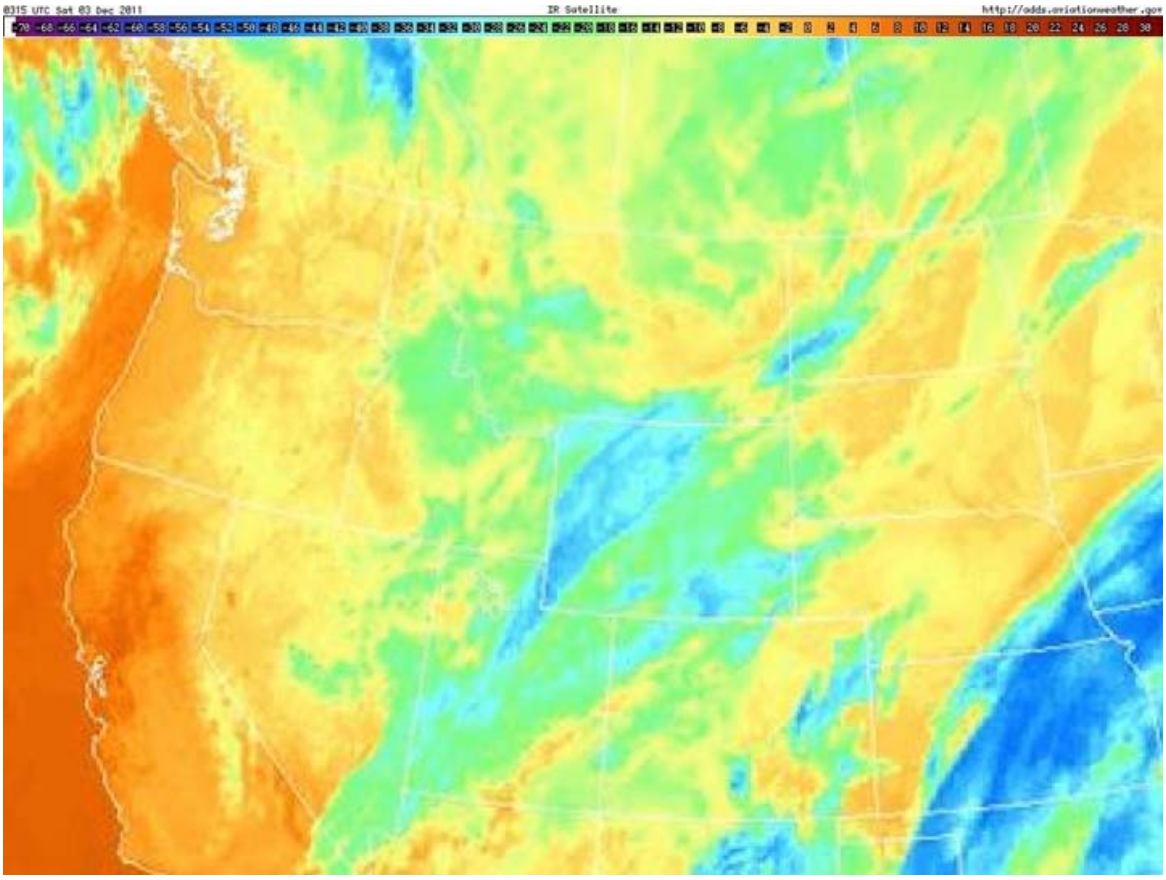

Figure 3.3 GOES IR satellite imagery at 0315 UTC, December 3, 2011. Cloud top temperatures (CTT) are -30°C over the Laramie Range.

Cloud base (CB) heights above ground level (AGL) and wind observations were collected from the Casper, Wyoming Airport METAR (KCPR) for instances that fell within the "representative time" window for this event (0300 UTC, +/- 45 min.). If no METAR data was available within the representative time window, null values were added to the database, because cloud base heights can vary considerably over a fairly short period of time. In order to have all the data on a common MSL vertical coordinate the measured AGL cloud bases were converted to MSL. The cloud base heights on December 3, 2011 were 6700 ft MSL (1400 ft AGL), with the winds from the north-northeast at 20 knots (kts)(Figure 3.4).

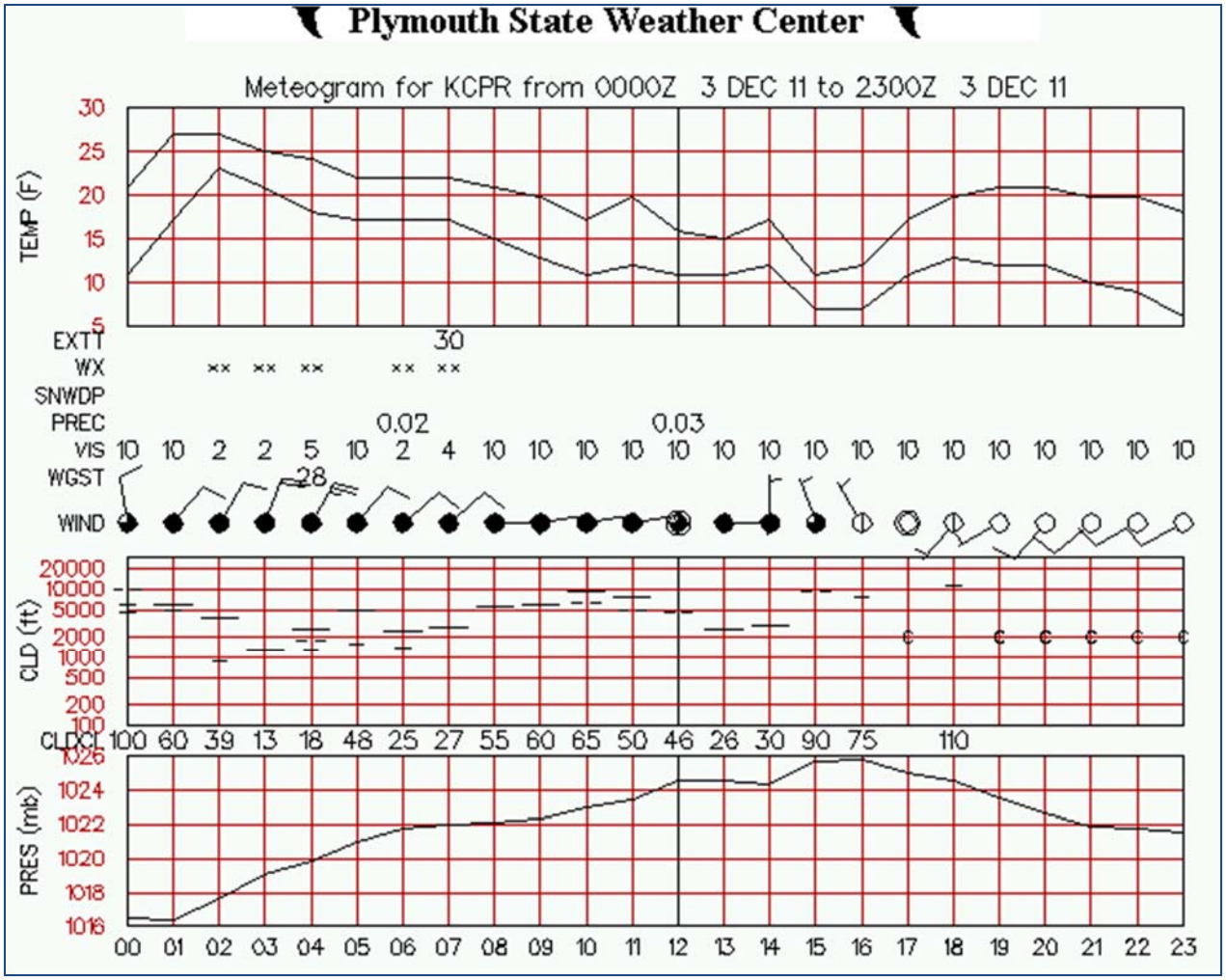

Figure 3.4 KCPR (Casper, WY) meteogram for December 3, 2011. Panel 3, cloud (labeled CLD (ft)), shows CB heights over Casper in ft. AGL.

RAP model images (00 hour forecasts) of the 500 hPa and 700 hPa surfaces were examined for temperatures, geopotential height, wind direction, and wind speeds over the Laramie Range. Using the 700 hPa (10,000' MSL; Laramie Range peak altitudes) analysis (Fig. 3.5) for the December 3, 2011 case at 0300 UTC, the temperature is determined to be -12°C, winds out of the northeast at 20 kts, and the geopotential height over the range was 2970 meters (m) (9741 ft).

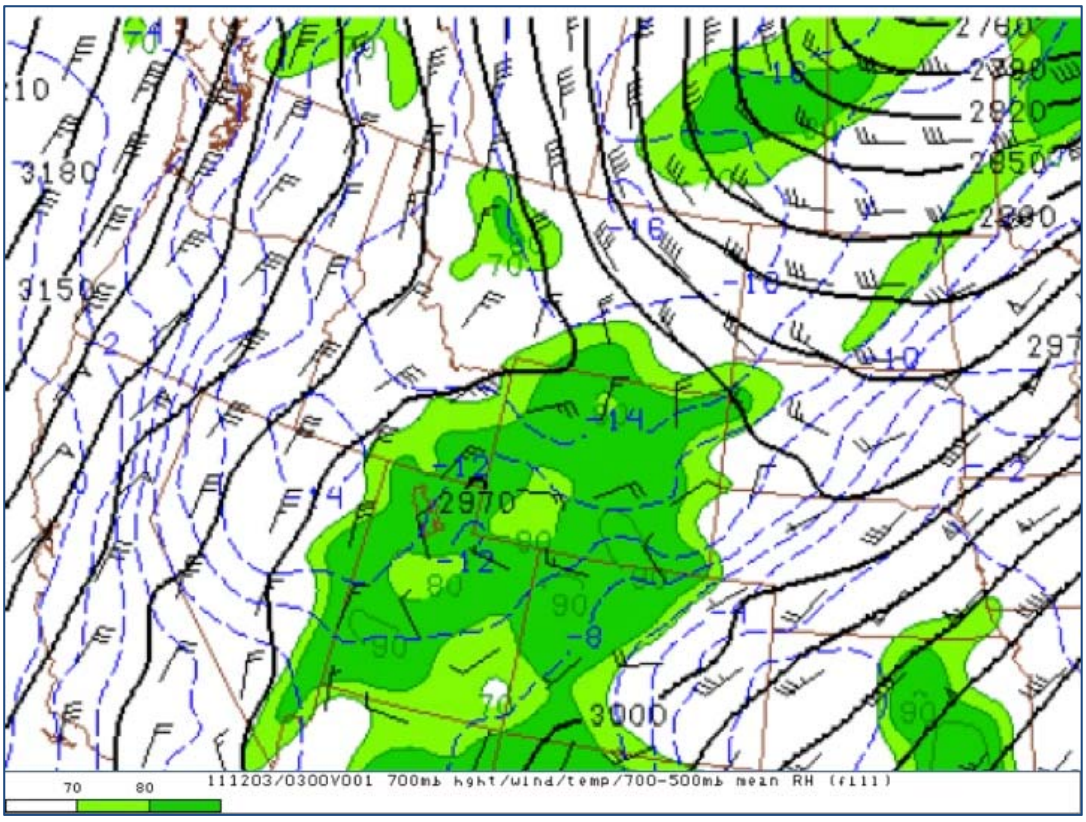

Figure 3.5 The 700 hPa SPC Experimental Mesoscale RAP Analysis for 0300 UTC, December 3, 2011. 700 hPa temperature (-12°C), wind speed (20 kts), wind dir (45°), and geopotential height meters (2970 m) over the Laramie Range.

A similar method was followed for the 500 hPa layer (Figure 3.6), but only wind direction and wind speed were archived. In this case, winds at 500 hPa are from the southwest at 35 kts.

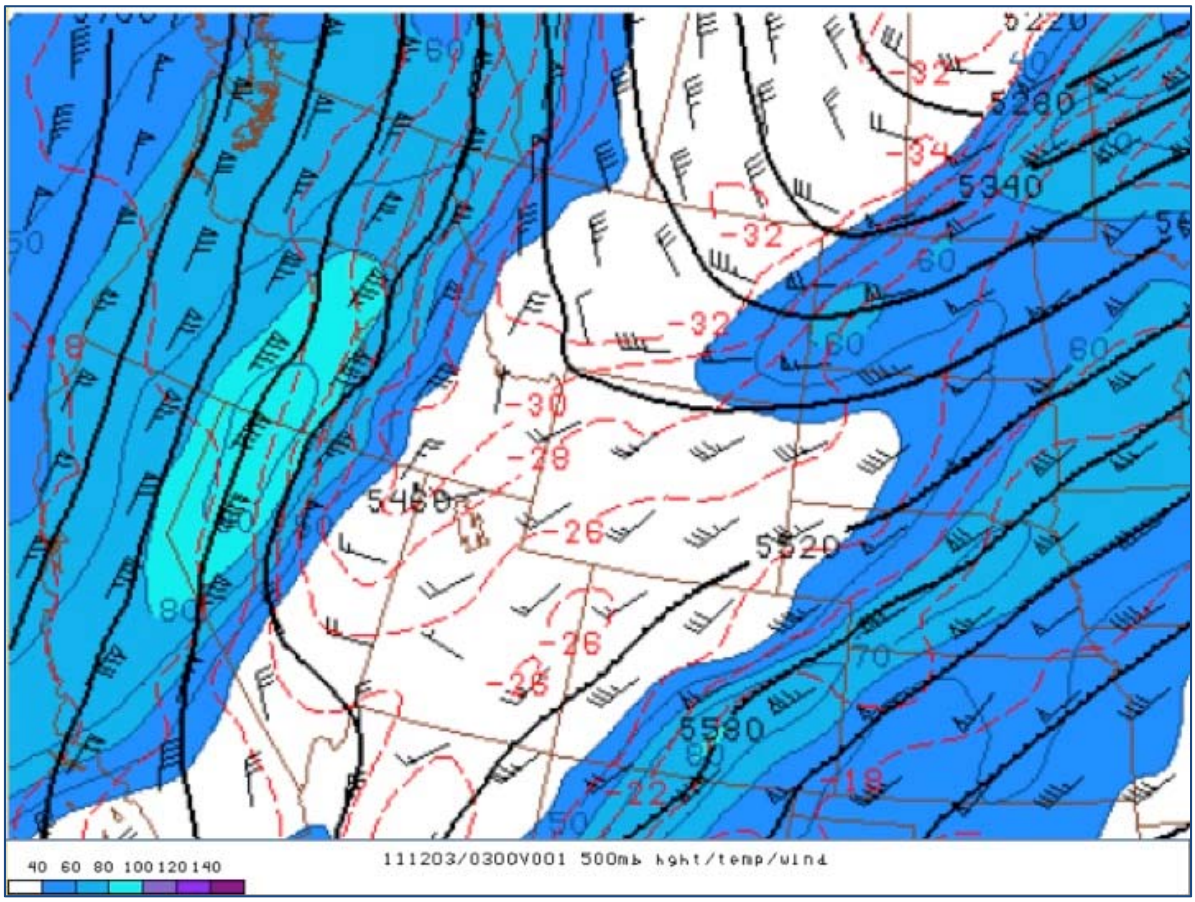

Figure 3.6 The 500 hPa SPC Mesoscale RAP Analysis with wind speed (35 kts) and wind direction (235°).

Two additional data sets were also included in the observed climatologhical database. The first of these data sets were the positive icing PIREPS. When ice forms on an aircraft while in flight it is a direct indication that a SLW cloud is present at the aircraft location. Any low-level positive icing pilot reports found within a defined polygon around the greater target location (43.14, -107.25; 41.25, -105.80; 41.50, -104.30; 43.03, -104.71), and within the storm time period, are denoted "Y" in the database. The lack of an icing PIREP cannot be used to infer an absence of icing as there may be no air traffic to report conditions. When PIREPS were absent during a given storm, the PIREP flag was denoted "N". For the December 3, 2011 case, two icing PIREPs were available within the polygon. The number of PIREPS for each case, along with remarks, which include icing type, intensity, and altitude, were also listed in the observed climatological database.

The observed climatology utilized the 1-km WRF (see Chapter 3.3) soundings developed for this project to calculate Froude numbers:

$$F = U/NH$$

$$N = [(g/\theta)*(\partial\theta/\partial z)]^{1/2}$$

These were calculated at three point locations (Casper Mountain: 42.73, -106.29; Glenrock: 42.87, -105.87; Shirley Basin: 44.44, -106.10) adjacent to the target area.

Synthesizing the data collected for case 1214, the seeding potential and best generator location(s) for this particular case's representative time can be determined. Given that CB heights at 0300 UTC are 6700 ft MSL, cloud tops are near 18,000' MSL (CTT -30°C at 500 hPa), and icing conditions were reported by aircraft, it can be inferred that the target area, located entirely above 8000 ft, is in clouds with SLW likely present. A 700 hPa temperature of -12°C coupled with northeast (NE) winds at 20 kts, suggests that a high-elevation, ground-based generator located roughly 11.5 miles northeast of the target area would be useful in conducting seeding operations for this type of case. The ideal temperature range for ground-based generator operations (i.e., AgI cloud seeding) is from -6°C to -16°C, with the natural peak in riming occurring at the cooler end of the temperature range (Wallace and Hobbs 2006) (Figure 3.7).

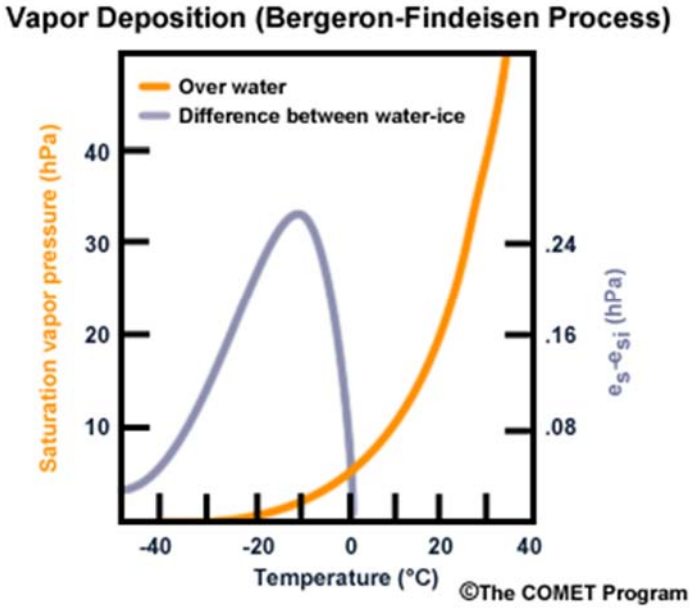

Figure 3.7 ©The COMET Program graphic showing saturation vapor pressure for liquid water (orange curve) and the difference in saturation vapor pressure for liquid minus that for ice (blue curve), both against temperature (°C). The peak in saturation vapor pressure of water-ice occurring between -10°C and -20°C indicates the region of most efficient, natural riming.

Aircraft operations for this particular case would be highly dependent on the altitude of flight. The CTTs suggest the 500 hPa level is at cloud as top and the 700 hPa level is in cloud. Therefore cloud seeding could potentially be conducted at a range of different altitudes. For this case, using the 500 hPa winds, a flight track roughly 20 miles southwest (SW) of the range would be identified for seeding, however, basing a flight track off the 700 hPa winds, requires a much closer track to the NE of the range. Successful aircraft seeding with this case could be difficult due to the strong directional shear between 700 hPa and 500 hPa and fairly cold temperatures above 12,000 ft. MSL (the minimum altitude for the seeding aircraft). The shear would make targeting the area more difficult and since temperatures at 700 hPa are -12°C the temperatures higher in the atmosphere, where the aircraft would be required to fly, may be too cold for effective cloud seeding.

3.2.2 Results and Observed Climatology

The same method applied to the December 3, 2011 case as described above, was repeated for each of the 447 total cases identified in the observed climatology. In order to generate a set of case bins for the observational data from the storms, winter weather patterns over the Laramie Range during the 2005-2014 water years were defined, and some simple statistical methods were utilized. Looking first at the typical duration of storm systems, all day storms (listed in the database as 23-hr; 0000 UTC through 2300 UTC) dominate by a large percentage (Figure 3.8).

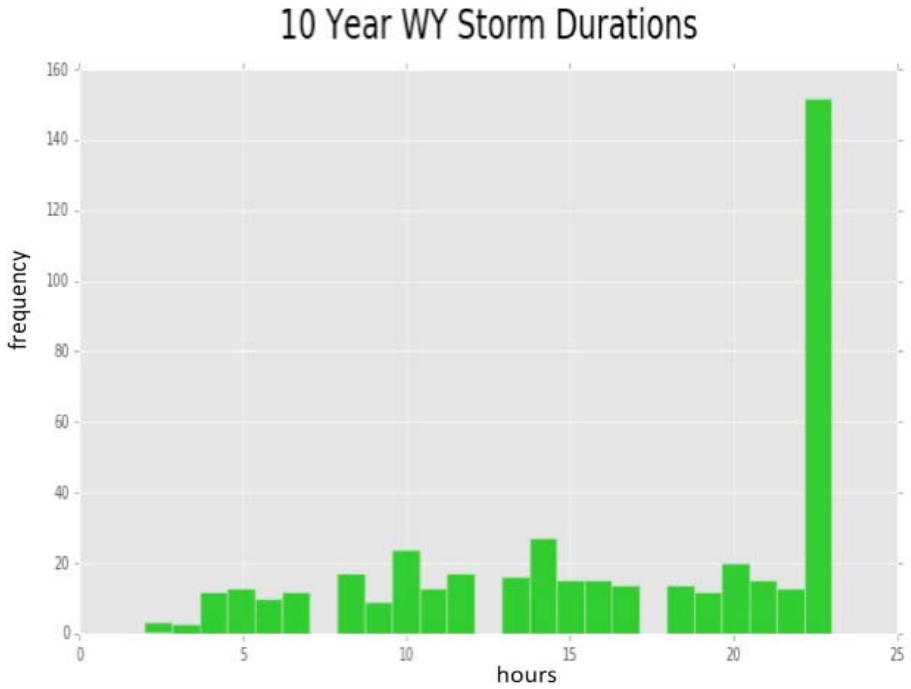

Figure 3.8 Frequency of 10-year observed climatological storm durations. Hours per storm shown on x-axis, frequency of storms in each bin on y-axis. Minimum storm duration possible: 1 hour; maximum: 23 hours.

The total winter storm system hours over the ten-year climatology was 7296 hours. The SWE distributions at both Reno Hill and Laprele Creek SNOTEL sites show most storms produce less than 0.5" of SWE (Fig. 3.9 and 3.10). Assuming a snow-to-liquid ratio of 10:1 on average, 5 inches of snow or less was observed during most storms. The Reno Hill SNOTEL compared favorably with Laprele Creek SNOTEL for many storms.

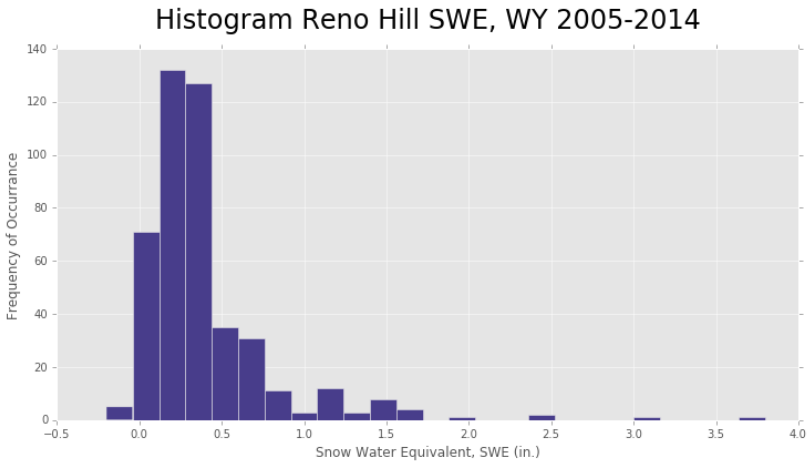

Figure 3.9 Histogram of Reno Hill SNOTEL SWE values over the 10-year climatology.

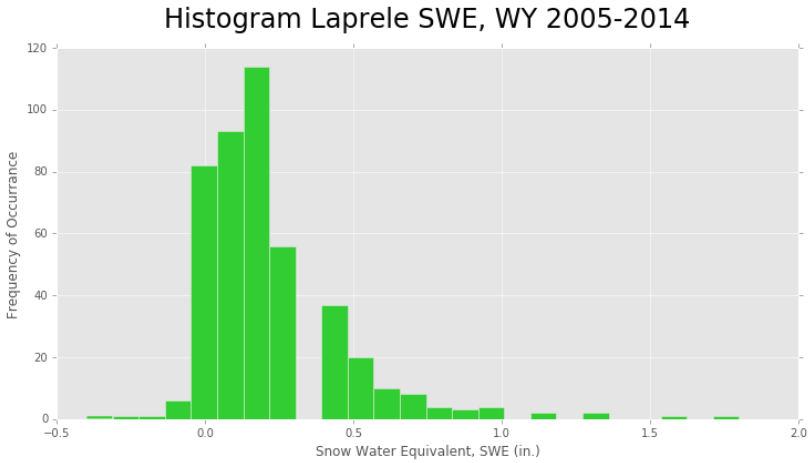

Figure 3.10 Histogram of Laprele Creek SNOTEL SWE values over the 10-year climatology.

Figure 3.11 shows that a slightly bimodal distribution of CTTs was present over the ten years of winter storms for the Laramie Range, with most cases having CTTs colder than -40°C.

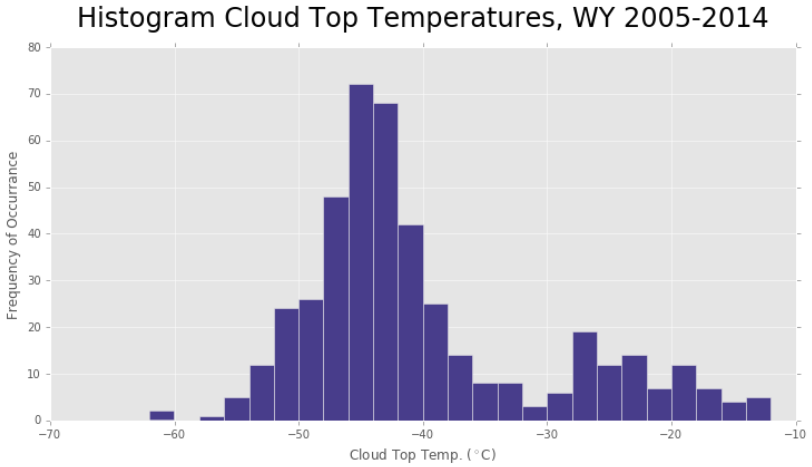

Figure 3.11 Histogram of cloud top temperatures (CTTs) observed via satellite, over the Laramie Range for the 10-year period examined.

The majority of observed CTTs in the Laramie Range at the case representative time are colder than those defined as typical for seeding (warmer than -26°C) by Griffith et al. (2012). Colder clouds have more natural ice crystals and are thought to have less SLW available for cloud seeding. The cold CTTs observed by satellite may be due to cold cirrus clouds overlaying lower warmer clouds containing SLW as is discussed in Bernstein et. al. 2005. Alternatively, strong upward motions, enhanced by complex terrain in mountainous regions in orographic winter precipitating clouds can result in the maintenance of supercooled water saturation. Korolev and Mazin 2003 show that SLW can be maintained even as heavy snow falls through a cloud layer and cloud tops remain cold. Given the 45.4% frequency of PIREPS for the cases within the ten water years examined, the ≥-26°C CTT criteria presented by Griffith et al. (2012) is not particularly valid for observed SLW in the Laramie Range.

Cloud base heights at (KCPR) were often below the Laramie Range mountain top level, with the highest frequency of CB heights in the range of 6000-8000 ft. MSL (Figure 3.12), below the peaks of the Laramie Range. This is important for cloud seeding as precipitation exiting the low cloud bases will not evaporate or sublimate and will reach the ground. In addition low cloud bases suggest the presence of SLW.

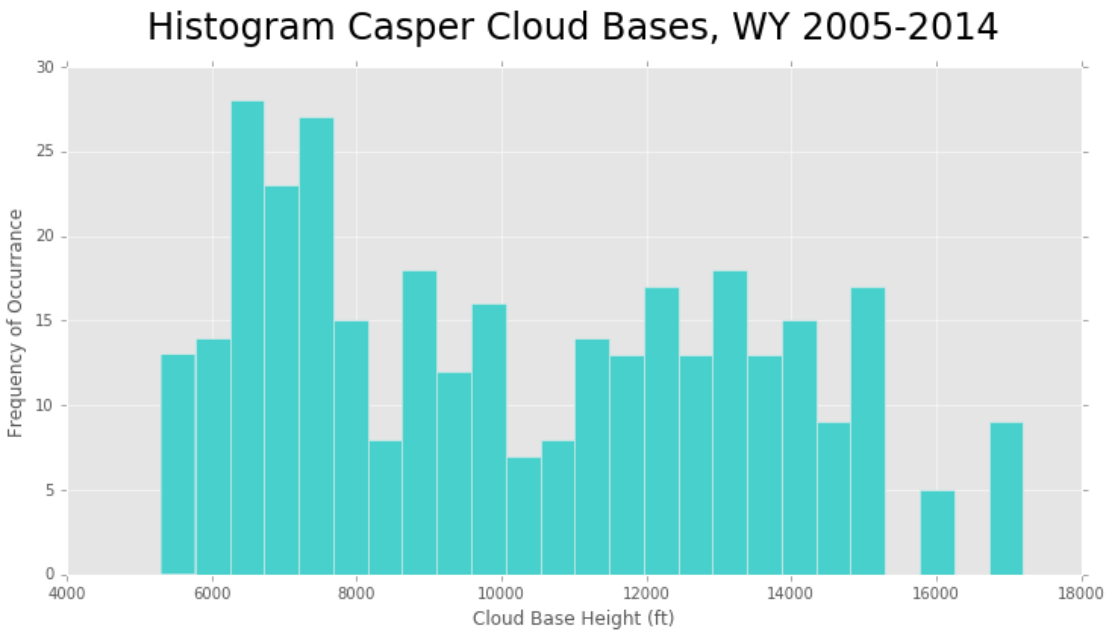

Figure 3.12 Histogram of KCPR (Casper, WY) cloud base heights over the 10-year climatological period. The Laramie Range mountain tops are between 9,000 ft and 10,000 ft.

The distribution of 700 hPa temperatures over the region suggests many of the cases fall into the ideal temperature range for AgI seeding (-6°C to -16°C), and (-2°C to -16°C) for liquid propane (LP) seeding (Figure 3.13).

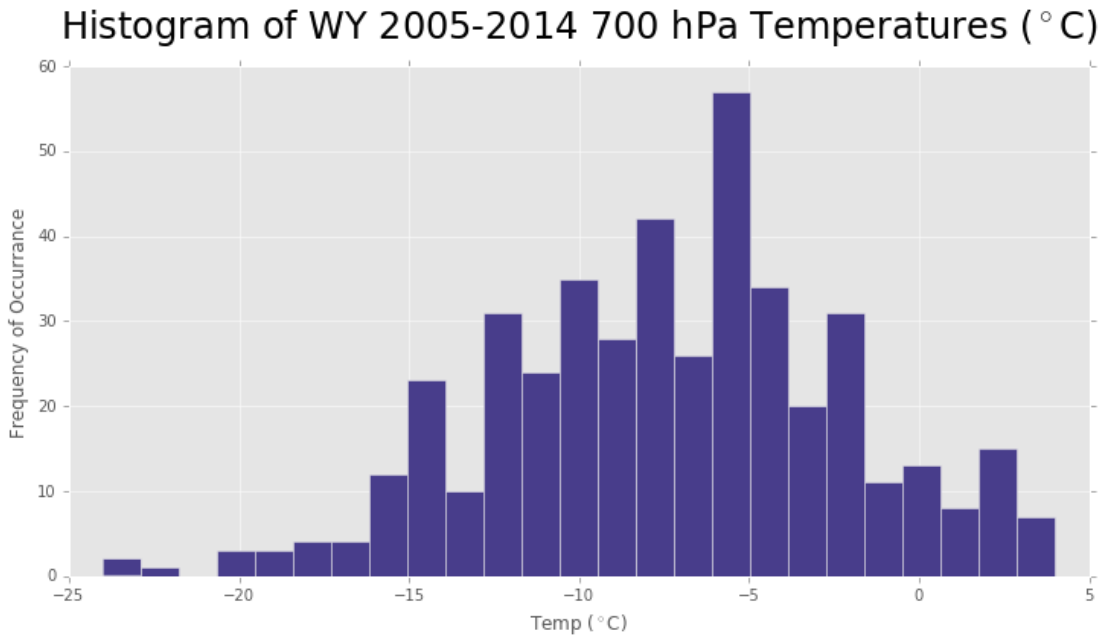

Figure 3.13 Histogram of 700 hPa temperatures over the 10-year climatology.

For this study, ground-based generators and aircraft, both employing AgI, were considered, as well as ground-based (LP) generators. Using only a temperature threshold (recall that clouds and likely precipitation are present at this time), out of 447 cases 268 (60.0%) had 700 hPa temperatures appropriate for ground AgI seeding (-6°C through -16°C), 405 (90.6%) had temperatures appropriate for aircraft seeding (-14°C or warmer below 700 hPa), and 390 (87.2%) had temperatures appropriate for LP seeding (temperatures of -2°C and colder).

The 500 hPa wind analysis (Figure 3.14), suggests the majority of the cases evaluated for this study had a westerly wind component.

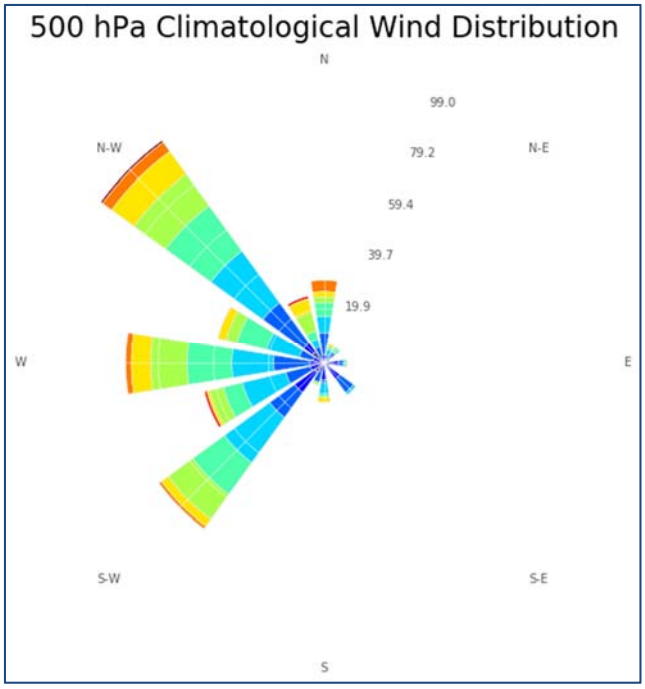

Figure 3.14 Wind rose of wind speed and direction at 500 hPa for the Laramie Range cases at the representative time.

While 500 hPa winds do provide some insight into the synoptic patterns associated with Laramie Range winter storms, and perhaps aircraft based cloud seeding activities, the actual altitude of flight operations will take place between 700 hPa and 500 hPa. Looking at the 700 hPa wind rose (Figure 3.15), there was a substantially large proportion of storms that fell into a more northwesterly flow pattern, as well as a noticeable frequency of storms with winds from the west and north. Examination of winds from KCPR suggests winds at the surface are frequently from the southwest and north though north-northeast (Figure 3.16).

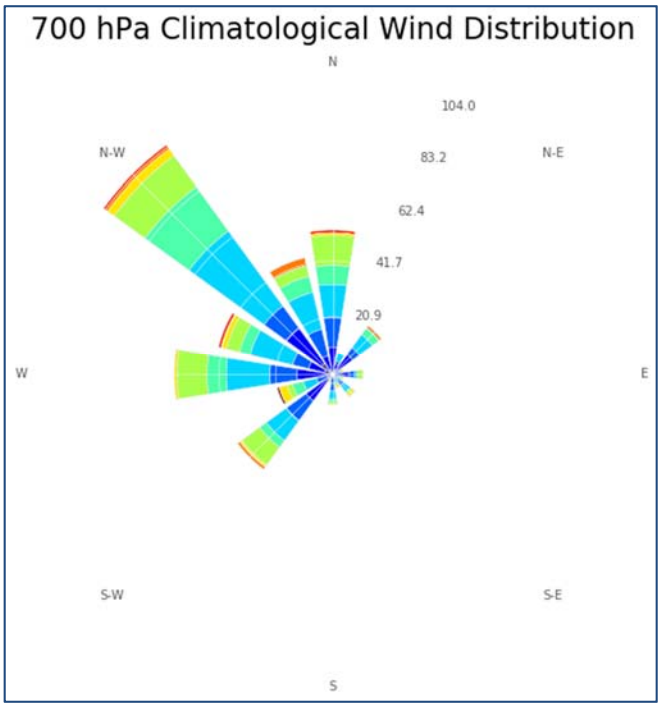

Figure 3.15 Wind rose of wind speed and direction at 700 hPa for the Laramie Range cases

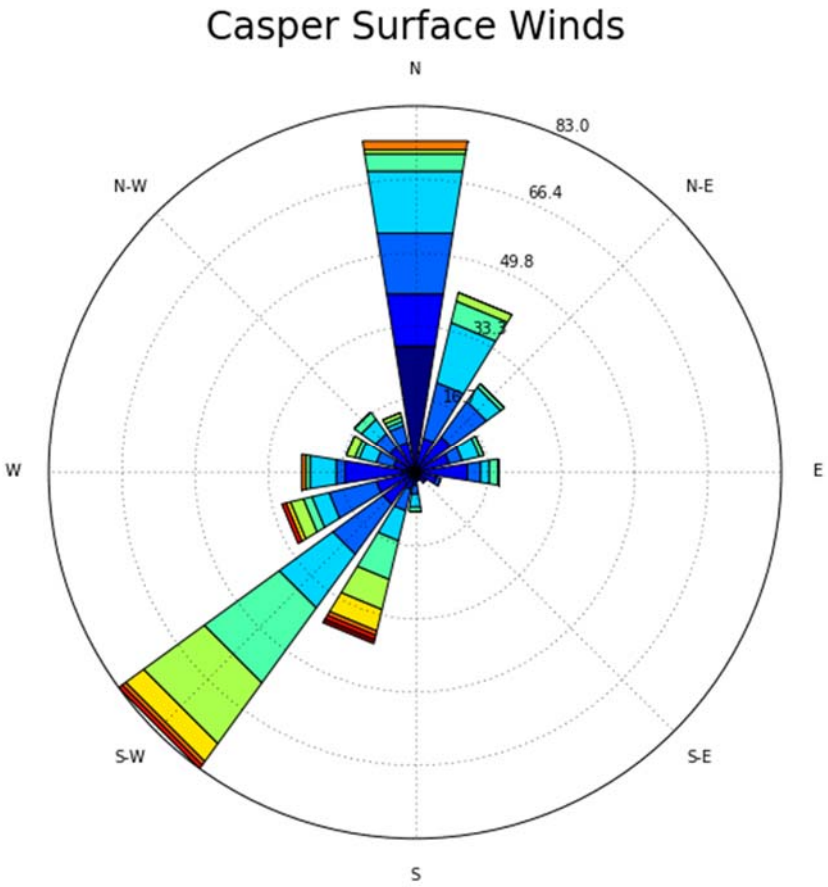

Figure 3.16 Wind rose of wind speed and direction at KCPR for the Laramie Range cases at the representative time.

Based on the 700 hPa and surface wind rose analysis of all 447 cases, two storm regimes were identified to be the most frequent – northwest and north-northeast wind flow. The northwest regime will be referred to as *Scenario 1 storms* (restricted to only cases with 700 hPa winds from W-NNW), and the north/northeast regime will be referred to as *Scenario 2 storms* (consisting of cases with 700 hPa and/or surface winds from north though east). The southwest wind surface scenarios were found to be matched the northwest 700mb wind scenarios. For each of the Scenarios, the statistics for potential cloud seeding using both ground-based AgI generators and aircraft AgI operations were considered. The parallel winds to the Laramie Crest in Scenario 1 caused the LP plumes to exit clouds prior to reaching the target area (see Section 4.3). Therefore the feasibility of LP generators was considered only for storms in Scenario 2.

Based on wind direction, Scenario 1 encompasses 249 of 447 cases (55.7% of all storms), and 3932 potential storm hours. Scenario 2 includes 97 of 447 cases (21.7% of all storms), and 1651 potential storm hours. In total, both Scenarios 1 & 2 encompass 346 of 447 cases (77.4% of all storms), which also accounts for 76.5% of the total potential storm hours (Table 3.1). In the next section the two scenarios will be characterized and considered for cloud seeding.

Storm Cases	Case Count	Total Storm Hours
Total Storm (all winds)	**447**	**7296**
Scenario 1 (W-WNW winds)	**249**	**3932**
Scenario 2 (N-E winds)	**97**	**1651**

Table 3.1 Total storm hours for Scenario 1, and Scenario 2.

3.2.2.1 Scenario 1 Storm Climatology

Scenario 1 storms that are potentially seedable are defined as having 700 hPa winds over the area from west-northwest though north-northwest, clouds observed via satellite, and 0.2" of SWE observed in the target area during the storm. Of the total 249 cases that fall into Scenario 1, 62.3% of the storms, or 155 cases, would have periods conducive to ground-based AgI seeding (700 hPa temperatures between -6°C and -16°C). Based solely on the temperature criteria of -8°C to -16°C between 12,000 ft MSL and 18,000 ft MSL, 92.0% of Scenario 1 storms, or 229 cases, would be conducive for aircraft seeding, whereas 30% of storm cases are too warm for ground based seeding and are suitable only for aircraft.

The most common characteristics found in Scenario 1 storms are temperatures at 700 hPa of -8°C, and median wind speeds of 30 kts. Icing PIREPs were reported for 104 (41.8%) of the 249 total Scenario 1 storms, directly indicating that there was indeed SLW present during periods of these storms. Using PIREPS, as indicators of SLW rather than model output has been shown to be more accurate in terms of identifying the actual presence of SLW. It has been documented that operational models, like the WRF RAP, glaciate clouds too quickly, and can significantly under-represent the frequency and quantity of SLW in potential icing clouds (Wolff and McDonough 2010). Unfortunately a lack of icing PIREPs cannot be used to determine if icing is present or absent.

The 249 Scenario 1 storms yield a total of 3932 potential winter season (November – April) storm hours. Using the start and end times for each storm event and assuming conditions remained suitable for seeding for the entire duration of the event. When broken down by type of seeding to be conducted, there was a winter season average of 247.9 maximum possible seeding hours via ground generators, an average of 360.5 maximum possible seeding hours using aircraft, and a maximum of 112.6 winter season seeding hours when only aircraft seeding could be conducted (temperatures are too warm for ground based cloud seeding). This is shown in Table 3.2, along with comparisons of seeding hours to total Scenario 1 hours and total overall climatology hours.

SCENARIO 1	Potential Seeding Hours	% of Scenario 1 Storm Hours	% Total Hours all Storms
Ground-based AgI	2479	63.05	33.98
Aircraft AgI	3605	91.68	49.41
Aircraft Only AgI	1126	28.64	15.43

Table 3.2 Scenario 1 storms (WNW-NNW) potential seeding hours for the 10-year climatology, compared to Scenario 1 percentage of storm hours and percentage of total storm hours.

The typical storm durations of Scenario 1 (Figure 3.17) match the overall distribution of the 10-year observed climatological storm durations (Figure 3.8) fairly well.

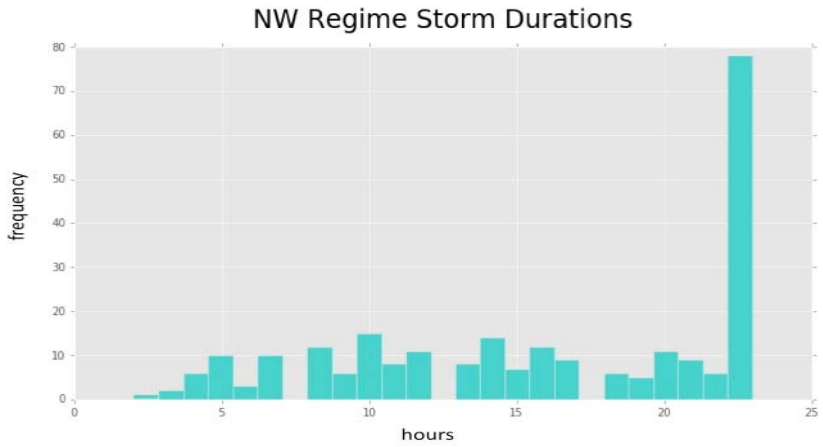

Figure 3.17 Histogram of Scenario 1 storm (WNW-NNW) durations. Most storms are full day storms.

The SWE distributions for Scenario 1 storms also generally match the overall SNOTEL SWE 10-year climatology, with Reno Hill receiving more precipitation than Laprele Creek (Figures 3.9, 3.10). The peak in SWE at the Reno Hill SNOTEL (Figure 3.18) was 0.25“. There were less than 20 of the 229 Scenario 1 storms with observed SWE greater than 1.0” and, one 24-hr storm producing just over 3.0 inches, showing that most storms produce moderate to light snowfall.

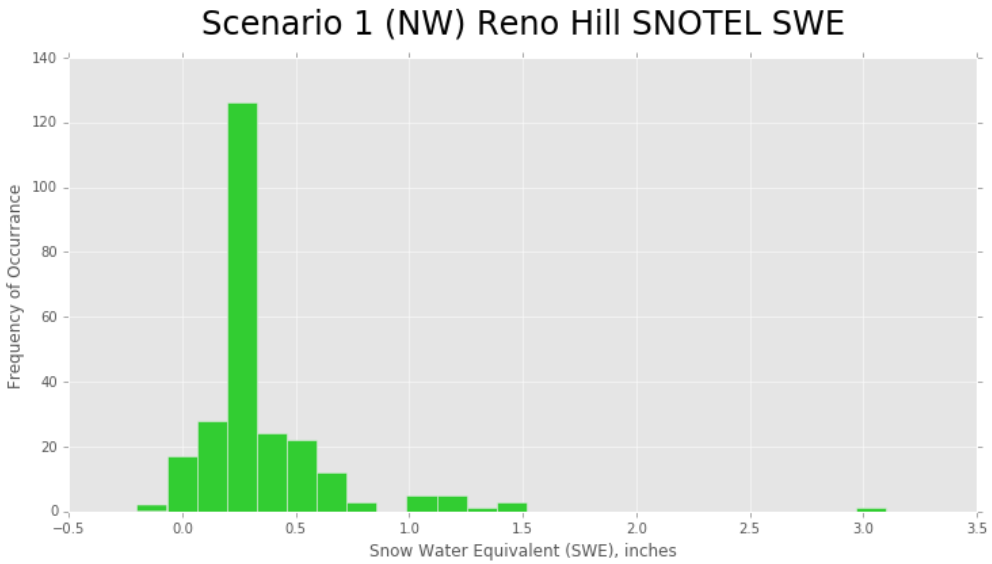

Figure 3.18 Histogram of Reno Hill SNOTEL measured SWE values over the ten-year climatology.

Analyzing the Laprele Creek SNOTEL SWE (Figure 3.19) shows that there were less than 15 storms with more than 1.0" of accumulated SWE. Given that winds in Scenario 1 storms are predominately from the NW, it is likely that the SWE totals at Reno Hill are higher because it is both further north and west than the Laprele Creek station.

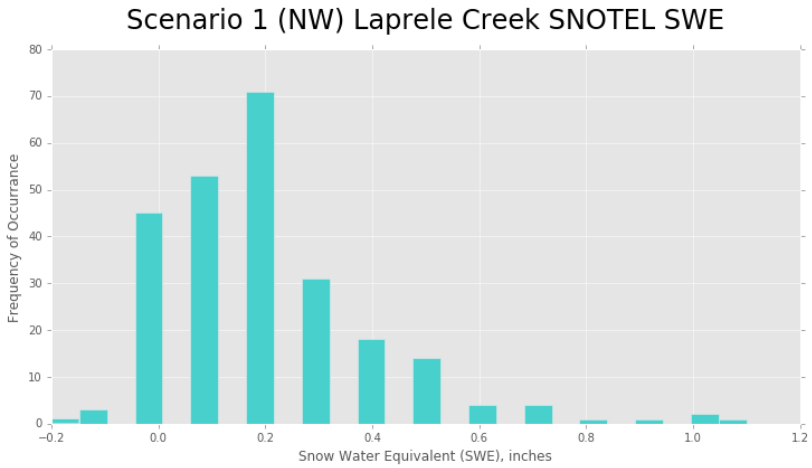

Figure 3.19 Histogram of Laprele Creek SNOTEL measured SWE values over the ten-year climatology.

CTTs within Scenario 1 storms (Figure 3.20) are consistent with the overall distribution of CTTs for the full 10-year climatology (shown previously in Figure 3.11). Scenario 1 storm CTTs also feature the bimodal distribution with peaks between -40°C and -50°C, and -20°C and -30°C. As previously discussed, it has been acknowledged that the satellite-derived CTTs used in this study may not be representative of the cloud layer where seeding would occur.

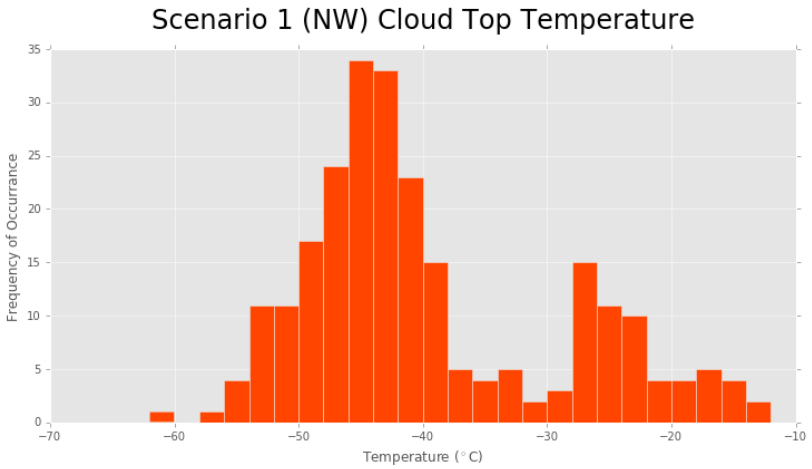

Figure 3.20 Histogram of Scenario 1 storm CTTs .

The only site that provides CB observations is the valley location of (KCPR). This site is north-northeast of the Laramie Range target area and may not be representative of cloud base heights during some of the Scenario 1 storms. The ten-year distribution of CB heights for Scenario 1 storms is shown in Figure 3.21. Rather than a clear maximum in CB heights, below the 9000 ft MSL mountain-tops, the Scenario 1 storm CB heights are more clustered between about 12000 ft and 15000 ft, with 16 cases having CB heights between 7000 ft and 7500 ft.

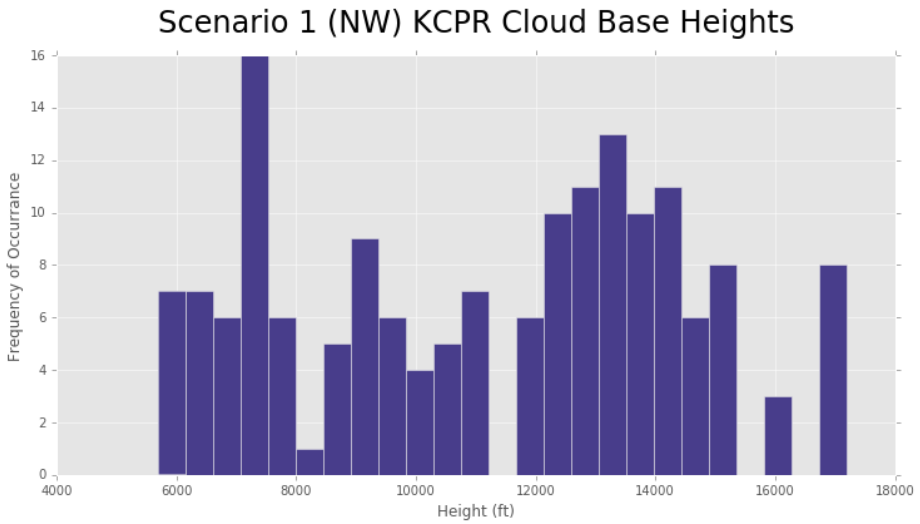

Figure 3.21 Histogram of cloud base heights for Scenario 1 storms at KCPR (Casper, WY, elevation: ~5200 ft).

The distribution of 700 hPa temperatures for Scenario 1 storms are presented in Figure 3.22. The majority of 700 hPa temperatures during Scenario 1 winter storms in the Laramie Range lie between -5°C and about -12°C, ideal for cloud seeding.

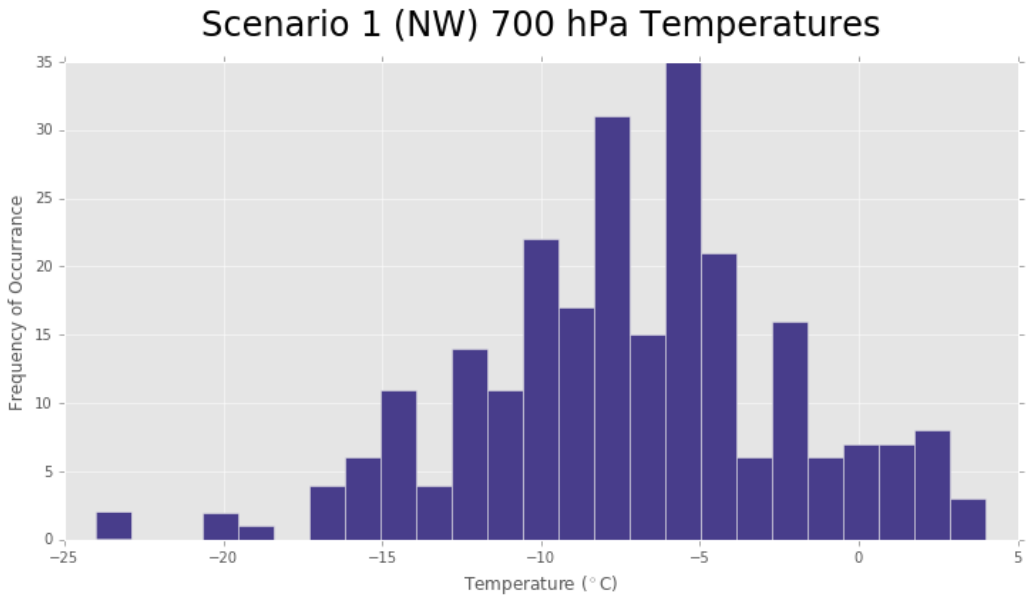

Figure 3.22 Histogram of Scenario 1 storm 700 hPa temperatures (degrees Celsius).

The most frequently occurring 700 hPa wind speed for Scenario 1 storms is 30 kts, with the next most frequent wind speeds at 35 kts and 20 kts (Figure 3.23). Only 7% of the Scenario 1 storms have winds greater than 50 kts. This suggests that ground based generators could be ideally sited 15 to 25 miles upstream of the target area in the Laramie Range peaks.

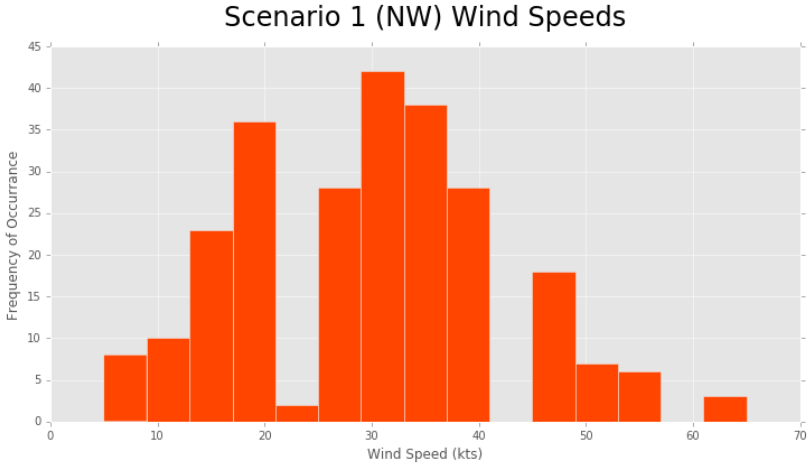

Figure 3.23 Histogram of wind speeds for Scenario 1 storms.

The 10-year climatological distribution of 500 hPa wind speeds for Scenario 1 storms are shown in Figure 3.24. The 500 hPa winds are exclusively between SW through N, with most storms consisting of winds from the NW. The laminar (similar direction) flow between the 700 hPa level and 500 hPa levels suggests that aircraft cloud seeding flights from the northwest at a variety of altitudes is feasible.

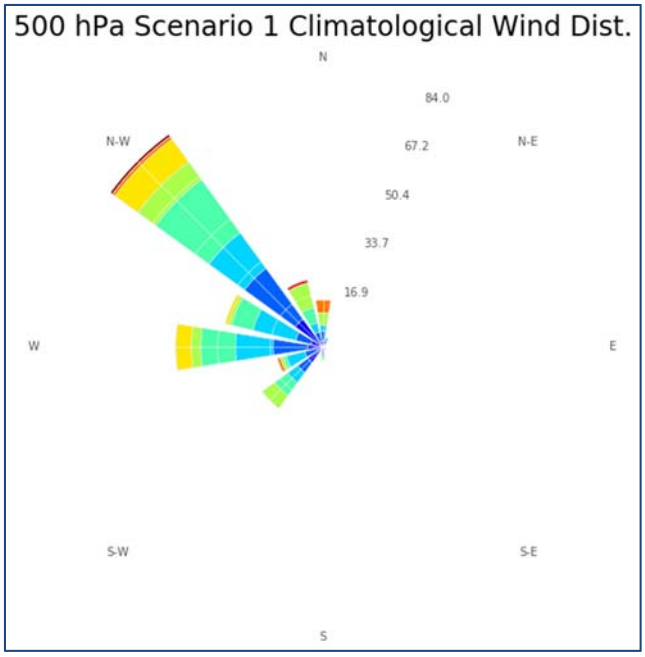

Figure 3.24 Wind rose showing distribution of wind speeds and wind directions at 500 hPa for Scenario 1 storms at representative times.

For Scenario 1 storms, Froude numbers were to used to calculate the atmospheric stability between two potential generator locations and the target area (represented by the Reno Hill SNOTEL location). The two source locations, Casper Mountain and a location near Shirley Basin, are located to the north and west of the target area (Section 4). Rather than the traditional Froude number calculation (Epifanio and Durran 2001, Galewsky 2008), the "mountain height", *h*, in our analysis is the distance between the generator (source) location and the target area, as opposed to the height of the mountain. The calculation is modified in this way in order to gain insight into the stability between potential generators and the target area. Figure 3.25 shows the distribution of Froude numbers between Casper Mountain (7,800 ft.) and the Reno Hill SNOTEL (8,400 ft).

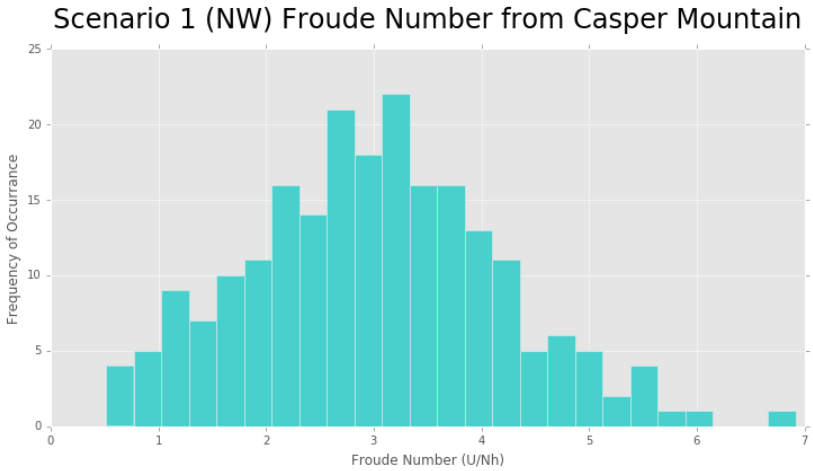

Figure 3.25 Histogram of (modified) Froude numbers calculated between Casper Mountain and the target area (represented by the Reno Hill SNOTEL).

The Froude numbers for the Casper Mountain source location suggests successful mixing and cloud seeding plume delivery from a location near Casper Mountain to Reno Hill (F > 1.0 = unstable). There are 4 storm events with Froude numbers below 1.0, although not below 0.5 (F < 0.5 = stable), which would indicate stronger stability and trouble mixing the seeding plume into the cloud over the target. Figure 3.26 shows the distribution of Froude numbers from near Shirley Basin (northwest of the target) to Reno Hill.

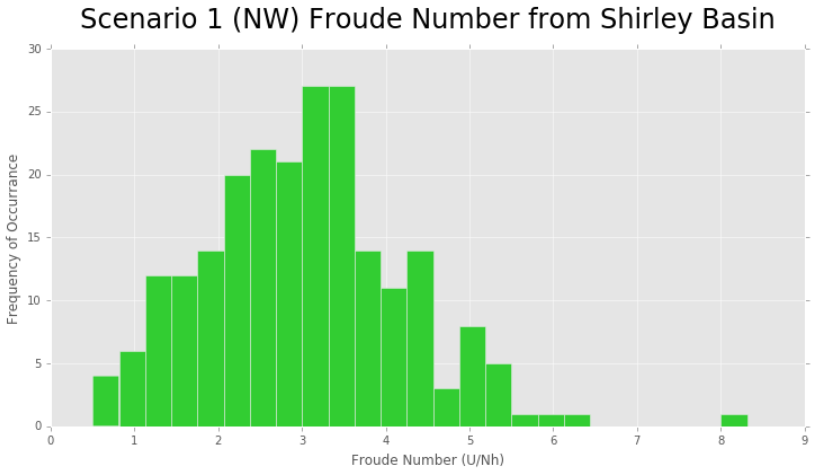

Figure 3.26 Histogram of (modified) Froude numbers calculated between a location near Shirley Basin and the target area (again, represented by the Reno Hill SNOTEL location).

The peak of the distribution for Froude numbers between Shirley Basin (7,200 ft.) and Reno Hill (8,400 ft) is also just above 3.0, indicating instability and successful mixing much of the time. There are only 4 cases of the 229 with Froude numbers below 1.0 from the Shirley Basin source location.

The results of the Froude number analysis suggest that cloud seeding plumes released from generators sited upstream of the target area for the Scenario 1 storms would reach the target area the majority of the time.

3.2.2.2 Scenario 2 Climatology

An additional 97 cases are identified by the Scenario 2 storm criteria, with 700 hPa and surface winds from KCPR from N through E. This represents 21.7% of all 447 cases. Of the Scenario 2 cases, considering temperature criteria alone, 77.3% (75 of the 97 cases) were conducive to ground-based AgI seeding, 85.6% (83 of 97) for aircraft seeding, and 94.9% of scenario 2 cases (92 of 97) for propane seeding. For LP seeding, it is crucial that the generator itself be fully immersed in a SLW cloud. To gain an idea of the likelihood of this occurring in Scenario 2 storms, an additional set of statistics for LP cloud seeding were generated by limiting cases based on the KCPR CB heights. Test one limited the CB heights to 10,000 ft MSL or lower, test two was for CB heights lower than 9,000 ft MSL, and test three for 8,000 ft MSL CB heights.

SCENARIO 2	Cases	% of Scenario 2 Cases
Ground-based AgI (700 hPa -6°C to -16°C)	75	77.32
Aircraft AgI (700 hPa T > -14°C)	83	85.57
Propane (700 hPa -2°C to -16°C))	92	94.85
Propane & (CB < 8000')	38	39.18
Propane & (CB < 9000')	46	47.42
Propane & (CB < 10000')	59	60.82

Table 3.3 Scenario 2 potential seeding methods broken down by number of cases. Compared to total Scenario 2 cases. Propane cases (700 hPa temperatures between -2°C and -16°C) include the cloud base height from KCPR.

Table 3.3 shows the number of potential seeding cases, with LP seeding cases broken down by CB height restrictions, as well as LP cases where just temperature between -16°C and -2°C are included for all CBs. A LP generator at an elevation of 8000 ft. would only be able to seed 38.2% of storms (38 of 92 storms) within the LP temperature thresholds. A LP generator at 9000 ft. could seed 47.4% (46 of 92) of Scenario 2 storms, and if a generator could be placed at 10000 ft, 60.8% (59 of 92) of Scenario 2 storms could be seeded using LP. These KCPR CB values are likely over estimate of the CBs over the upslope side of the Laramie Range, as the CB observation at KCPR is taken on the valley floor (5,300 ft MSL) and away from the orographic influences. During storms, CB heights found on the northeastern slopes of the Laramie Range would likely be lower than the KCPR reported cloud base heights.

Table 3.4 displays the number of maximum potential seeding hours for each seeding method in Scenario 2 storms, including all four LP options: without cloud base restrictions and with cloud bases restricted to below 10,000 ft, 9,000 ft, and 8,000 ft.

SCENARIO 2	Potential Seeding Hours	% of Scenario 2 Storm Hours	Winter Avg. (hrs)
Ground-based AgI	1274	77.17	127.4
Aircraft AgI	1439	87.16	143.9
Propane (all)	1580	95.70	158.0
Propane (< 10000')	1094	66.26	109.4
Propane (< 9000')	866	52.45	86.6
Propane (< 8000')	721	43.67	72.1

Table 3.4 Breakdown of maximum potential seeding hours for each method of seeding in Scenario 2 storms. Compared against total Scenario 2 storm hours. Winter average potential seeding hours also calculated.

The distribution of storm durations from the NE (Figure 3.27) still shows a clear maximum of all day (multi day) storms.

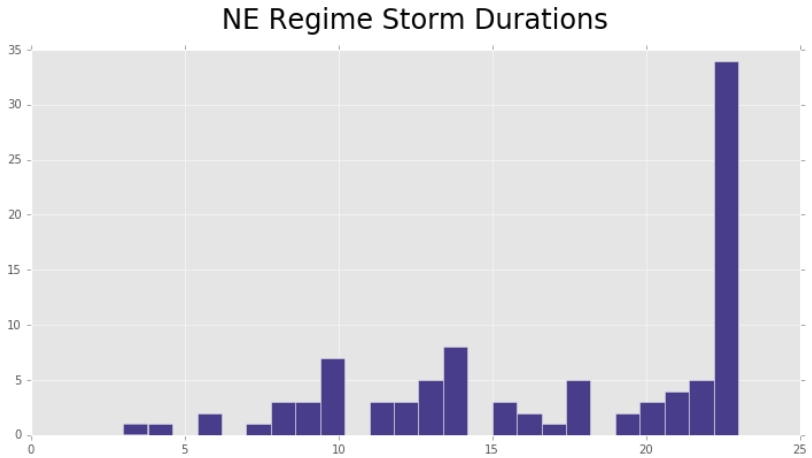

Figure 3.27 Histogram of Scenario 2 storm durations.

The Reno Hill SNOTEL had peak SWE accumulations of 0.2" during most Scenario 2 storms (Figure 3.28). Scenario 2 storms also showed a percentage of storms receiving between 1.0 inch and 3.0 inches of SWE, more than from Scenario 1. This suggests that heavier storms are associated with Scenario 2 weather conditions.

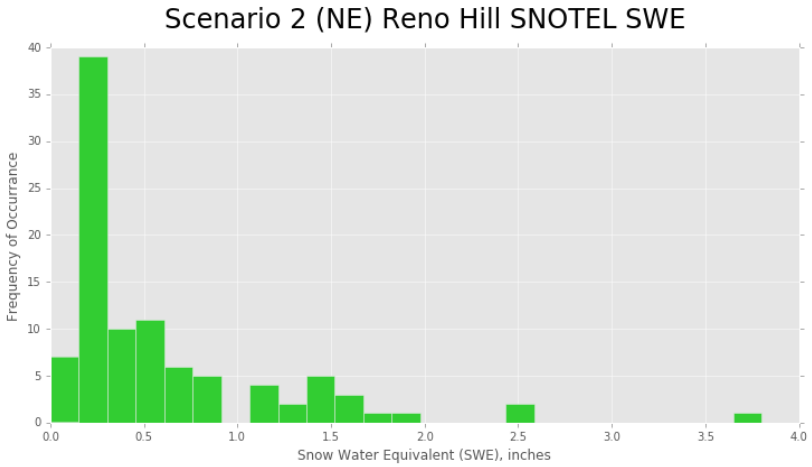

Figure 3.28 Histogram of Scenario 2 Reno Hill Scenario 2 measured SWE values over the ten-year climatology.

While many of the storms received 0.0 inches of SWE at the Laprele Creek SNOTEL, there were more storms receiving larger SWE accumulations, especially relative to Laprele Creek values in Scenario 1 storms (Figure 3.19). Laprele Creek is located further to the east than Reno Hill, which may explain why Laprele Creek also has its (relatively) large storms during Scenario 2 storms (N-NE regime).

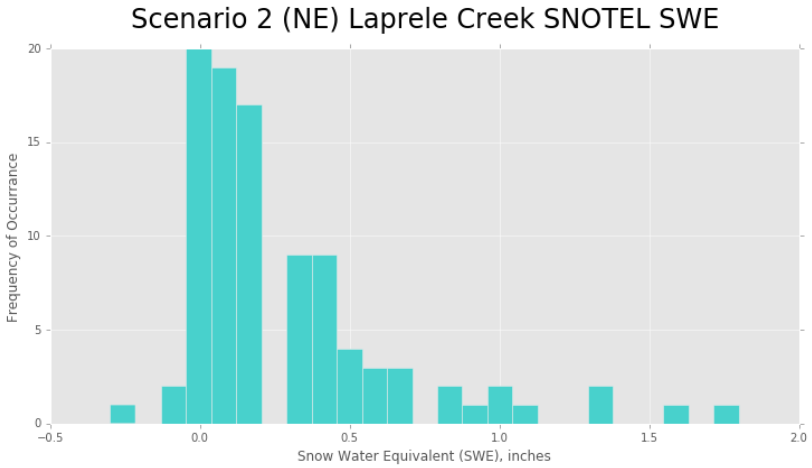

Figure 3.17 Histogram of Scenario 2 Laprele Creek Scenario 2 measured SWE values over the ten-year climatology

Most of the CTTs in Scenario 2 storms are cold (Figure 3.30). This was a similar finding compared to Scenario 1 storms and the overall climatology. The most frequent temperatures were between -40°C and -50°C, and a few cases had CTTs of -20°C. There were 52.6% (51 of 97 cases) of Scenario 2 storms accompanied by icing PIREPS.

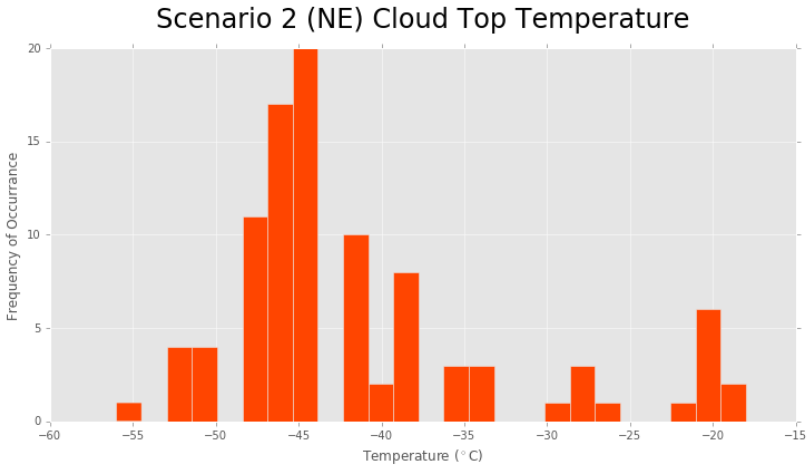

Figure 3.30 Histogram of Scenario 2 CTTs over the Laramie Range.

The KCPR, 20 miles upstream of the target, CB heights in Scenario 2 storms are much lower on average than the CB observed for the Scenario 1 storms (Figure 3.31). The majority of Scenario 2 storm CB heights are below 10,000 ft MSL, with a maximum just above 6,000 ft. MSL.

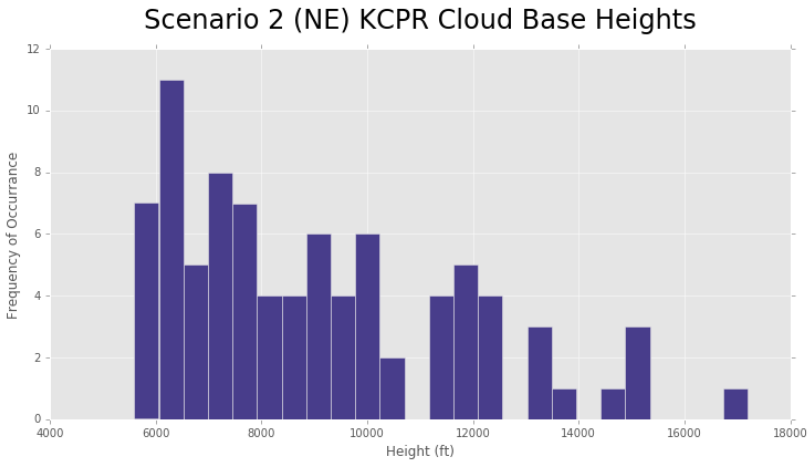

Figure 3.31 Histogram of Scenario 2 storm cloud base heights at KCPR (Casper, WY).

The 700 hPa temperatures in Scenario 2 storms (Figure 3.32) are also a bit colder than those in Scenario 1 storms, with the most frequently occurring 700 hPa temperature at -12°C.

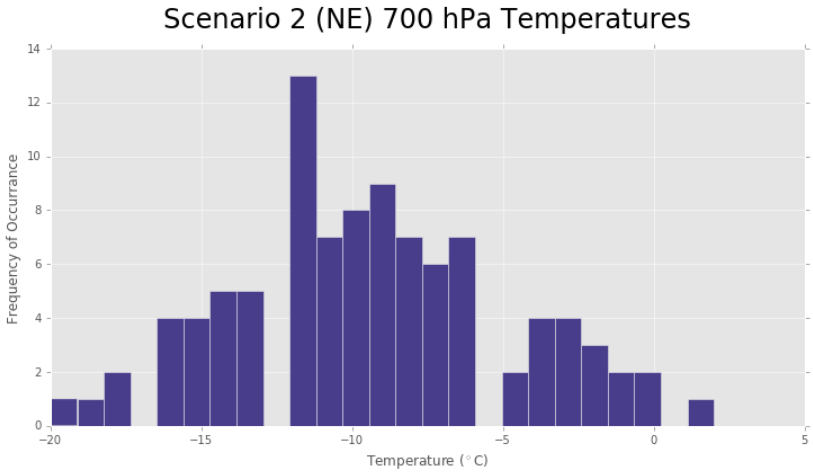

Figure 3.32 Histogram of Scenario 2 storms 700 hPa temperatures.

Wind speeds during Scenario 2 storms (Figure 3.33) are a bit weaker than those in Scenario 1 storms, although both distributions still have their maximum frequency at 30 kts for 700 hPa winds. The majority of Scenario 1 storm winds speeds are between 15 and 40 kts, whereas wind speeds in Scenario 2 storms range between 15 and 30 kts. This suggests that optimal siting of generators would be 10 to 20 miles upstream of the target.

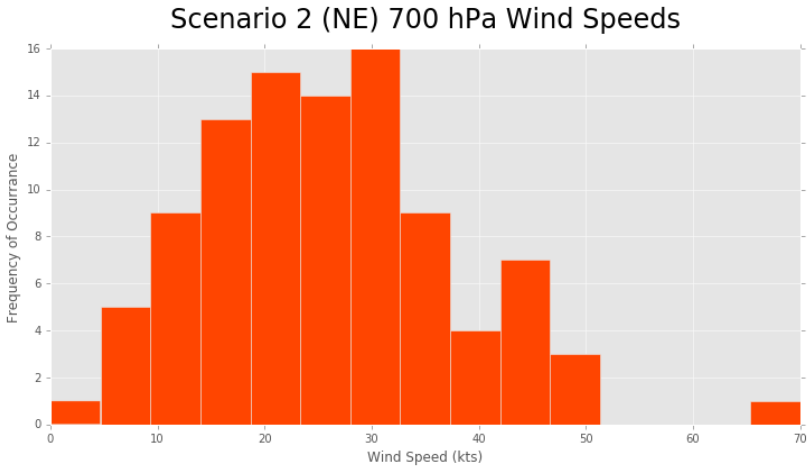

Figure 3.33 Histogram of 700 hPa wind speeds from Scenario 2 storms.

500 hPa winds in Scenario 2 storms (Figure 3.34) vary much more than 500 hPa winds in Scenario 1 storms. An additional difference in the Scenario 2 storm 500 hPa winds is the lack of intensity in speed. This suggests directional shear between 500 hPa and 700 hPa, making planning cloud seeding flight tracks more difficult.

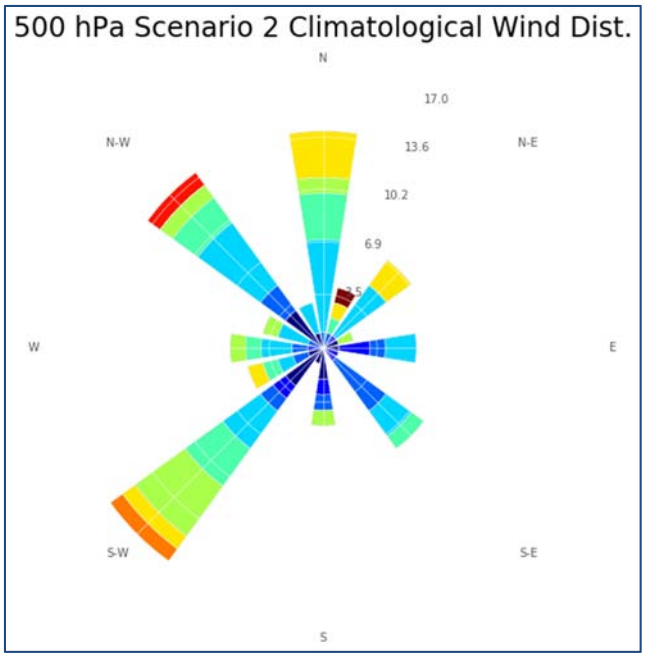

Figure 3.34 Wind rose of 500 hPa winds for Scenario 2 storms (N-E).

The Froude numbers examined for Scenario 2 storms were calculated from Casper Mountain and a location near Glenrock, WY along the North Platt River, to the Reno Hill SNOTEL site. Again, *h* is modified, representing the vertical distance between each of these locations and the Reno Hill SNOTEL site. Figure 3.35 shows the distribution of Froude numbers for Scenario 2 storms from Casper Mountain. Most cases have Froude numbers between 1.25 and 2.0, indicating adequate instability for delivering the cloud seeding plume into clouds

and targeting the high peaks of the Laramie Range. As in Scenario 1 storms, there are not many cases with Froude numbers below 1.0.

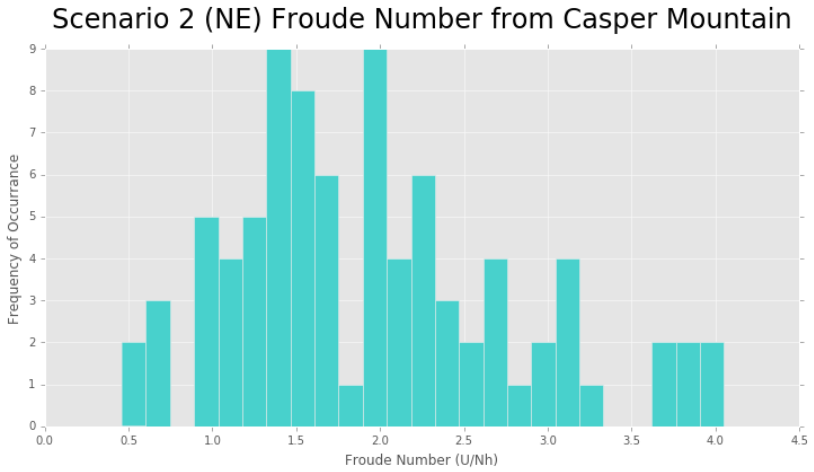

Figure 3.35 Histogram of Scenario 2 storms (modified) Froude numbers, calculated between Casper Mountain and the Reno Hill SNOTEL.

The distribution of Froude numbers from Glenrock up to the Reno Hill SNOTEL site is similar to Casper Mountain in this scenario (Figure 3.36). The maximum in the distribution occurs between about 1.3 and 2.0, and there are few storms with Froude numbers below 1.0.

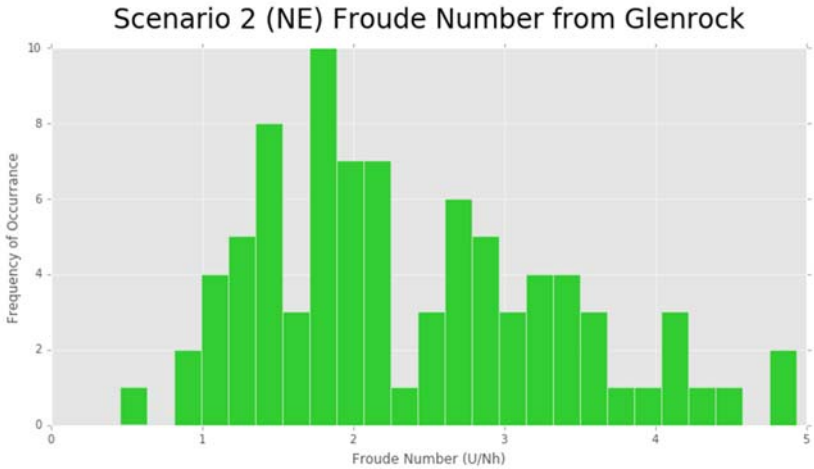

Figure 3.36 Histogram of Scenario 2 storm Froude numbers, calculated between Glenrock and the Reno Hill SNOTEL site.

The relatively unstable environments indicated by Froude numbers above 1.0 are encouraging, and seeding plumes should have little issue mixing into the targeted clouds.

3.2.3 Summary

The total number of storm cases identified in the observed climatology was 447. There were 249 cases categorized as Scenario 1 storms (NW 700 hPa flow), and 97 cases as Scenario 2

storms (N-E flow at 700hPa or at KCPR). . Temperatures were shown to be favorable for cloud seeding for majority of the cases during the "representative time" window. Icing PIREPs were present during 41% of the Scenario 1 storms, and 53% of the Scenario 2 storms, suggesting that SLW was present, and conditions would be suitable for seeding. Wind speeds in majority of the cases ranged from 15 to 40 kts, with only 7% of Scenario 1 storms exceeding 50 kts. Thus siting generators 10 to 25 miles upstream of the target area would deliver the cloud seeding plume to the high peaks of the northern Laramie Range. Cloud base heights evaluated at KCPR were much lower during the Scenario 2 storms, thereby supporting potential cloud seeding using LP generators. In fact, the Scenario 2 storms with the lowest cloud base heights suggested that nearly 40 hours or more of LP seeding would be possible. Based off the results of the observed climatology, aircraft seeding would be more efficient under Scenario 1 due to the higher number of cases that meet the necessary seeding criteria, and the high frequency of consistent northwesterly winds at both 700 hPa and 500 hPa. It is estimated that 30% of Scenario 1 storms are too warm for ground-based operations, but could be seeded by aircraft. The modified calculation of Froude numbers determined from test generator locations to the target area, show that the atmosphere is well-mixed for nearly all storms evaluated.

3.3 WRF Modeling

3.3.1 The Regional Climate Model Simulations

Regional Climate Models (RCMs) can be used in conjunction with reanalysis data or global climate models (~100km) to produce high-resolution numerical simulations (10 km or even 1 km) of the climate over a region of interest. RCMs are becoming important tools in evaluating climate and estimating winter precipitation processes. This is due to their ability to produce high spatial and temporal resolution (~kilometer and sub-hourly, respectively) simulations in areas with complex topography and sparse observational networks (Silverman et al. 2013; Xue et al. 2014). The approach is known as "dynamical downscaling" and uses large-scale atmospheric fields from reanalysis products to explicitly simulate regional and local-scale climate features that are not resolved by large-scale modeling or data observation systems. Dynamical downscaling is an efficient and resource-inexpensive tool that provides accurate climate scenarios on the regional scale.

A fine-resolution RCM simulation based on the WRF (Skamarock and Klemp, 2008; Skamarock et al. 2008) model was developed to produce climatological fields of cloud seeding potential (CSP; "a.k.a. seedability") for the Laramie Range region, and examine the flow regimes leading to a high seedability. These simulations consist of 11 cold season periods (Nov-April) extending from 2005-2015. The model domains consist of 9 km, 3 km, and 1km nested domains with the 3 km grid size domain covering all of Wyoming and the 1 km domain centered over the Laramie Range (Fig. 3.37). All model results shown in this report are for the 1km grid size domain, unless otherwise specified.

We used the best RCM configuration practices for long-term integration, which are recommended to add physical consistency and have been shown to improve RCM skill (Rummukainen 2010; Mearns et al. 2003). The RCM configurations follow the DRI-Regional Climate Modeling (RCM; Dorman at al. 2013) strategies with some modifications outlined below. The selection of model setup was designed through basic and common knowledge of the prevailing physical processes that dominate regional climate variations over Wyoming and the Western United States (Leung et al. 2003; Rasmussen et al. 2011; Liou et al. 2013; Silverman et al. 2013; Zhang et al 2013; Dorman et al. 2013). However, it is well known that the selection of all of optimal parameters and physics configuration within a RCM is a challenging task that depends on many factors, including: the boundary conditions implemented, reanalysis data sets, regional climate and its variability, and simulation grid sizes (Liang et al. 2012; Fernández-González et al. 2015). Controlling and testing all of these and other factors is out of the scope of work, and requires time and resources that were not available for this project. However the modeling configuration used for these simulations were tested and validated and were shown to accurately represent the observed weather conditions.

The RCM was driven by lateral boundary conditions (LBC) throughout the simulation period. Our RCM uses state variables provided by the North American Regional Reanalysis (NARR; Mesinger et al. 2006), while integrating the dynamic equations and physics parameterizations at the interior grids at finer spatial and temporal scales. NARR is produced and recurrently updated by the National Centers for Environmental Prediction (NCEP). The horizontal grid spacing for the NARR data is 32 km, and there are 45 vertical layers. The NARR provides LBC of surface, atmospheric, and soil variables every three hours. The NARR data input includes all available surface and upper-air observations from various national and local networks.

The NARR is currently the best available resource of LBC data as it is dynamically consistent in the atmospheric and hydrologic fields. The NARR has been rigorously evaluated over the Great Plains and Eastern US (Mesinger et al., 2006; Kennedy et al. 2011; Li et al., 2010; Zhong et al. 2012; Walter et al. 2014). Of interest for this study, the evaluation of the NARR at KLBF (the North Platte, NE upper-air balloon radiosone (raob) site) in Walter et al. (2014) shows that the re-analysis system is capable of constraining all the mesoscale structures as observed by the RAOBs. Over the Rockies and over Wyoming, NARR skill to retain the upper-air observed climatological features is more challenging due to scale constrains and the complex orography of the region. We argue that providing adequate large-scale flow conditions, NARR combined with the WRF model, can add value and meaningful small scale and adequate orographic structures. In order to gain additional confidence in the results of the climatology, this study systematically evaluated both NARR data and the WRF model output in an effort to examine the added value skill of this dynamical downscaling work.

RCM simulations are continuous within each cold season, with weak spectral nudging of NARR reanalysis data at upper-levels to preserve large-scale observed/assimilated synoptic patterns (von Storch et al. 2000). Previous studies have shown that weak spectral nudging can yield better synoptic variability, reduce error at the interior or region of interest (e.g., Miguez-Macho et al. 2004; Spero et al. 2014; Bullock et al. 2014; Lo et al. 2008; Bowden et al.

2012), and improve simulation of surface parameters such as precipitation and wind (Omrani et al. 2015). Internally and in the upper troposphere, spectral nudging was implemented to constrain low variability modes. The weak spectral nudging factors were used for temperature, moisture, and wind fields above the planetary boundary layer (PBL). Of note is the use of weak nudging factors towards the moist upper-level fields as suggested by Spero et al. (2014). Spero et al. show that this approach tends to improve representation of precipitation, clouds and surface radiation fields. It has also been shown this nudging approach is expected to reduce the domain location and geometry dependency (Miguez-Macho et al. 2004; Lo et al. 2008); model simulations are also configured to prescribe the reanalysis slow varying parameters within the ground and associated fluxes as assimilated in the 0-1 m soil layers within WRF Land Surface Model (LSM). A summary of the nudging and other model configurations are shown in Table 3.5.

Settings	Domain 1 9 km grid size	Domain 2 3 km grid size	Domain 3 1 km grid size
Horizontal and vertical grid cells	141x131x55	217x187x55	166x157x55
Nudging	3 hourly; no_pbl; wavenumbers x=5 and y=4; nudged parameters u,v,t,q,h (Omrani et al. 2015); nudging coefficients as reported by Spero et al. 2014.	No	No
Deep soil temperature	Updated	Updated	Updated
Slope radiation	On	On	On
Topographic shading	On	On	On
Albedo	Monthly	Monthly	Monthly
Downscaling	One-way	One-way	One-way
Output time increments	hourly	hourly	½ hourly
Time step	54 seconds	9 seconds	3 seconds
Physics Parameterizations:			
Boundary Layer	MYJ (Janjic 1994)	MYJ (Janjic 1994)	MYJ (Janjic 1994)
Cumulus	Explicit	Explicit	Explicit
Microphysics	Thompson (Thompson et al. 2008)	Thompson (Thompson et al. 2008)	Thompson (Thompson et al. 2008)
Land Surface Model	Unified-Noah (Tewari et al. 2004)	Unified-Noah (Tewari et al. 2004)	Unified-Noah (Tewari et al. 2004)
Radiation (SW and LW)	Dudhia (Dudhia 1989) and RRTM (Mlawer et al. 1997)	Dudhia (Dudhia 1989) and RRTM (Mlawer et al. 1997)	Dudhia (Dudhia 1989) and RRTM (Mlawer et al. 1997)

Table 3.5 Model setting for WRF used in this work (climate mode).

Note that the DRI siting design strategies makes use of a Lagrangian modeling framework for plume dispersal that works best when very fine resolution atmospheric simulated output is available (~ 1km; sub-hourly). At the time this project was developed, this level of spatial-temporal resolution was not publicly available for use, therefore DRI elected to develop the model climatology using in-house model runs. Any proposed simulation cannot be considered "deterministic" (Warner 2011), hence, our simulation efforts are to be considered as an attempt to make current modeling frameworks over Wyoming more robust. This strategy addresses some of the internal modeling uncertainty and those derived from the implemented forcing data,

During the preliminary design of the simulations, we tested the effect of the initial conditions by changing the length of the spin-up period using 12-month, 6-month, 3-month, and 1-month spin-ups. Our results indicated that a 1-month (Oct 1-31; only tested for 2005) spin-up was enough to reach an equilibrium state in the downscaling of surface atmospheric boundary layer parameters. We believe this relatively short spin-up is likely due to the dry state of the soil during this time of the year (the beginning of the water year) and semi-arid climate. Also, this could be due to the coarser domain being relatively small (~1000 km), yet retaining the synoptic variability variance as observed by NARR. However, we only tested the sensitivity of the spin-up period for the cold season 2005. A rigorous evaluation of the effect of initial conditions for each year is recommended as wet/dry anomalous warm season states can have significant effects on the equilibrium states within the WRF-LSM (Yang et al. 2011). During the course of the RCM simulations, each cold season simulation was run separately allowing for the optimal scalability of DRI's high-performance computing system.

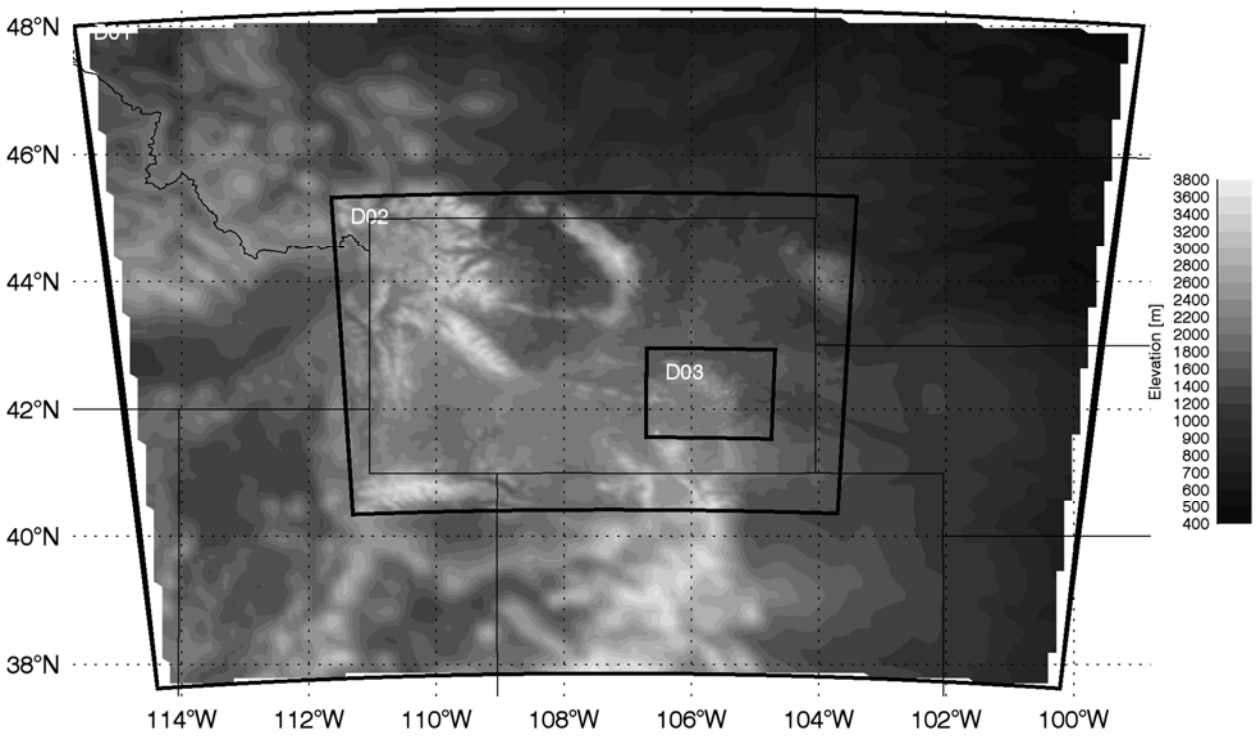

Figure 3.37 DRI-RCM model nested domains using D01=9km, D02=3km, and D03=1km (grid sizes). Shaded contours correspond to the terrain elevation using the actual domain resolution.

3.3.2 Model Climatology Results

In this study, we define the Cloud Seeding Potential (CSP) using a simple approach that estimates the frequency of supercooled liquid water hydrometeors (cloud, rain, or both) using modeled meteorological conditions. Our approach is performed by a locally defined index that finds windows of opportunity meeting the following seedability criteria for two different seeding agents:

- for AgI
  - If -6°C < T(t ,x, y, p) < -18°C and $Q_{liquid} \geq 0.001$g/kg, then, $CSP_{AgI}(t, x, y, p) = 1$, else, $CSP_{AgI}(t, x, y, p) = 0$,

- for LP
  - If -2°C < T(t ,x, y, p) < -18°C and $Q_{liquid} \geq 0.001$g/kg, then, $CSP_{LP}(t, x, y, p) = 1$, else, $CSP_{LP}(t ,x, y, p) = 0$,

where t is the model output time increments (30 min for the 1-km Laramie Range WRF runs), T is the temperature field in the three-dimensional space (x: east-west direction, y: north-south, p: pressure as the vertical coordinate), and Q_{liquid} is liquid water defined as $Q_{liquid}=Q_{cloud}+Q_{rain}$. Of note is that our approach contrasts from Ritzman et al. (2015), who defined seedability over the Sierra Madre and Medicine Bow Mountains using modeled non-local, upstream conditions (700-hPa temperatures ≤−8°C, 700-hPa winds between 210° and 315°, and the presence of supercooled liquid water upstream the target area). Compared to Ritzman et al., our CSP local definition is less aggregated, as a seedable condition is defined per pixel, per time (e.g., 1 km grid size, every 30min, during 11 cold season/years). Our local definition of CSP takes advantage of the fine scale of the model, as it resolves clouds explicitly.

Additionally, our approach enables us to derive the flow pathways around complex terrain from and into the target seedable clouds (or those meeting the CSP condition) by using a forward and backward Lagrangian approach. This is presented in the Section 5

3.3.2.1 Decade-long Mean Cloud Seeding Potential

Figure 3.38 shows the horizontal projection of maximum WRF AgI CSP frequencies during 11 cold season periods (Nov-April) extending from 2005 through 2015. The left panel covers the entire state of Wyoming at the 3 km grid size model domain and the right panel covers the Laramie Range at the 1 km grid size model domain. The target area over the higher terrain in the Laramie Range suggests that AgI cloud seeding opportunities are present up to 10% of the time. In addition it can be clearly seen that the CSP opportunities are enhanced as orographic lifting near the mountains amplifies the SLW cloud occurrences.

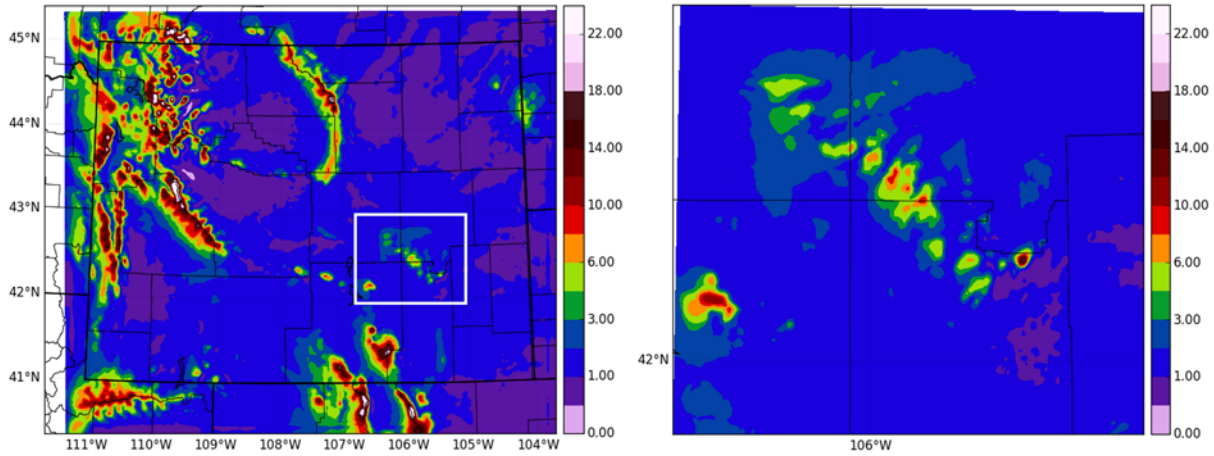

Figure 3.38 Horizontal projection of the percent of time when AgI cloud seeding potential is present in the column over the WRF 11-year climatology. 3 km domain on left and 1 km domain over the northern Laramie Range (white box) on right.

The vertical structure of the mean AgI cloud seeding potential at both 3-km and 1-km is presented in Figure 3.39. The enhanced SLW is clearly observed in the higher resolution domain. The results suggest that most of the cloud seeding opportunities are below 3,500 m. Validation of this field is difficult due to the lack of direct or indirect observations of cloud microphysical properties in the region. We are not certain about the model skill in representing such CSP spatial patterns. However, when comparing model data to observations of cloud particles, other studies have shown that finer grid sizes from 3 km to 1 km or finer can led to significantly improved simulations of cloud liquid water content due to better-resolved terrain features (Nygaard et al. 2011).

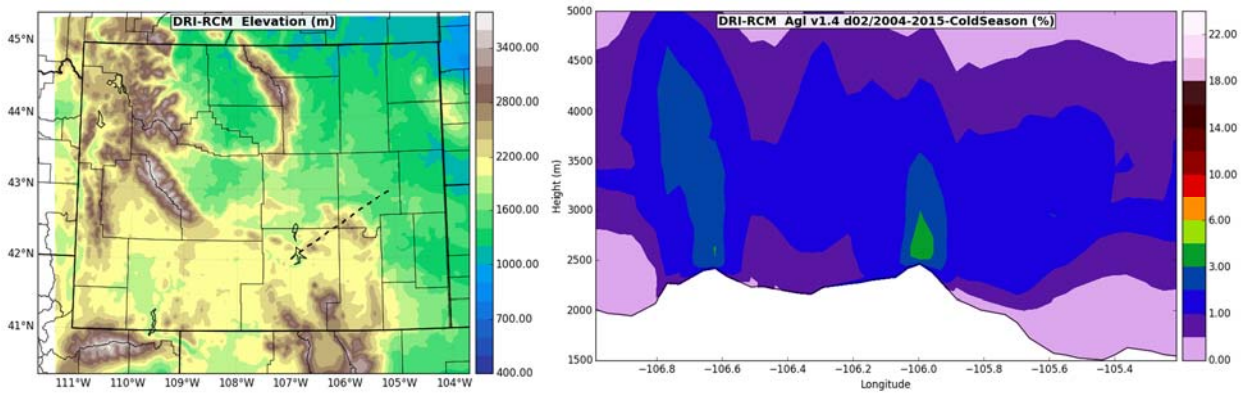

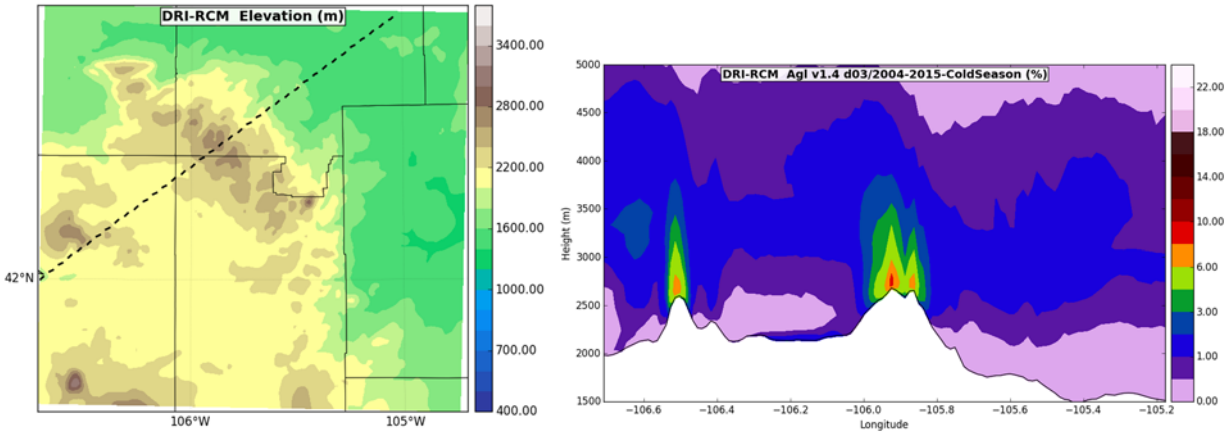

Figure 3.39 Vertical cross-section at 3-km (top) and at 1-km (bottom) for of the percent of time when AgI cloud seeding potential is present in the column over the WRF 11-year climatology.

As expected, when the winter CSP_{LP} frequencies across the 11-year WRF 1 km climatology are plotted (Fig. 3.40) slightly more opportunities for seeding are present. This is obviously due to the 4°C larger temperature range. The CSP_{LP} frequencies are 3 to 4% greater than the CSP_{AgI} frequencies, with values in the core of the range reaching 10% over the highest peaks for CSP_{AgI} and 14% for CSP_{LP}. Even though the CSP_{LP} shows more windows of opportunity for seeding operations, propane generator siting is more challenging since the LP generators need to reside in the cloud and the new ice nucleated crystals must remain in cloud until precipitation sized particles are formed. Due to this constrain, generation siting and efficiencies using Lagrangian trajectories (Section 5) are only performed using CSP_{AgI} thresholds. The results from the observed climatology suggests that LP cloud seeding may be possible for up to 72-hours per year on average

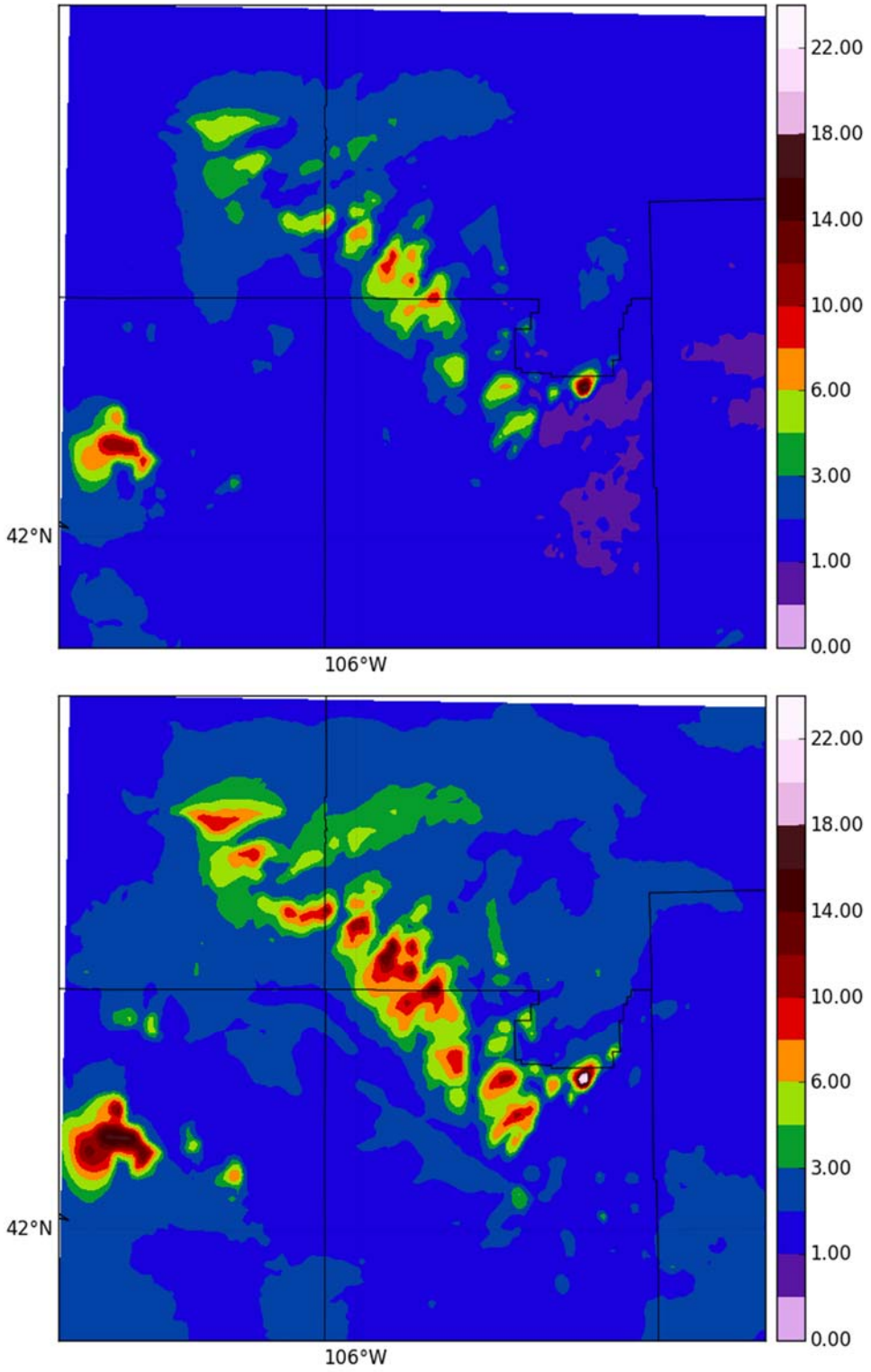

Figure 3.40 Horizontal projection of the maximum percent of time when AgI (top) and LP (bottom) cloud seeding potential is present in the column.

The predominant wind directions were estimated during CSP occurrences. For each CSP event (CSP_{AgI} = 1 or CSP_{LP} =1) horizontal wind vectors were composited and averaged in the vertical as shown in Figure 3.41. During the cold season, westerly flow dominates the entire state of Wyoming at CSP levels, while over the Laramie Range, the wind composites show a west-northwesterly flow with a wind component crossing over the mountains. Note that these wind composites provide a broad view of the mid-to-low level synoptic flow patterns responsible for CSP occurrences. Since most of the CSP occurrences are forced by the terrain, the wind barbs only represent the horizontal wind direction at the CSP level and do not necessarily represent the upstream/downstream trajectories of the flow near the surface. Overall the higher western slopes and peaks of the Laramie Range show more seeding opportunities than the eastern slopes, which aligns with the observed climatology.

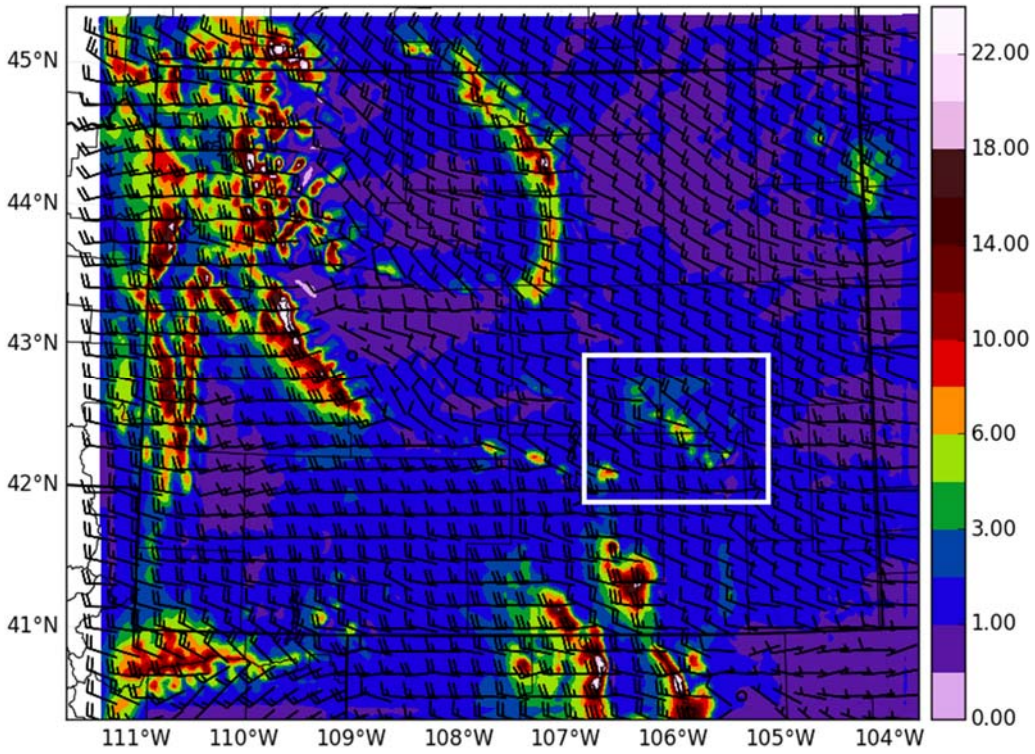

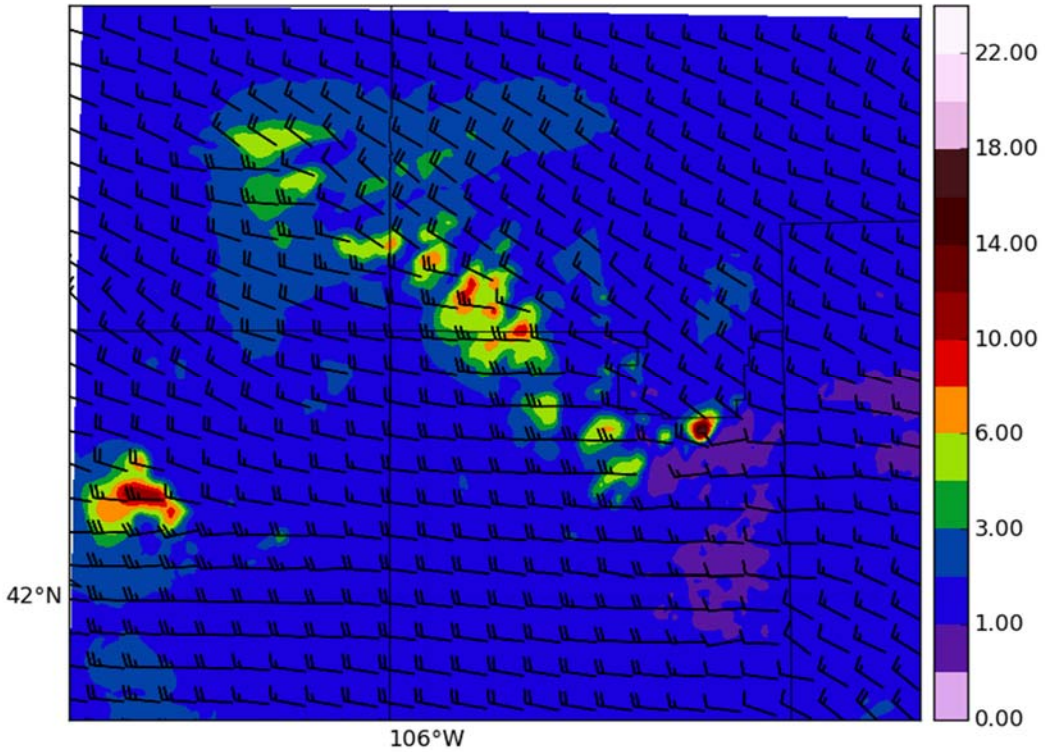

Figure 3.41 The mean AgI Cloud Seeding Potential (CSP_{AgI}; filled contours) frequency of opportunities (% of total simulation period) estimated over the state of Wyoming domain (3 km grid size; top panel) and Laramie Range (1 km grid size; lower panel) during 11 cold season periods (Nov-April) extending 2005-2015. Wind barbs indicate the mean flow patterns at the CSP levels. To avoid cluttering, barbs are plotted only every 6 grid points and using the regular meteorology chart convection: a circle for wind < 2.5 knots, half barb = 5 knots, full barb = 10 knots.

3.3.2.2 Seasonality

Flow regimes are seasonally dependent and are worth examining as they can influence siting and generator operations. Figure 3.42 shows monthly mean CSP fields ("seeding opportunities") and their related winds for February and April 2012. During February, the wind pattern showed a stronger northwesterly flow regime creating more CSP opportunities than during weaker northerly winds that occurred in April. Note the increased CSP over the eastern slopes in April 2012.

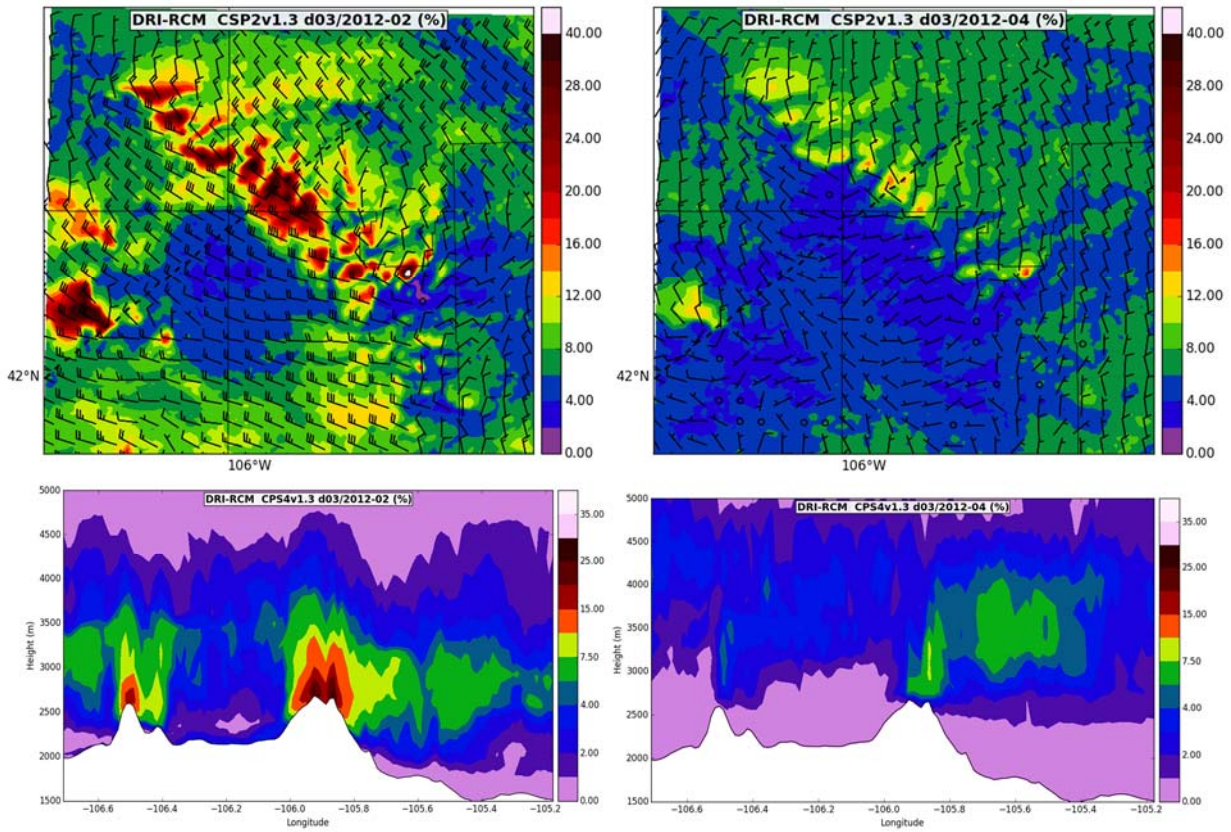

Figure 3.42 The mean AgI Cloud Seeding Potential (CSP; % of time) and predominant flow for February 2012 (upper left panel) and April 2012 (upper right panel). To avoid cluttering, barbs are plotted only every 6 grid points. Barbs use the regular meteorology chart convection: a circle for wind < 2.5 knots, half barb = 5 knots, full barb = 10 knots. Vertical cross-section of the mean AgI Cloud Seeding Potential for February 2012 (bottom left panel) and April 2012 (bottom right panel).

Figure 3.43 shows the monthly mean CSP from the 1 km WRF climatology near Buffalo Peak with an estimated average mid-winter maximum of 8.5% of the time for AgI and 11.5% for LP, which is equivalent to 57 and 77 potential seeding hours, respectively. Average AgI seeding opportunities drop to about 4-5% of the time (28-36 hours) in the late fall and spring. Figure 3.44 shows the monthly seeding opportunities highlighting a considerable year-to-year variability in CSP with AgI long-term mean of 6.3% 3.27% standard deviation. The results suggest that mid-range forecasting products providing intraseasonal storminess and related flow regimes can provide valuable information in the seeding generator operation.

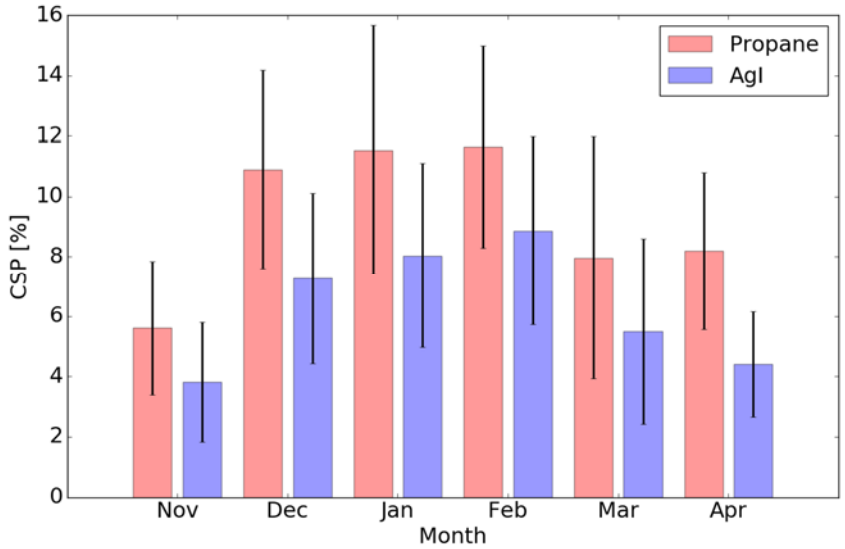

Figure 3.43 Monthly mean Cloud Seeding Potential (CSP; % of time in the month) mean (bars) and standard deviation range (error bars) for AgI and liquid propane seeding frequencies over the Laramie Range. Statistic estimates retrieved from corresponding CSP values averaged over the circumference with center point near Buffalo Peak (42.50°N, 105.89°W) and radius of 8km for 11 cold season periods (Nov-April) extending 2005-2015.

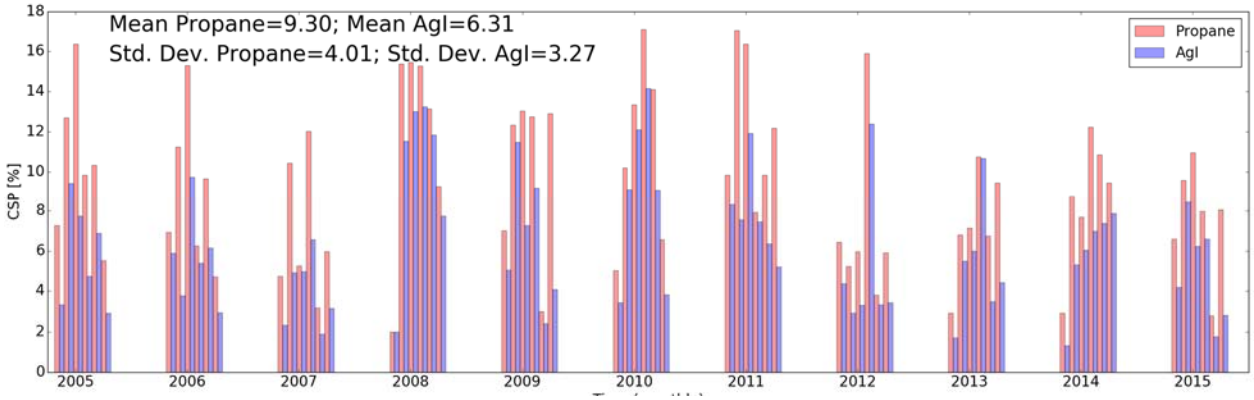

Figure 3.44 Monthly Cloud Seeding Potential (CSP; % of time in the month) for AgI and liquid propane over the Laramie Range. Statistic estimates retrieved from corresponding CSP values averaged over the circumference with center point near Buffalo Peak (42.50°N, 105.89°W) and radius of 8km.

3.3.2.3 Model Potential Precipitation Augmentation

Previous research studies, including the WWMPP, have estimated the average potential precipitation augmentation from cloud seeding strategies at about 10% of total precipitation (American Meteorological Society 1998; Hunter 2006). Arguably, this value provides an upper end limit as not all winter precipitation is produced by candidate "seedable" storms. Ritzman et al. (2015) performed a more detailed analysis using model output to estimate the fraction of precipitation that falls during seedable opportunities. The results for their study showed that 27%-30% of the precipitation events were seedable. In this study, we used our locally-defined CSP approach to estimate the precipitation accumulations that fell up to 1 hour after each CSP event occurred. We also estimated the amount of precipitation that fell during non-CSP events. To apply this approach, we assumed that precipitation is originated

in the same column where the one of the CSP is categorized as seedable. This could be a strong limitation as vertical and horizontal advection can displace the glaciated particles from where the nucleation took place.

Figure 3.45 shows the model total cold season (Nov-April; 2004-2015) precipitation accumulation and the precipitation accumulated during the CSP_{AgI} and CSP_{LP} windows of opportunity over the Laramie Range (d03 = 1km grid size domain). The smoother seasonal precipitation contrasts the sharper, and more topographically defined CSP-related precipitation estimates. This is not surprising as our approach was based on relatively fine scale grid sizes (1 km) and the CSP was designed to capture local 'seedable' conditions that are enhanced by orographic forcing.

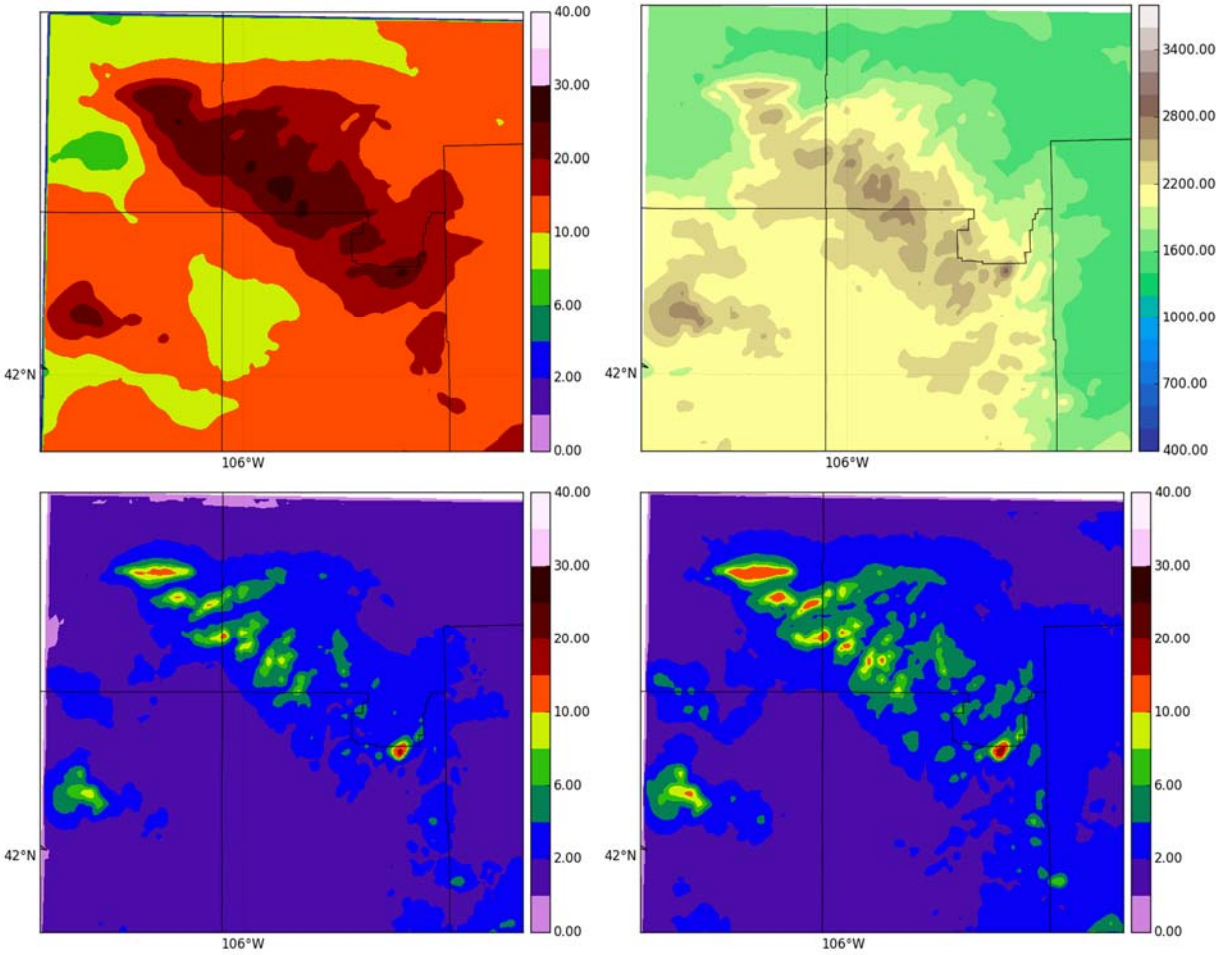

Figure 3.45 Total precipitation accumulated during 11 cold season periods (Nov-April) extending 2005-2015 (in; upper left panel), digital elevation WRF model (m_MSL; upper right panel), total precipitation during CSP_{AgI} and $CSP_{propane}$ clouds (in; bottom left and right panels, respectively).

The ratio of CSP-related precipitation and total cold season precipitation defines the proportion of precipitation that can potentially be seeded (Fig. 3.46). This ratio can be factored by the potential precipitation augmentation of 10% to obtain a first guess water yield, assuming that all windows of opportunities are seeded. Note that over the Laramie

Range peaks, and the northern end of the target the proportion of CSP-related precipitation can reach up 60-70%, perhaps yielding nearly ~7% of the total precipitation. Away from the peaks, CSP-related precipitation drops rapidly to values below 4-5%, yielding less than 0.5% of the total precipitation.

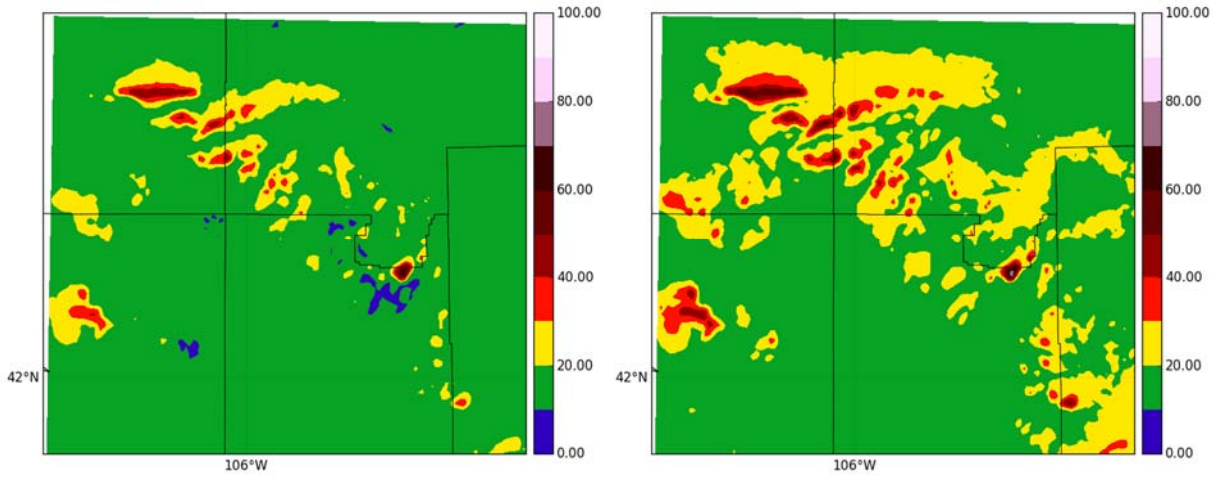

Figure 3.46 The ratio of CSP_{AgI} (left) and $CSP_{propane}$ (right) opportunities to total precipitation.

Figure 3.47 shows the fraction of CSP events related to non-precipitating clouds (e.g. precipitation values < 0.001 in). Overall, the model results indicate that nearly all CSP-related events are related to precipitation accumulations of any kind at the ground.

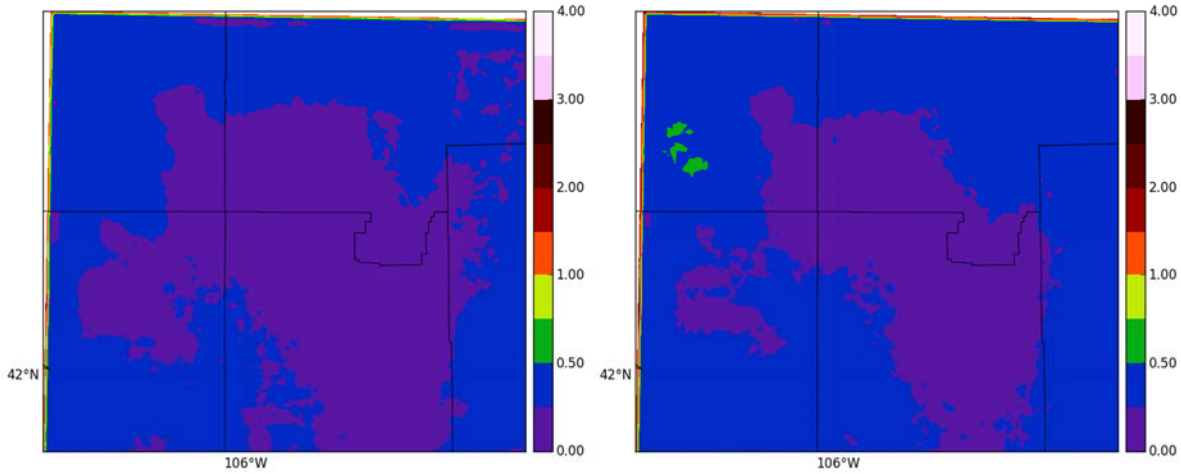

Figure 3.47 Proportion of events meeting CSP_{AgI} (left) and $CSP_{propane}$ (right) criteria without any trace of precipitation accumulation at the ground.

3.3.2.4 Summary

The model climatology closely matches the results of the observational climatology. The highest frequency of seedable storms occurs under northwesterly flow with a secondary maximum occurring under northeasterly flow. Most of the seeding opportunities are found below 12,000 ft MSL. The average mid-winter frequency of AgI cloud seeding opportunities is ~54 hour per month, with an additional ~27 hours per month possible in spring and fall. The seeding opportunities are tied to areas of highest terrain and decrease quickly away

from the peak. Annual precipitation increases up to 7% may be realized over the peaks, were an average of 15" to 20" of SWE was annually observed.

3.4 Model Evaluations

3.4.1 Upper-Air Regional Climate Model (RCM) Performance

Evaluation of the model increases confidence in the results of the climatology and is often done as part of a RCM. The NARR was evaluated and the model's ability to retain the mean large-scale flow and synoptic variability assessed. This was achieved by evaluating the reanalysis (NARR) and the RCM output against upper-air in-situ observations. Tropospheric parameters from NARR data are typically adequately constrained by the *in-situ* upper-air observations. However, long-term integration studies over the Western U.S. have shown that part of the errors exhibited by WRF upper-air simulated output can be inherited from NARR data around the lateral boundary conditions [e.g., Castro et al. 2005; Brands et al. 2012]. Brands et al. (2012) highlighted that this is particularly the case for the moist parameters (e.g., specific humidity) as their statistics tend to differ from the observations. Additionally, previous studies have shown that the model adds uncertainty and tends to degrade and drift towards its own climatology (Leung et al. 2003). Therefore, a comprehensive evaluation of the WRF, relative to NARR, and constrained by the observations, is then necessary to assess overall model's uncertainty.

The vertical resolution of a radiosonde sounding varies from one observation to another and with the different segments of the rawinsonde record, including changes in technology (Walters et al. 2014), whereas the vertical resolution for WRF output archive is based on 55 exponentially distributed vertical sigma levels from sigma=1 close to the terrain to the top level of the model at 50 hPa). For fairness in the model evaluation, we only retrieved simulated upper-level data at times (typically at 00 and 12 UTC) and levels (mandatory and additional levels) that were observed. Note that this is only possible because the model is forced with "observed" boundary conditions from NARR. All interpolation requirements were performed using the height as the vertical coordinate. No homogenization technique was performed on the upper-air data, which is often needed when technology changes can alter the observational uncertainty (McCarthy et al. 2009).

The RCM simulations successfully produce the observed vertical structure of temperature, specific humidity, zonal and meridional winds as indicated by different distance metrics such as bias and root-mean-square-error regardless of the domain evaluated. The agreement between the simulations and the NARR at Riverton, WY (KRIW) is better for temperature fields and errors are larger for specific humidity and wind components (See Figure 3.48 and 3.49). In the upper-tropospheric median temperature biases are small and well within the observational uncertainty (Philipona et al. 2013). However near the surface, the model shows a warm systematic bias over all evaluated sites (not shown). In general the spread of the bias is smaller at the mid-levels gradually increasing at the lower-tropospheric levels. The lack of nudging on the PBL, the uncertainty added by the Land Surface Model, and the

complex topography seems to affect the model skill at these levels. Similar difference patterns are observed for North Platte, NE (KLBF), Rapid City, SD (KUNR), and Denver, CO (KDNR). Overall, the RCM correctly simulate the large-scale flow distribution at mid- and upper-levels. This is not surprising, for two reasons, first, the model domain is relatively small when compared to the characteristic scales dominating the flow dynamics in the region, and secondly, the interior nudging has been implemented above the boundary layer for our simulations. One remarkable feature from Figs 3.48 and 3.49 is that error is growing (Table 3.6), but retaining similar vertical distribution over the upper atmosphere. In general, the model adequately simulated the median and flow variation statistics (as shown by the high correlation of the pairs and the range of variability at different percentiles at upper-levels), which is consistent for all the RAOBs sites evaluated. Although there are not RAOBS sites within the 1 km domain (D03), we believe that biases have a similar structure around and over Laramie Range.

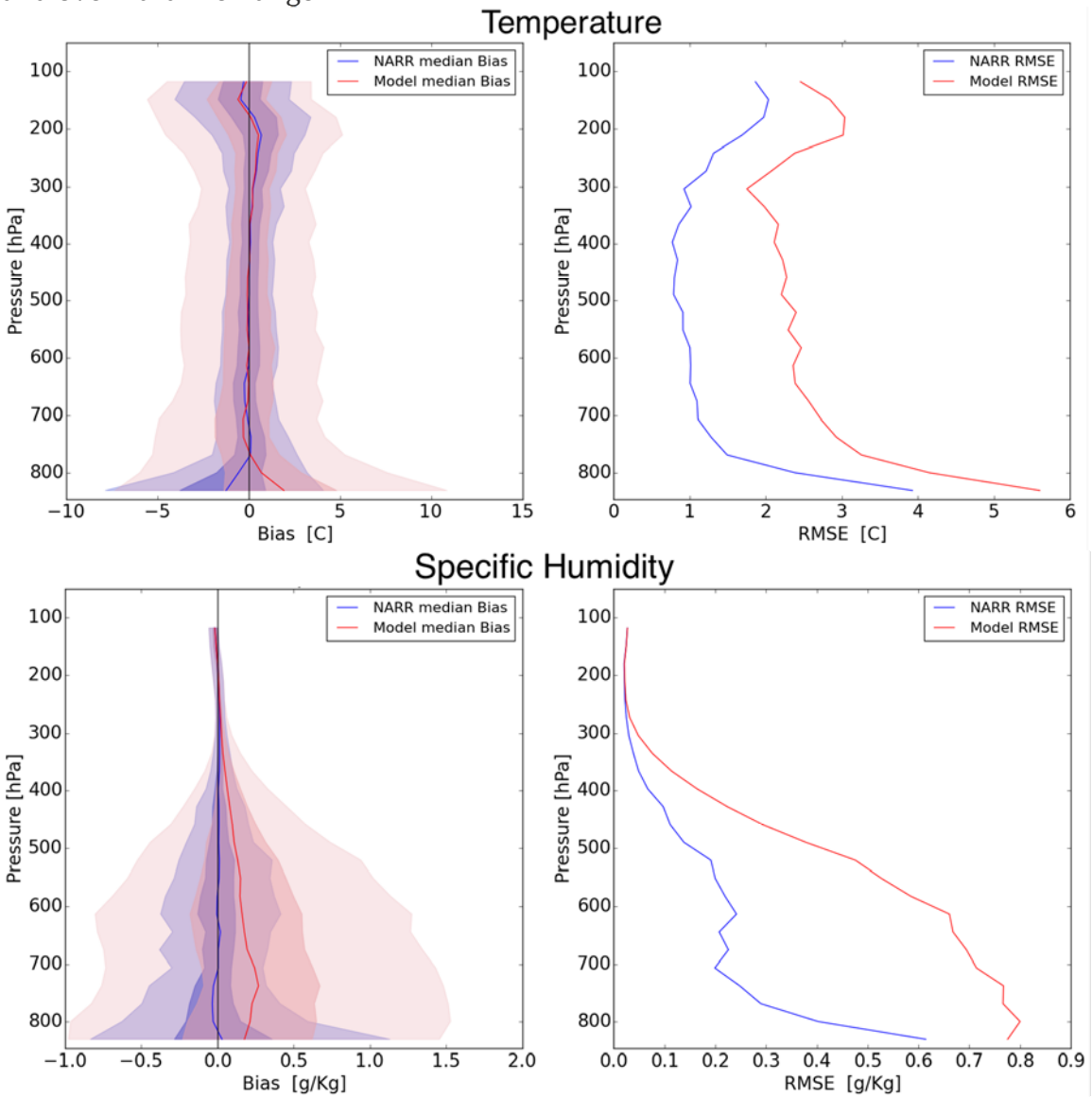

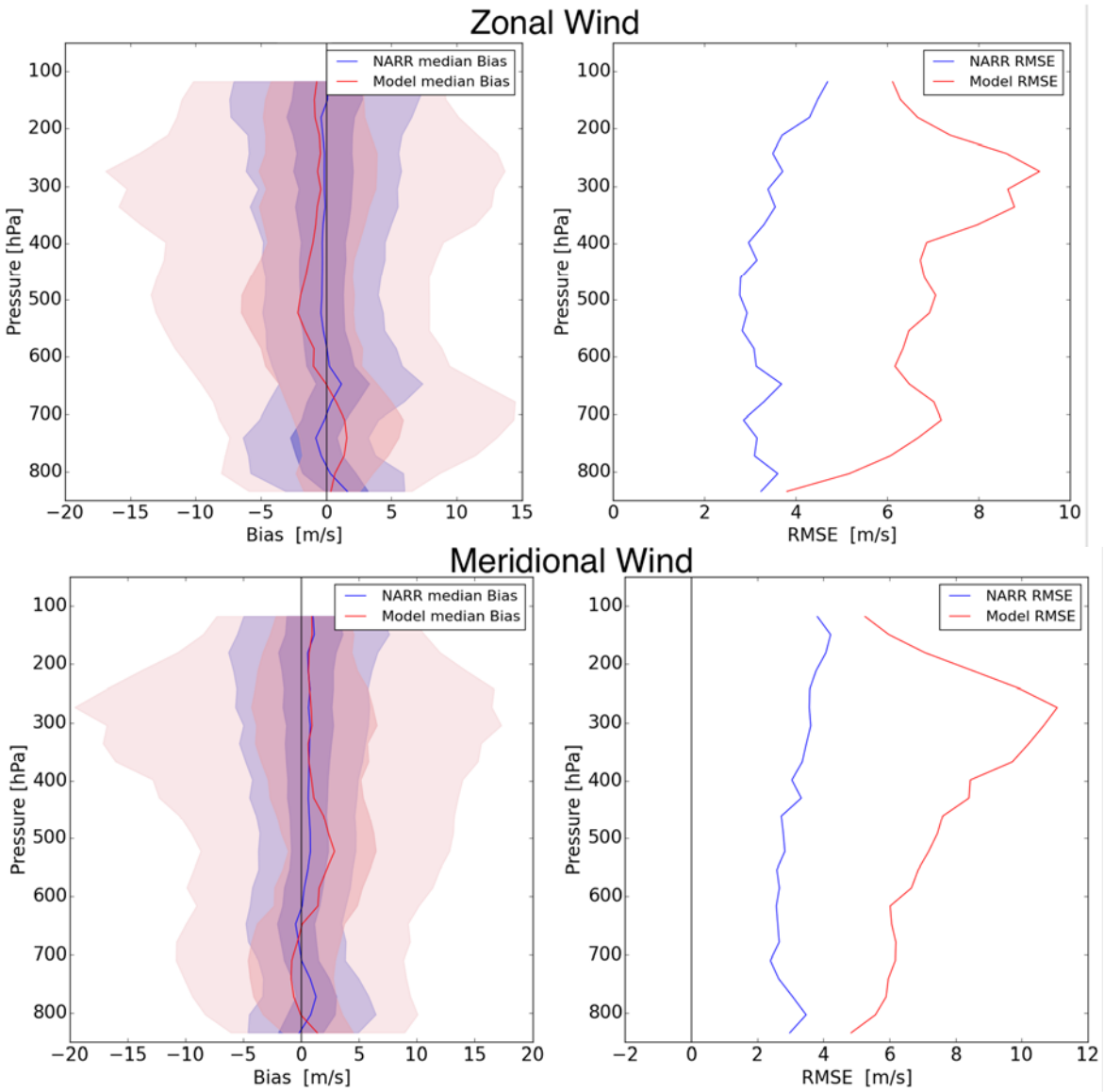

Figure 3.48 NARR and 9km (D01) model upper-air bias distribution (left) and root mean square error (RMSE: right) at the Riverton, WY (KRIW) raob site (top to bottom panels) for temperature (T; C). specific humidity (Q: g/kg), and zonal (Uma/sec) and meridonal (V: m/sec) win components during the 2004-2015 cold seasons (Nov _April). Bias distribution is shown by the median (solid lines), interquartile range (dark shades), and the 5th and 95th percentile range (light shades).

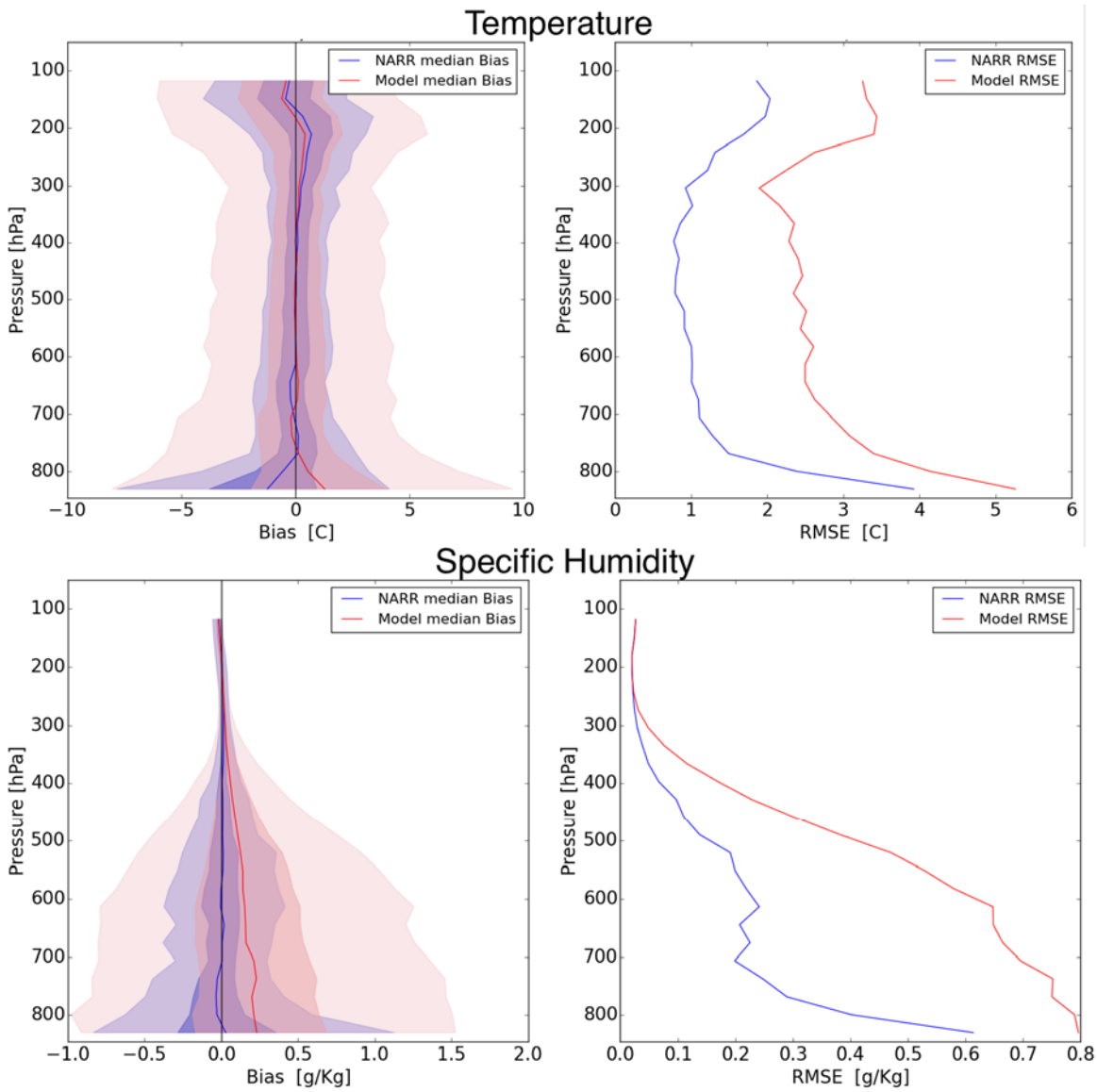
Temperature
NARR median Bias
Model median Bias
Pressure [hPa]
Bias [C]
NARR RMSE
Model RMSE
RMSE [C]
Specific Humidity
NARR median Bias
Model median Bias
Pressure [hPa]
Bias [g/Kg]
NARR RMSE
Model RMSE
RMSE [g/Kg]

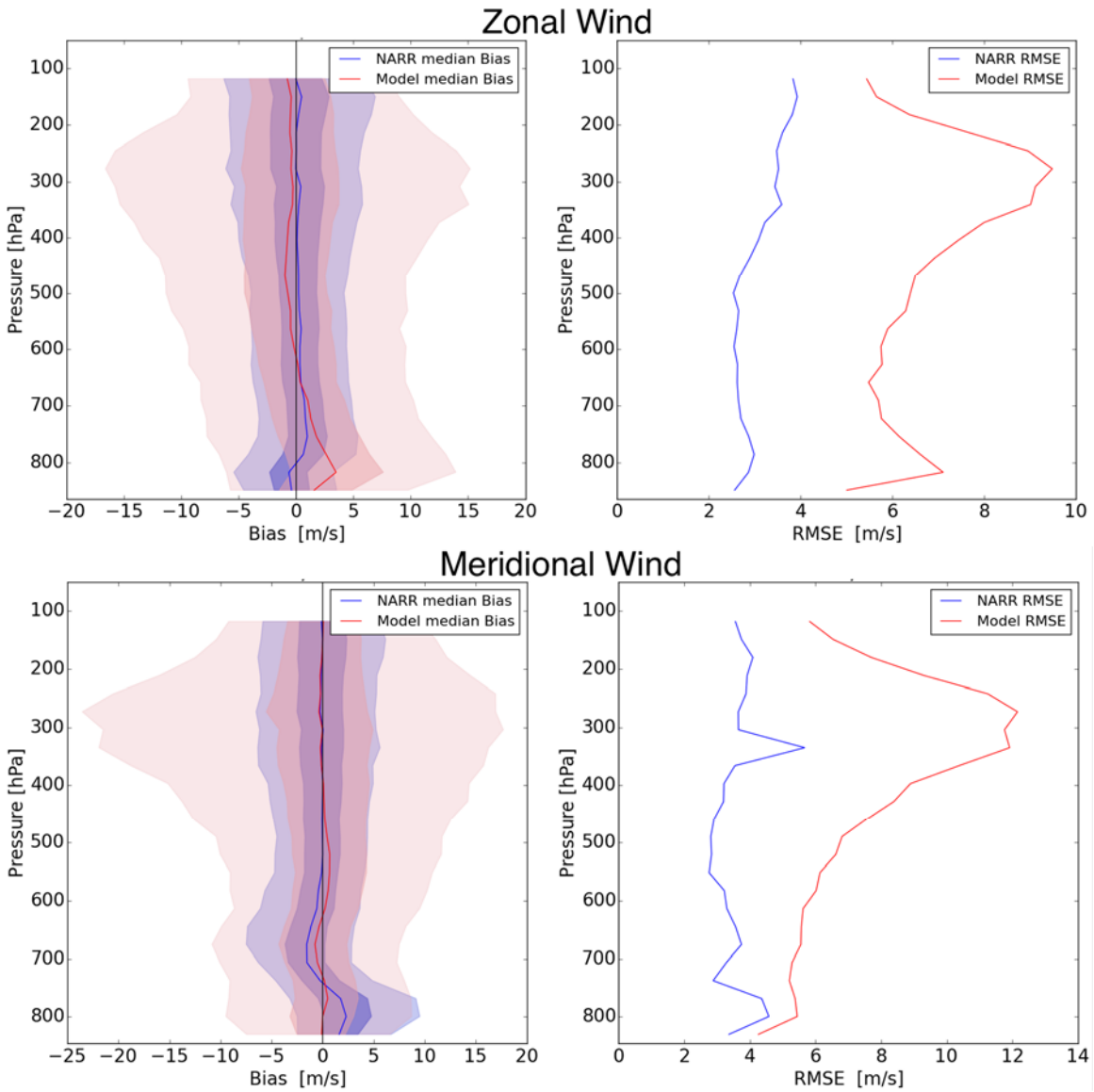

Figure 3.49 As in Fig 3.48 except for the 3-km domain (D02).

Sounding Site	Reanalysis/ Downscaling	T	Q	U	V
RIW D02	NARR	0.99	0.96	0.92	0.92
	Model (3km)	0.98	0.84	0.71	0.69
UNR D02	NARR	0.99	0.97	0.93	0.94
	Model (3km)	0.98	0.79	0.71	0.7
LBF DO1	NARR	0.99	0.96	0.93	0.94
	Model (3km)	0.98	0.8	0.77	0.69
DNR D01	NARR	0.99	0.95	0.92	0.93
	Model (3km)	0.98	0.82	0.74	0.71

Table 3.6 Pearson correlation estimates between the contemporaneous pairs of NARR and observations and the model and observations. Evaluated parameters are: T, Q, U, V during the 2004-2015 cold seasons (Nov – April). See Fig 3.37 for domains. Model output is evaluated only for the domain with the finest grid size available at the sounding location (D01=9km, D02=3km).

The model performance in simulating the wind field has less skill relative to temperature and specific humidity and shows similar performance when comparing the downscaled winds from NARR to D01 and D02 (see Fig 3.37). Notwithstanding is that the lower-atmosphere shows some significant/systematic median biases. Regionally, however, the biases vary with location and have a tendency to grow downstream (west-northwesterly flow; not shown), resulting likely from a systematic distortion of the large-scale circulation (i.e., synoptic wave trains) that crossed Rocky Mountains over the coarser domain. The RCM surface wind speeds show relatively small biases when compared to long-term climatological means derived directly from observations, or from NARR. These biases can be attributed to aspects of the parameterization of unresolved orography and surface roughness.

A striking feature in our model results is the lower troposphere wet bias exhibited in all the evaluated soundings over all the evaluated sites (Fig 3.50) We highlight that this biases are rather large (1-2g/kg) and larger than the reported operational biases (McCarthy et al. 2009). The observation of water vapor in the atmosphere is an inherently difficult measurement. Note that absolute specific humidity values decrease by orders of magnitude as one ascends from the surface to the upper troposphere. This has limited our ability to detect emerging meaningful biases within the model. In a similar situation, Bullock et al. (2014) suggested that their model setup, based on the WRF model, may have had an unbalanced hydrologic cycle that was returning moisture from land to the atmosphere too quickly. We have not shown any additional sources of moisture in the model, and which model component is to blame (e.g., land surface model or PBL). Other modeling studies reported systematic model deficiencies in the model moist parameters without providing any conclusive evidence of such error sources (Leung et al. 2003; Katragkou et al. 2015).

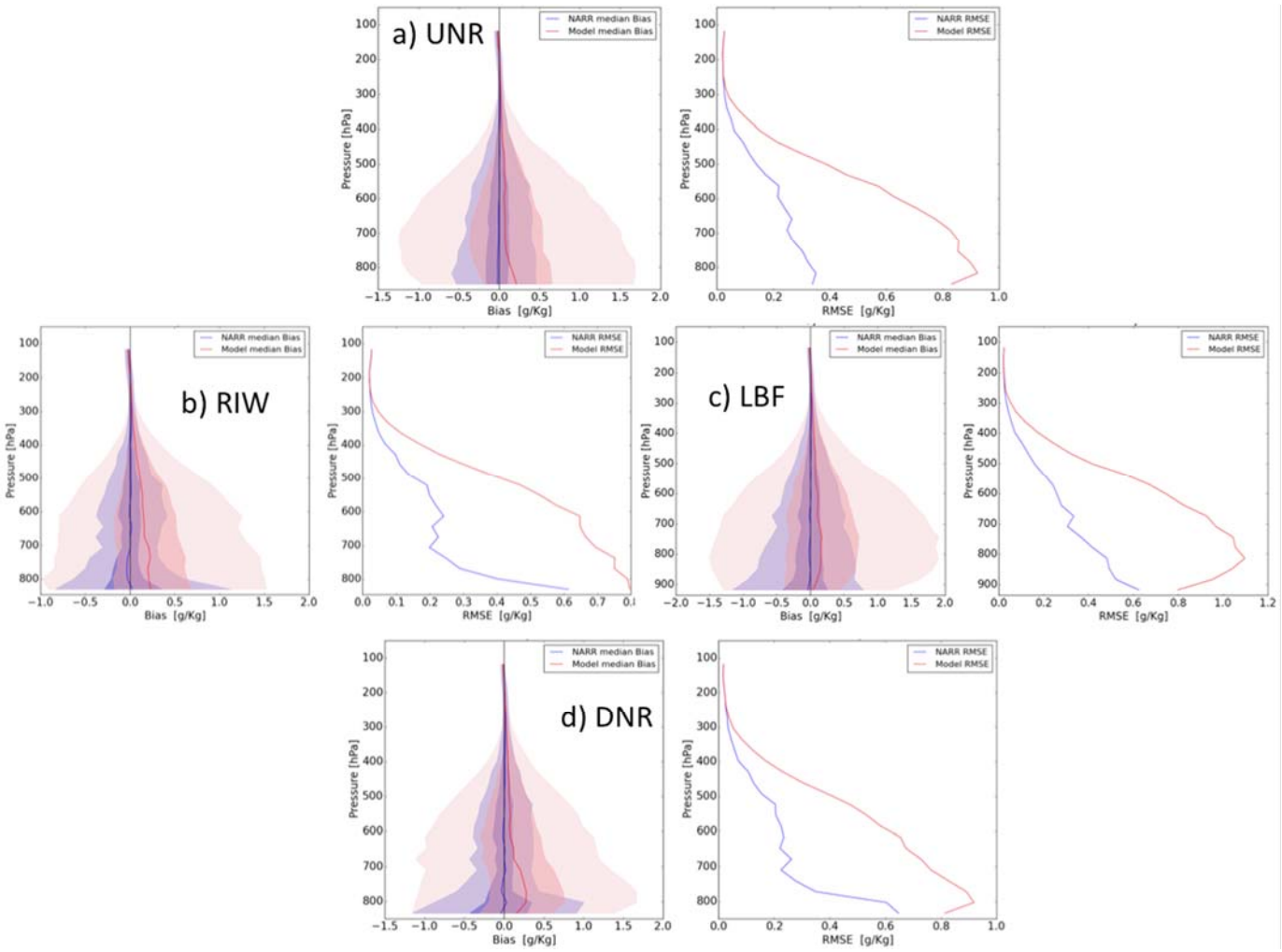

Figure 3.50 Specific humidity biases and RMSE for NARR and the model relative to contemporaneous RAOBS data evaluated at a) Rapid City (KUNR), b) Riverton (KRIW), c) North Platte (KLBF), and Denver (KDNR).

3.4.2 Near-surface RCM Performance

The accurate simulation of near-surface atmospheric conditions is one of the most important and difficult tasks in RCMs, as several factors must be represented properly, including: topography, land use and land cover, surface heat flux transport, and mixing properties of the lower atmosphere (Cheng and Steenburgh 2005). Owing to our limited understanding of near-surface atmospheric processes and the uncertainties in model physics parameterizations, a verification of the RCM performance in simulating near-surface variables becomes a necessary step for model improvement.

We focused the surface station analysis of the four SNOw TELemetry (SNOTEL) sites spread across the northern Laramie Range. The SNOTEL observations were quality assured and controlled. Of note is that SNOTEL measurement uncertainty can include local biases caused by abrupt topography at high elevations, misrepresentation in space due to local microclimates, and precipitation undercatch due to turbulent flows (Silverman et al. 2013). Furthermore, measurement errors due to sensor resolution can be important as reports of

precipitation are provided only at one tenth of an inch, creating trace underestimates. Issues of quality of the SNOTEL observations have been studied over Western U.S. (Meyer et al. 2012; McEvoy (2014) and the sites over the Laramie Range appear to suffer some of the widely reported issues. Particularly, all sites implemented in this evaluation study showed years in which the SWE unrealistically outpaced accumulated precipitation. Figure 3.51 shows the WRF model (D03 1-km) compared to the Casper Mountain SNOTEL. Panel (d) shows that SWE remains below the accumulated precipitation before mid-January 2012, but then increases to exceed and outgrow precipitation until early April 2013. Meyer et al. (2012) attributed this feature to substantial precipitation undercatch and overemphasis of SWE by drifting of snow.

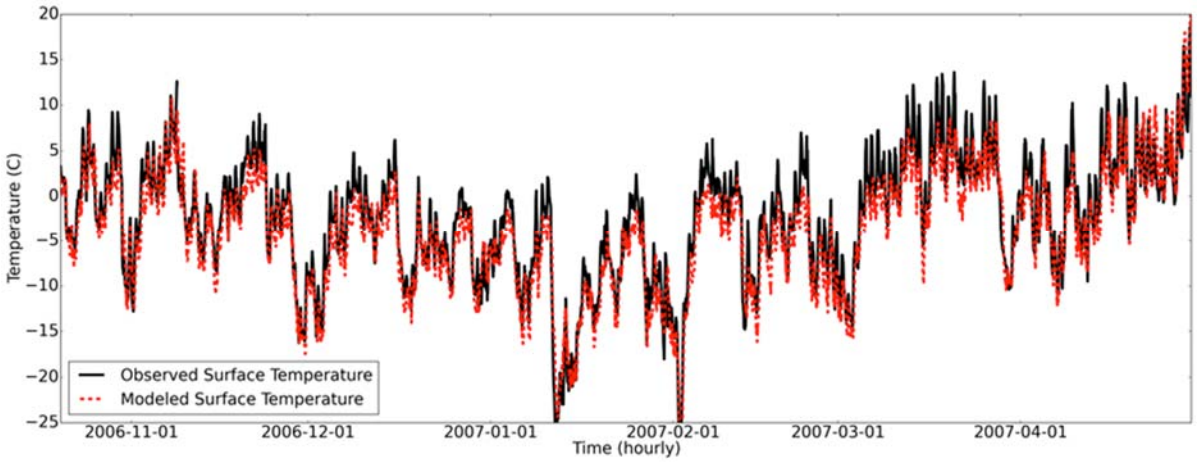

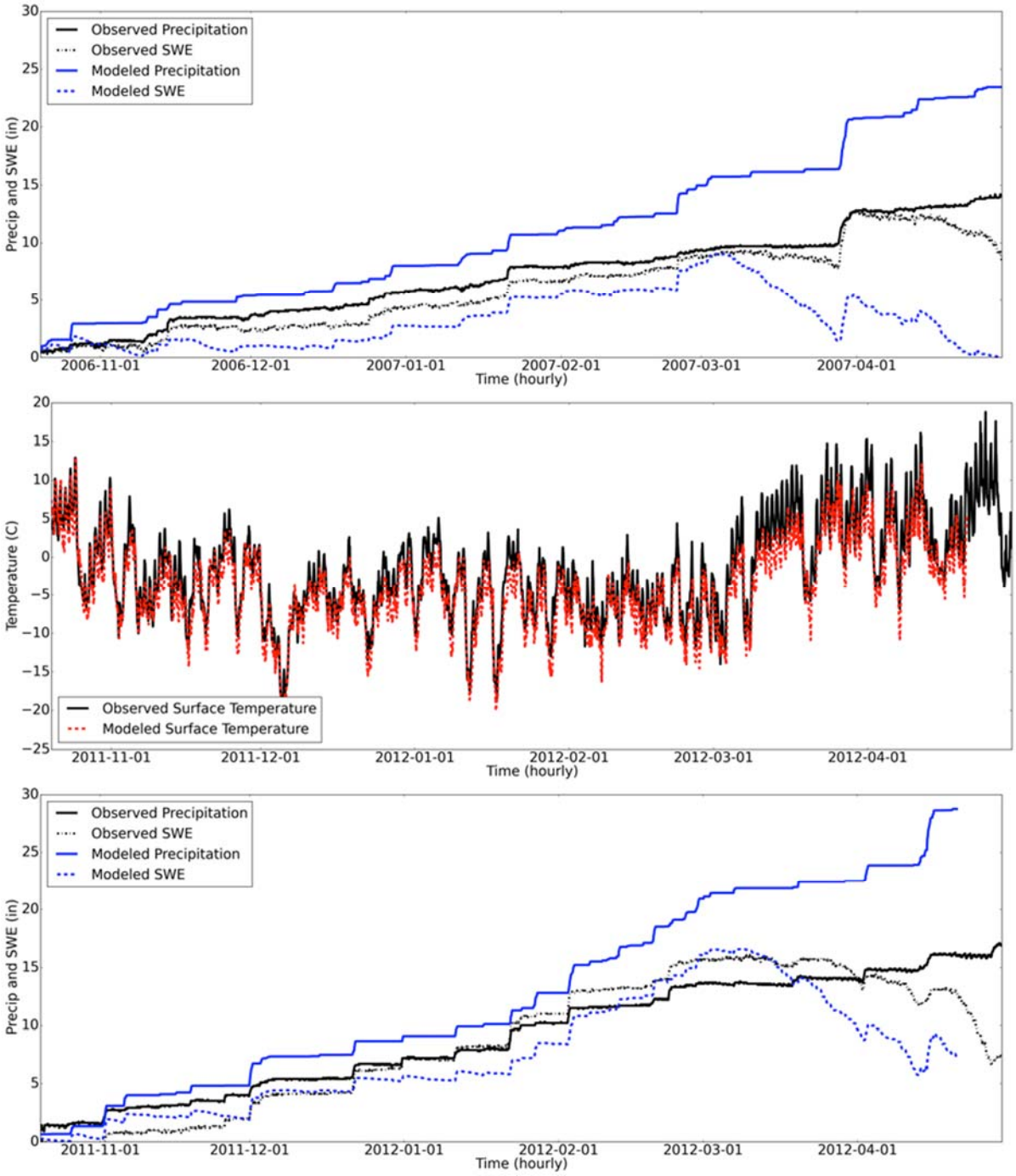

Figure 3.51 Temperatures and snow water equivalent (SWE) for 2007 and 2012 (winter) water years at Casper Mountain the SNOTEL site.

The observed surface temperature, precipitation, and SWE at the 4 SNOTEL sites for the Nov 1 through April 30 time frame during 11 years between 2004 and 2015 were compared against the equivalent model output at 3 km and 1 km grid sizes. Of note is that the sensitivity of the results below were tested for different model grid-to-point data retrieval schemes, including nearest neighbor grid point, randomly selecting between the four nearest grid

points, and bilinear interpolation using all these points. Results herein only show results using the bilinear interpolation scheme.

Evolution of modeled surface temperature shows that the WRF model is able to reproduce synoptic weather or "day-to-day" phenomena reasonably well (Fig 3.52a and 3.52c)) with some apparent systematic errors. Over all sites, the model shows a systematic cold bias of about -1.5°C. These biases tend to be smaller (~ -0.6 to -1°C) early in the water year and tend to increase by the end of the cold season (-2 to 2.5°C). Surface Temperature error statistics at the SNOTEL sites do not show an improvement by increased resolution from the 3km to the 1 km grid size (Table 3.7). Although better detail of the land use/land cover and topography is expected, biases and RMSE are rather stable, also suggesting that information is not degraded by adding an additional nested domains (when using the RCM to downscale from 3 km to 1 km grid size). Our results agree with findings from other studies showing that the model performance decreases by increasing grid size (Mass et al. 2002; Mejia et al. 2012; Zhang et al. 2013). However, other studies suggested that the accuracy of regional climate simulation over complex terrain tend to increase with decreasing grid size resolution (Leung and Qian 2003; Rife and Davis 2005). In complex terrain, simulations not only suffer from the model's inability to reproduce accurate atmospheric conditions in the lower troposphere, but also struggle with representative issues due to scale issues between the model and the actual terrain.

The precipitation biased at SNOTEL sites were significantly large ranging from 32% at Reno Hill to nearly 80% at Laprele Creek (Table 3.9) with relatively large inter annual variations (not shown). However, SNOTEL network have a margin of measurement error between 10% and 50%, possibly more in mountainous regions (WMO 2008). Of note is that these results are consistent with the mid-tropospheric wet biases found upstream at the KRIW sounding site and consistently over all of Wyoming and the surrounding upper level measurement sites. The positive bias found for both low-level mixing ratio and precipitation suggests that the WRF model, as configured here, may have an unbalanced hydrologic cycle that is recycling precipitation and moistening the lower atmosphere.

RCM studies using WRF have shown that the model tends to over predict precipitation. Wet biases could have been introduced by the driving boundary conditions data set, but in our case we will show this is unlikely as we are using internal nudging and the NARR moisture fields are unbiased (see upper-air evaluation), suggesting that such biases are more likely due to internal drifting of the WRF and its physics parameterizations (Caldwell et al., 2009, Silverman et al. 2013; Katragkou et al. 2015). Silverman et al. (2013) overviews and briefly describes some of the common WRF wet biases issues. For example, a logical reason could be related to less topographic smoothing for smaller grid sizes, improving representation of higher elevations, which tends to increasing orographic effects and making it possible for higher precipitation amounts to exist (Mass et al. 2002; Leung and Qian 2003; Chin et al. 2010).

The exact source of the wet and cold biases over the Laramie Range highlands is out of the scope of this study (e.g., land-atmospheric vs. cloud-radiation interaction). Results shown here illustrate that model errors in near surface variables depend strongly on the diurnal

variation in surface conditions, especially late in the cold season. Additionally, cold biases appear to be consistent with the wet precipitation biases as indicated by the surface temperature biases diurnal cycle (Fig. 3.53), which indicate that biases are enhanced during the daylight, likely due to wetter mid-tropospheric atmosphere, which tend to develop more clouds and precipitation, therefore creating cooler surface due to direct reduced incoming solar radiation. Cold biases could have been exacerbated by the indirect cooling effect due to higher albedo over the snowy surfaces.

As mentioned earlier, several WRF schemes configurations tend to produce systematic wet biases (Katragkou et al. 2015). Therefore, the disagreement between error structure and the scale dependency, the influence of the flow regime and the seasons, and the complex interaction between parameterization schemes, make error characterization and attribution a complicated and challenging tasks. Although the aforementioned surface biases around the SNOTEL sites are rather large, they do not preclude the use of WRF flow dynamics and cloud phase in this feasibility study (Silverman et al. 2013). The flow dynamics and cloudiness responses are expected to behave reasonably well, allowing the examination of the high-resolution flow regime patterns and their implications for realistic cloud seeding potential. The feasibility results derived from this modeling study will be discussed in the light of this biases.

Despite the NOAH snow physics being somewhat oversimplified (single slab snow layer lumped with the topsoil; no liquid water; fixed snow density; One vegetation type in one grid cell; 4-layer temperatures and moisture and frozen soil) relative to other approaches (e.g., CLM Jin and Wen (2012)), the model SWE performed relatively well. Figure 3.52 time evolution shows simulated SWE results for selected years over the Casper Mountain SNOTEL site, in which snow accumulations and the snowmelt evolution follow closely to those observed, but with larger differences late in the cold season and early spring; visual inspection indicate this is typical behavior for most years and other sites (not shown).

Figure 3.52 mean plots show that the model exhibits a faster snowmelt when compared to observations, which is a typical behavior in NOAH as it lumps the albedo effect by multiple land use types (e.g., vegetation and snow surfaces) in one grid cell. In agreement with previous studies (Leung and Qian 2003), there are noticeable improvements in the model SWE performance using finer resolution from 3km to 1km grid size (Table 3.10). In light of the systematic cold surface temperature and wet precipitation biases outlined earlier, we speculate that this SWE performance is likely affected by error compensation.

Precipitation and surface temperature systematic biases exhibited by WRF indicate there is a potential for bias correction when best precipitation forecast/projections are needed for hydrologic modeling and water resource management strategies. Of note is that the accuracy of WRF surface parameters for individual events were not evaluated. However, a thorough evaluation of individual events is necessary, as the model tends to depend on the flow regime and season transition. Easterly flow and spring season synoptic flow patterns appear to enhance the errors. However, these flow patterns could be important as the easterly flow systems create cloud seeding potential opportunities over the eastern slopes of the Laramie Range (Fig. 3.40).

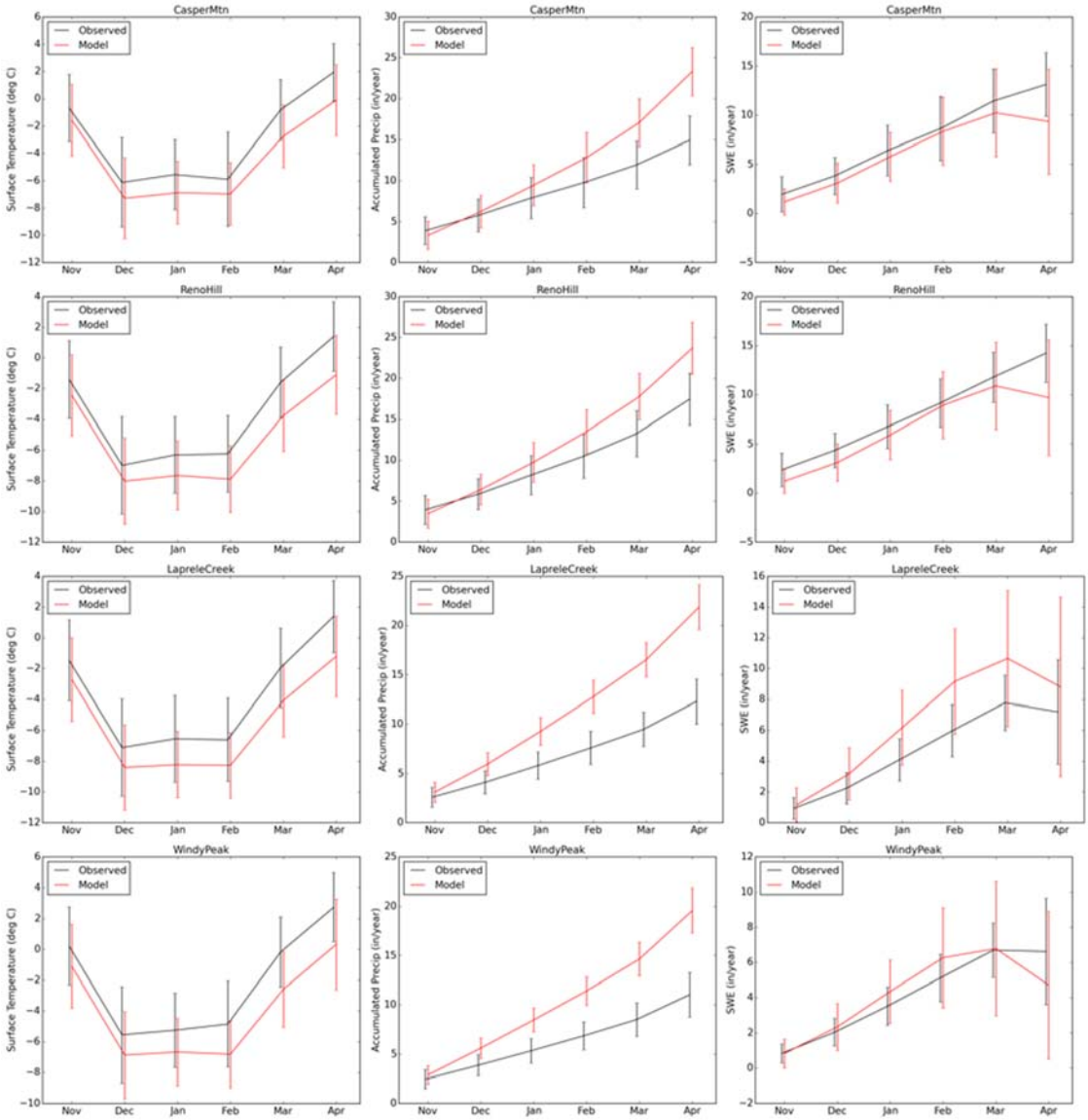

Figure 3.52 (Nov 2004- April 2015) monthly mean observed and modeled temperature, precipitation, and snow water equivalent (SWE). Median and ±Standard Deviation. All SNOWTEL sites available over Laramie Range

		Nov	Dec	Jan	Feb	Mar	Apr	Cold Season
Casper Mountain	**1 km**	-0.87	-0.99	-1.32	-1.42	-1.97	-1.62	-1.37
	3 km	-0.69	-0.89	-1.30	-1.36	-1.83	-1.35	-1.24
Laprele Creek	**1 km**	-1.23	-1.28	-1.44	-1.58	-2.15	-2.11	-1.63
	3 km	-1.24	-1.22	-1.32	-1.49	-2.09	-2.21	-1.59
Reno Hill	**1 km**	-1.03	-1.03	-1.36	-1.65	-2.17	-2.07	-1.55
	3 km	-1.20	-1.25	-1.66	-1.86	-2.37	-2.21	-1.76
Windy Peak	**1 km**	-1.14	-1.28	-1.36	-1.86	-2.42	-1.92	-1.66
	3 km	-1.23	-1.42	-1.52	-1.96	-2.50	-2.00	-1.77

Table 3.7 Modeled monthly mean surface temperature bias (°C) evaluated at SNOWTEL sites over Laramie Range. Model output is evaluated for D02 (3km gridsize) and D03 (1km grid size).

		Nov	Dec	Jan	Feb	Mar	Apr	Cold Season
Casper Mountain	1 km	1.6	1.6	2.1	1.9	2.4	2.4	2.0
	3 km	1.5	1.6	2.1	1.9	2.3	2.3	1.9
Laprele Creek	1 km	1.9	1.9	2.0	2.2	2.7	2.8	2.3
	3 km	1.9	1.9	1.9	2.1	2.7	2.9	2.2
Reno Hill	1 km	1.7	1.7	1.9	2.1	2.6	2.7	2.1
	3 km	1.8	1.9	2.2	2.3	2.9	2.9	2.3
Windy Peak	1 km	1.9	2.0	2.3	2.5	3.0	2.8	2.4
	3 km	2.0	2.1	2.4	2.6	3.1	2.8	2.5

Table 3.8 Modeled monthly mean surface temperature RMSE (°C) evaluated at SNOWTEL over Laramie Range. Model output is evaluated for D02 (3km gridsize) and D03 (1km grid size).

		Observed	Model	Bias	Relative Difference
Casper Mountain	**1 km**	15.0	23.2	8.4	56.1
	3 km	15.0	21.9	6.9	46.2
Laprele Creek	**1 km**	12.3	22.1	9.7	78.9
	3 km	12.3	21.8	9.5	76.9
Reno Hill	**1 km**	17.3	23.7	6.4	37.1
	3 km	17.3	23.0	5.5	31.9
Windy Peak	**1 km**	11.1	19.7	8.6	77.8
	3 km	11.1	19.4	8.4	75.7

Table3.9 Cold season precipitation bias (in) and relative difference (%). Model output is evaluated for D02 (3km gridsize) and D03 (1km grid size).

		Observed [in]	Model [in]	Bias [in]	Relative Difference [%]
Casper Mountain	**1 km**	13.0	9.1	-3.9	-30.1
	3 km	13.1	6.2	-6.9	-52.9
Laprele Creek	**1 km**	7.4	8.9	1.5	19.9
	3 km	7.1	9.4	2.3	32.0
Reno Hill	**1 km**	14.2	9.6	-4.6	-32.4
	3 km	14.2	8.6	-5.7	-39.9
Windy Peak	**1 km**	6.8	4.7	-2.1	-31.2
	3 km	6.6	4.1	-2.5	-38.2

Table 3.10 Cold season SWE bias (in) and relative difference (%). Model output is evaluated for D02 (3km gridsize) and D03 (1km grid size). SWE comparisons.

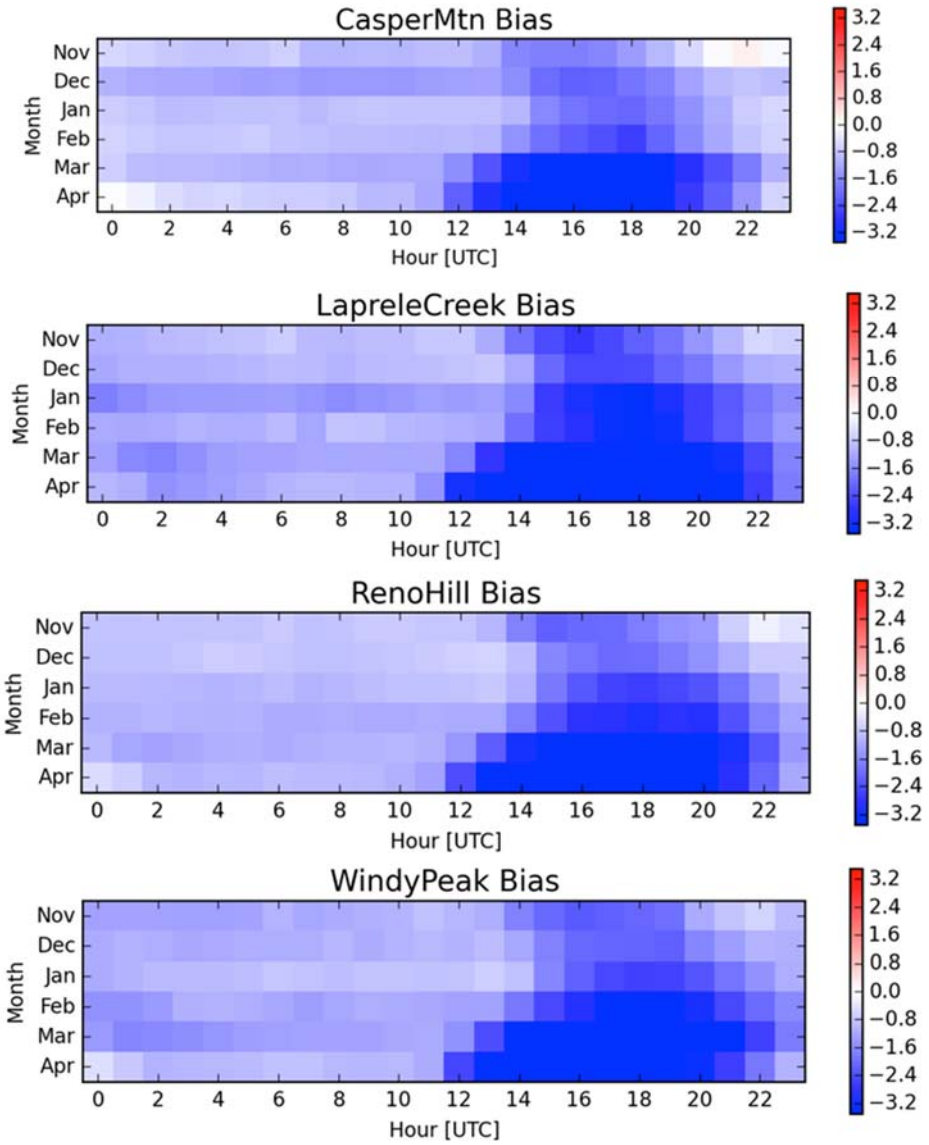

Figure 3.53 Cold season diurnal cycle of the model surface temperature bias (°C) at SNOWTEL sites.

4 Development of a Preliminary Project Design

4.1 Introduction

Building off the results from the climatology, a preliminary project design was created. This section discusses the types of seeding generators available to the project, how the generators create snowfall, and where the initial siting locations were placed.

4.2 Cloud Seeding Methods

The effectiveness of AgI cloud seeding is dependent on temperature, with cloud temperatures below -8°C being most effective, but temperatures as warm as -5°C initiating some freezing events. DRI has used AgI mixed with a hygroscopic salt as the seeding material for several decades. This improves the probability of condensation taking place in droplets with the AgI ice nuclei present, improves the probability of the droplets freezing, and makes cloud seeding more efficient. It is recommended that the project use this seeding agent. The required time to create a precipitation-sized snowflake depends on the CB height, vertical motion, temperatures, and SLW content in the targeted clouds. Figure 4.1 shows an AgI remote controlled cloud seeding generator getting installed in Colorado.

Figure 4.1 AgI high altitude cloud seeding generator.

LP cloud seeding was discussed in a feasibility study for Colorado Winter Mountain Clouds by Arlen Super and James Heimbach stating that: *"The final topic concerns expansion of liquid propane to chill cloudy air below 40°C. This produces vast numbers of embryonic ice crystals by homogeneous nucleation. This is a method of higher elevation ground seeding with an agent and mechanism different than AgI seeding. It is given emphasis in this report because the method is not widely known, but recent results from a randomized propane seeding experiment in Utah are very encouraging. Propane seeding may provide an adjunct or alternative to AgI seeding in Colorado. Propane releases can produce abundant ice crystals at temperatures as*

warm as -1°C and with little temperature dependence below -2°C. A disadvantage of propane seeding is that it must be released within SLW clouds or just beneath in ice saturation conditions. Consequently, high altitude remote-controlled dispensers are required for propane seeding." Super and Heimbach (2005) discuss this method in more detail.

DRI has embraced this seeding method and this study has tested its feasibility in the Laramie Range project. DRI has built and operated LP generators on the Grand Mesa in Colorado and analysis of this project suggests the technology can be useful, has low costs, and the dispensers require low maintenance (Fig 4.2).

Figure 4.2 DRI LP cloud seeding generator on the Grand Mesa in Colorado.

Aircraft cloud seeding is a highly effective method to deliver AgI directly into clouds upstream of the target area. The aircraft is not impacted by low-level inversions and the temperature and wind direction targeting challenges associated with ground-based generators. The technology has very high efficiencies in producing increased precipitation. The downsides are:

1. Costs: More than $1000/hr to ferry the aircraft and more than $2000/hr while the aircraft is conducting operations.
2. Safety: Cloud seeding conditions are also aircraft icing conditions. Icing on the exposed airframe can cause the aircraft to become difficult to operate. In winter in

Wyoming the freezing level is below the ground so there is limited opportunity escape the condition when the aircraft if icing conditions become dangerous.

3. Minimum altitudes: The climatology suggested that the supercooled liquid clouds were often at altitudes below 12,000 ft MSL. The highest peaks in the target are above 9,000 MSL so the aircraft may need to operate and the lowest possible legal altitudes to be effective.

4.3 Project Design

After an assessment of the climatological results, a preliminary set of generator sites and aircraft flight tracks were prepared to target the 620,000 acres in the northern Laramie Range above 8,000 ft MSL. These initial sites were iterated though the plume dispersal model (See a snapshot of Chapter 5 results in Fig 4.3) and the final sites identified.

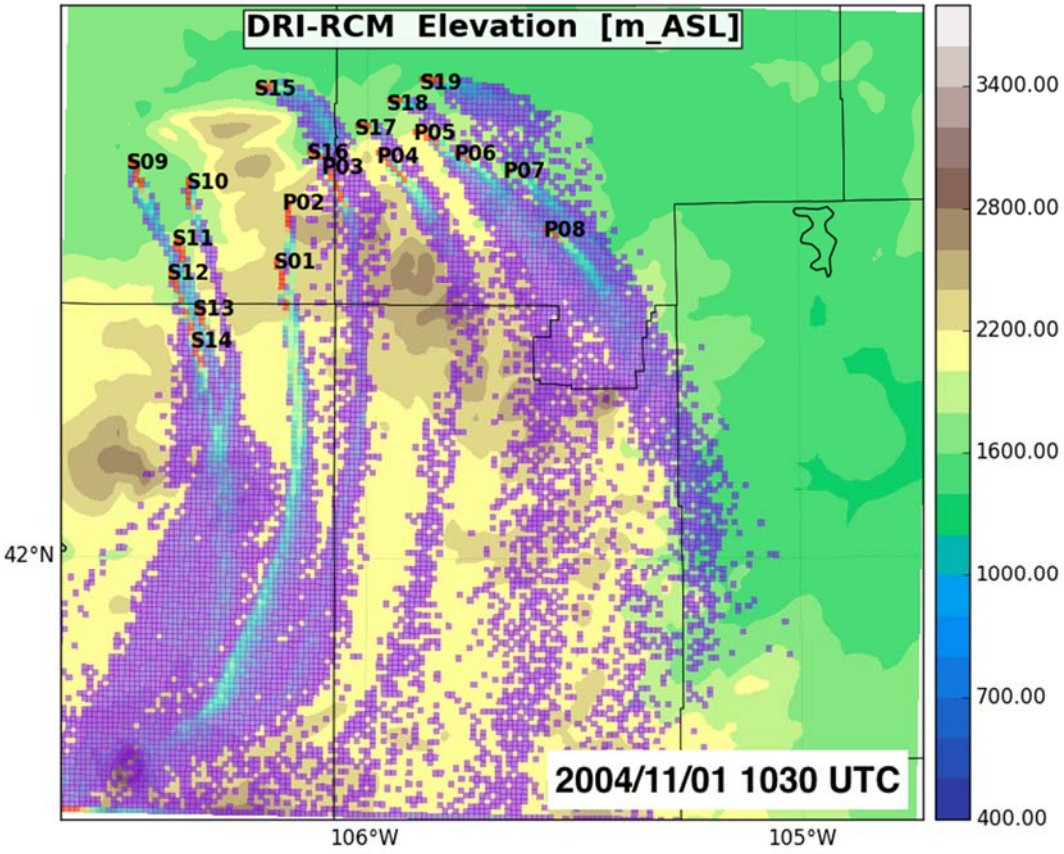

Figure 4.3 Snapshot of the seeding material dispersion modeling based on the Lagrangian plume model (Section 5 of this report) valid for Nov 1, 2004 at 1030 UTC. Concentration of particles contours (# particles per unit volume) are shown over the model elevation contours (m_ASL). Seeding material is released from generator locations identified as *"S"* for AgI sites and *"P"* for LP/AgI sites.

Figure 4.4 shows a map of the potential project in the Laramie Range designed following the results of the climatology and plume modeling. The project includes 12 ground-based AgI generators (yellow pins; Fig. 4.4), 7 LP and/or AgI generators (green pins; Fig 4.4), and AgI aircraft tracks (red dashed lines: Fig 4.4).

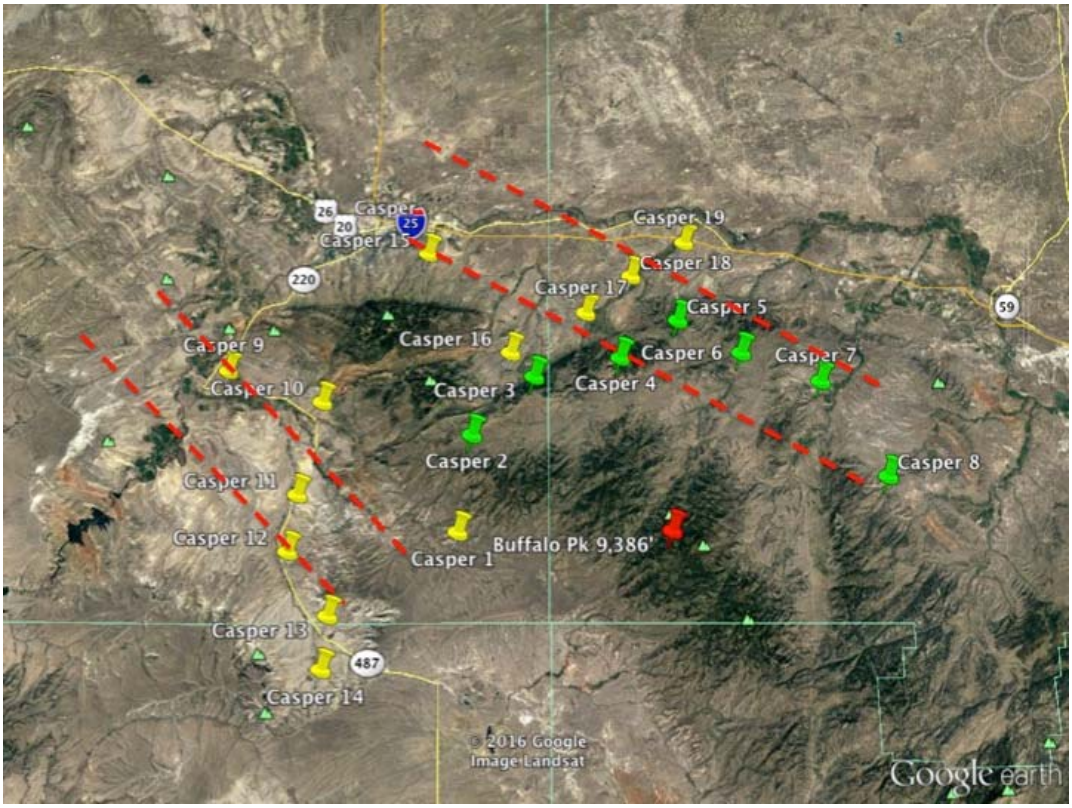

Figure 4.4 The preliminary design for generators and flight tracks. Yellow pins indicate ground-based AgI, green pins indicate Agi or LP generator locations, and red dashed lines potential aircraft flight tracks. The red pin identifies the center of the target area.

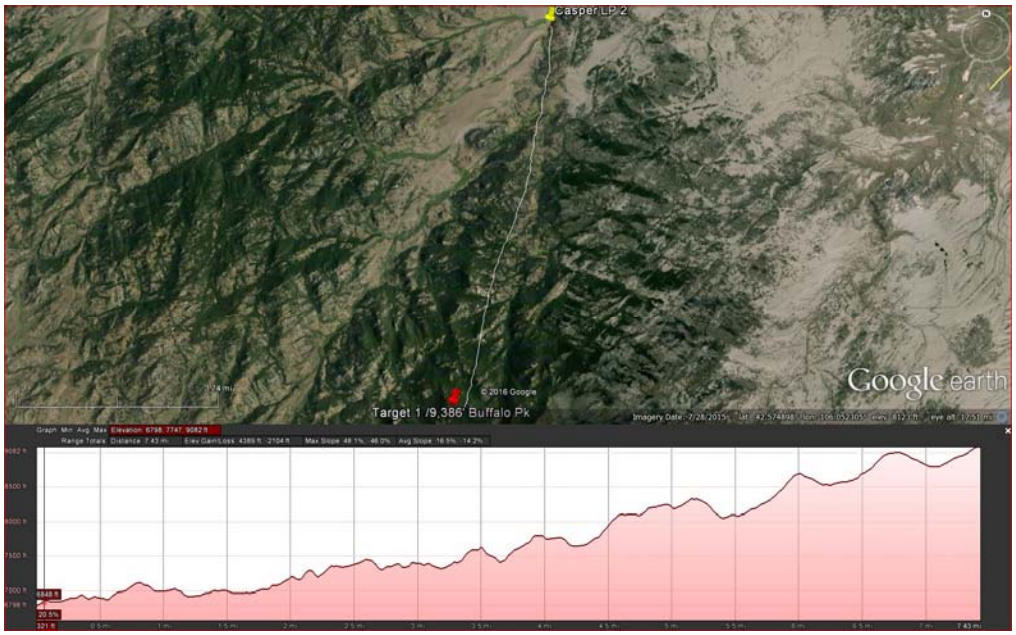

Figure 4.5. Profile from a proposed liquid propane generator site (yellow pin: Casper 5 in Figure 4.4) to the target area (red pin) under north to north-northeast flow. The inset shows the vertical profile along a north-northeast to south-southeast transect from the potential release point to the target.

This siting plan takes into account both Scenario 1 and Scenario 2 storms as well as the results from Task 5. The locations of the generators and flight tracks are expected to maximize the seeding potential for both northwesterly flow regimes and north through northeasterly flow regimes. Plume modeling also showed that LP releases from the northwest were not feasible since they were found not remain in cloud due to periods of downward vertical motions as the plume moved southeasterly along the upstream crest of the ridge. LP seeding was shown in the model to be effective for Scenario 2 storms (Figure 4.5).

5 Model Evaluation of the Preliminary Design

5.1 Lagrangian Dispersion Model: Ground-based Siting Considerations

The DRI dispersion model uses a combination of gridded wind and turbulence to simulate transport of gas plume/passive constituents (e.g., cloud seeding agents, dust, pollutants) using a Lagrangian Stochastic Particle Dispersion Model (LSPDM). Lagrangian methods consider particles as discrete units and tracks their pathways. By studying the statistics of particle trajectories, the Lagrangian method is also able to calculate the particle concentration at a receptor site. The LSPDM has been developed at DRI (Koracin et al. 2011) and it has been evaluated using field experiment data, and has shown significant capabilities in complex atmospheric and environmental conditions on a variety of scales. The LSPDM estimates dispersion of passive particles using inverse- and direct-time integration of the trajectory equations. The model uses the 3-D wind field to pinpoint either source (inverse) or receptors (direct) and incorporates turbulent dispersion, dry deposition, and convection "buoyancy" terms. The current version of the LSPDM assumes no interaction of seeding agent (i.e. ice nuclei) with the clouds, hence, neither crystal growth, fall speed, or sedimentation rate of the crystals are considered. However, each LSPDM particle has attributes or tags (spatial-time, ambient meteorology, physical and chemical composition, suspension time, source metadata), which allow particles from different grid cells to be tracked over space and through time to estimate their relative impact upon a chosen receptor site. Therefore, the LSPDM permits to locally evaluate whether seedable conditions are found along each trajectory (e.g., Cloud Seeding Potential-CSP defined in Section 3 of this report).

The LSPDM is suitable in complex atmospheric and environmental conditions on a variety of scales. Recent LSPDM applications include modeling implemented for regional emission sources over the eastern U.S. (Koracin et al. 2011); dust emissions at micrometeorological scales by rotorcrafts (McAlpine et al. 2010); regional dispersion of Radiation Plume from Japan's Fukushima Nuclear Reactors Explosions (Mejia and Koracin 2011). Other applications include Luria et al. (2005), Koracin et al. (2007), Weinroth et al. (2008), and Lowenthal et al. (2010). Recently, DRI uses the LSPDM as a forecasting tool to estimate transport of cloud seeding agents as a function of weather forecasting products for DRI's weather modification program.

5.1.1 The Backward Integrations

The LSPDM is reversible in the sense that it can be used to locate sources (e.g., cloud seeding generators) or used to optimize the location of detectors. For backwards trajectories, the irreversibility of turbulent diffusion and deposition (He 2011 and Xu et al. 2016) prevents exact estimates of dispersion simply using back trajectories and the resultant solution does not represent emission concentration fields. Instead, the output of backward simulations is

a source-receptor sensitivity field that provides probabilities of possible source locations. Once the most probable source locations are known, the LSPDM model can be integrated in forward mode using idealized flow under different atmospheric or emission scenarios (laminar flow, low and high turbulence flow; logarithmic/exponential wind profiles; wind orientations; emission rate and locations), or realistic simulated flow conditions (e.g., WRF model output). If solved using adequate resolution, the modeling framework enables characterization of stagnant (or separation) zones and high ventilation zones around complex terrain. This strategy was implemented to guide the optimal seeding generator (ground-based) siting zones around the Laramie Range.

Figure 5.1 shows backward integration results using model output for all 11 cold season periods (Nov-April) extending from 2005-2015. From each grid point in the 3D space meeting the seedable criteria or CSP_{AgI} = 1 (Section 3.3.3), a trajectory was integrated backwards up to 90 minutes. A collection of backward trajectories (only low-level trajectories or first 10 model layers) forms an ensemble of the source location, from which the frequency --number of touchdowns per grid point-- is estimated relative to the total number of released backward trajectories. Trajectories were ended when they intersected the lowest model layer (10 m AGL). We suggest that regions of high source frequency can be treated as potential generator site locations. Figure 5.1 shows that the northwestern and northeastern flanks are the regions with the highest frequency values around the Laramie Range, regardless of the backward integration duration. Of note is that these results are consistent with CSP_{AgI} level predominant flow shown earlier. The value of our source frequency results is that they highlight low-level trajectories, from which a better-informed (best guess) scenario generator siting was created. Note that the high source frequency or siting zones outlined in Chapter 4 are only constrained to our simulated meteorology and these backward integration probabilities. However, these results were used as guidance to inform other siting constrains including considerations such as permitting and accessibility.

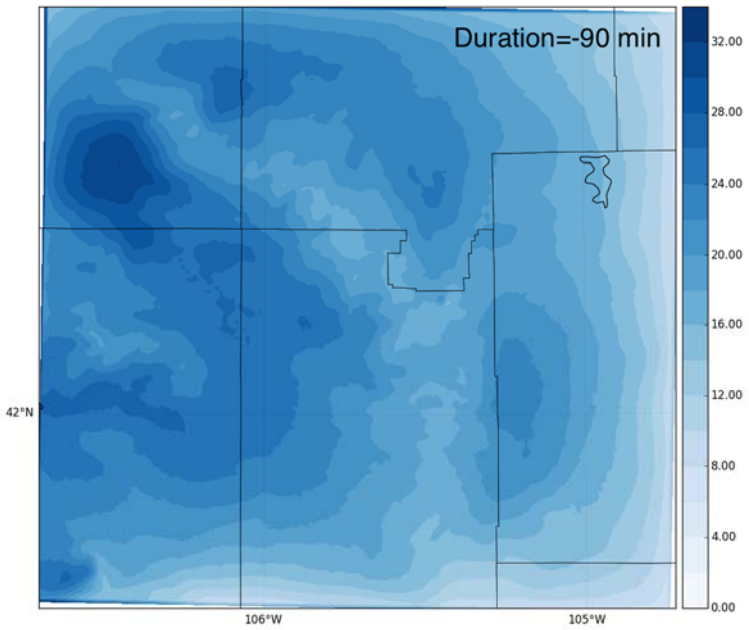

Figure 5.1 Source probability (%) estimated using backward trajectories released from all seedable opportunities (CSP_{Agl} = 1; in the 3D space) and composited for trajectory duration of 90 minutes (see text for details). Backward integrations performed during 11 cold season periods (Nov-April) extending 2005-2015.

5.1.2 The Forward Integrations

The LSPDM is well suited for investigating transport of cloud seeding particles in multi-scale turbulent environments under advection-dominated flows. Theoretically, and under inviscid flow assumption, the basis of our approach does not impose restrictions for any type of velocity fields or complex geometric layouts. They take direct advantage of the inherent Lagrangian advection of cloud seeding particles as a tracer before the particle is glaciated. The number of particles from different sources can be released as a function of the emission estimates. The final distribution of many (tens of thousands to millions) particles gives a stochastic estimation of dispersion patterns. The LSPDM estimates the particle as a single drifting point, and the final distribution of numerous particles is used to estimate concentration fields. The final concentration fields are estimated by a simple box-counting or cluster analyses approaches.

For forward trajectories of particles, we use the Thompson assumption for separation of the mean and perturbed motion. The net result is a trajectory velocity for each particle that is given by the sum of the grid point mean Eulerian velocity and a velocity perturbation. Our LSPDM model uses the mean wind fields from the Eulerian framework (e.g., our model output based on WRF) and parameterizes velocity perturbation from the turbulence fields using a local closure approach (e.g, k-ε turbulence model), which in turn is a function of the flow regimes (laminar, transitional, turbulent). The stochastic components of the model follows a modified version of the Lagrangian stochastic model of Thomson for 3D flows (Weil 2007) and estimates diffusion of particles from a probability distribution function (PDF) estimated of perturbed particles being released (thousands) in each integration time. Of note

is that this approach imposes the well-mixed criterion and satisfies the Fokker–Planck equation under the inertial sub-range.

The forward LSPDM was implemented using pre-selected siting zones from our backward LSPDM results (i.e., optimal zones over which cloud seeding generators can be installed to increase the likelihood of reaching supercooled liquid clouds). These zones were used to adjust the initial sites from the climatological analysis for new feasible sites (Table 5.1). For illustration purposes, we run the LSPDM during Nov 1st, 2004 storm event. This was a Scenario 2 storm (see Chapter 3). Seeding particles were released for 24 hours from 0000 to 2400 UTC. Figure 5.2 shows the pre-defined sites with all the generators (19) using AgI as seeding agent. As mentioned in Section 4, sites that were originally planned as potential LP sites were also tested as AgI sites. Figure 5.2 also shows four snapshots of the three-dimensional particle distribution dispersion projected into the horizontal plane. Note that the dispersion of cloud seeding plumes is evident due to the turbulent diffusion nature of the LSPDM integrations. Figure 5.3 shows the seeding efficiency of individual generators during the same snapshot times shown in Figure 5.2. In this analysis approach, each generator is kept independent and their efficiency is evaluated according to the number of particles reaching CSP_{AgI} environments. Early during the storm day, all generators showed low efficiency in reaching supercooled liquid clouds. Later around 1500 UTC, generators 02-08 located over Laramie Range northeastern slopes improved and showed better efficiency relative to all others, likely due to their location relative to the storm's northerly flow. This also suggests that if low cloud bases were present LP seeding would have been effective. Also note that for this specific storm. As expected AgI generators 09-14 located over the northwestern slopes do not show a significant response throughout the storm event. The evolution of the seeding response averaged over all generators is shown in Figure 5.4 highlighting what appears to be a narrow window of seeding opportunity (from 1300UTC-1900UTC) for the given storm and siting scenario. Note that this modeling framework constitutes a powerful prognostic tool for seeding generator operations as the simulated efficiency of individual generators can be also retrieved as a function of the forecasting window.

Location	Temperature Range (°C)	Latitude	Longitude	Elevation (ft MSL)	Land Owner
01	-6 to -18	42.505963°	-106.214819°	7321	State Trust lands
02	-6 to -18	42.605939°	-106.195254°	7245	Private
03	-6 to -18	42.667358°	-106.103773°	7557	Private
04	-6 to -18	42.687352°	-105.975915°	6916	Private
05	-6 to -18	42.727203°	-105.889336°	6705	Private
06	-6 to -18	42.691921°	-105.796812°	6510	Private
07	-6 to -18	42.661432°	-105.680472°	5765	Private
08	-6 to -18	42.561286°	-105.588496°	5733	Private
09	-6 to -18	42.674399°	-106.558531°	5444	Private
10	-6 to -18	42.64089°	-106.416681°	5734	Private
11	-6 to -18	42.544309°	-106.449208°	5936	Private
12	-6 to -18	42.486128°	-106.46042°	6098	BLM
13	-6 to -18	42.421897°	-106.399764°	6421	Private
14	-6 to -18	42.369024°	-106.407131°	6697	BLM
15	-6 to -18	42.801583°	-106.262845°	5468	Private
16	-6 to -18	42.693266°	-106.138796°	5848	State Trust lands
17	-6 to -18	42.735953°	-106.026635°	5556	State Trust lands
18	-6 to -18	42.776137°	-105.951596°	5254	State Trust lands
19	-6 to -18	42.813054°	-105.876253°	5328	State Trust lands

Table 5.1 Laramie Range Cloud Seeding Generators implemented by the LSPDM forwards dispersion modeling. All generators use AgI as seeding agent.

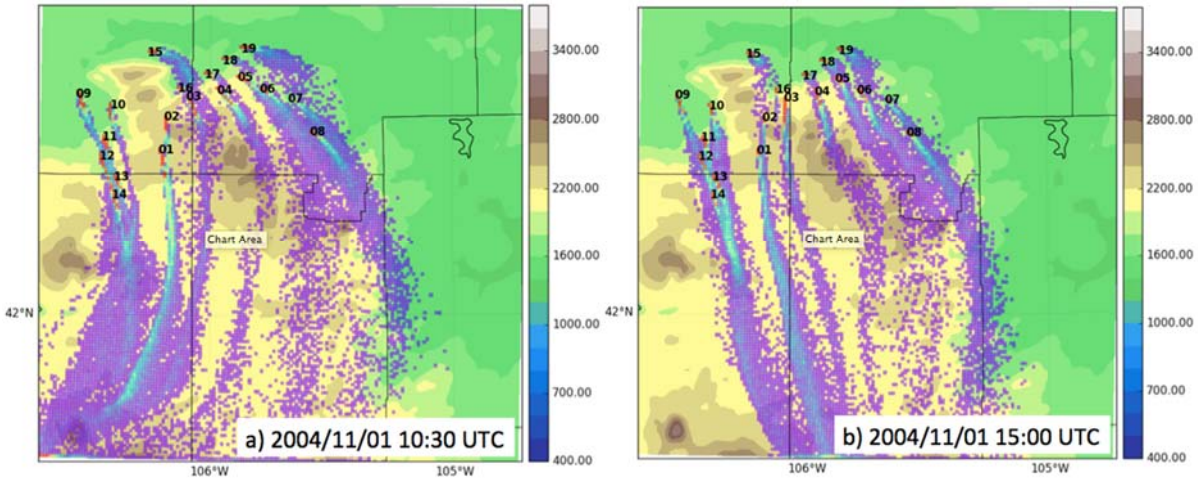

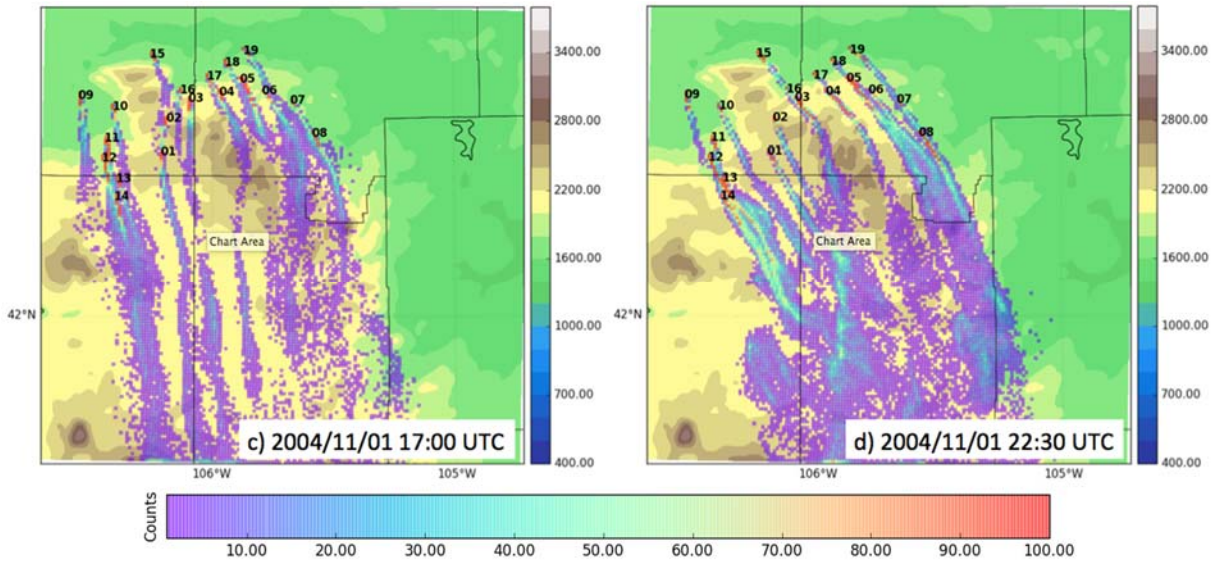

Figure 5.2 (Left panels) LSPDM cloud seeding plume concentration (#particles) during Nov 1st, 2004 cold season storm at a) 10:30 UTC, b) 15:00 UTC, c) 17:00 UTC, and d) 22:30 UTC. The model digital elevation model (m_ASL) is used as background.

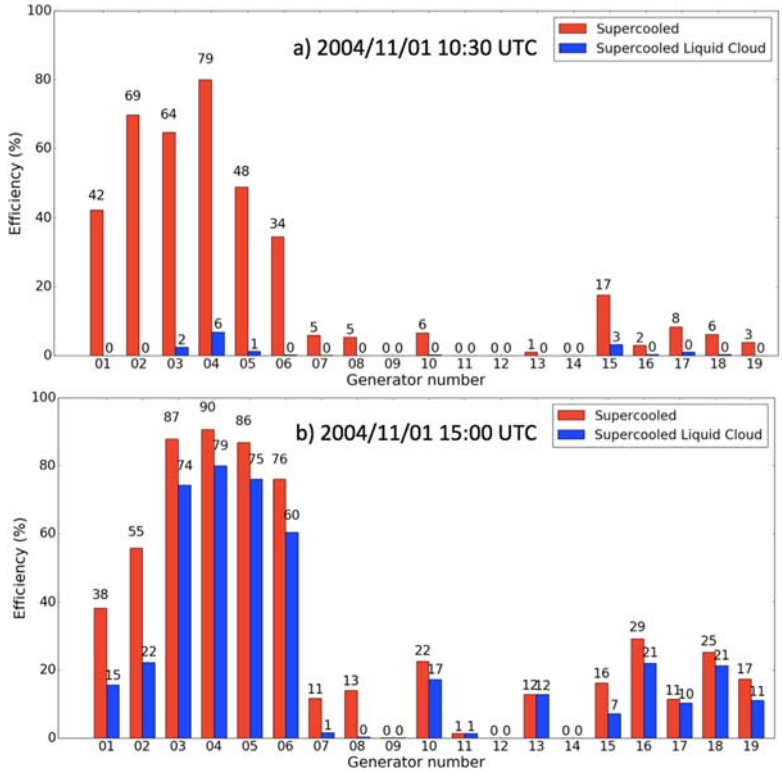

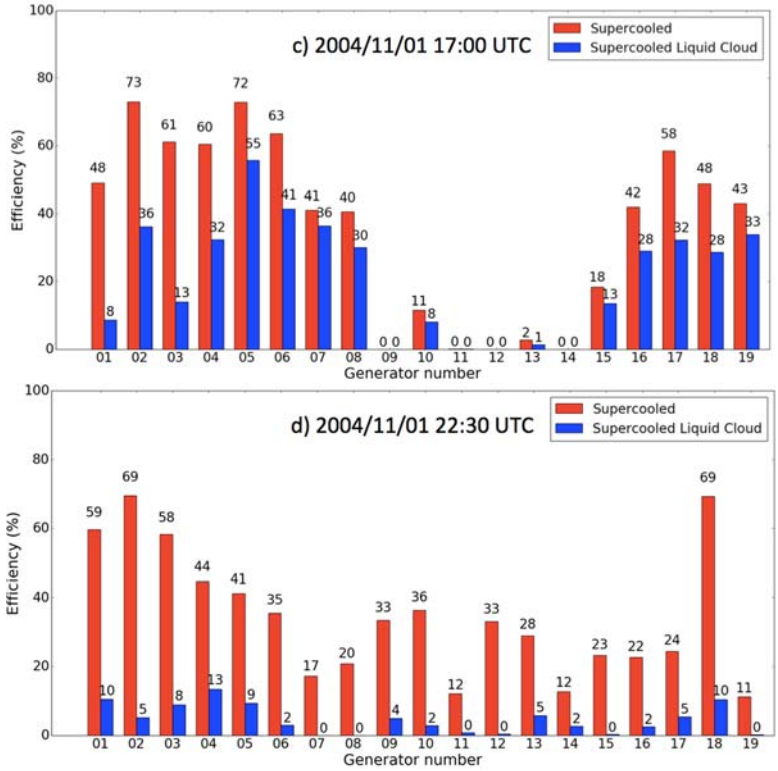

Figure 5.3 Generator efficiency (%) evaluated as the proportion of released AgI particles that reach a supercooled environment (red bars) or seedable supercooled liquid clouds (blue bars; environments defined as CSP_{AgI}=1). Top to bottom the panels show four snapshots during the same times shown in Figure 5.2. Generator locations are shown in Fig. 4.4.

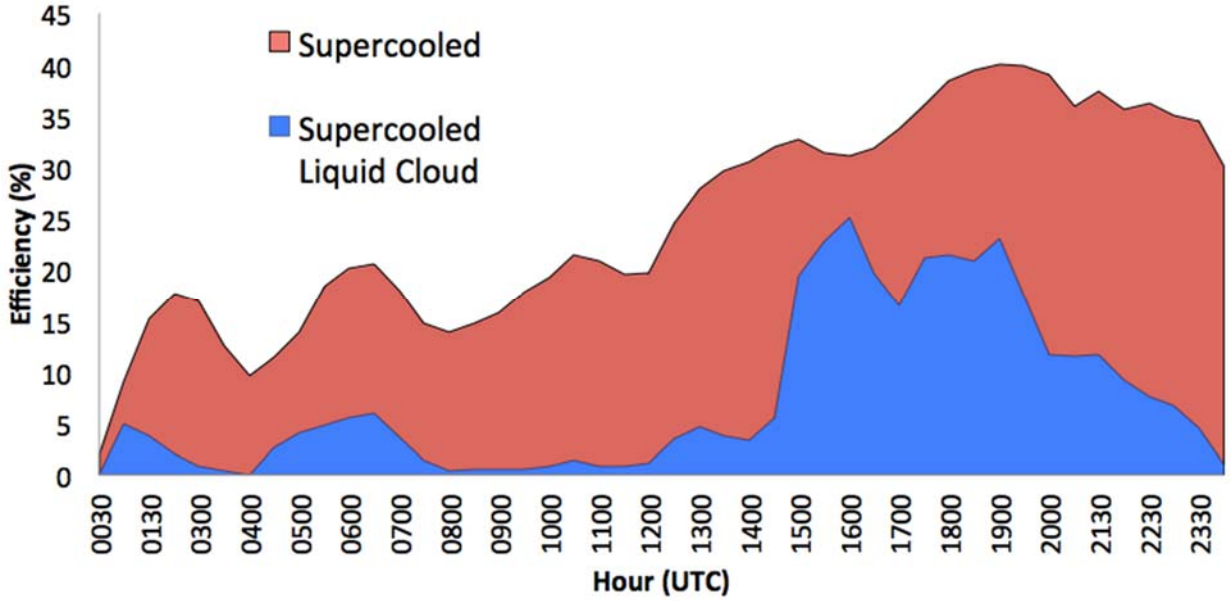

Figure 5.4 Generator efficiency (%) evolution for the Nov 1st, 2004 storm event. Red shaded area represents the evolution efficiency of AgI particles reaching supercooled environment, while the blue shaded area show the proportion of AgI particles reaching the seedable supercooled liquid clouds (environments defined as CSP_{AgI}=1). Cloud seeding efficiency averaged over all generator sites during the 1 Nov 2004 cold season storm event shown in Figures 5.2 and 5.3.

5.1.3 Efficiency of the proposed ground-based siting

We examined the overall simulated efficiency of the proposed generator siting for the set of cold season storms identified during 10 cold season periods (Nov-April) extending 2005-2014. The events were selected according to their precipitation accumulation over Laramie Range and using SNOTEL data. Following the approach shown above for a single storm event, we examined the seeding efficiency of all pre-defined cloud seeding generator locations as an average of the efficiency of all the individual storms.

Figure 5.5 shows the individual generators mean efficiency highlighting the proportion of AgI particles reaching the seedable supercooled liquid clouds and their relative impacts according to their location around the Laramie Range. In this analysis, we assume the seeding generator start operating above an efficiency threshold value of 10%. The relative efficiency of the different generators is not affected by this threshold and the same patterns emerge for efficiency values ranging from 10-50%. On average, generator 3-6, located in the northern slopes, appear to deliver the largest number of particles (up to 35%) into the seedable environments, whereas Generators 9-10 and 18-19 show relatively lower efficiency (26-28%). These results suggest that the northern slopes appear to favor upslope flow more frequently than locations farther away.

Figure 5.6 shows the mean number of operating hours per generator showing two distinct patterns with the best (1-6 and 11-14) and the worst (7-10 and 15-19) performing generators, which tends to agree with the optimal zoning provided by the source probability results examined earlier.

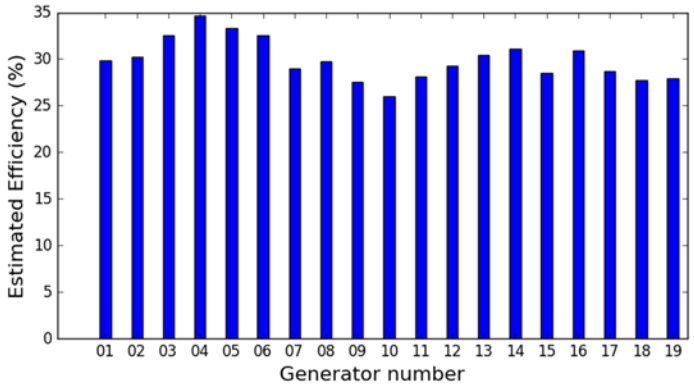

Figure 5.5 Generators efficiency [%] averaged for 448 cold season storms events during Nov-April extending 2004-2015. Efficiency is defined as the proportion of AgI particles reaching the seedable supercooled liquid clouds (environments defined as CSP_{AgI}=1). Generator locations are shown in Fig. 4.4.

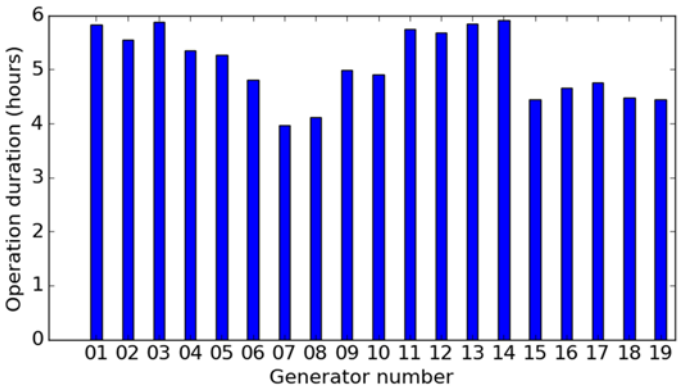

Figure 5.6 Operation duration (hours) averaged for 448 cold season storms events during Nov-April extending 2004-2015. Number of operating hours estimated for consecutive efficiency values above 10%. Generator locations are shown in Fig. 4.4.

6 Field Surveys- Proposed AgI Ground Generator and AgI/Liquid Propane Dispenser Locations

6.1 Preliminary selection of locations before site visits

Sites were originally selected to target the higher terrain of the northern Laramie Range from a both a NW and N-NE storm track. They were laid out with dirt road access in mind and spread out to provide ample coverage at approximately 15 miles from the target. No sites were selected in the south end of the range so as to not impact the Interstate 80 and Highway 34 travel corridors and also due to a lack of high altitude target areas.

Eight sites were initially selected in the Deer Creek range area and in the Duck Flats area above the Deer Creek and Boxelder creek drainages to cover NW to N to NE storm tracks. All sites except one were on private land to simplify the landowner access process.

Upon running the WRF Lagrangian plume dispersal model it was determined that sites further away (approx. 25 - 30 miles) would also target the areas above 8,000 ft MSL (i.e Buffalo Peak) so alternate sites (Casper 9-19) were selected in two general areas, the Bates Hole area and the other in the Deer Creek Road area. New sites were selected along existing roads for ease of access (Fig 6.1).

The first selection of sites (Casper 2-8) were kept to be used as LP dispenser type as they cause an immediate nucleation of available SLW at the dispenser and could benefit the upper Deer Creek and Boxelder creeks drainages. Also the LP type are less prone to midseason maintenance and repairs so having winter road access is not thought to be a significant issue. It was determined in the climatology (Chapter 3.2) that up to 77 hours per year, or more, may have favorable LP seeding conditions from these sites. These locations were also found to be favorable for AgI ground based cloud seeding generator sites. The purchase of LP cloud seeding dispenser are on the order of $10,000 per unit whereas remote high output AgI generators are on the order of $50,000 per unit. So 5 LP dispensers could be purchased at the same cost as 1 AgI generator. Additional observations of cloud base at the sites is needed to confirm the efficiency of the LP cloud seeding potential

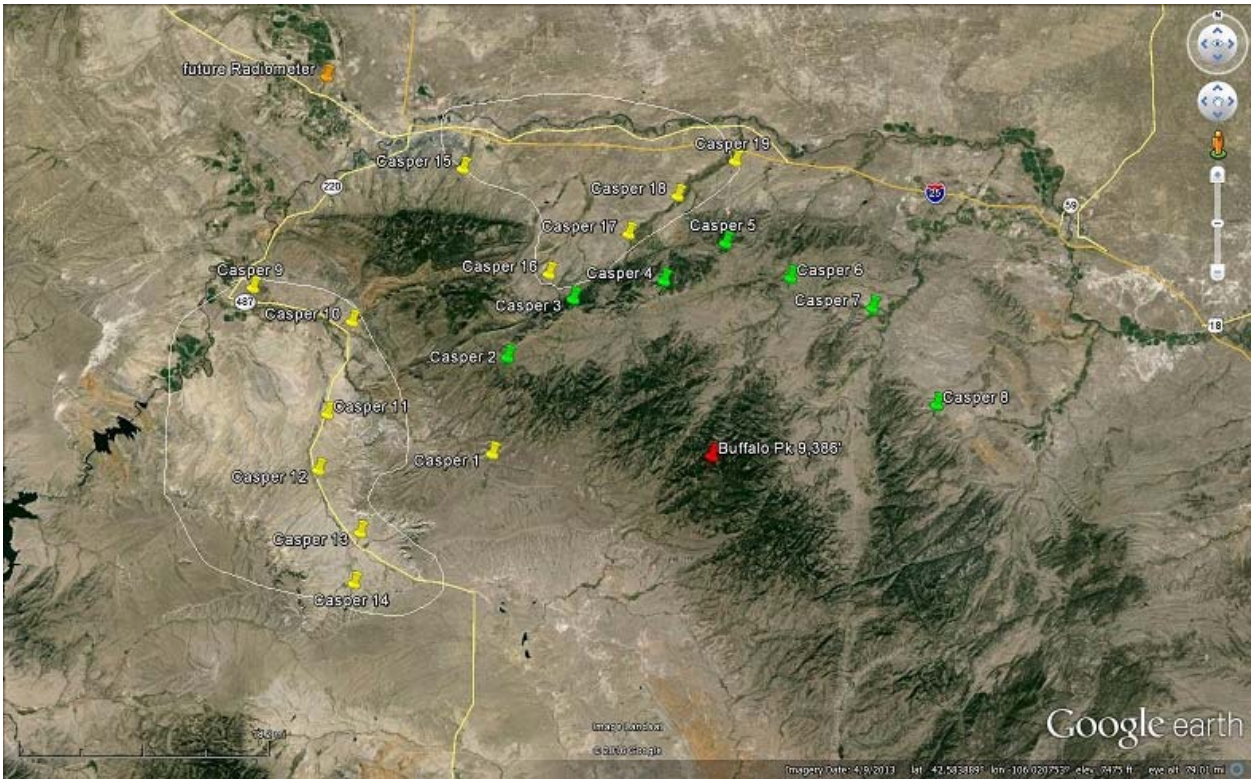

Figure 6.1 The superset of potential generator sites in the Laramie Range. Yellow pins are the ground bases AgI sites, and the green pins are the LP sites. Center of target red pin.

location	type	lat	lon	elev	land owner
Casper 1	AgI	42.505963°	-106.214819°	7321'	State Trust lands
Casper 2	LP/AgI	42.605939°	-106.195254°	7245'	private
Casper 3	LP/AgI	42.667358°	-106.103773°	7557'	private
Casper 4	LP/AgI	42.687352°	-105.975915°	6916'	private
Casper 5	LP/AgI	42.727203°	-105.889336°	6705'	private
Casper 6	LP/AgI	42.691921°	-105.796812°	6510'	private
Casper 7	LP/AgI	42.661432°	-105.680472°	5765'	private
Casper 8	LP/AgI	42.561286°	-105.588496°	5733'	private
Casper 9	AgI	42.674399	-106.558531	5444'	private
Casper 10	AgI	42.64089	-106.416681	5734'	private

Casper 11	AgI	42.544309	-106.449208	5936'	private
Casper 12	AgI	42.486128	-106.46042	6098'	private
Casper 13	AgI	42.421897	-106.399764	6421'	private
Casper 14	AgI	42.369024	-106.407131	6697'	BLM
Casper 15	AgI	42.801583	-106.262845	5468'	private
Casper 16	AgI	42.693266	-106.138796	5848'	State Trust lands
Casper 17	AgI	42.735953	-106.026635	5556'	State Trust lands
Casper 18	AgI	42.776137	-105.951596	5254'	State Trust lands
Casper 19	AgI	42.813054°	-105.876253	5328'	State Trust lands

Table 6.1 Generator locations and altitudes as well as land ownership.

6.2 Post Visit Site Selection

A site visit trip was scheduled for May 16th with the TREC Inc. Environmental Scientist who accompanied the DRI field technician to all the sites that were accessible during that very wet and stormy day.

All the upper elevation sites (Casper 1-8) were not visited due to the roads being extremely muddy and very high runoff in the creek crossings.

Sites Casper 9-19 were visited with some exceptions due to muddy conditions. A few of the sites were moved (Casper 14 -19) to allow better access due to wintertime road closures. Some sites were moved to get them on top of bluffs and out of valleys thus potentially preventing the seeding plume from getting trapped within inversion and not reaching the target. Local ranchers could be contacted and the sites further refined to be closer to the target if this is determined to be favorable.

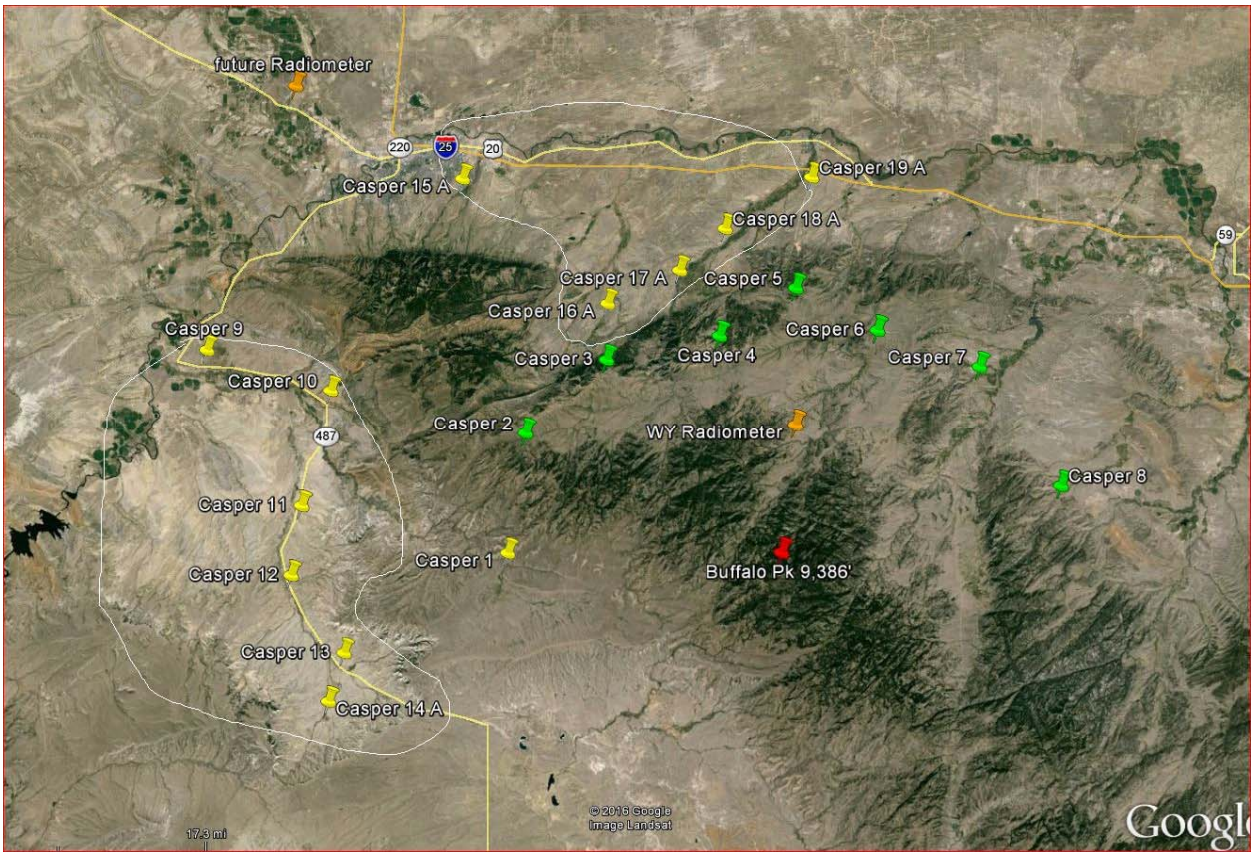

Figure 6.2 The final set of potential generator sites in the Laramie Range. Yellow pins are the ground bases AgI sites, and the green pins are the LP sites. Center of target red pin.

location	let	long	notes
Casper 1	42.505963°	-106.214819°	Off hwy SR 487 then on the Bates Creek RD CR 402 to north of the Bates Creek Reservoir. Site is on private land.
Casper 2	42.605939°	-106.195254°	Just south of the West Fork Deer Creek. Site would be accessed off hwy SR 487 then on the Bates Creek RD CR 402. Site is on private land. Recommend LP dispenser due to remote location and limited winter time access. Future road improvements for wind generation farm may improve access and possible upgrading to an AgI remote site.
Casper 3	42.667358°	-106.103773°	Off of Hat Six Rd SR 253 and then up CR 606 to Negro Hill. Site is on private land. Recommend LP dispenser due to remote location and limited winter time access. Future road improvements for wind generation farm may improve access and possible upgrading to an AgI remote site.
Casper 4	42.687352°	-105.975915°	Off Mormon canyon Rd CR 18 then east of Portuguese Pasture next to Little Deer Creek. Site is on private land. Recommend LP dispenser due to remote location and limited winter time access. Future road improvements for wind generation farm may improve access and possible upgrading to an AgI remote site.
Casper 5	42.727203°	-105.889336°	West of Mormon Canyon Rd CR 18 at Rocky Ridge. Site is on private land. Recommend LP dispenser due to remote location and limited winter time access. Future road improvements for wind generation farm may improve access and possible upgrading to an AgI remote site.
Casper 6	42.691921°	-105.796812°	Off of Boxelder Rd CR 17 just before Windy Ridge Rd CR 14 between Root Creek and Windy Ridge Creek. Site is on private land.
Casper 7	42.661432°	-105.680472°	Accessed from CR 13 west of La Prele then south along Spring Canyon Rd CR 11 along the Sawmill Creek. Site is on private land.
Casper 8	42.561286°	-105.588496°	Off of SR 94 then to Poison Lake RD CR 4 past the Raeber ranch the Maneater Creek area. Site is on private land.
Casper 9	42.674399	-106.558531	Off SR 220 on the west side of the range. On the north side of SR 487 on a knoll by sand pit. Site is on private land. Cattle in area so fencing may be required.
Casper 10	42.64089	-106.416681	Off SR 487, to the east on a ranch just south of the CR 402 Rd. Site is on private land just east of the school house.

Casper 11	42.544309	-106.449208	Off SR 487, to the east, in the open area north of CR 403. The site is NW of the Twin Buttes. Site is on federal BLM land.
Casper 12	42.486128	-106.46042	Off SR 487 a little past Lawn Creek. To the west in the open area, just north east of the Stinking Creek and it is on private land.
Casper 13	42.421897	-106.399764	Off SR 487, just before the turn off for SR 77. To the east, just inside the gate. Site is on private land. This site would have good potential to seed the Shirley Basin area.
Casper 14 A	42.381612°	-106.416902°	Off SR 77, this site was moved to the Stinky Rd ranch due to the end of hwy vehicle access during winter. This site would have good potential to seed the Shirley Basin area. Site is on private land.
Casper 15 A	42.818537°	-106.268354°	Moved this site to Casper Country Club for better mid-season access. Site is on private land in the Golf Club maintenance yard.
Casper 16 A	42.714455°	-106.102677°	Moved this site to ridgeline road above the valley to achieve a better line of site to the range and access during the winter months.
Casper 17 A	42.742279°	-106.020870°	Moved this site to east side of road on private land, in a field. This site could be moved closer to the foothills and on private ranch land (Kimball Ranch).
Casper 18 A	42.777256°	-105.969194°	Moved to the bluff above the ranches, out of the low valley area. Cell coverage available here. Site is on private land.
Casper 19 A	42.820233°	-105.870513°	Moved to top of bluff before dropping into the valley. This site has great cell signal and line of site to the range. Site is on private land.

Table 6.2 Final generator locations and notes.

6.3 Summary of Site Visits

Upon visiting these select sites and the favorable cost and climatological findings DRI has determined that using LP dispensers at the higher, non-paved road inaccessible sites (Casper 2-8) would be a better choice than ground-based remote AgI generators as they tend to be less prone to needing mid-season maintenance and they produce an immediate nuclei due to temps at the nozzle of near -40^{o}C. This would be an advantage as these sites are often in cloud with likely SLW enough of the time to warrant this type of equipment.

The AgI type generators deployed in the North to Northwest areas the project design cover the majority of seedable events for Scenario 2. The plume model results and high Froude numbers for most cases suggests that the seeding material will travel from the release areas

along the west slope and then turn east up the slopes to the higher altitude target areas near Buffalo Peak.

Access to the sites for the entire season would have difficulties, but siting along roads and using the LP dispensers at the higher elevations would mitigate this. Many rancher –land owner contacts are necessary to ensure gaining access to suitable sites that have maintained roads, and are in ideal locations to deliver the seeding agents to the target areas.

Photos taken during the Site visits (below):

Figure 6.3 Site 9

Figure 6.4 Site 10

Figure 6.5 East of Site 12

Figure 6.6 Site 14 access road

Figure 6.7 Site 16 access road

Figure 6.8 Below Site 18 at CR 19/20 intersection

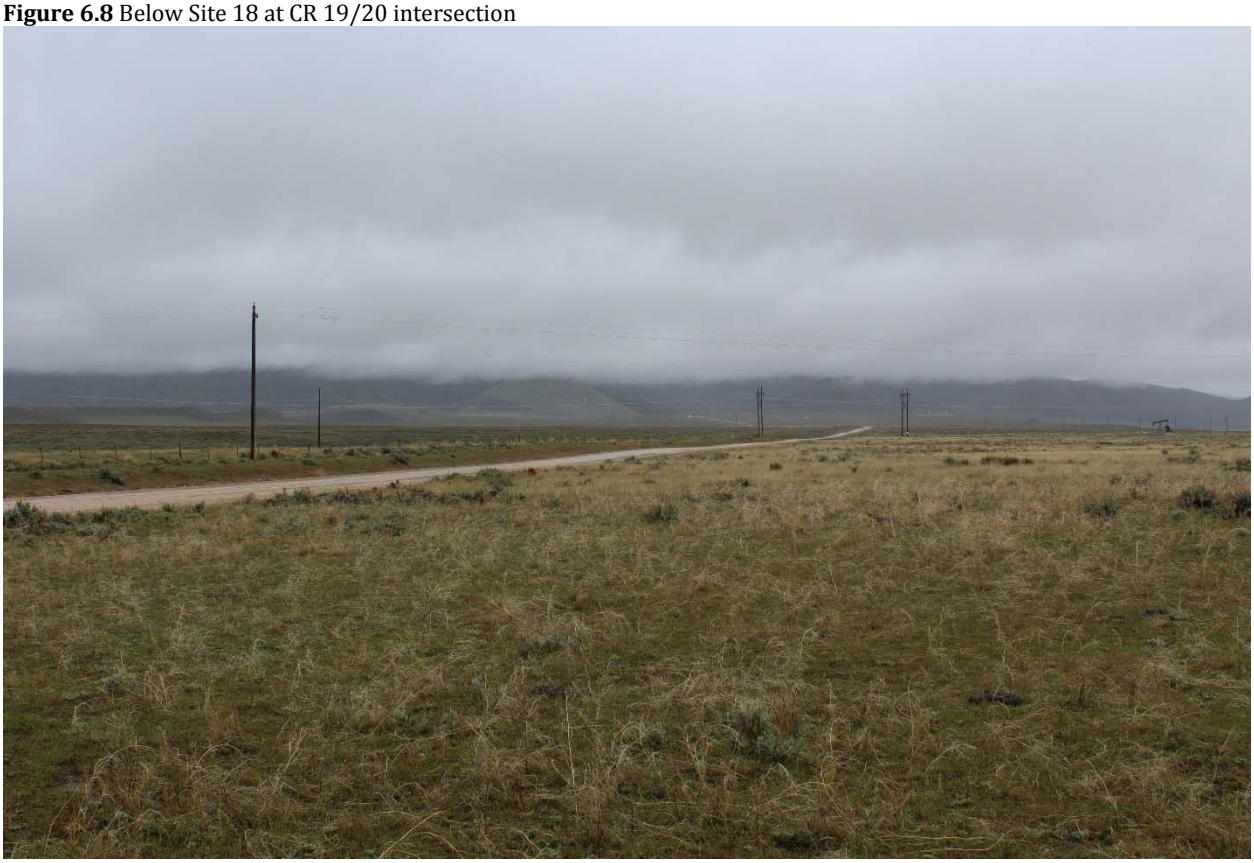

Figure 6.9 Site 19 looking along CR 18

7 Access/Easements and Environmental Permitting/Reporting

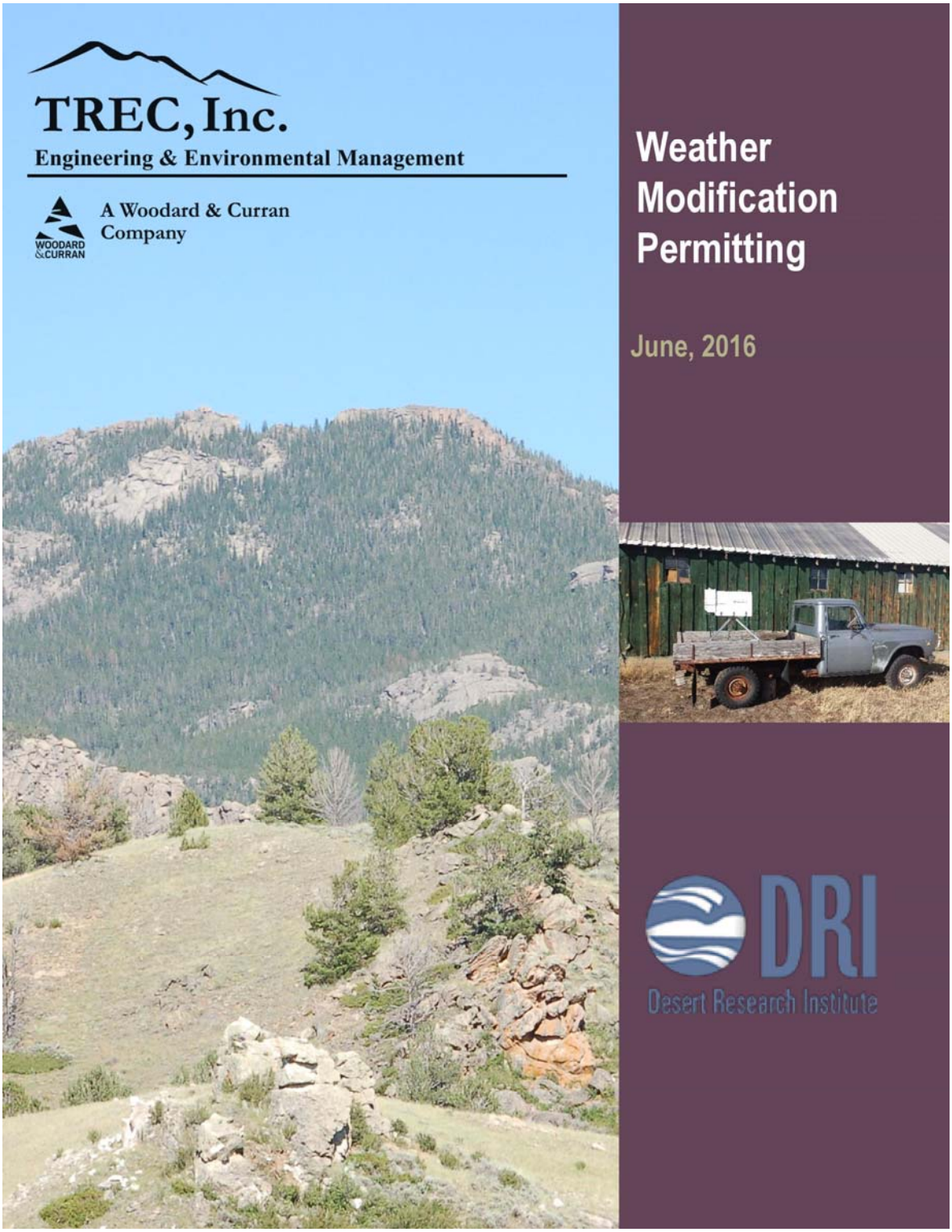

Executive Summary

TREC, Inc. (TREC) is providing this report to Desert Research Institute (DRI) to be included in the Laramie Range Siting and Design, Level III Study as contracted by the Wyoming Water Development Commission. This study is one of three mountain ranges being evaluated for cloud seeding based on the preliminary summary of the Wyoming Weather Modification Pilot Project.

This report provides a summary of necessary permits, certificates, and approvals required to commence weather modification operations for the Laramie Range, Wyoming. The information provided covers both siting of ground-based ice-nucleus generators and the activity of aerial cloud seeding.

DRI has identified eleven locations for siting of the silver iodide generating stations best suited for producing favorable weather modification results. These locations are generally situated at the northern end of the Laramie Range along two separate routes as shown in Figure 1:

- Highway 487 between Highway 220 and the base of the Shirley Basin; and
- The Hat Six / Deer Creek road loop between Casper and Glenrock.

As locations may shift during final siting, the location of the generators may include a mix of private, state, and Federal lands. Currently there are Federal and private lands identified (Table 1). Access and easements required to site the generators varies between the agencies with the Bureau of Land Management being responsible for Federal Lands and the Office of State Lands and Investments managing the state lands in the area. Both agencies require a "special use" permit for the siting of the generators, with no other permits required for the operation of the equipment or access to the generator. Private lands in Wyoming have no formal permitting process for the siting of generators; however, it is recommended that a formal access agreement is executed between the land owner and the generator station operator.

The activity of cloud seeding for the purposes of weather modification can only be conducted in Wyoming with approval from the Wyoming State Engineers Office (WSEO). The WSEO reviews applications for weather modification and approves only those operations which are conducted by qualified individuals. This is the only permit needed in the State of Wyoming for the activity of weather modification. The application requires a written description of activities such as aerial, propane, or other seeding methods. The approvals required for siting the generators and conducting weather modification within Wyoming are described in Tables 2 through 4.

If it is determined aircraft seeding is best alternative for agent dispersal, the proposed project will have to adhere to Federal Aviation Administration (FFA) regulations as cloud seeding is considered a restricted flight category and requires additional airworthiness certification as outlined in Table 5.

The National Oceanic and Atmospheric Administration (NOAA) is the federal agency to which weather modification activities conducted in the United States must be reported. Prior to the

beginning of each project season, an initial report will need to be submitted and subsequent interim and final reports based on the duration of the proposed project. Table 6 provides more detailed information regarding NOAA reporting requirements.

Currently, there are no US Forest Service (USFS) administered lands within the proposed project area. If future operation plans have the potential to impact USFS administered lands, an application, Standard Form 299, and supporting documentation will need to be prepared. Based on previous weather modification projects in the State of Wyoming, the USFS has determined weather modification fell within a category of actions listed in Chapter 30 of the Forest Service NEPA Handbook (FSH) that are excluded from documentation in an Environmental Assessment or Environmental Impact Statement (FSH 1909.15, Chapter 31.11 [a] [3]). Therefore, a Categorical Exclusion (CE) and supporting documentation will need to be prepared to analyze potential impacts to the environment. The CE will require scoping studies, site surveys (biological assessment), other agency consultation performed under the National Environmental Policy Act (NEPA). In addition, an annual Operations Plan will need to submitted to the USFS prior to commencement of operations and for each subsequent operating season. Table 7 provides more information regarding the Annual Operations Plan.

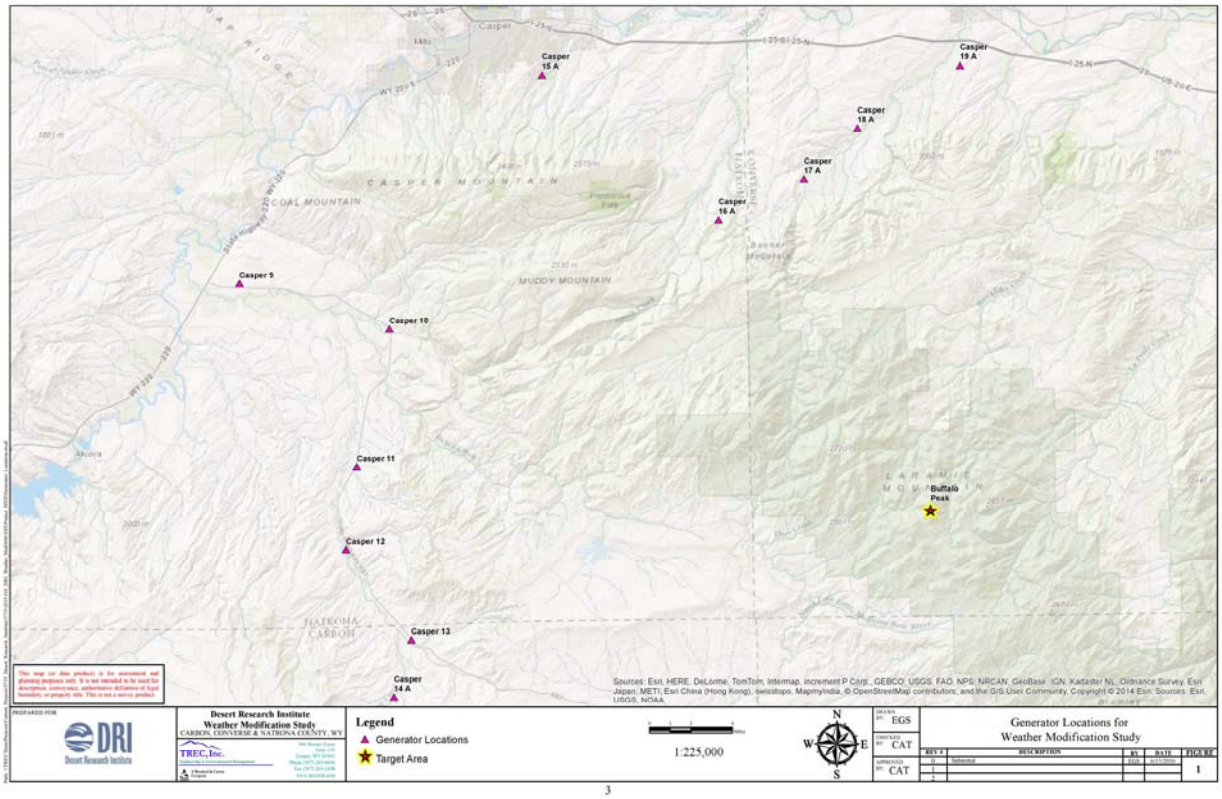
Casper 15 A
Casper 19 A
Casper 18 A
Casper 17 A
Casper 16 A
Casper 9
Casper 10
Casper 11
Casper 12
Casper 13
Casper 14 A
Buffalo Peak
CASPER MOUNTAIN
CORAL MOUNTAIN
MUDDY MOUNTAIN
SOUTH CASPER
LARAMIE MOUNTAIN
NATRONA CARBON
Alcova
Casper
I-25 N
WY 220
WY 253
Sources: Esri, HERE, DeLorme, TomTom, Intermap, increment P Corp., GEBCO, USGS, FAO, NPS, NRCAN, GeoBase, IGN, Kadaster NL, Ordnance Survey, Esri Japan, METI, Esri China (Hong Kong), swisstopo, MapmyIndia, © OpenStreetMap contributors, and the GIS User Community, Copyright © 2014 Esri. Sources: Esri, USGS, NOAA
This map (or data product) is for assessment and planning purposes only. It is not intended to be used for description, conveyance, authoritative definition of legal boundary, or property title. This is not a survey product.
PREPARED FOR
DRI
Desert Research Institute
Desert Research Institute
Weather Modification Study
CARBON, CONVERSE & NATRONA COUNTY, WY
TREC, Inc.
Legend
Generator Locations
Target Area
1:225,000
N
W
E
S
DRAWN BY: EGS
CHECKED BY: CAT
APPROVED BY: CAT
Generator Locations for
Weather Modification Study
REV #
DESCRIPTION
BY
DATE
FIGURE
0
Submittal
EGS
12/15/2014
1

3

Table 1: List of Proposed Sites and Ownership

Location	Latitude	Longitude	Elevation	Land Ownership
Casper 9	42.674399	-106.558531	5444'	private
Casper 10	42.64089	-106.416681	5734'	private
Casper 11	42.544309	-106.449208	5936'	Federal (BLM)
Casper 12	42.486128	-106.46042	6098'	private
Casper 13	42.421897	-106.399764	6421'	private
Casper 14 A	42.381612°	-106.416902°	6697'	private
Casper 15 A	42.818537°	-106.268354°	5468'	private
Casper 16 A	42.714455°	-106.102677°	5848'	private
Casper 17 A	42.742279°	-106.020870°	5556'	private
Casper 18 A	42.777256°	-105.969194°	5254'	private
Casper 19 A	42.820233°	-105.870513°	5328'	private

Table 2: Wyoming Office of State Lands and Investments

Permit Name	Application for Temporary Use Permit
Regulatory Agency	Wyoming Office of State Lands and Investments (OSLI)
Statute/Regulation	
Application Process	• Determine site grazing lessee • Have grazing lessee sign "Surface Lessee Notification and Comment" form (if applicable) • Complete "Application for Temporary Use Permit" form • Typically, the Wyoming Game and Fish Department (WGFD) reviews all applications on State of Wyoming lands and will require their approval
Application Development Time	Approximately one month to coordinate with grazing lessee and complete application
Permit Fees	• $50 one-time permit application fee • $50 one-time payment to grazing rights lessee • $100 annual fee per site
Filing Date	At least one month prior to deployment of equipment
Processing Time	Approximately three weeks
Expiration Date	Permit is valid for five years, renewable
Other Notes	• One permit application may be submitted for multiple sites • Permit must be approved by State Board of Land Commissioners at board meeting, temporary authorization is typically granted by OSLI staff
Useful Resources	Application for Temporary Use Permit form: http://slf-web.state.wy.us/Surface/TemporaryUseApplicationRevised2015.pdf Surface Lessee Notification Form: http://slf-web.state.wy.us/surface/easements/surface_lessee.doc
Contacts	Brenda Davis: (307) 777-3331

Table 3: Bureau of Land Management

Permit Name	Land Use Application and Permit
Regulatory Agency	Bureau of Land Management (BLM)
Statute/Regulation	USC 1732
Application Process	• Complete Land Use Application and Permit Form (BLM Form 2920-1)
Application Development Time	Approximately two weeks
Permit Fees	• $428 one-time permit processing fee • $122 one-time monitoring fee
Filing Date	At least two months prior to deployment of equipment
Processing Time	Approximately 30-60 days
Expiration Date	Permit is good for three years, renewable
Other Notes	• One permit application may be submitted for multiple sites • BLM will conduct site specific reviews for ecological resource impact potential (Sage Grouse, Critical Big Game Habitat, etc.) • Contact BLM very early to verify process and requirements as process may vary
Useful Resources	Application for Land Use Permit form: http://www.blm.gov/style/medialib/blm/noc/business/eforms.Par.26383.File.dat/2920-001.pdf
Contacts	Randy Sorenson: (307) 262-0328

Table 4: Wyoming State Engineers Office

Permit Name	Application for Permit to Engage in Weather Modification Activities in the State of Wyoming
Regulatory Agency	Wyoming State Engineers Office (WSEO)
Statute/Regulation	W.S. 9-1-905 – 9-1-909, 1977
Application Process	• Complete application form (attached) • Application includes full description of activities proposed
Application Development Time	Approximately two weeks
Permit Fees	$50 Application fee
Filing Date	At least 30 days prior to commencement of project
Processing Time	Approximately one week
Expiration Date	One Year
Other Notes	• Weather modification may only be conducted by individuals deemed adequately qualified by the State Engineers Office • Reporting to SEO required within 30 days of a commencement of activities • Monthly reports must be provided for the duration of the seeding season. Detailed information includes date and length of each seeding event and the amount of seeding agent burned
Useful Resources	• ***Attachment 1*** of this report provides the WSEO application form • ***Attachment 2*** are the Weather Modification Rules • SEO Office Website: https://sites.google.com/a/wyo.gov/seo/
Contacts	Lee Arrington: (307) 777-6171

Table 5: Federal Aviation Administration

Permit Name	Application for U.S. Airworthiness Certificate (FAA Form 8130-6)
Regulatory Agency	Federal Aviation Administration (FAA)
Statute/Regulation	49 USC 44103 – 14 CFR Part 21
Application Process	• Complete application form • Present modified plane for inspection
Application Development Time	Approximately two weeks
Permit Fees	N/A
Filing Date	Prior to commencement of restricted flight
Processing Time	Approximately one month – dependent on inspection
Expiration Date	N/A
Other Notes	• Likely prior obtained by contracting flight company • Required for restricted flight (Cloud Seeding)
Useful Resources	• Application Form: http://www.faa.gov/documentLibrary/media/Form/Approved_OMB_8130-6_Expires_2015.pdf
Contacts	Denver Aircraft Certification Office: (303) 342-1080

Table 6: National Oceanic and Atmospheric, Department of Commerce

Report Name	Weather Modification Activities Report
Agency	National Oceanic and Atmospheric (NOAA)
Statute/Regulation	• Section 6(b) of Public Law 92–205 • 15 CFR Part 980
Reporting Process	Initial Report (Form 17-4) Describes the intended target, the seeding agent(s), the firm or person(s) conducting the operations, the project start and end dates, and the sponsor Interim Reports (Form 17-4a) Provides number of days of actual modification activities, net hours of agent release, and total amount of agent used. Final Report (Form 17-4a) The content of the final report is the same as the interim report(s) *15 CFR Part 980 provides a more detailed account of information requirements for all reports. Forms 17-4 and 17-4a are provided in ***Attachment 3*** of this report
Filing Date	Initial Report 10 days prior to commencement of project or activity and/or prior to the beginning of each season Interim Report January 1 in any year, not later than 45 days thereafter. Only required if the project long term (six months continuous duration) Final Report No later than 45 days after the completion of the project
Other Notes	• Although not required, copies of NOAA filings can be submitted to the WSEO • 15 CFR Part 980 provides a more detailed account of information requirements for all reports • Respondents have a choice of either electronic or paper forms. Methods of submittal include email of electronic forms, mail and facsimile transmission of paper forms.
Useful Resources	• ***Attachment 3*** of this report provides NOAA Forms 17-4 and 17-4a
Contacts	Karen Williams: (301) 734-1196 (NOAA)

Table 7: US Forest Service

Report Name	Annual Operating Plan
Agency	US Forest Service (USFS)
Statute/Regulation	National Forest Management Act
Reporting Process	Submit an Annual Operating Plan including general project information such as dates for each season, generator maintenance, ground generator locations, design criteria, suspension criteria, and plans for monitoring and evaluation
Filing Date	Submitted prior to commencement of project or activity and/or prior to the beginning of each season
Other Notes	• The Operating Plan is only required if USFS administered lands have the potential to be impacted by the proposed weather modification project • The permittee and the USFS will review and discuss potential changes to the Operating Plan prior to each new operating season • The USFS supervisor or their designee, must approve, in writing and in and advance, any changes to the Standards of Operation in the Annual Operating Plan
Useful Resources	• Medicine Bow National Forest Website: http://www.fs.usda.gov/main/mbr/home
Contacts	Medicine Bow National Forest: (307) 745-2300

Attachment 1:

WSEO Application Form

STATE OF WYOMING
STATE ENGINEER'S OFFICE
CHEYENNE, WYOMING

APPLICATION FOR PERMIT
TO ENGAGE IN
WEATHER MODIFICATION ACTIVITIES
IN THE STATE OF WYOMING

I, _____ of_____

_____, County of _____,

State of _____, hereby apply for a permit to engage in weather modification experiments and activities in the State of Wyoming provided under the provisions of W.S. 9-1-905 - 9-1-909, 1977, and being duly sworn according to law, upon my oath say:

1. The name of the applicant is:_____

_____

2. The address of the applicant is:_____

_____

3. As required by law, the following named member(s) of our firm, institution or agency has (have) adequate qualifications in the atmospheric sciences (please attach resumes):_____

_____

_____

In the case of a corporation or partnership, a copy of a resolution signed by all officers is attached, providing the above-named individual(s) the authority to act on the behalf of said corporation or partnership and said corporation or partnership to assume full responsibility for the above-named individual(s) as their designated agent.

4. The following equipment and trained personnel will be utilized in conducting the experiments or activities (describe fully):

5. Describe fully the previous experience by the individual(s) and the firm, corporation or agency in weather modification experiments or activities:

(NOTE: ITEMS 6, 7 AND 8 ARE NOT APPLICABLE TO INSTITUTIONS OR GOVERNMENTAL AGENCIES.)

6. Evidence of financial responsibility of the applicant and liability accompanies this application as follows:

7. It is agreed that evidence of adequate liability insurance will be furnished prior to the time the permit is issued. The minimum amount of liability coverage required will be Three Hundred Thousand Dollars ($300,000.00). The State Engineer may require more than Three Hundred Thousand Dollars ($300,000.00) of liability coverage if the circumstances indicate desirability of additional coverage.

8. The applicant agrees, if the permit herein applied for is granted, to indemnify and save harmless the State of Wyoming, and any and all State officials or employees, from any liability or responsibility, resulting from activities engaged in under such permit.

9. References:

(Give names and addresses of five responsible people, companies or corporations having personal knowledge of the applicant(s) character and professional reputation.)

Name	Address
_____	_____
_____	_____
_____	_____
_____	_____
_____	_____

10. List proposed activities with dates and locations and attach a map showing the general location of target area and generators or other equipment and facilities. (Describe fully the proposed activities, techniques, procedures and the specific areas covered. Attach additional pages or report(s) as necessary to complete this item).

11. The applicant agrees to notify the State Engineer of commencement of each separate activity or operation and to file a written report with the State Engineer of the activity covered by the Permit within thirty (30) days of completion of the activity. Progress reports will also be filed with the State Engineer every 30 days if in the opinion of the State Engineer it appears necessary or advisable.

12. All weather modification activities shall be conducted under the actual and personal supervision of the following named individual or individuals:

_____

_____

_____

13. The following named individual, a resident of the State of Wyoming, is designated for service: (This portion is to be completed by out-of-state corporations or firms only.)

Name:_____

Address _____

14. Articles of Incorporation for out-of-state corporations must be filed with the Secretary of State's Office and evidence of such filing is attached to this application.

STATE OF WYOMING)

)

County of _____)

I, _____ hereby affirm that the statements and information contained in this application are true in every respect to the best of my knowledge and belief.

_____

Signature of Applicant

Subscribed and sworn to before me this _____ day of _____, 20 ___ .

_____

Notary Public

My Commission Expires _____.

Attachment 2:

WSEO Weather Modification Rules

CHAPTER II.

POWERS AND DUTIES OF BOARD

Section 1. Weather' Modification Operations. Weather modification operations shall be conducted in the case of individuals holding permit only under the direct and actual supervision of the person holding such permit, and in.case of a corporation, a partnership, institution, association, or governmental agency, shall be conducted only under the actual and personal supervision of a person or- persons designated by such corporation, partnership, or association, submitted to the Board and by such Board approved; provided such person or persons can demonstrate to the Board's satisfaction that he has or they have adequate qualifications in the atmospheric sciences. (Amended W-25

Section 2. Permit Required. It shall be unlawful for anyone to engage in weather modification activities except under and in accordance with a permit issued by the State, Engineer. The State Engineer may issue such permit only upon the recommendation of the Weather Modification Board, and in such form as prescribed by the Board. (5 9-270, Wyo. Stat. 1957.)

Section 3. Permits-to Conduct-Weather-Modification Experiments or Activities. A permit shall be issued for. each experiment or activity within a specific period of time, and shall be revocable by the State Engineer upon recommendation of the Board, in accordance with such procedures as the Board shall establish.- (S 9-271, Wyo.-Stat., 1957, as amended by S 1, C..104, S.,L. of W o..1.971.)
(Amended, *MAY* 2 3 1971

a. A fee of Twenty-Five Dollars ($25.00) shall be charged for each permit, or renewal thereof, so, issued. (S 9-2 ' 71,,Wyo. Stat. 1957, as amended by S 1, C..104,-.S. L. of Wyo. 1971.) (Amended..

b. A permit shall be issued only to a person or @ persons who can demonstrate to the Board's satisfaction, that he has or they have adequate qualifications in the atmospheric sciences, pursuant to 5 9-271, Wyoming Statutes 1957, as amended by S 1, Chapter, 104, Session Laws of Wyoming 1971. (Amended *MAY* 2 *@, 1971*

c. Said permit will be issued for a 1-year period, extending from October 1 of one (1) year to September 30 of the following year. All permit ' s shall terminate on September 30. The granting of a-permit shall not guarantee the holder thereof any right of-renewal whatsoever.

Section 4. Rules Governing Permits. A permit shall be issued for each experiment or activity specifying a definite period of time within which such experiment or activity may be conducted and a definite area of terrain over which the experiment or activity may extend. Such permit must contain the following:

. a. A requirement that the applicant will notify the Board of commencement of each separate activity or operation, and that progress reports in writing shall be made to the Board every thirty (30) days during the period of the experiment if in the opinion of the Board, it appears necessary, or advisable.

b.A complete report in writing covering the whole of every experiment shall be filed with the Board within thirty (30)days after the experiment or activity is completed.

Section 5. Service of Process. All licensees shall designate a resident of the State of Wyoming for service.

Section 6. Corporation and Partnerships.

a. Articles of Incorporation for out-of-state corporations must be filed with the Secretary of State's Office, and evidence of iddh"filings must accompany the application for permit filed with the Board.

b. A copy of a resolution signed by all officers, of a corporation or partnership must accompany the application for permit., I giving the member or members of the firm who can demonstrate to the Board's satisfaction that he has or they have adequate qualifications in the atmospheric sciences, power of attorney to act for said corporation or partnership', and indicating that s . aid -corporation or partnership agrees to assume full responsibility for this individual or individuals as their designated agent.or agents.
(Amended MAY 2 3 1971

Section 7.Responsibility and Liability. All applicants, except for institutions or governmental agencies, shall furnish the following evidence of responsibility and liability either at the time their application is submitted or before a permit is issued:

a. Evidence to adequate liability insurance will be furnished prior to the time a permit is issued. The minimum of liability coverage required will be Three Hundred.Thousand Dollars ($300,000.00). 'The Board may require more than, Three Hundred Thousand Dollars ($300,000.00) of liability coverage if the circumstances indicate desirability of additional coverage.

b. A certified copy of a Performance Bond, the amount of which shall be equal to or greater than the contract price for the weather modification activities, is to be furnished prior to the time a permit is issued.

c. The application for permit and the permit shall contain a statement holding the Board, the State of Wyoming and any State officers, officials, and employees harmless from any liability. (S 9-276, Wyo. Stat. 1957.)

Section 8. Fees. A fee of Twenty-Five Dollars ($25-00) shall be charged for

each permit, or renewal thereof, so
issued.(S 9-271, Wyo. Stat. 1957, as amended by S 1, Ch. 104, S. L. of Wyo. 1971.)
(See also Chapter I, Section 7 -
Funds.) (Amended MAY 2 3 1971

Section 9. Authority to Receive and Accept Funds. The Board is authorized to receive and accept for and in behalf of the State, any and all funds which may be offered or become available from federal grants or appropriations, private gifts, donations or bequests, or any other source, and to expend such funds for the expenses of administering this Act [SS 9-267 to 9-276], and for the encouragement of experimentation in weather modification by the University of Wyoming, or any other appropriate State or public agency, either by direct grant, by contract, or other cooperative means. (S 9-275, Wyo. Stat. 1957.)

Section 10. Failure to Obtain Permit, Penal@Z. Any person, persons, corporation, institution, or group engaging in a weather modification experiment without a permit shall be guilty of a felony, and upon conviction, subject to a fine not to exceed One Thousand Dollars ($1,000.00) or by imprisonment in the penitentiary for not less than one (1) nor more than five (5) years. (S 9-274, Wyo. Stat. 1957.)

Section 11. Amendment of Rules. Any amendments to these Rules shall become effective as provided by SS 9-276.21 and 9-276.22, Wyo. Stat. 1957, as enacted by SS 3 and 4, Ch. *108,* S. L. of Wyo. 1965.

Attachment 3:

NOAA Forms 17-4 and 17-4a

Complete in accordance with instructions on reverse and forward copy:

TO: National Oceanic and Atmospheric Administration
Office of Oceanic and Atmospheric Research
1315 East-West Highway SSMC-3 Room 11216
Silver Spring, MD 20910

Form Approved: OMB No. 0648-0025 Expires 09/30/2014

NOAA FORM 17-4 (4-81) U.S. DEPARTMENT OF COMMERCE
NAT'L OCEANIC AND ATMOSPHERIC ADM.

INITIAL REPORT ON WEATHER MODIFICATION ACTIVITIES (P.L. 205, 92ND. CONGRESS)

1. PROJECT OR ACTIVITY DESIGNATION, IF ANY

2. DATES OF PROJECT

a. DATE FIRST ACTUAL WEATHER MODIFICATION ACTIVITY IS TO BE UNDERTAKEN

3. PURPOSE OF PROJECT OR ACTIVITY

b. EXPECTED TERMINATION DATE OF WEATHER MODIFICATION ACTIVITIES

4. (a) SPONSOR			**4. (b) OPERATOR**		
NAME			NAME		
AFFILIATION		PHONE NUMBER	AFFILIATION		PHONE NUMBER
STREET ADDRESS			STREET ADDRESS		
CITY	STATE	ZIP CODE	CITY	STATE	ZIP CODE

5. TARGET AND CONTROL AREAS (See Instructions)

TARGET AREA		CONTROL AREA	
LOCATION	SIZE OF AREA SQ.MI	LOCATION	SIZE OF AREA SQ.MI.

6. DESCRIPTION OF WEATHER MODIFICATION APPARATUS, MODIFICATION AGENTS AND THEIR DISPERSAL RATES, THE TECHNIQUES EMPLOYED, ETC. *(See Instructions)*

7. LOG BOOKS: *Enter name, affiliation, address, and telephone number of responsible individual from whom log books or other records may be obtained.*

NAME		
AFFILIATION		PHONE NUMBER
STREET ADDRESS		
CITY	STATE	ZIP CODE

THIS REPORT IS REQUIRED BY PUBLIC LAW 92-205; 85 STAT 735; 15 U.S.C. 330b. KNOWING AND WILLFUL VIOLATION OF ANY RULE ADOPTED UNDER THE AUTHORITY OF SECTION 2 OF PUBLIC LAW 92-205 SHALL SUBJECT THE PERSON VIOLATING SUCH RULE TO A FINE OF NOT MORE THAN $10,000, UPON CONVICTION THEREOF.

8. SAFETY AND ENVIRONMENT

☐ YES ☐ NO Has an Environmental Impact Statement, Federal or State been filed? If yes, please furnish a copy as applicable.

☐ YES ☐ NO Have provisions been made to acquire the latest forecasts, advisories, warnings, etc. of the National Weather Service, Forest Service, or others when issued prior to and during operations? If yes, please specify on a separate sheet.

☐ YES ☐ NO Have any safety procedures *(operational constraints, provisions for suspension of operations, monitoring methods, etc.)* and any environmental guidelines *(related to the possible effects of the operations)* been included in the operational plans? If yes, please furnish copies or a description of the specific procedures and guidelines.

9. OPTIONAL REMARKS *(See Instructions. Use Separate Sheet.)*

NAME			**CERTIFICATION:** I certify that the above statements are true, complete and correct to the best of my knowledge and belief.	
AFFILIATION			SIGNATURE	
STREET ADDRESS			OFFICIAL TITLE	
CITY	STATE	ZIP CODE	DATE	PHONE NUMBER

NOAA FORM 17-4A (4-81)

U.S. DEPARTMENT OF COMMERCE
NATIONAL OCEANIC AND ATMOSPHERIC ADMINISTRATION

Form Approved OMB No. 0648-0025
Expires 09/30/2014

INTERIM ACTIVITY REPORTS AND FINAL REPORT

This report is required by Public Law 92-205; 85 Stat. 735; 145 U.S.C. 330b. Knowing and willful violation of any rule adopted under the authority of Section 2 of Public Law 92-205 shall subject the person violating such rule to a fine of not more than $10,000, upon conviction thereof.

NOAA FILE NUMBER

☐ INTERIM REPORT ☐ FINAL REPORT

Complete in accordance with instructions on reverse and forward one copy to:
National Oceanic and Atmospheric Administration
Office of Oceanic and Atmospheric Research
1315 East-West Highway SSMC-3 Room 11216
Silver Spring, MD 20910

REPORTING PERIOD

FROM | TO

MONTH	(a) NUMBER OF MODIFICATION DAYS	(b) NUMBER OF MODIFICATION DAYS PER MAJOR PURPOSE				(c) HOURS OF APPARATUS OPERATION BY TYPE		(d) TYPE AND AMOUNT OF AGENT USED				
		INCREASE PRECIPITATION	ALLEVIATE		OTHER	AIRBORNE	GROUND	SILVER IODIDE	CARBON DIOXIDE	UREA	SODIUM CHLORIDE	OTHER
			HAIL	FOG								
JANUARY												
FEBRUARY												
MARCH												
APRIL												
MAY												
JUNE												
JULY												
AUGUST												
SEPTEMBER												
OCTOBER												
NOVEMBER												
DECEMBER												
TOTAL	0	0	0	0	0	0	0	0	0	0	0	0
TOTALS FOR FINAL REPORT												

DATE ON WHICH FINAL WEATHER MODIFICATION ACTIVITY OCCURRED *(For Final Report only.)*

CERTIFICATION: I certify that all statements in this report on this weather modification project are complete and correct to the best of my knowledge and are made in good faith.

NAME OF REPORTING PERSON

AFFILIATION

SIGNATURE

STREET ADDRESS

OFFICIAL TITLE

CITY | STATE | ZIP CODE

DATE

8 Establishment of an Operational Criteria

8.1 Introduction

The operational criteria includes defining the meteorological conditions in which cloud seeding can be successfully conducted, creating a set of resources to identify those meteorological conditions, creating a web site to communicate the cloud seeding operations to the public and interested stake holders, identifying sources of weather and climate conditions that would cause suspensions of cloud seeding operations.

The initiation of cloud seeding operations requires the identification of clouds containing supercooled liquid water at the altitudes that can be reached by seeding plumes, identification of temperatures suitable for cloud seeding, identification of winds suitable to deliver the seeding material from the source to the target area, and the identification of the atmospheric stability profile (Fig 8.1) that will allow the seeding material to vertically mix into the proper layer of the clouds.

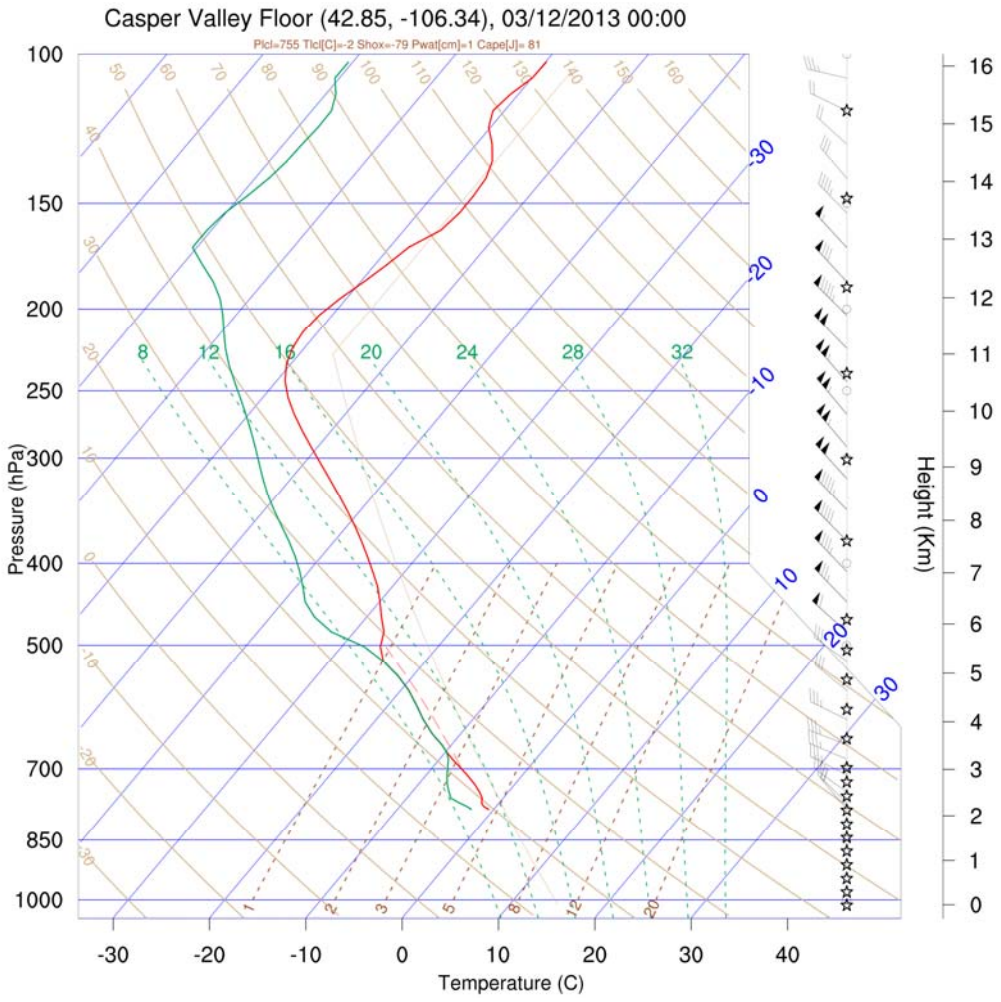

Figure 8.1 Model sounding showing supercooled clouds and northwesterly flow over the Laramie Range.

8.2 Forecasting

Identification of clouds containing supercooled liquid water is critical to initiate and continue cloud seeding operations. This is often a difficult task as no direct observations of these properties routinely collected. The set of rules to define inflight icing in the NOAA operational current icing product (CIP) have been shown to be among the most robust available to identify clouds containing supercooled liquid water (Bernstein et. al. 2005). These are described below.

8.2.1 Satellite

The GOES imager data contains 3 channels useful for identification of operational cloud seeding conditions. This data set has excellent 1 to 4 km horizontal resolution over the Laramie Range and updates every 30 minutes. The visible channel, since it consists of reflected solar energy, is only available during daylight hours. This channel gives an indication about the presence of cloud, and the optical thickness of clouds (i.e. how much condensate is present in the clouds). It does not give any indication of cloud temperatures or heights. The long-wave infrared channel provides data both day and night. These images provide the temperatures of the highest cloud levels, CTT, or the ground temperature in the absence of clouds. They give no indication about cloud thickness, cloud base height, or multiple cloud layers. The shortwave infrared channel paired with the longwave infrared channel provides estimates of cloud particle sizes at cloud top and this can be inferred as a surrogate for cloud top phase (i.e. ice or liquid).

8.2.2 Numerical Model

Several operational numerical models provide output over the Laramie Range. These include the North American Mesoscale (WRF-NMM) run at 12 km horizontal resolution. It runs every six hours, produces output at 3-hour granularity and includes explicit microphysical predictions. The WRF-RAP, which runs at 13 km horizontal resolution, and the High Resolution Rapid Refresh, which runs at 3 km also cover the Laramie Range. These models are the backbone of the Current Icing Product and Forecast Icing Products.

https://www.aviationweather.gov/adds/icing/icingnav

Both of these models update every hour, and produce hourly output. Useful data from these models include temperatures, winds, soundings than can estimate stability and the vertical wind structure, as well as moisture, clouds, and the cloud microstructure.

8.2.3 Surface Observations

METARs provide at least hourly information on cloud cover, cloud base heights, temperatures, dew point temperatures and winds. Several of these stations are located at

airports in the North Platte Valley and are useful for cloud seeding forecasting in the Laramie Range. The cloud base height information is the most useful. When clouds (not low-level fog) are present over the METAR sites they are also likely present over the higher terrain of the mountains. The cloud base height information can be paired with numerical model soundings. Additional surface observations that include temperatures and snowfall rates are available from the four Laramie Range SNOTEL instrument suites. There are two Remote Automated Weather Stations (RAWS) useful for monitoring weather in the

Laramie Range, these include Casper Mountain and Esterbrook. Additional surface (temperatures and winds) are available from additional weather stations at Shirley Basin and Pathfinder Dam in the northwestern generator siting area. Several of the cloud seeding generators would be expected to have low cost weather stations that measure temperatures, moisture and winds. Figure 8.2 shows the surface network (SNOTEL sites are absent).

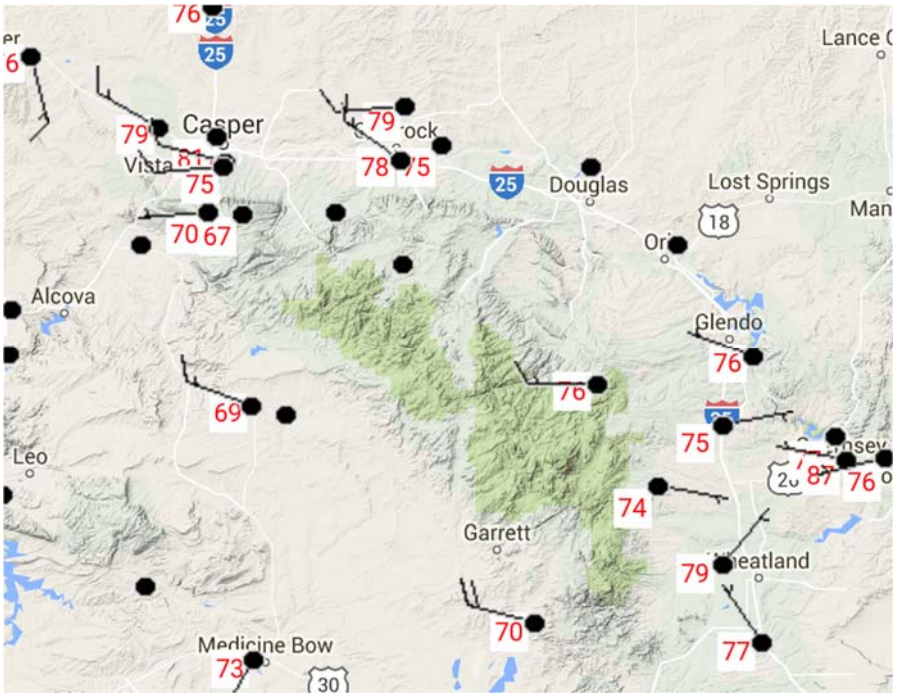

Figure 8.2 Surface network available for realtime forecasting in the Laramie Range.

8.2.4 Radar Observations

Radar observations from Cheyenne and Riverton, the closest radar sites, are of limited utility due to the long distances for the Laramie Range. The distance from Cheyenne to the target area is 180 km and from Riverton to the target area the distance is 200 km, putting the lowest radar beam height near the 11,500 ft MSL level. Some microphysical and cloud details in the mid and upper cloud levels can be inferred from these instruments but information in the targeted clouds, below 10,000 ft MSL is missing.

8.2.5 Icing Pilot Reports

Voice pilot reports are routinely available from air traffic as they takeoff, land, and traverse the greater Laramie Range region (Fig 8.3). When aircraft report icing they also often report cloud layer information and temperatures. These reports provide direct information to the project that clouds containing supercooled liquid water are present and the altitudes of the supercooled liquid layers. The PIREPs are available in real time.

https://www.aviationweather.gov/adds/pireps

CPR UA /OV CPR090020/TM 1305/FL105/TP E45X/TA M11/IC MOD RIME ICE

Figure 8.3 Icing PIREP in the Casper, WY area for moderate rime ice at 10,500 ft MSL at a temperature of -11°C.

Identification of supercooled liquid water clouds (SLW FCAST)* proceeds as follows:

Using the strengths and weaknesses from the above data sets a determination of the presence of SLW in the targeted clouds can be inferred.

1. Clouds need to be present in the target area.
   (and)
2. CTTs in the cloud layer that is in the target area and at seedable altitudes ideally are warmer than -25°C, although strongly forced clouds in which vertical velocities are strong enough to maintain liquid supersaturation can contain SLW at CTTs much cold than -25°C.
   (or)
3. Numerical model clouds should have supercooled liquid condensate in the target area.
   (or)
4. Positive icing reports are present. These are direct indicators of SLW in the clouds.
   (and)
5. CB should be below ridge top and be warmer than -10°C.

Ground-based AgI cloud seeding
Clouds present over the area
Supercooled liquid present (SLW_FCAST)
10,000 ft MSL winds from 260° through 60°
10,000 ft MSL winds speeds <50 MPH and >10 MPH
Low level stability suitable to vertically transport seeding plume
Temperatures in seeding target clouds -6°C< and >-18°C
Cloud bases below 10,000 ft MSL

Ground-based Propane cloud seeding
Clouds present over the area
Supercooled liquid present (SLW_FCAST)
10,000 ft MSL winds from 350° through 60°

10,000 ft MSL winds speeds <40 MPH and >5 MPH
Temperatures in seeding target clouds -2°C< and >-18°C
Cloud bases at or below generator height

Aircraft cloud seeding
Clouds present over the area
Supercooled liquid present (SLW_FCAST) at flight level
Flight level winds from 250° through 60°
Winds speeds <50 MPH and >10 MPH
Temperatures in seeding target clouds -6°C< and >-18°C
Cloud bases at or below 10,000 ft MSL

8.3 Suspension of Seeding

In the event of any emergency, which affects public welfare in the region of the seeding operations being carried by the cloud seeding operators, the seeding operations in that region will be suspended until the emergency conditions are no longer a threat to the public. Seeding suspensions would be expected to occur due to one or more of the following conditions.

1) When an extreme avalanche danger exists as determined by the U.S. Forest Service.
2) When the National Weather Service (NWS) forecasts a warm winter storm (freezing level >8000 ft.) with the possibility of considerable rain at the higher elevations which might lead to local flooding.
3) When Flash flood warnings are issued by the NWS.
4) When forecasts of excessive runoff issued by the River Forecast Center.
5) Quantitative precipitation forecasts issued by the NWS that would produce excessive runoff in or around the project area.
6) When the water content of the snowpack in the target area, as measured at existing snow courses or SNOTEL sites, exceeds the accumulation envelope defined by the following percentages to date of long-term averages on the same date. NRCS SNOTEL data and reports are used to monitor the snowpack (Fig 8.4).

December 1...175%	February 1...150%	April 1...140%
January 1.....150%	March 1....150%	May 1....140%

Intermediate limits shall be derived by linear interpolation between the percentages given above.

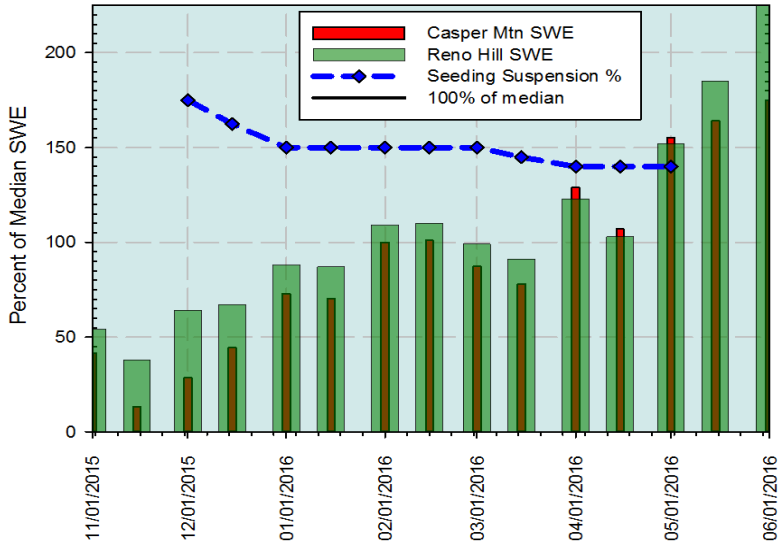

Figure 8.4 2016 northern Laramie Range snow water equivalent percent of median and suspension criteria. Seeding would have been suspended in late April prior to the end of the season.

In addition to the above seeding suspension thresholds, special consideration will be paid to recent forest fire-impacted areas. These areas will be identified prior to the start of the seeding project by local stakeholders and a set of seeding rules or perhaps generator siting adjustments will be developed prior to initiation of operations.

9 Environmental Considerations

The DRI Laramie Range cloud seeding study for the Laramie Range includes both LP and AgI seeding. In this section we discuss the potential environmental and legal considerations in conducting cloud seeding using these compounds.

9.1 Liquid Propane

LP is the molecule C_3H_6 stored under high pressure. The boiling point of propane is -42°C at the standard atmospheric pressure (1013 hPa) and lower at higher altitudes. The conversion of liquid propane under pressure to gas at the dispenser nozzle produces a stream of air cooled below -42°C and instantly freezes all cloud drops adjacent to the stream. One gallon of liquid propane creates 36 ft^3 of propane gas.

The propane dealers association notes that propane is non-toxic, non-caustic, and will not create an environmental hazard if released as a liquid or a vapor. The primary concern is freezing of organisms if a large amount of propane is spilled, and a low potential for fire. The only damage and potential danger exists if the vapor is ignited following a spill. And even then, there are no long-term effects of ignited propane that can be damaging to the environment when the ground is moist and humidity is high during storms.

Observations of dry forest and grasslands will cause a suspension of potential LP cloud seeding operations. Therefore range and forest fires will not be a hazard. In addition, propane liquid and vapor are not an environmental threat in their unused states (prior to combustion) if released.

- Propane is not considered a greenhouse gas.
- Propane is not damaging to freshwater or saltwater ecosystems, underwater plant or marine life.
- Propane is not harmful to soil if spilled on the ground. Propane will not cause harm to drinking water supplies.
- Propane vapor will not cause air pollution. Propane vapor is not considered air pollution.
- Propane vapor is not harmful if accidentally inhaled by birds, animals or people.
- Propane will only cause bodily harm if liquid propane comes in contact with skin (boiling point -42°C).
- Propane has a narrow range of flammability when compared with other petroleum products. In order to ignite, the propane-air mix must contain from 2.2 to 9.6 percent propane vapor. If the mixture contains less than 2.2 percent gas, it is too lean to burn. If it contains more than 9.6 percent, it is too rich to burn.
- Propane won't ignite when combined with air unless the source of ignition reaches at least 940 degrees Fahrenheit. In contrast, gasoline will ignite when the source of ignition reaches only 430 to 500 degrees Fahrenheit.

- If liquid propane leaks, it doesn't puddle but instead vaporizes and dissipates into the air.
- Because it is released from a pressured container as a vapor, propane can't be ingested like gasoline or alcohol fuels.

9.2 Silver Iodide

The environmental effects of AgI smoke, produced by ground-based generators and aircraft mounted flares, have been extensively studied by numerous cloud projects. Jane LaBoa an Environmental Specialist with Colorado Network Staffing, and with significant input from the Desert Research Institute produced a National Environmental Policy Act (NEPA) Environmental Assessment for the Walker Basin Cloud Seeding project. Much of the analysis of the role of silver iodide from that study is presented in the below discussion.

Several 1970s-era studies examined the environmental and health impacts of cloud seeding in the United States, including such as Harris (1981), Howell (1977), and Klein (1978). A more comprehensive list of worldwide laboratory and field studies is contained in the Weather Modification Association's 2009 Position Statement on the Environmental Impact of Using Silver Iodide as a Cloud Seeding Agent*." The conclusion of the policy statement is: The published scientific literature clearly shows no environmentally harmful effects arising from cloud seeding with silver iodide aerosols have been observed, nor would any be expected to occur. Based on this work, the WMA finds that silver iodide is environmentally safe as it is currently being used in the conduct of cloud seeding programs."*

Williams and Denholm (2009) provide an in-depth literature review of the toxicity of AgI on the environment, as well as the most recent monitoring results of the large-scale Snowy Precipitation Enhancement Study (SPERP), an eleven-year cloud seeding research program designed to assess the technical, economic and environmental feasibility of augmenting snowfall in the Snowy Mountain Region of New South Wales, Australia. The literature review summarizes findings from both field and laboratory toxicity studies, including studies on fish and amphibians. The authors concluded that there is compelling evidence that the use of silver iodide for the SPERP will not result in an adverse ecotoxicological impact on the study area environment.

Monitoring by the Desert Research Institute of past cloud seeding projects in and near the proposed project area for the WWMPP has not been able to detect an increase in silver above levels naturally present in soil and streams (i.e., baseline numbers are not elevated). DRI uses ultra sensitive laboratory methods, which can detect parts-per-trillion concentrations (Huggins personal communication).

All of these studies are consistent in concluding the contribution of AgI to the environment from cloud seeding is negligible (i.e., in quantities too small to be measured) compared to background levels and are well below threshold limits for human safety, aquatic organisms, and water quality standards.

Overall, the conclusions reached in the published scientific literature center around these points:

- Background levels of silver far exceed silver contributed from cloud seeding projects. Silver is found naturally and through industrial emissions. Silver is a trace element in many organisms. Numerous studies report no detected AgI in samples of cloud seeded areas vs. control areas.

- In studies where silver (all compounds and all sources) was detected it was in the range of 0.1 to 0.01 micrograms per liter. The U.S. Public Health Service established a concentration limit of 50 micrograms/liter in public water supply. In a 1978 study, cloud seeding AgI was estimated to contribute 0.1 percent of overall silver emissions (Eisler 1996).

- The quantities of AgI used in cloud seeding are minute because very little material is needed to form the desired ice crystals. Furthermore, cloud seeding material is dispersed over very large areas. In sampling waterbodies in mountain areas of California subject to long-term cloud seeding, no detectable silver above the natural background was found in seeded target area water bodies, precipitation and lake sediment samples, or any evidence of silver accumulation after more than fifty years of continuous seeding operations (Stone et al 1995; Stone 2006).

- AgI is considered water insoluble and not able to bio-accumulate to toxic levels. This insoluble property is what makes AgI maintain its structure and serve as an effective cloud seeding agent. Some silver compounds are toxic, especially to aquatic organisms in laboratory studies. However, in an environmental setting AgI is immobilized and is not bio-active. Studies were conducted as part of an environmental monitoring effort to determine if cloud seeding was impacting Sierra Nevada alpine lakes. No evidence was found that silver from seeding operations was detectable above the background level. There was also no evidence of an impact on lake water chemistry, which is consistent with the insoluble nature and long times required to mobilize any silver iodide released over these watersheds. Comparisons of silver with other naturally occurring trace metals measured in lake and sediment samples collected from the Mokelumne watershed (northeast of the proposed project area but in comparable ecosystems) in the Sierra Nevada indicate that the silver was of natural origin (Stone 2006).

Material Safety Data Sheet
Silver Iodide MSDS
Available online at:
Http://www.espimetals.com/msds's/silveriodide.pdf

9.3 Downwind "extra-area" Effects

A common misconception regarding cloud seeding is that causing additional precipitation in one area will cause decreased precipitation in an area downstream. A conceptual model to demonstrate the impact of cloud seeding on the moisture budget is demonstrated in Figure 9.1.

Prior to cloud formation 100% of the moisture in the air is water vapor. As clouds form, up to 20% of the vapor will be condensed into cloud with 80% remaining as vapor. As precipitation forms, 6% of the cloud will be converted from cloud to precipitation, with 14% of the vapor remaining with the cloud and 80% remaining as vapor in the clear air.

Cloud seeding in a Wyoming storm can, on average, be expected to add 5% to 15% more precipitation than would naturally occur. Assuming a 10% increase in precipitation from cloud seeding, 6% of the precipitation would be natural and an additional 0.6% of the cloud would be converted precipitation from cloud seeding. This leaves 80% as vapor, 13.4% as cloud and 6.6% of the moisture exiting as precipitation, with 0.6% from cloud seeding.

The total change in atmospheric water vapor following a cloud seeded storm compared to a similar unseeded storm is 0.6%. Turbulent mixing and evaporation downstream of the seeding location can quickly overcome the 0.6% vapor deficit.

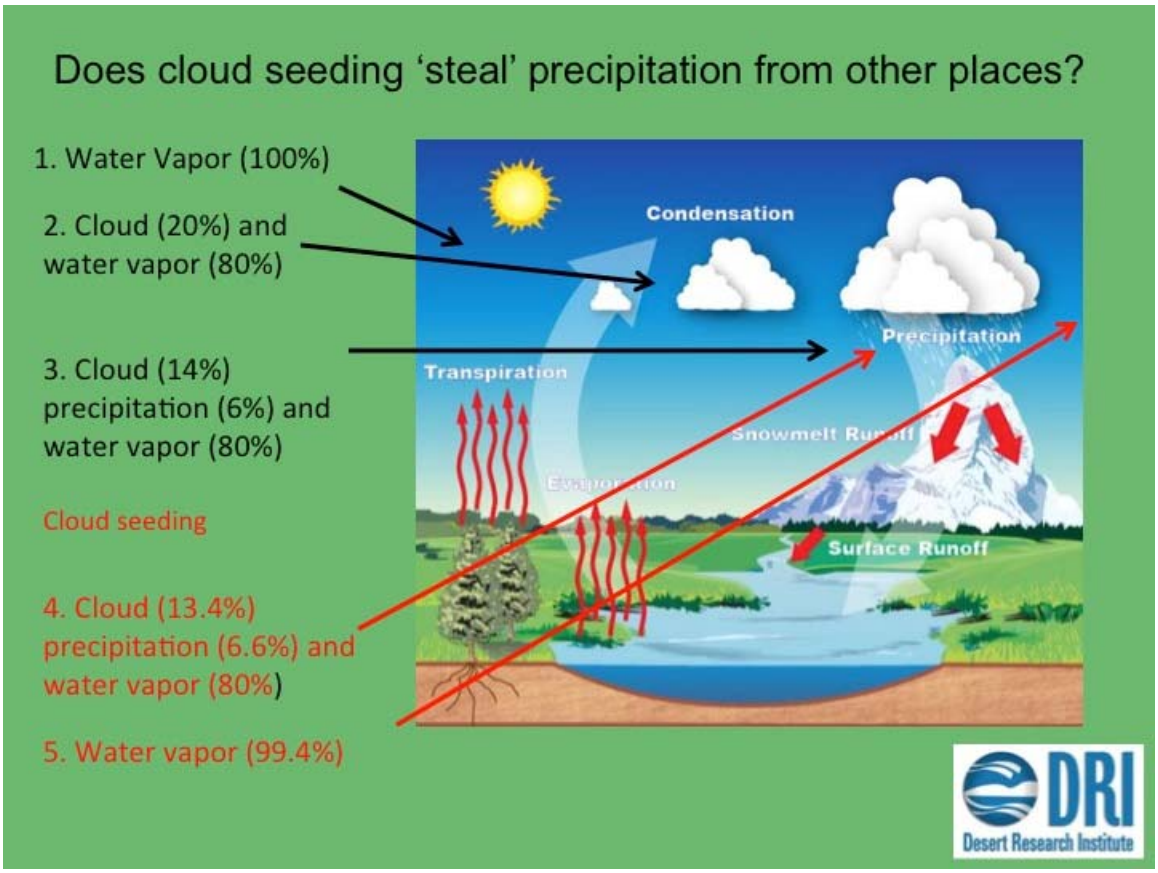

Figure 9.1 Atmospheric water cycle in relation to the role of cloud seeding.

A set of cases analyzed by DeFelice et al. (2012) suggests that the seeding material is potentially transported downwind of the target and may increase precipitation beyond the target area. A California study showed no decrease in precipitation downwind of the Sierra Nevada (Hunter 2007). This confirmed the findings from the Project Skywater and the 1981 Sierra Cooperative Project, which concluded that AgI seeding does not cause a decrease in downwind precipitation and may increase precipitation as far as 100 miles downwind.

9.4 Legal Considerations

In order to legally conduct the potential Laramie Range Cloud Seeding Project the contractor will closely follow the suspension guidelines outlined in Task 8. In addition the state of Wyoming and the contractor will post notice and then host public meetings informing the public that cloud seeding will be taking place and the scope of the operations. All legal obligations as outlined in Task 7 will be followed in a timely manner.

It is recommended that the state require the contractor to carry liability insurance or provide proof of financial responsibility and/or post a bond. To date no cloud seeding provider has been successfully sued for flood or other consequences resulting from cloud seeding

operations. A compilation of past cases where lawsuits were brought and dismissed are discussed by attorney Ronald B. Standler.

http://www.rbs2.com/weather.pdf

9.5 Summary

A properly conducted cloud seeding program is an environmentally safe method to potentially increase winter precipitation. LP dispenser cloud seeding can be safely conducted with proper siting locations, although this has not been not widely studied. All available research shows cloud seeding with AgI also has no environmental impact. The AgI is not bioavailable to flora and fauna, and doesn't accumulate in soil and water compared to background values. The available evidence suggests that cloud seeding has none to slightly positive impacts up to 100 miles downwind of target area.

10 Evaluation Methodology

10.1 Background

Determining the effects of cloud seeding on the snowpack is a difficult problem. The measured success of any cloud seeding activity requires (1) statistical evidence of a significant increase in the response variable (water year stream flow or snowfall) presumably due to seeding and (2) physical evidence that establishes the plausibility that the effects suggested by the statistical evidence could have been caused by the seeding intervention (AMS, 1998).

Statistics can be computed by comparing snowfall ratios between project locations and appropriate non-project locations, both before and after the cloud seeding has started (Griffiths et al. 2015). This method has also been used to compare stream flow data in a similar manner (Silverman 2007). Large research projects have used a randomization approach to statistically show the seeding effect (i.e. WWMPP Breed et. al, 2014, Manton and Warren 2011). This is not appropriate for most operational programs, as randomization requires extended time periods requiring withholding cloud seeding and additional snowfall during seedable conditions.

Physical measurements of the required sequence of events for cloud seeding is a second approach to validation. This includes detecting supercooled liquid water in the targeted clouds, proving that the seeding material has reached the target and had an effect. In the Bridger Range Experiment (Super 1974), snow chemistry was done within the target and an aircraft equipped with cloud physics equipment was also flown through the seeded clouds. Manton and Warren (2011) also describe a successful physically based validation technique. For the Laramie Range potential project a combination of new instrumentation and NWS remote sensing would be used in the physical validation exercise.

A third method to estimate the cloud seeding effects is through a well validated and high-resolution numerical model as was done for the WWMPP (Rasmussen et al. 2015). This cloud be done for the Laramie Range.

10.2 Validation Plan

Should this project move forward, a lower cost version of a physical based validation plan, a target-control validation for both snowfall and stream flow, as well as a numerical model validation are all proposed.

A proposed validation plan would be designed using several of the below:

1) Install an ice detector and heated weather station at the top of Hogadon Mountain Ski area at 7,900 ft MSL on Casper Mountain to determine the approximate mountain temperatures and winds as well as when and how much SLW is present.

2) Install web cams pointing at the highest terrain on one of the Scenario 1 cloud seeding generators and on one of the Scenario 2 generators to determine cloud presence over the target area.
3) Collect NWS operational data such as outlined in the observational climatology (Task 3).
4) Collect snowfall in real time during seeding events both within and outside the seeding plume during 1 or 2 cases.
5) Collect snow full layer snowpack samples late in the winter for chemical analysis.
6) Conduct snow chemical analysis for #4 and #5.
7) Define target and control statistics for stream flow at Deer Creek (within the target) and at Sybillie Creek (outside the target in the southern Laramie Range)
8) Create a target and control regressions Scenario 1 and Scenario 2 storms for the northern Laramie Range SNOTEL and the Cow Creek SNOTEL in the southern Laramie Range
9) Run the high resolution WRF that was used in the climatology but add the cloud seeding cloud physics parameterizations as was done for the WWMPP validation.

11 Potential Benefits/Hydrologic Assessment

11.1 Introduction

Section 11 describes the steps necessary for successful implementation of a hydrologic model to assess the benefits of cloud seeding on the river drainage basin. Steps necessary for successful implementation of a hydrologic model include: selecting the model code; collecting/synthesizing and identifying gaps in data; defining conceptual model (basin characteristics and boundary conditions); and calibration, evaluation, and sensitivity analysis. As we went through the process of outlining these steps, it became possible to conduct limited hydrologic modeling on the Box Elder and Deer Creek basins within the Laramie Range. Limited modeling offered the opportunity to exercise these steps, estimate precipitation changes, and, on a preliminary basis, and make estimates of changes to streamflow from cloud-seeding in Box Elder and Deer Creek basins. Concurrently, we used a linear approach to estimate changes to streamflow in multiple basins in the Laramie Range for an estimate of changes to Glendo reservoir. Advantages of the limited modeling approach –as opposed to linear approaches only- are discussed.

11.2 Review of Approaches to Estimate Streamflow Changes

There are various approaches for estimating changes to streamflow from changes in precipitation. Regardless of complexity, all approaches seek to describe the predictability of streamflow from precipitation based on the underlying relationship between the two. Linear techniques can provide rapid first-order approximations. It is widely recognized that these techniques suffers from uncertainties due to non-linearities in the hydrologic cycle, incomplete spatial and temporal data sources, non-physical assumptions, and misleading estimates of the fraction of winter snow pack affected by cloud–seeding. Changes in streamflow are attributed not only to changes in snowpack but also to changes including: warming temperatures during winter and spring (Rood et al. 2008); land cover and forest management regimes (Kelly et al., 2016); and soil moisture content, vegetation patterns, as well as meteorological observations (Toth, 2013). Dixon et al. (2014) used a regression tree approach to show that elevation, wind, canopy cover, and solar radiation were influential factors to changes in streamflow, with their order of importance changing during different years of the study.

Benefits of cloud seeding can be modeled with software such as Variable Infiltration Capacity model (VIC), WRF-Hydro, and the Groundwater and Surface water Flow model (GSFLOW). Acharya et al. (2011) used the VIC model to show that a 1-5% increase in precipitation from cloud seeding produced a 0.3–1.5% increase in annual streamflow over an area between the Medicine Bow and Sierra Madre mountains (Acharya et al., 2011). The model considered vegetation coverage – portions covered by evergreen forest generated more streamflow as compared with portions covered by shrubland/grassland. For a project in Eastern Nevada, we compared VIC with United States Geologic Survey (USGS) streamflow gages at four creeks

and made some observations. Inter-annual variability of streamflow at USGS gauges was well-captured in VIC. VIC had a dry bias, and VIC runoff showed peak streamflow occurring three to four months earlier in the water year than what was shown by the USGS stream gauges. The elevation of each USGS gage was significantly higher than the elevation of its equivalent VIC cell. This negative elevational bias in VIC may explain the early peak streamflow, since lower elevations favor a "flashy" regime, while observed streamflow suggested a snowmelt dominated watershed. It is unclear if similar observations could be made for the VIC model around the Laramie Range - while Eastern Nevada and Wyoming experience similar topography and climate, the two locations are not identical. Given the spatial scale of the VIC (1/8 degree or ~12km) data set, there is an inherent challenge in making comparisons at all.

Unlike VIC, WRF-Hydro can downscale to needed resolution. It has the advantage of being able to directly couple the climate to the land surface. GSFLOW, however, has an advantage over WRF-Hydro in that it can capture the physically based process of groundwater flow and also stream leakage. A more detailed discussion on this will follow. For the objectives of this project, GSFLOW best suits the needs to balance numeric complexity and grid cell resolution with numeric efficiency. During the course of this project, it became possible to conduct hydrologic modeling on the Box Elder and Deer Creek basins using a limited version of GSFLOW. Limited modeling offered the opportunity to make estimates of changes to streamflow and compare with the linear approach.

11.3 Linear Approach

The goal was to estimate stream flow changes from cloud seeding with Glendo reservoir as the final target. Linear regression was used to estimate streamflow changes based on the relationship between streamflow measured at USGS gages and snow water equivalent measured at NRCS SNOTEL sites in each basin (Figure 11.1, Table 11.1). Basins along the 50-mile northwest to southeast transect are: Muddy Creek, Deer Creek, Box Elder Creek, Laprele Creek, Wagonhound Creek, and La Bonte Creek. The US Geological Survey (USGS) measures streamflow at various locations that are not consistent over the time of interest. The NRCS measures climate -including SWE - at four locations starting in 1983; three are used in this study.

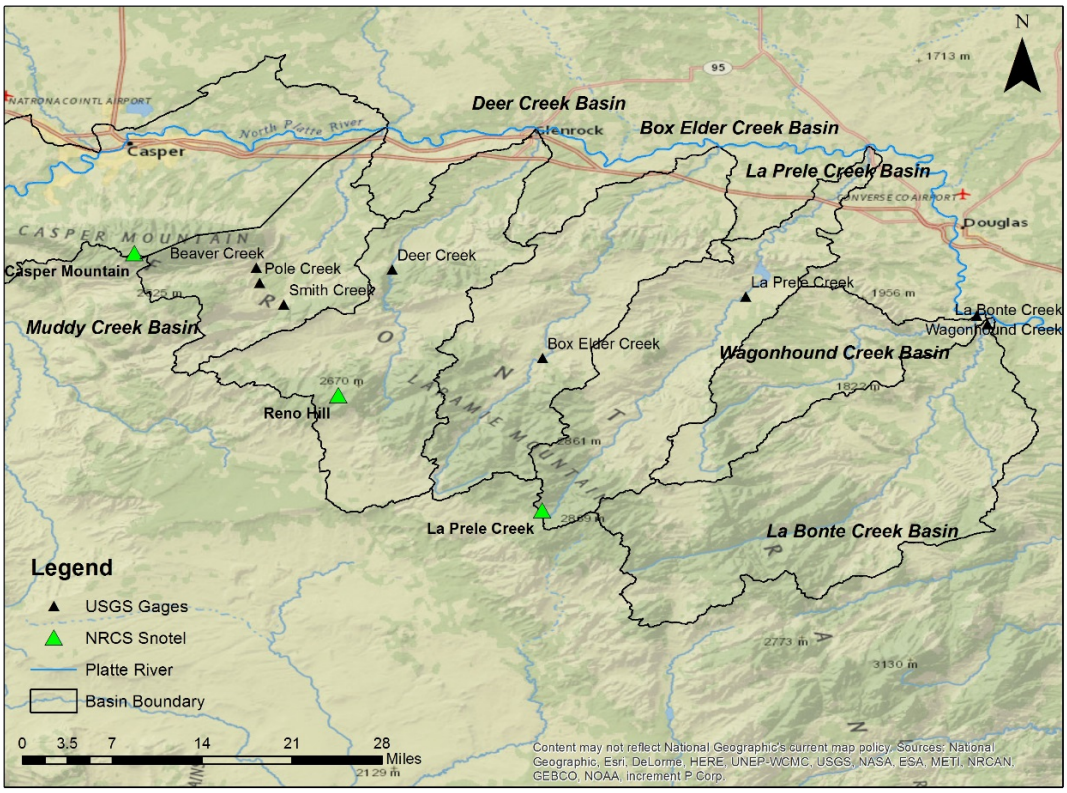

Figure 11.1 Map of study area. Shown are: locations of US Geological Survey (USGS) streamflow gages, Natural Resources Conservation Service (NRCS) Snotel sites, and basin boundaries.

USGS	Name	Area Drained mi^2	Elev	Years Active
06645178	Pole Creek near Casper	2.7	5880	1987-1996
06645174	Beaver Creek above Pole Creek	4.67	5800	1987-1996
06645166	Smith Creek below Otter Creek	18.5	5980	1987-1996
	Sum of Pole, Beaver, and Smith creeks	25.9	5890*	1987-1996
06646000	Deer Creek in Canyon, near Glenrock	139	5640	1985-2002
06647500	Box Elder Creek at Boxelder	63	6710	1945-2016
06649000	Laprele Creek near Douglas	135	5600	1919-1992
06651500	La Bonte Creek near La Bonte	287	4752	1916-1969
06650500	Wagonhound Creek near La Bonte	112	4741	1916-1969
NRCS	Name		Elev	Years Active
389	Casper Mountain		7900	1983-2016
571	Reno Hill		8375	1983-2016
716	Laprele Creek		8400	1983-2016
872	Windy Peak		7900	1983-2016

*Elevation is average of Pole, Beaver, and Smith

Table 11.1 Name and location information for US Geological Survey (USGS) streamflow gages and Natural Resources Conservation Service (NRCS) Snotel sites.

Pearson's ρ and a linear regression coefficient of determination were used to describe the relationships between SWE and streamflow at these locations. Pearson's ρ is a measure of linear correlation and measures the strength of the relationship – as one increases, the other increases and ρ is positive (Helsel, 2002). When there is no correlation, ρ is 0. Linear regression was used to calculate the coefficient of determination R^2, which is the fraction of data that can be predicted by regression – closer to 1 is better predictability.

Several criteria were applied in the approach. Gages without a minimum of seven years of continuous streamflow were omitted. If a gage had a period of record during which less than seven years of continuous flow was recorded, those particular records were omitted (e.g. Deer Creek 1985-2002, 2014-2015 were omitted). Water years 1983 to 2015 were used, because SWE is only available for these years. Linear regression was applied basin-by-basin. For basins where neither SWE nor streamflow was available, information from co-located basins was used and the basin with higher ρ and R^2 values was preferred. Maximum SWE values were used for each water year.

The approach made some assumptions. Increases from cloud seeding are based on snow increases of 5% to 15% estimated by previous research (AMS, 1998; WMA, 2005). A 15% increase is assumed for cloud seeding on 100% of the storms, but not all storms experience cloud seeding. A 2% increase in precipitation is suggested from 13% of storms experiencing cloud seeding, and a 10% increase in precipitation is estimated from 67% of storms

experiencing cloud seeding. We assumed seasonal SWE changes in increments of 2%, 4%, 6%, 8%, and 10% at the SNOTEL.

It is important to note that all changes in streamflow were estimated at the USGS gages and not the basin outlets, or the basin mouths at the Platte. All SWE and streamflow changes occurred in the area drained above the gage elevation. There are likely contributions from SWE and streamflow occurring below the gages, but it was not possible to account for these contributions at this time. Thus, since some flow is being missed, estimates from the linear approach may be considered conservative.

11.3.1 Muddy Creek Basin

The Muddy Creek basin is the southeast portion of the larger Muddy Creek – North Platte basin above the USGS gages. The Casper Mountain Snotel is located in the Muddy Creek Basin along with three USGS gages: Smith Creek below Otter Creek (06645166), Beaver Creek above Pole Creek (06645174), and Pole Creek (06645178). The three were summed to better represent streamflow, spatially, across the basin. The regression equation shown in Figure 11.2 upper was used to calculate the estimated changes in streamflow for each change of SWE shown in Figure 11.2 lower. Average, minimum, and maximum values are summarized in Table 11.2. Changes in SWE resulted in approximately corresponding changes in streamflow. Calculations suggest a slightly greater change in streamflow at higher values of SWE.

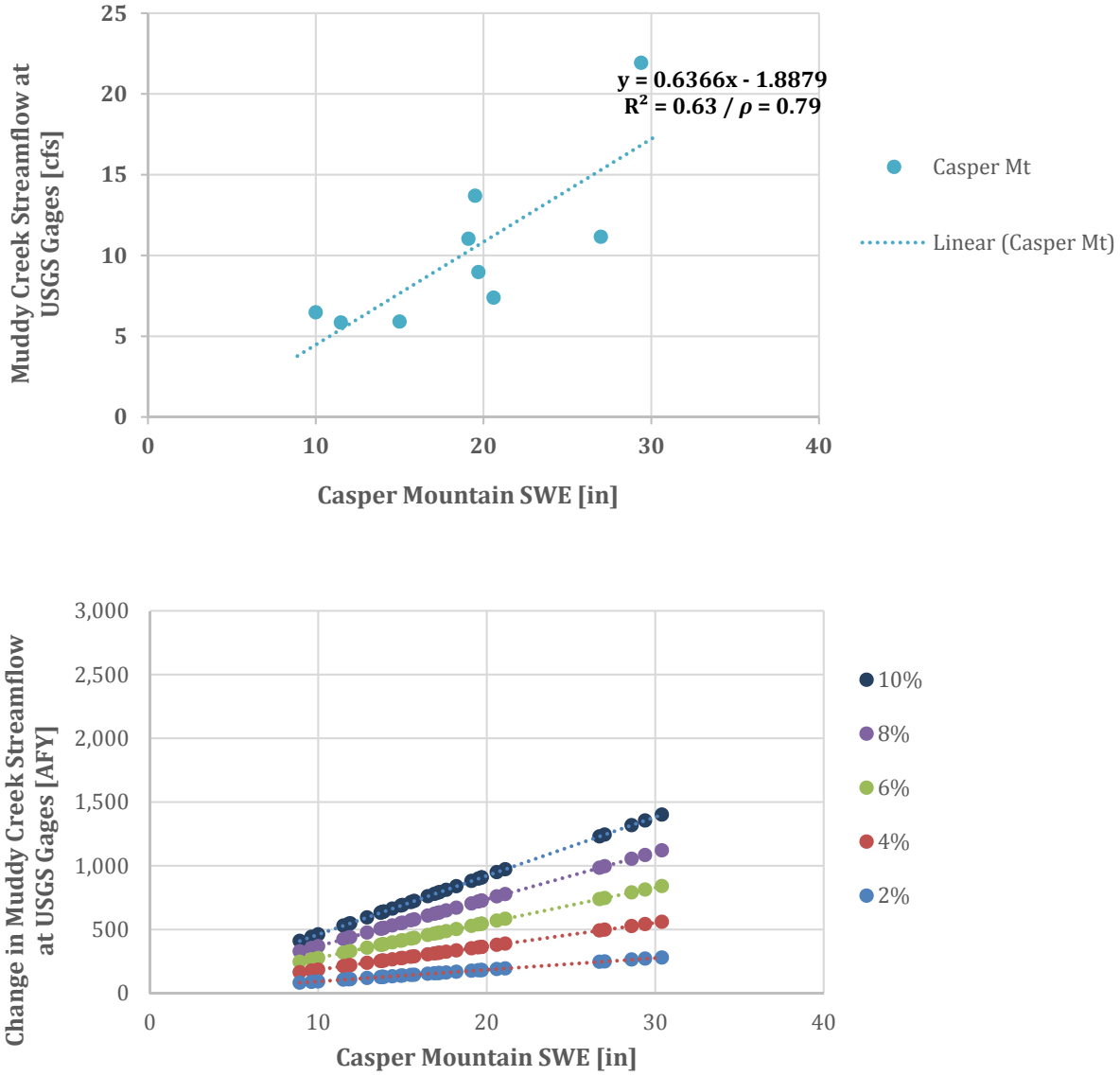

Figure 11.2 Upper shows linear regression equation, coefficient of determination R^2, and Pearson's ρ for predictability of streamflow based on SWE in the Muddy Creek basin. Lower shows estimated changes in streamflow for 2%, 4%, 6%, 8%, and 10% changes of SWE based on the linear regression equation.

Change	2%	4%	6%	8%	10%
Average (AFY)	160	320	480	640	800
Minimum (AFY)	82	164	246	328	410
Maximum (AFY)	280	560	841	1121	1401
% of Annual Average	2.2%	4.3%	6.5%	8.6%	10.8%

Table 11.2 Average, minimum, and maximum estimated changes for Muddy Creek basin streamflow.

11.3.2 Deer Creek Basin

The Reno Hill SNOTEL is located in the Deer Creek Basin along with the USGS gage at Deer Creek in the Canyon (06646000). The regression equation shown in Figure 11.3 upper was used to calculate the estimated changes in streamflow above the USGS gage for each change of SWE shown in Figure 11.3 lower. Average, minimum, and maximum values are summarized in Table 11.3. Changes in SWE resulted in larger changes in streamflow. Calculations suggest a greater change in streamflow at higher values of cloud-seeding and SWE i.e. a "wet" year may yield more streamflow for 10% cloud-seeding than a "dry" year.

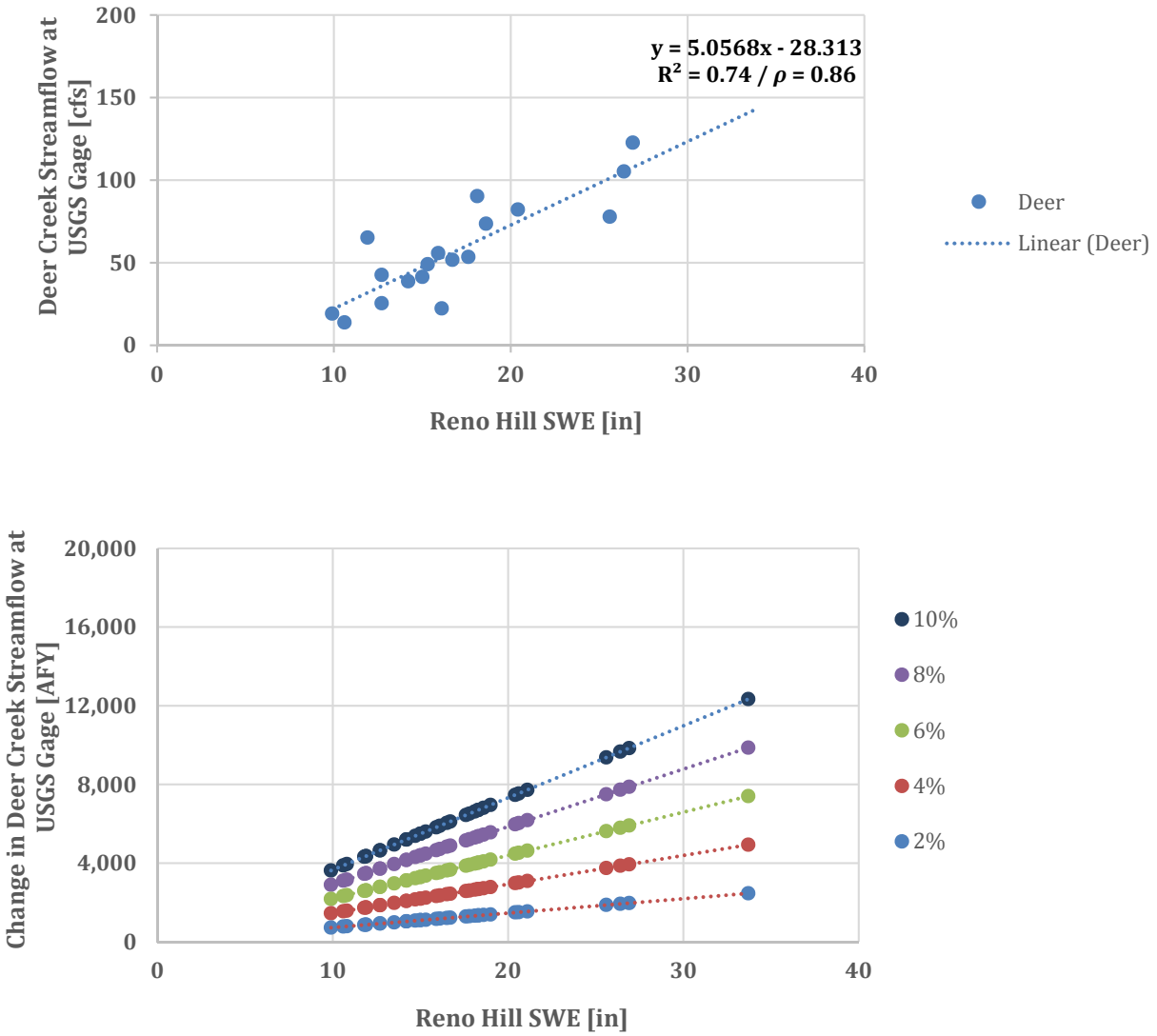

Figure 11.3 Upper shows linear regression equation, coefficient of determination R^2, and Pearson's ρ for predictability of streamflow based on SWE in the Deer Creek basin. Lower shows estimated changes in streamflow for 2%, 4%, 6%, 8%, and 10% changes of SWE based on the linear regression equation.

Change	2%	4%	6%	8%	10%
Average (AFY)	1247	2493	3740	4986	6233
Minimum (AFY)	725	1450	2175	2899	3624
Maximum (AFY)	2467	4935	7402	9870	12337
% of Annual Average	3.0%	6.0%	9.0%	12.0%	15.0%

Table 11.3 Average, minimum, and maximum estimated changes for Deer Creek basin streamflow.

11.3.3 Box Elder Creek Basin

Box Elder Creek Basin has no SNOTEL located within it. Co-located SNOTELs are Reno Hill to the northwest in Deer Creek Basin and La Pelé Creek to the southeast in Laprele Creek Basin. The USGS gage is Box Elder at Box Elder Creek (06647500). Higher R^2 and ρ values were calculated for the relationship between streamflow and Reno Hill as compared with Laprele, so Reno Hill was preferred for linear regression. Since Reno Hill has higher SWE this may slightly bias the results somewhat in favor of cloud seeding. The regression equation shown in Figure 11.4 upper was used to calculate the estimated changes in streamflow for each change of SWE shown in Figure 11.4 lower. Average, minimum, and maximum values are summarized in Table 11.4. Similar to Deer Creek Basin, changes in SWE resulted in larger changes in streamflow; i.e. greater changes during wet years.

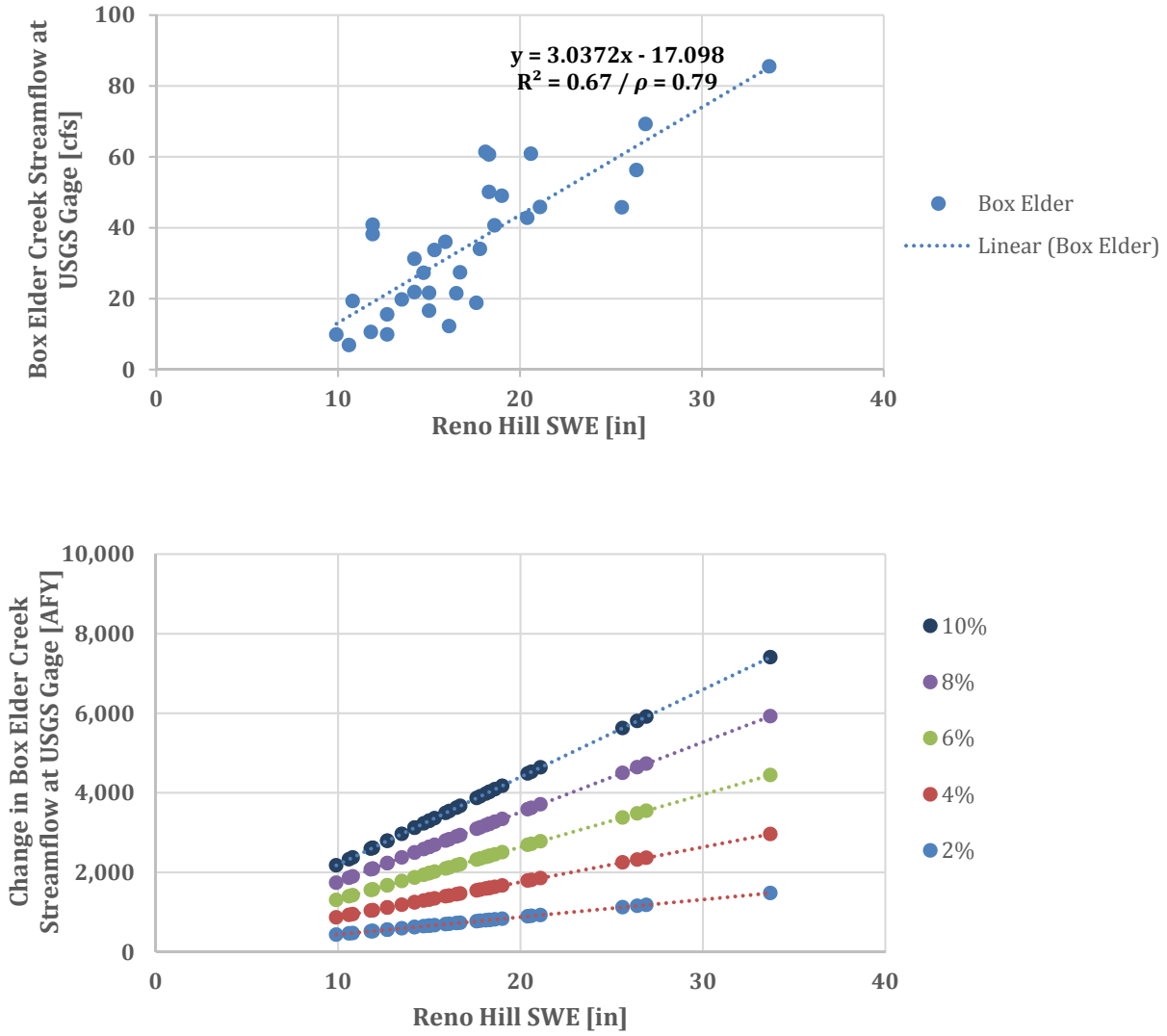

Figure 11.4 Upper shows linear regression equation, coefficient of determination (CoD) R^2, and Pearson's ρ for predictability of streamflow based on SWE in the Box Elder Creek basin. Lower shows estimated changes in streamflow for 2%, 4%, 6%, 8%, and 10% changes of SWE based on linear regression equation.

Change	2%	4%	6%	8%	10%
Average (AFY)	749	1497	2246	2995	3743
Minimum (AFY)	435	871	1306	1741	2177
Maximum (AFY)	1482	2964	4446	5928	7410
% of Annual Average	3.0%	6.0%	9.0%	12.0%	14.9%

Table 11.4 Average, minimum, and maximum estimated changes for Box Elder Creek basin streamflow.

11.3.4 Laprele Creek Basin

The Laprele SNOTEL is located in the Laprele Creek Basin along with the USGS gage at Laprele Creek near Douglas (06649000). The regression equation shown in Figure 11.5 upper was used to calculate the estimated changes in streamflow for each change of SWE shown in Figure 11.5 lower. Average, minimum, and maximum values are summarized in Table 11.5. In this basin, changes in SWE resulted in the largest changes in streamflow. Reasons are unclear – basin size and gage elevation are similar to those at Deer Creek. However, SWE recorded at Laprele (18 to 20 in) is lower as compared with other stations (10 to 33 in).

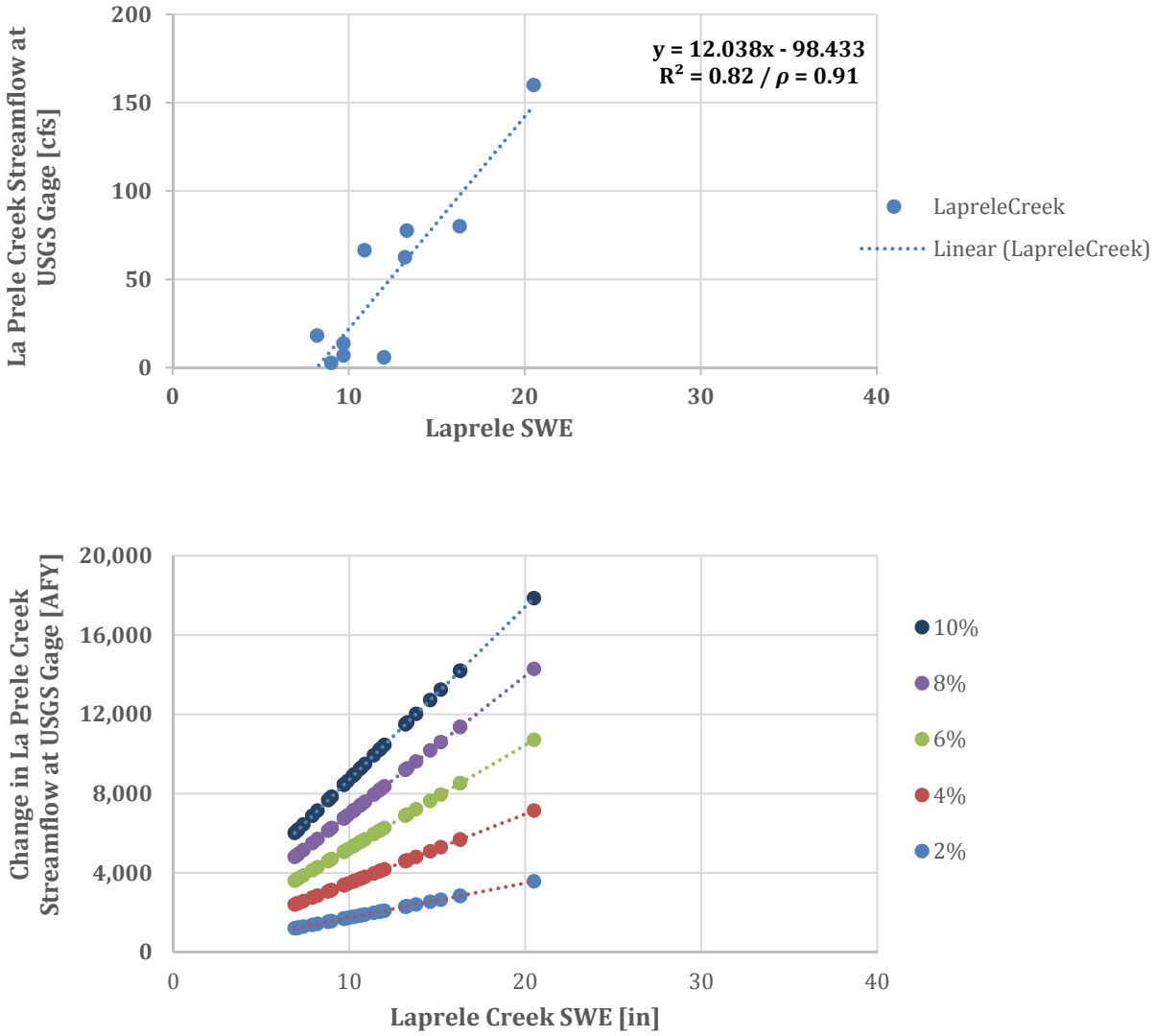

Figure 11.5 Upper shows linear regression equation, coefficient of determination (CoD) R^2, and Pearson's ρ for predictability of streamflow based on SWE in the Laprele Creek basin. Lower shows estimated changes in streamflow for 2%, 4%, 6%, 8%, and 10% changes of SWE based on linear regression equation.

Change	2%	4%	6%	8%	10%
Average (AFY)	1921	3841	5762	7682	9603
Minimum (AFY)	1203	2405	3608	4811	6013
Maximum (AFY)	3573	7146	10720	14293	17866
As % of Average	5.4%	10.7%	16.1%	21.5%	26.9%

Table 11.5 Average, minimum, and maximum estimated changes for Laprele Creek basin streamflow.

11.3.5 Wagonhound Creek and La Bonte Creek Basins

Estimates for streamflow changes were more difficult for Wagonhound Creek and La Bonte Creek Basins. Neither basin has a SNOTEL station. The USGS gages located in the basins cover a long amount of time (1919-1969), but do not overlap with years during which SWE was measured at co-located basins. The USGS gages also do not overlap enough with other gages so as to extrapolate streamflow values from another basin to either Wagonhound or La Bonte. A linear approach was not possible.

We made crude estimates for these two basins based on several assumptions. Table 1 summarized basins characteristics used to calculate ratios of streamflow and area drained shown in Table 11.6. Ratios were fairly consistent among the summed creeks, Deer Creek, and Laprele Creek. All of these gages are in the 5600 to 5900 elevation range. Box Elder Creek drains a relatively smaller basin but the gage is at a higher elevation, which may explain the higher ratio of streamflow generated.

Name	Area Drained mi^2	Elev	Average Flow	Ratio Flow/mi^2
Sum- Pole, Beaver, Smith Creeks	25.9	5890*	10.26	0.40
Deer Creek in Canyon	139	5640	57.26	0.41
Box Elder Creek at Boxelder	63	6710	34.61	0.55
Laprele Creek near Douglas	135	5600	49.39	0.37

Table 11.6 Basins, areas drained by gages, elevations, average annual streamflow, and the ratio of area drained to average flow.

We continued using the assumption that all SWE and streamflow changes occurred in the areas above the gages. Figure 11.6 shows an orange contour line of 5900 ft elevation (chosen slightly higher to be conservative) across the Wagonhound Creek and La Bonte Creek Basins. The areas above the contour are approximately 37 mi^2 and 170 mi^2, respectively. Applying the 0.37 conservative ratio of area drained to average flow for Wagonhound Creek and La Bonte Creek Basins, we calculate 13.7 cubic feet per second (cfs) and 62.9 cfs average annual flow, respectively. Applying changes calculated for Muddy Creek Basin, which were the smallest and most conservative, gives the estimated listed in Table 11.7. Minimum and maximum values could not be calculated.

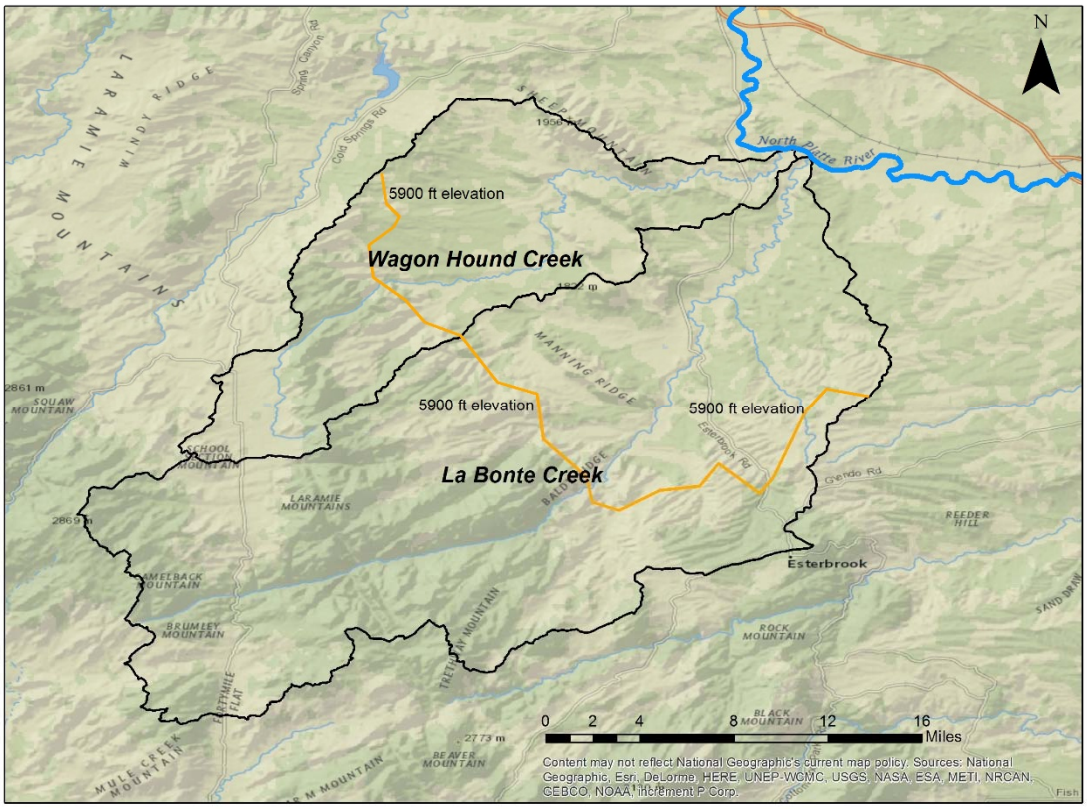

Figure 11.6 Orange contour line of 5900 ft elevation delineating areas of Wagonhound Creek and La Bonte Creek Basins.

SWE	2%	4%	6%	8%	10%
% Annual Streamflow (Muddy Basin)	2.2%	4.3%	6.5%	8.6%	10.8%
Wagonhound Creek (AFY)	218	426	645	853	1071
La Bonte Creek (AFY)	1002	1958	2960	3916	4918

Table 11.7 First-order estimates of streamflow changes in Wagonhound and La Bonte Creek Basins.

11.3.6 Laramie Range

The goal was to estimate stream flow changes from cloud seeding with Glendo reservoir as the final target. First order approaches were used to estimate changes to streamflow across the Muddy Creek, Deer Creek, Box Elder Creek, Laprele Creek, Wagonhound Creek, and La Bonte Creek Basins above the USGS gages. Average, minimum, and maximum values of changes to streamflow from changes in SWE were calculated and summed for each basin in acre-feet per year. Minimum and maximum values could not be calculated for Wagonhound and La Bonte basins. Table 11.8 shows values summed from all basins and is the amount of change that may be captured in Glendo Reservoir. Figure 11.7 shows the amount over average annual inflow. Average annual inflow at Glendo is 1,046,543 AFY and is calculated by the Bureau of Reclamation (http://www.usbr.gov/gp-bin/arcweb_gler.pl).

Inflow to Glendo	2%	4%	6%	8%	10%
Average (AFY)	5,297	10,535	15,833	21,072	26,368
Minimum (AFY)	2,445	4,890	7,335	9,779	12,224
Maximum (AFY)	9,022	17,989	27,014	35,981	45,003

Table 11.8 Inflow values summed from all basins and is the amount of change that may be captured in Glendo Reservoir.

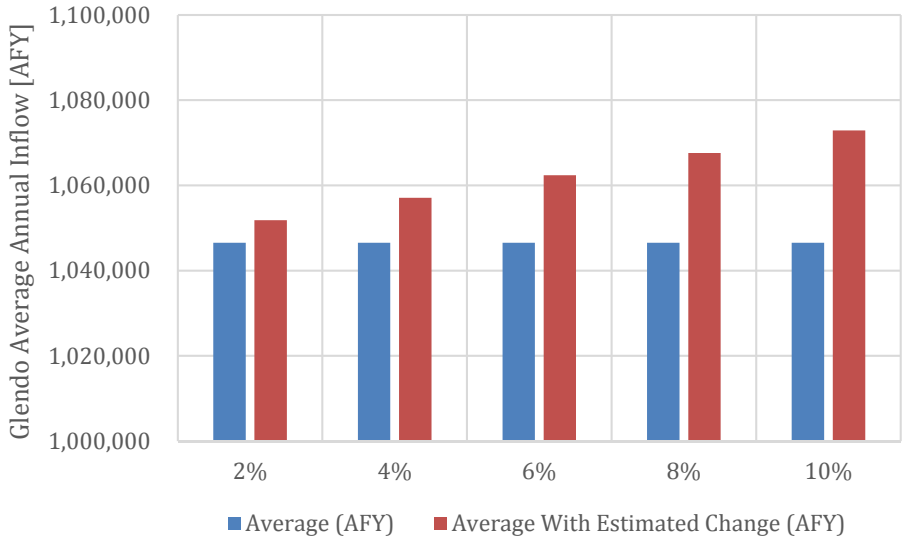

Figure 11.7 Estimated capture over average annual inflow at Glendo. Average annual inflow is 1,046,543 AFY and is calculated by the Bureau of Reclamation (http://www.usbr.gov/gp-bin/arcweb_gler.pl).

It is noted that the ratio approach for calculating changes at Wagonhound and La Bonte is crude. In general, the linear approach for estimating changes in streamflow form changes in SWE is simplistic. As already discussed, changes in streamflow are attributed the factors including spring warming, land cover and forest management regimes, soil moisture content, as well as meteorological observations beyond SWE. Reasons for the relatively higher percentage changes at Laprele Creek cannot be explained in the linear approach.

11.4 Outline Steps for Hydrologic Model – GSFLOW Approach

Integrated hydrologic models offer a physically-based numeric approach that couples atmospheric forcing, land surface processes and groundwater movement to balance both energy and water at the watershed scales. These numeric models allow practitioners to analyze complex water resources problems including feedback mechanisms and timing of important water budget components. Specifically, evapotranspiration (ET), soil-zone flow (interflow), runoff and groundwater interactions with surface feature such as streams. Three potential numeric models were considered for application to weather modification (WM) scenario testing. These models include the Variable Infiltration Capacity model (VIC; Liang et al., 1994), the Weather Research and Forecasting Model Hydrological modeling

extension package (WRF-Hydro; Goctis et al., 2015) and the Groundwater and Surface water Flow model (GSFLOW; Markstrom et al., 2008). All codes allow for 3-dimensional climate forcing and simulate a 2-way coupling with a land surface model with a terrain routing model to quantify overland and subsurface flow, as well as a 1-2 way coupling with channel routing to quantify streamflow interactions with groundwater. We identified GSFLOW as the model that best suits the project objectives based on the competing demands of computational expense, inclusion of physically based processes and the resolution of model grid structure.

GSFLOW combines the U.S. Geological Survey (USGS) Precipitation-Runoff Modeling System (PRMS, Leavesley et al., 2005) with the USGS Modular Groundwater Flow model (MODFLOW-NWT, Harbaugh, 2005; Niswonger et al, 2011) to account for flow within and between the plant canopy and soil zone, streams and the shallow groundwater system. PRMS is considered a modular, deterministic, distributed parameter and physical-process watershed model. Hydrologic flow is partitioned into reservoirs representing each watershed compartment (Figure 11.8) for each hydrologic response unit (HRU). HRUs are discretized, homogenous units generally based on hydrologic and/or physical characteristics that promote a uniformed hydrologic response to modeled stress (climate). Defining characteristics can include features such as drainage boundaries, elevation, slope, aspect, plant type or cover, land use, soil characteristics, etc. The HRU resolution is often the scale at which the model grid is defined and for watershed processes in mountainous terrain a scale of 100 m allows for numeric efficiency while capturing both topographic and vegetative gradients.

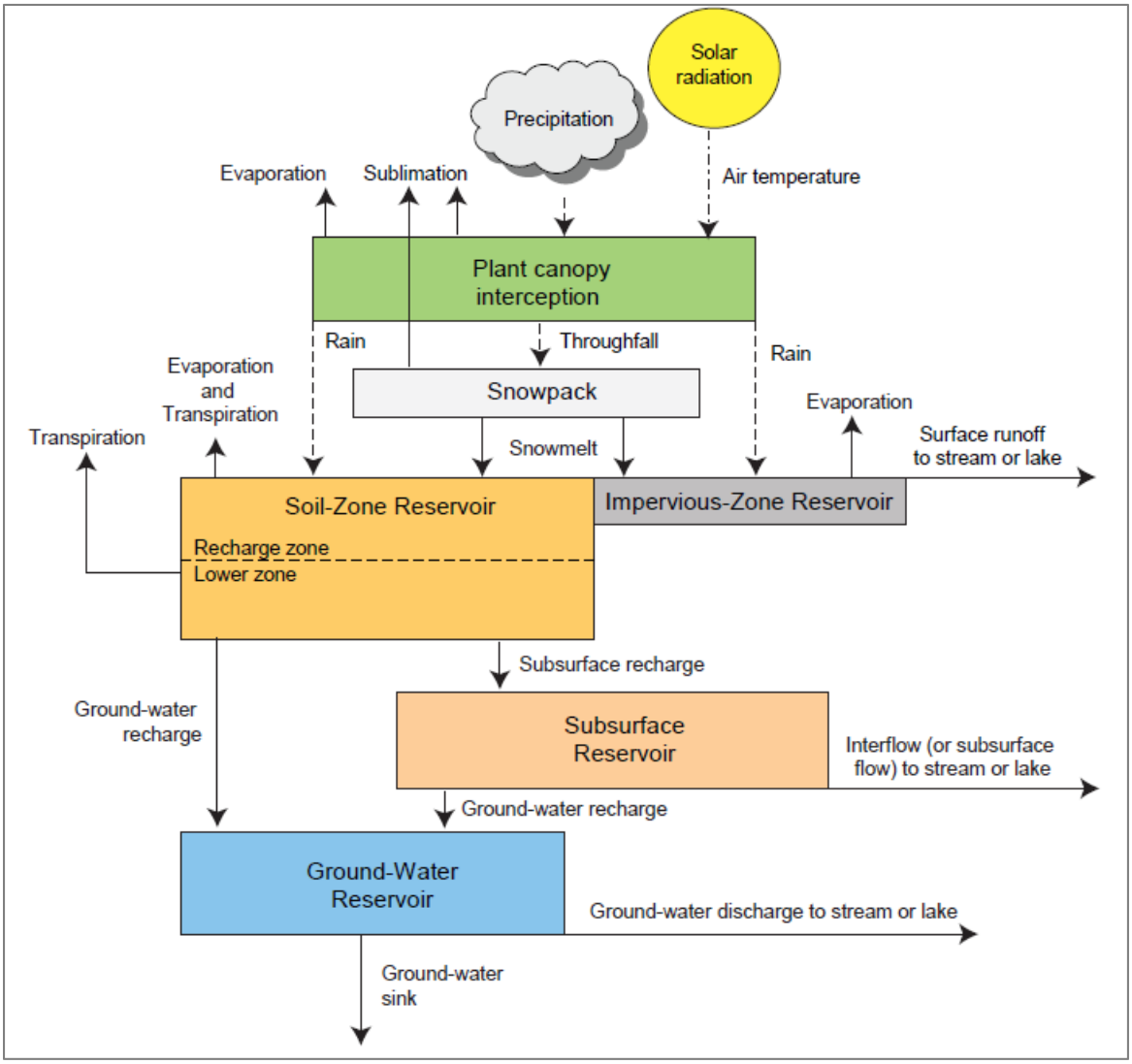

Figure 11.8 Schematic diagram of PRMS modeled hydrologic inputs and reservoirs in GSFLOW (modified from Markstrom et al., 2008).

Water and energy balances are computed daily for each HRU while climate inputs to PRMS reservoirs defining plant canopy interception, snowpack and the soil zone. Outflows from these zones include calculated evaporation, transpiration, sublimation and surface runoff. Soil storage is routed to either lateral flow through the soil zone (interflow), or to the groundwater system. Overland flow and subsurface flow in the soil zone are simulated using a lateral kinematic routing approach that does not depend on downstream conditions and takes advantage of this upstream dependent routing from cell to cells to solve the problem using a predefined order recursive algorithm to provide a significant computational efficiency advantage over other codes that solve using a matrix (simultaneous) solution. Precipitation type is a function of air temperature with snowpack simulated as a two-layered system and simulated dynamically as both water and heat reservoir to account for accumulation, sublimation and melt. Figure 11.9 illustrates the energy balance components used by PRMS.

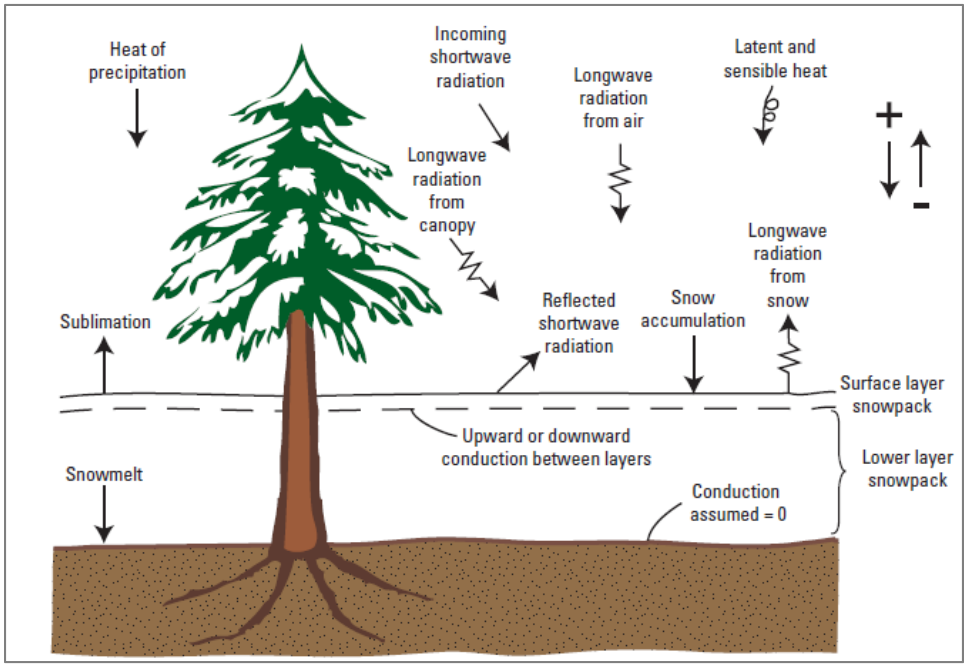

Figure 11.9 Components of the snowpack energy balance, accumulation, snowmelt and sublimation (modified from Leavesley et al., 1983).

GSFLOW integrates PRMS with groundwater flow model MODFLOW-NWT (NWT) to replace the groundwater reservoir in PRMS. Figure 11.10 shows the exchange of flow between the three primary regions in GSFLOW and the inclusion of soil moisture and head dependence on flow calculations. NWT is the latest installment of the USGS modular groundwater program that uses a finite-difference numerical method to obtain a solution to the 3-dimensional groundwater flow equation. NWT relies on the Newton solution method and an unstructured, asymmetric matrix solver to efficiently calculate groundwater head (Knoll and Keyes, 2004). NWT uses a 1-dimensional approximation of Richard's equation for unsaturated conditions for numerical efficiency and is designed to work with the Upstream Weighted (UPW) package to solve complex, unconfined groundwater flow simulations to maintain numeric stability during wetting and drying of model cells and able to describe groundwater flow within thin, steeply dipping aquifers of mountainous terrain (Zaidel, 2013). Streams are an important link between surface and groundwater systems and are modeled using MODFLOW's streamflow routing package (SFR2; Prudic et al., 2004; Niswonger and Prudic, 2005). SFR2 is a head-dependent boundary condition that allows for complex stream routing, intermittent streams and stream diversions. Flow into and out of stream reaches is often based on surface runoff routing as a function of topography and the hydraulic gradient between stream stage and the groundwater system as well as the connectivity between systems as defined by streambed conductivity.

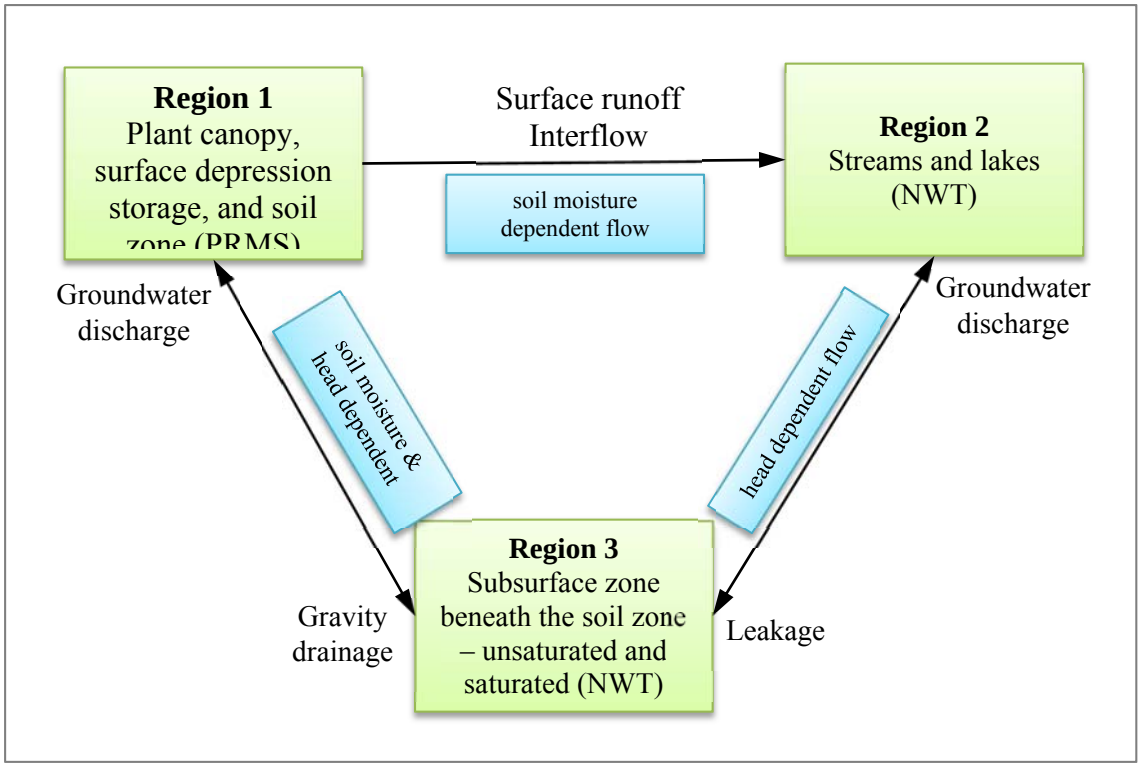

Figure 11.10 Schematic diagram of the exchange of flow among the three regions in GSFLOW. Modified from Markstrom et al., 2008.

GSFLOW implements a cascading flow procedure to route surface runoff and interflow among HRUs and streams. Flow paths start at the highest upslope HRU and continue through downslope HRUs until reaching a stream segment or lake. Cascading flow is also included in the groundwater flow for PRMS-only simulations by assuming topography is a good analogue for groundwater movement. In contrast, NWT solves for head dependent groundwater flow with unconfined conditions based on topography, stratigraphy and hydrogeological parameters defining aquifer conductance and storage. PRMS input parameters define flows between one HRU and another and derived on the basis of flow accumulation and direction analysis of a digital elevation model (DEM) and land surface altitudes. As an example is Figure 11.11, which is modified from Henson et al. (2013). The cascade routing tool (CRT; Henson et al., 2013) was used to correct the DEM for undeclared swales in topography and route flow for Box Elder and Deer Creek.

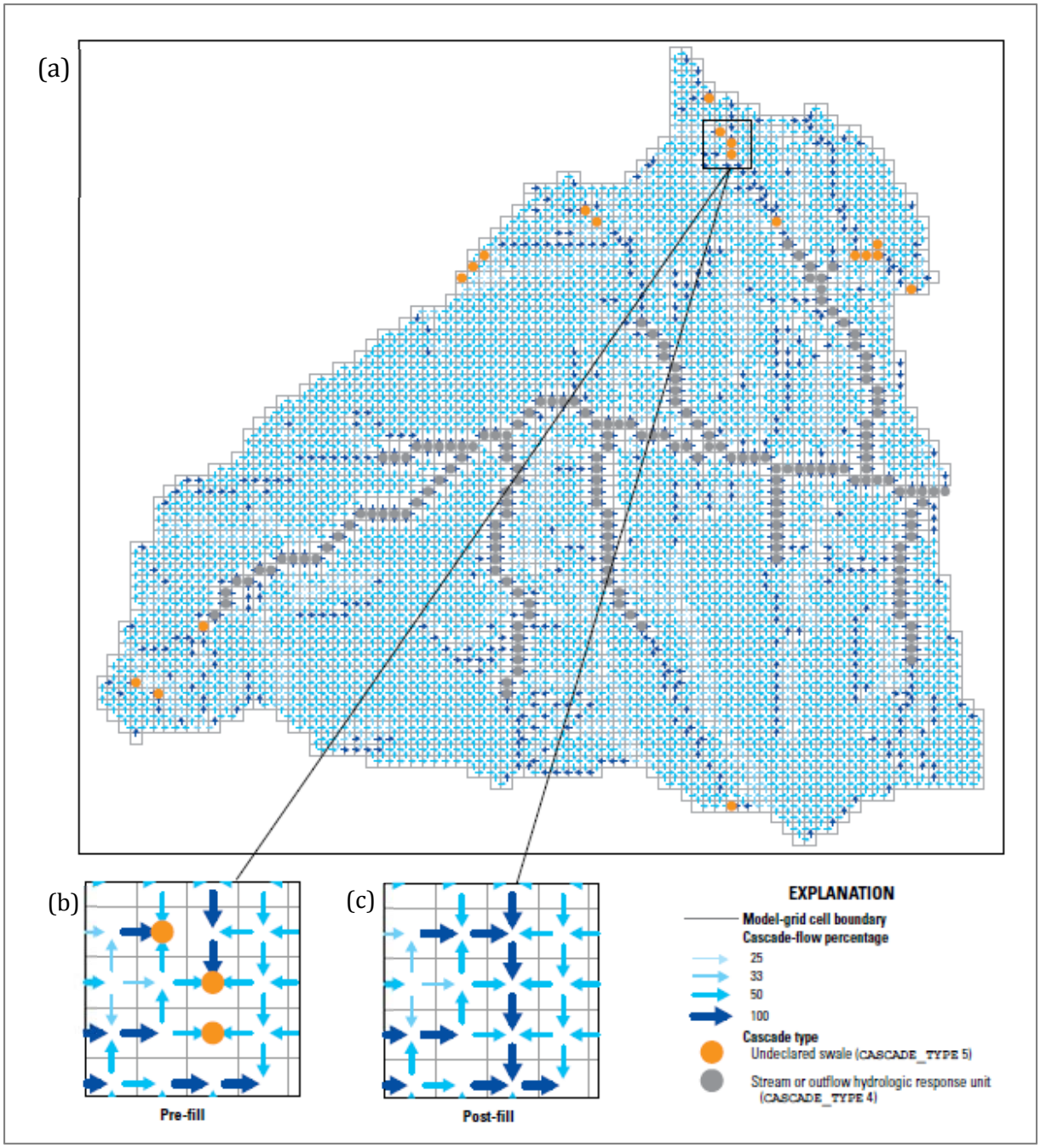

Figure 11.11 An example of the CRT application to a watershed. (a) Model domain with HRUs (grid) showing stream network, cascade flow arrows and undeclared swales, (b) detail of the model domain showing the undeclared swales and cascade flow arrows before the land-surface model is corrected, (c) the same detail of the model domain after elimination of the undeclared swales in the CRT fill procedure. Modified from Henson et al. (2013).

11.4.1 Collect and synthesize data required – Limited Modeling Approach

With GSFLOW in mind, we began a process of outlining a conceptual model. This outlining process included collecting and synthesizing available information including remote sensing, geophysical, observational, and point data. As we went through the outlining process, it became possible to conduct limited hydrologic modeling on the Box Elder and Deer Creek basins within the Laramie Range. Data needed for hydrologic modeling included a digital elevation map (DEM), precipitation and climate data, streamflow data, vegetation, and basin boundary. Figure 11.12 shows basins outlined in yellow, approximate USGS hydrologic unit code (HUC) delineations outlined in white, SNOTEL sites as red dots, and USGS gages as green dots. Numbers correspond as follows: 06646000 – Deer Creek, 06647500 - Box Elder Creek, 06652000 – Platte River at Orin, 06652800 - Platte River below Glendo Reservoir. Basin delineation was conducted using a 30 m DEM to include the HUC-12 basins contributing flow to the USGS streamflow gaging stations with model grids established at the 100 m grids shown and in Figure 11.13. Box Elder is 103 mi^2 with elevations spanning 5400 to 9000 feet; while Deer Creek is 148 mi^2 and elevations 6400 to 9300 feet.

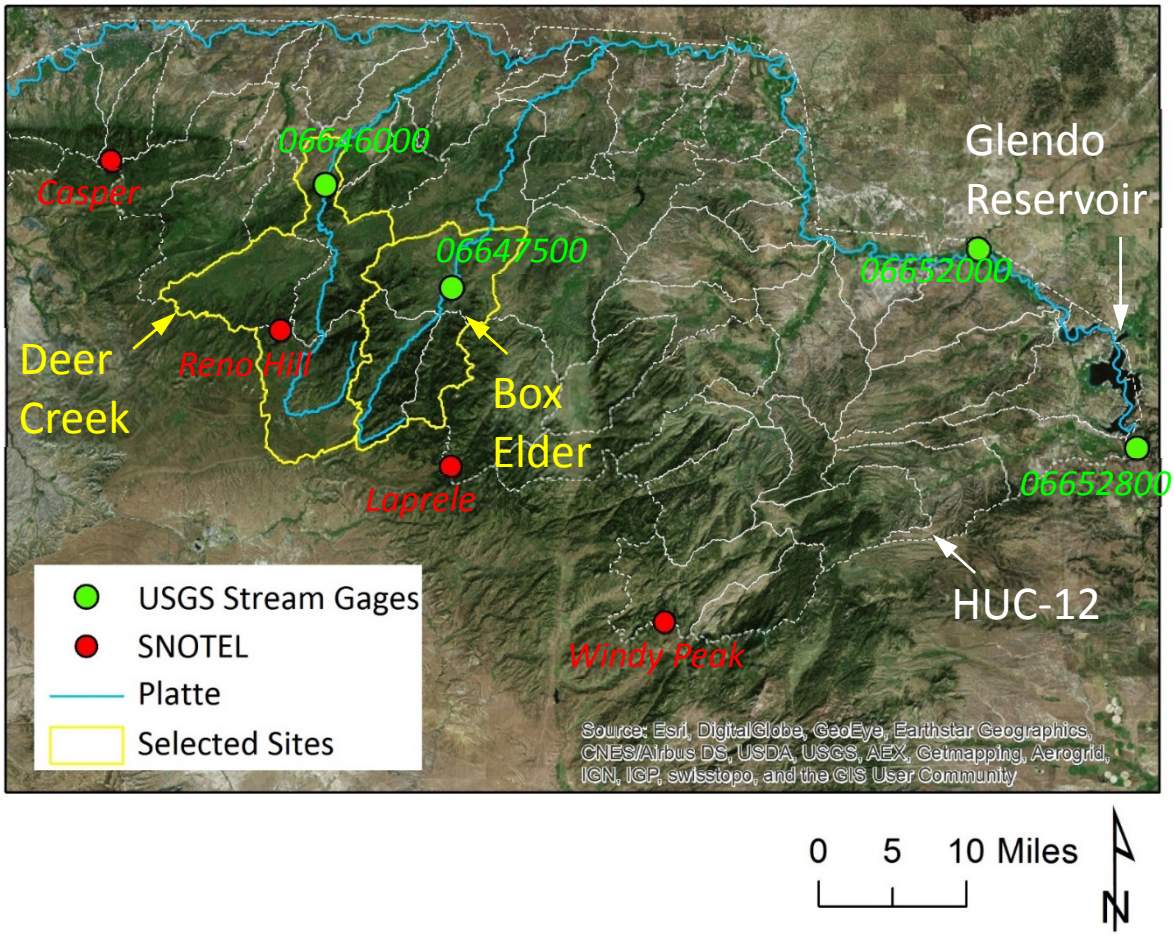

Figure 11.12 The Laramie Range with identified climate stations (Natural Resources Conservation Service Snow Telemetry; SNOTEL) and stream gages (United States Geological Survey site ID provided). Hydrologic unit code (HUC) level 12 watersheds delineated.

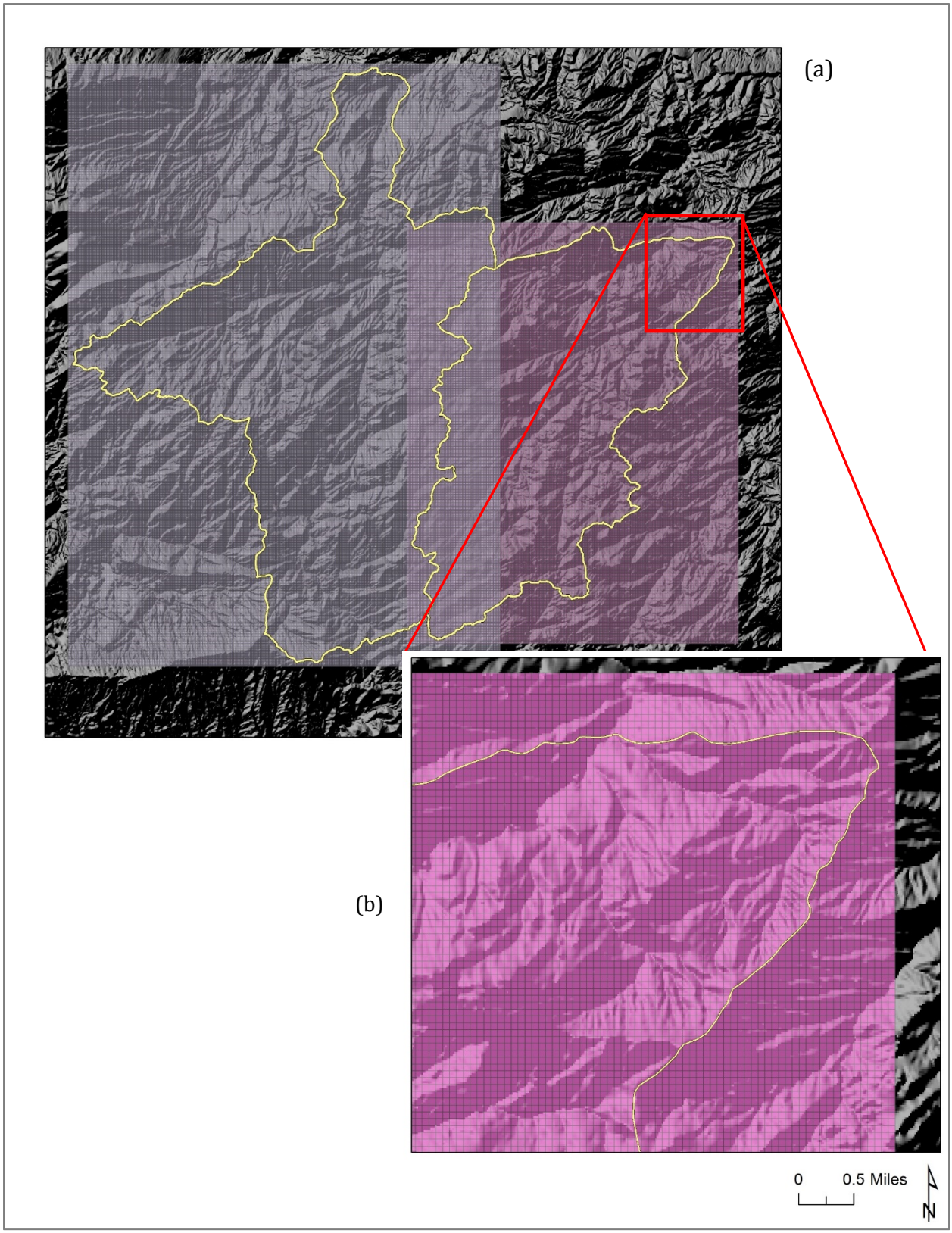

Figure 11.13 (a) Deer Creek (left) and Box Elder (Right) GSFLOW grids, (b) detail of 100 m grid resolution GSFLOW climate inputs are daily precipitation, maximum and minimum air temperature and (optionally) solar radiation.

Air temperature and solar radiation are used to compute evaporation, transpiration, sublimation and snowmelt. Three-dimensional climate forcing (x, y and time) of precipitation, air temperature, potential evapotranspiration (PET), and solar radiation obtained from WRF modeling can be spatially and temporally distributed to GSFLOW HRUs via the climate distribution module. The finest WRF resolution of the Laramie Range is at the 1 km grid resolution with output every 30 minutes and would require aggregation to the daily level for GSFLOW use. GSFLOW provides alternative mechanisms to distribute climate in space and time.

For the limited demonstration with Box Elder and Deer Creek daily air temperature lapse rates were determined using Reno Hill and Windy Peak SNOTEL stations (water years, WY, 1989 to 2015) and extrapolated across each watershed based on elevation with adjustments based on aspect. Monthly regressions of daily temperature between stations were used to backfill missing data with daily lapse rates constrained by the observed monthly standard deviation over the simulated time period. Solar radiation and PET for each HRU were not input as boundary conditions but calculated internally within PRMS. Daily potential solar radiation was calculated using approached described by Frank and Lee (1966) and Swift (1976) while shortwave radiation is computed using the degree-day method (Leaf and Brink, 1973) developed for the Rocky Mountain region and applicable to the study site where clear skies generally occur on days with no precipitation. PET was calculated using a modified Jensen-Haise formulation (Jensen et al., 1969) that relies on air temperature, solar radiation, altitude, vapor pressure and plant cover.

Daily precipitation for both basins was defined by precipitation at Reno Hill SNOTEL and spatially distributed by the ratio with mean monthly Parameter-elevation Regression on Independent Slopes Model (PRISM; 1981 to 2010; Daly, 1994). The center of each 800 m PRISM cell was linearly interpolated to the 100 m PRMS grid. Figure 11.14 provides an example of the January ratios for both domains. Values less than 1.0 signify a decrease in precipitation in comparison to Reno Hill. Precipitation type is a function of air temperature with snowpack simulated as a two-layered system and simulated dynamically as both water and heat reservoir to account for accumulation, sublimation and melt. Figure 11.15 provides simulated snow water equivalent (SWE) for a dry year (2002) and a wet year (2008) in the Box Elder watershed for March and May. Results show how PRMS spatially distributes SWE as well as the reduction of SWE over time. Additionally, PRMS output illustrates that during wet years the persistence (even accumulation) of late season SWE in the upper elevations with potentially important ramifications on peak streamflow discharge.

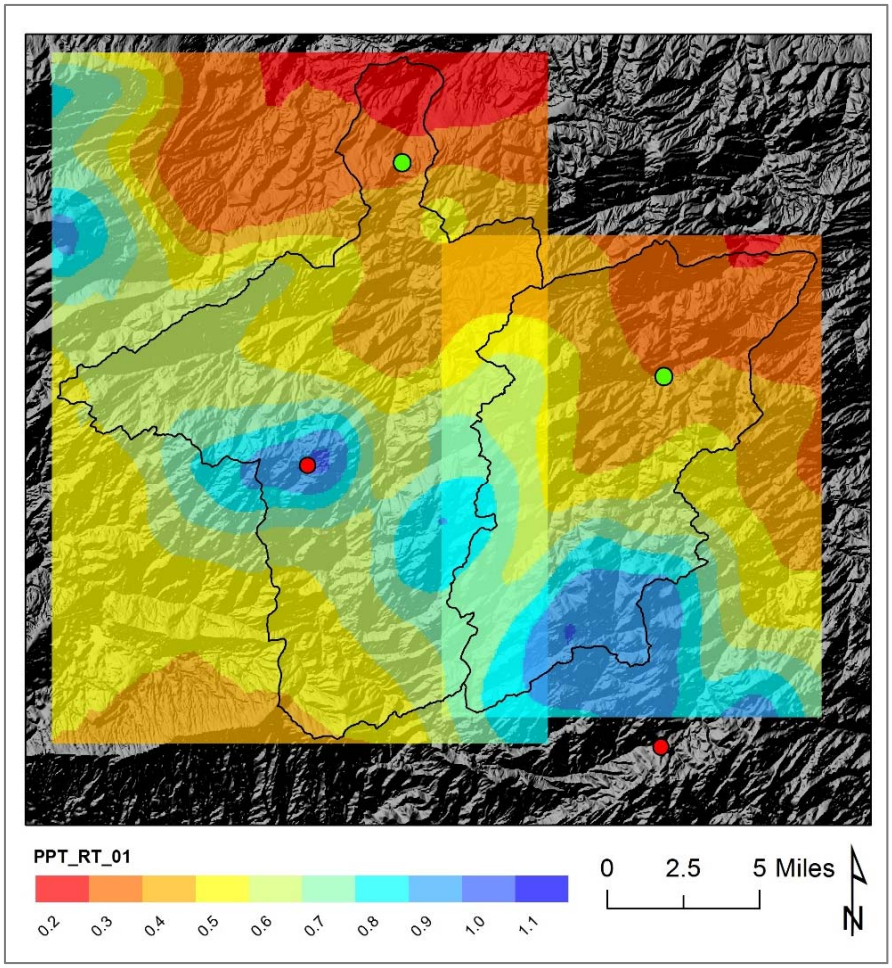

Figure 11.14 PRISM precipitation ratios for simulated domains used to distribute Reno Hill observed daily precipitation for the month of January.

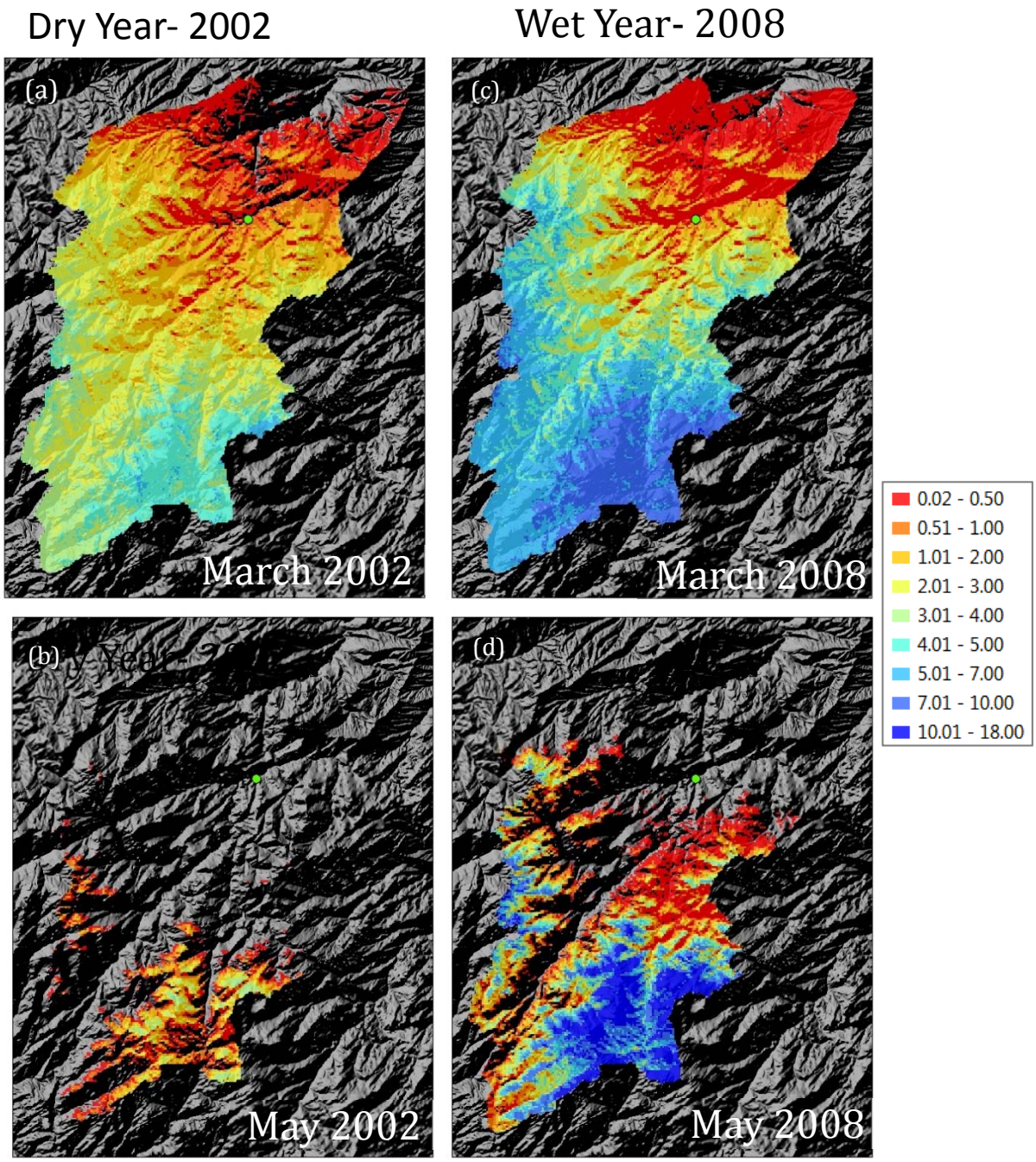

Figure 11.15 Example of SWE output from PRMS (a) March 2002, (b) May 2002, (c) March 2008 and (d) May 2008).

Basin characteristics and boundary conditions are largely based on the DEM to define topographic parameters related to elevation, slope, aspect, latitude, longitude, and cascading flow. Landuse classification uses the USGS LANDFIRE (2008) 30 m raster data set. This information was used to derive PRMS parameters of dominant cover type (Figure 11.16), summer and winter cover density, canopy interception characteristics for snow and rain, rooting depth and transmission coefficients for short wave radiation. Soil parameters were extracted from the Soils Survey Geographic Database (SSURGO) data set (NRCS, 1991). Geologic information was not required for the limited simulation, but would be required for

adding NWT to the analysis. Surface geology can be acquired through USGS mapping while depth and hydrogeologic properties of individual hydrostratigraphic units would need to be defined based on rock type, depth, observed borehole information and model calibration.

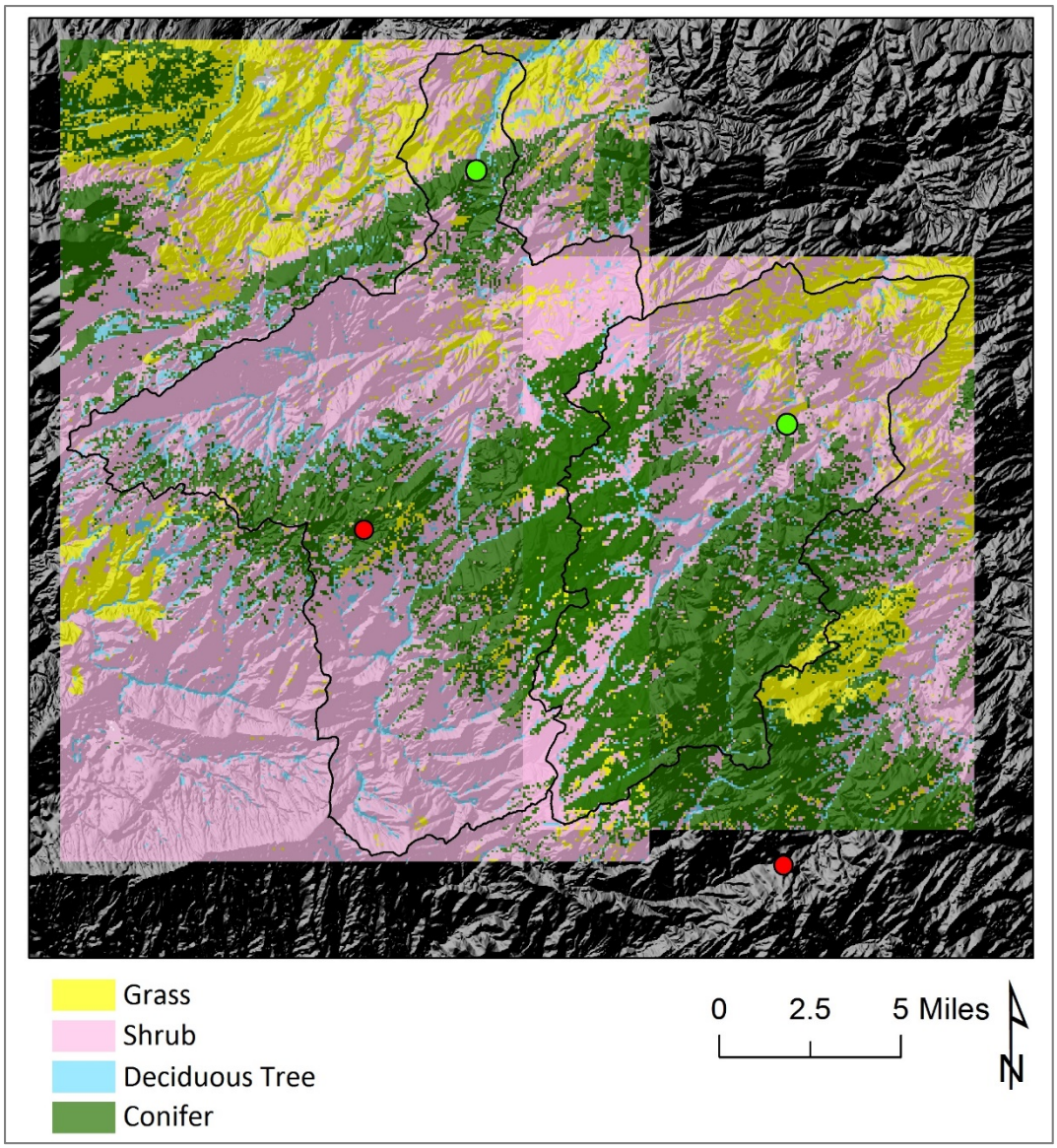

Figure 11.16 Cover types defined from species specific classifications provided by 30 m USGS LANDFIRE data sets.

11.4.2 Precipitation Changes

In the limited modeling approach, WM scenarios were developed using the calibrated, limited model to look at the effect of cloud seeding on streamflow. Precipitation type is determined internally by PRMS but it is possible to apply changes to snow only through alteration of the PRMS parameter *Snow_Adj*. For this demonstration, snow increases were applied across the entire basin and not restricted to a specific region within the model

domain. Obviously cloud seeding wound not impact the entire basin but the regions with heaviest snowfall and increased contributions would be within the cloud seeded domain. Using the model it is possible to fine-tune the seeding distribution to those portions of the watershed most likely to receive fall out from WM. The baseline scenario is the multi-decadal simulation from WY 1989 to 2015 with no augmentation of snowpack. On average, PRMS estimates annual snowfall at 65% and 56% of the precipitation for Deer Creek and Box Elder, respectively. Inter-annual variability is simulated (Figure 11.17) with lowest fraction of precipitation falling as snow occurring in 1992 despite the driest conditions simulated in 2002. Days with snowfall are estimated to occur approximately 70 days per year (61% of the precipitation events), or approximately 50 storms if individual storms are separated by at least one day of no precipitation. WM scenarios were run increasing snow precipitation by 2%, 4%, 6%, 8% and 10%. Snow increases of 5% to 15% are estimated by previous research (AMS, 1998; WMA, 2005). If one assumes that a 15% increase in snowfall is obtained when augmenting 100% of the storms, then simulating lower fractional increase from 15% implicitly assumes that not all snow precipitation events are augmented. For example, 2% augmentation would suggest only 13% of snow events are seeded, while 10% increase suggests 67% of snow events are seeded.

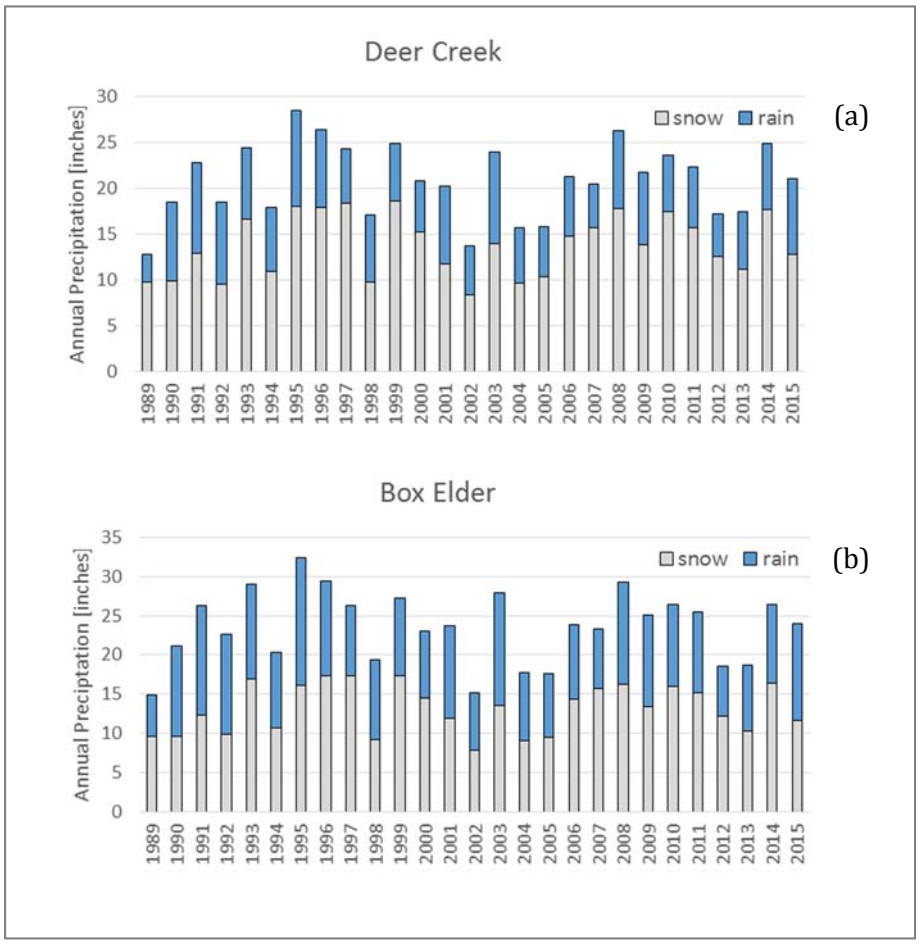

Figure 11.17 PRMS basin average precipitation totals for baseline simulation: (a) Deer Creek, (b) Box Elder.

11.4.3 Model Evaluation

GSFLOW calibration is a three step process. PRMS-only simulations only require the first calibration step. Adding NWT requires the additional two steps:

(1) Calibrate PRMS-only simulation. This generally includes adjusting PRMS parameters to match observed solar radiation (if not input as a boundary condition), PET and streamflow runoff. The latter is highly dependent on the PRMS parameter of maximum soil storage (SSP; inches) which can be conceptualized as a field capacity threshold above which water is partitioned as either interflow through the soil zone or percolates downward as gravity drainage into the groundwater reservoir (PRMS) or unsaturated zone (NWT). For Box Elder and Deer Creek, the spatial distribution of SSP was first estimated as the product of the rooting depth and available water content. Calibration is then done by scaling the spatially distributed SSP by a uniform factor. The SSP distribution was scaled by a factor of 10 for both watersheds modeled to best match streamflow. An increase in *SSP* allows for more water to be stored in the soil zone to available for losses related to evaporation and transpiration and thereby decreases water movement through processes of runoff, interflow or recharge.

(2) Calibrate a steady state NWT to best match stream baseflow. Average recharge into the groundwater system is obtained from step (1). Baseflow is the groundwater contribution to streams and represented by late summer streamflow with calibration typically done on the hydrostratigraphic unit conductance terms that is found most sensitive to streamflow estimates.

(3) Calibration of a fully coupled, transient GSFLOW with attention given to SSP and groundwater storage. In many cases it is necessary to determine length of model spin up to allow initial conditions to reach a dynamic equilibrium. GSFLOW's restart option (Regan et al., 2015) can then be used in all subsequent simulations.

Figure 11.18 shows observed and predicted streamflow at Box Elder Creek. Observed streamflow indicates that Box Elder has very low baseflow with streamflow in the summer months dipping to less than 1 cubic foot per second (cfs) all years and suggesting that Box Elder can be simulated with no groundwater reservoir in the model. Simulated results under-predict peak streamflow but are able to capture inter-annual variability. The Nash-Sutcliffe Efficiency (NSE) of simulated daily flow is 0.70 (log flow NSE = 0.56; emphasis on baseflow) and annual NSE = 0.80 indicates the model is capturing observed behavior. Figure 11.19 shows that Deer Creek has more baseflow as compared to Box Elder Creek. Summer streamflow is approximately 10 cfs and the model is improved by including a groundwater reservoir in PRMS. Figure 12 shows that, similar to Box Elder, the model is not capturing peak discharge but the daily NSE equal to 0.77 (log flow NSE = 0.72, emphasis on baseflow) and an annual NSE of 0.86 indicates the model is appropriately capturing hydrologic response.

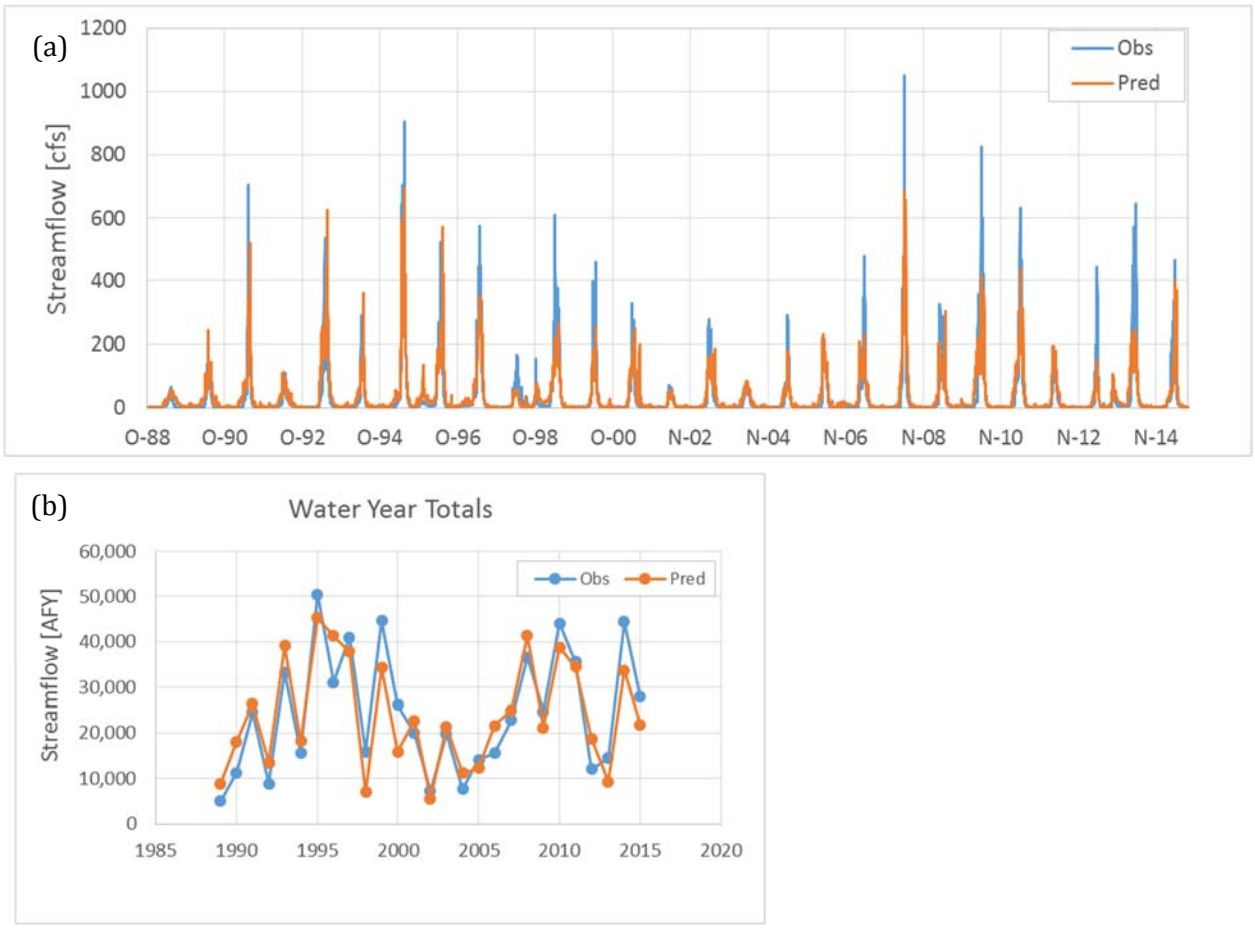

Figure 11.18 Observed and PRMS predicted streamflow at Box Elder USGS gage for WY 1989 to 2015: (a) daily and (b) annual.

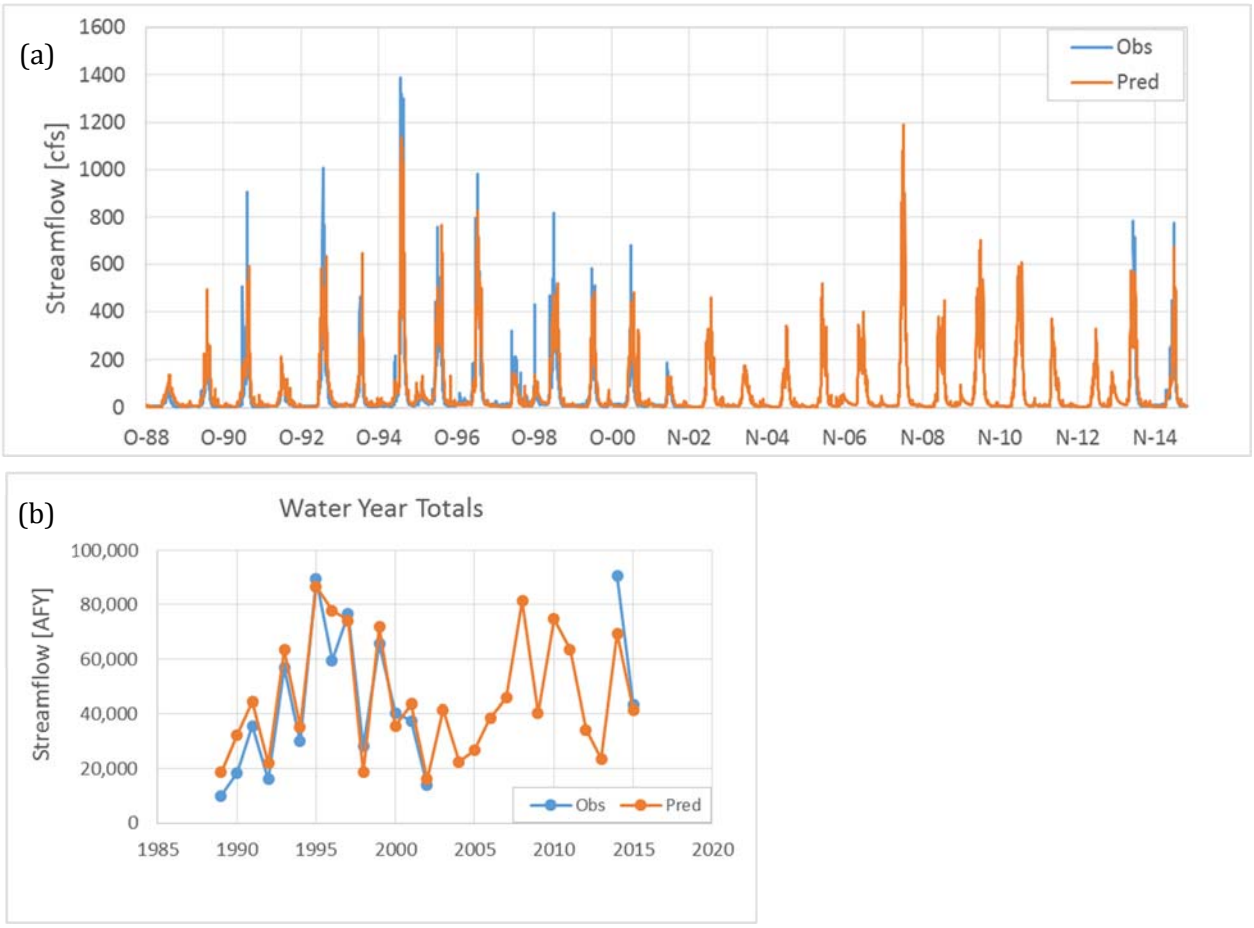

Figure 11.19. Observed and PRMS predicted streamflow at Deer Creek USGS gage for WY 1989 to 2015: (a) daily and (b) annual.

11.4.4 Results of Limited Model in Deer Creek and Box Elder

Results for modeled annual stream flow increases at the USGS gages at Deer Creek and Box Elder are given in Figures 11.20 and 11.21, respectively. Shown are changes in streamflow as a function of total precipitation (upper), total snowfall (middle), and peak SWE. The choice of using Reno Hill as the descriptive variable is based on availability of data at this location for quick assessment outside the PRMS modeling platform.

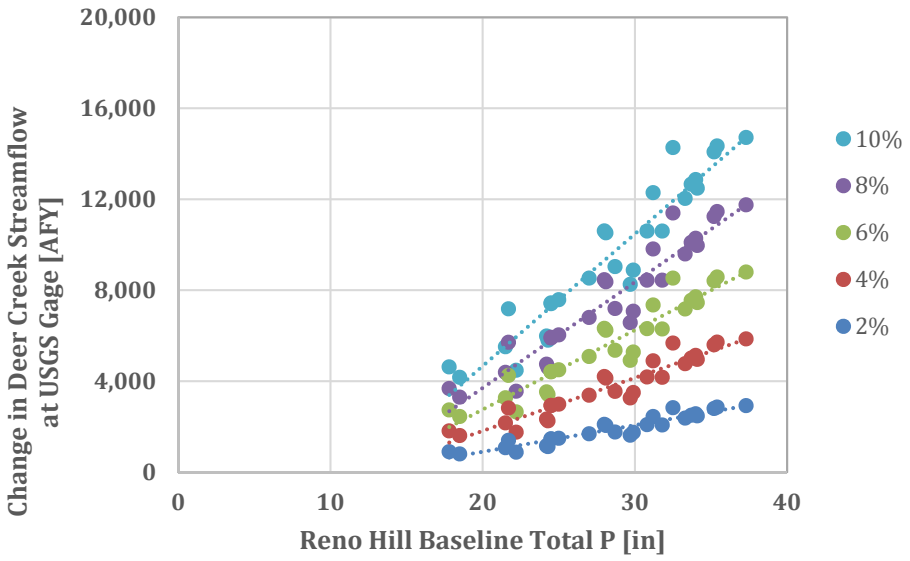
20,000
16,000
12,000
8,000
4,000
0
0
10
20
30
40
Change in Deer Creek Streamflow at USGS Gage [AFY]
Reno Hill Baseline Total P [in]
10%
8%
6%
4%
2%

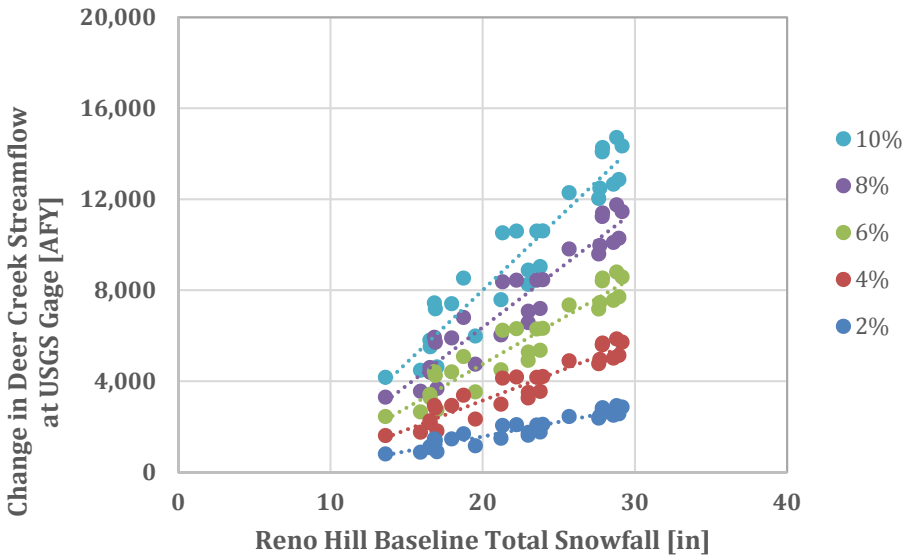
20,000
16,000
12,000
8,000
4,000
0
0
10
20
30
40
Change in Deer Creek Streamflow at USGS Gage [AFY]
Reno Hill Baseline Total Snowfall [in]
10%
8%
6%
4%
2%

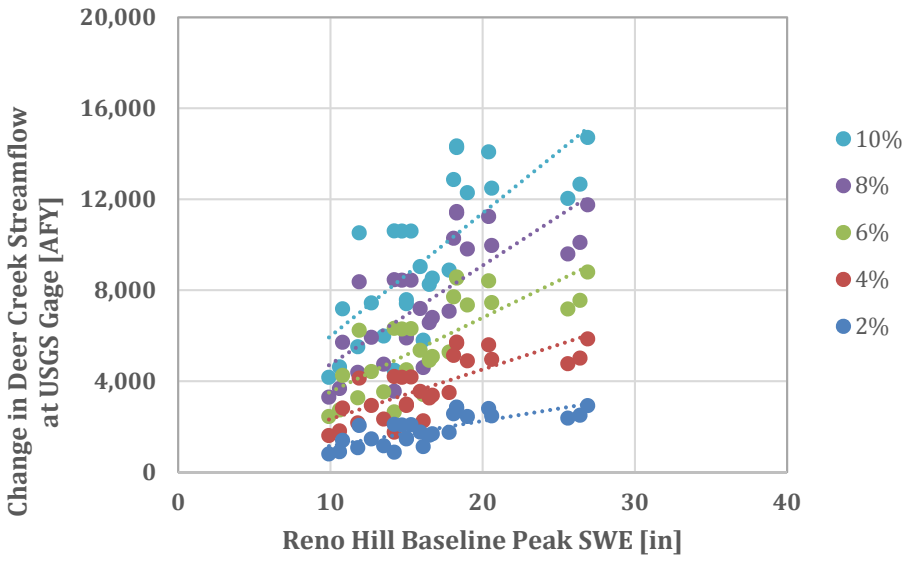

Figure 11.20 Model estimates of changes to streamflow (AFY) at the Box Elder USGS gage from cloud seeding as a function of change in: (upper) baseline total precipitation, (middle) baseline total snowfall, (lower) baseline peak SWE.

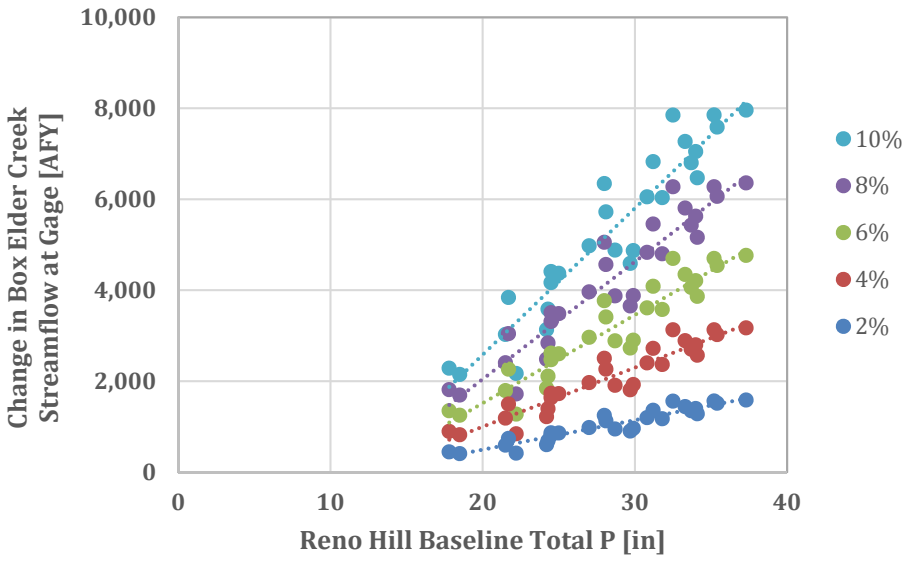
10,000
8,000
6,000
4,000
2,000
0
Change in Box Elder Creek Streamflow at Gage [AFY]
0
10
20
30
40
Reno Hill Baseline Total P [in]
10%
8%
6%
4%
2%

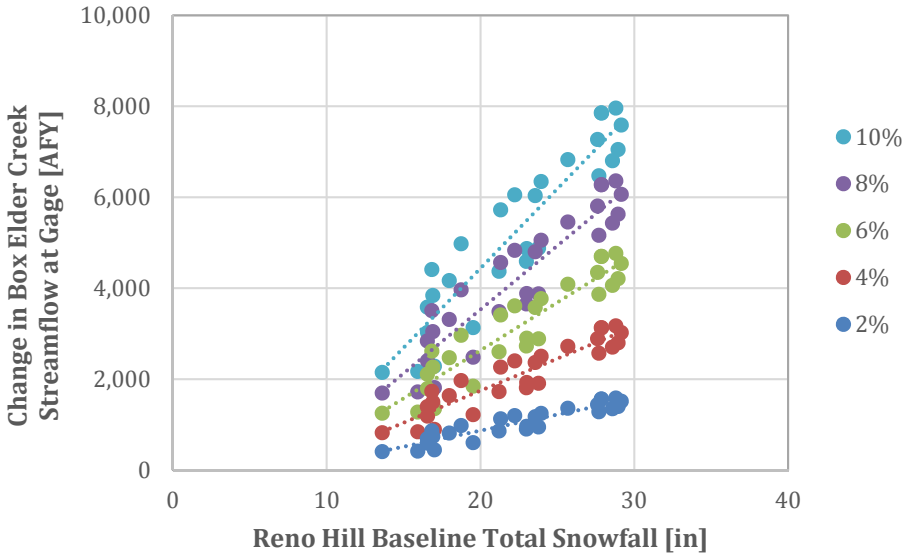
10,000
8,000
6,000
4,000
2,000
0
Change in Box Elder Creek Streamflow at Gage [AFY]
0
10
20
30
40
Reno Hill Baseline Total Snowfall [in]
10%
8%
6%
4%
2%

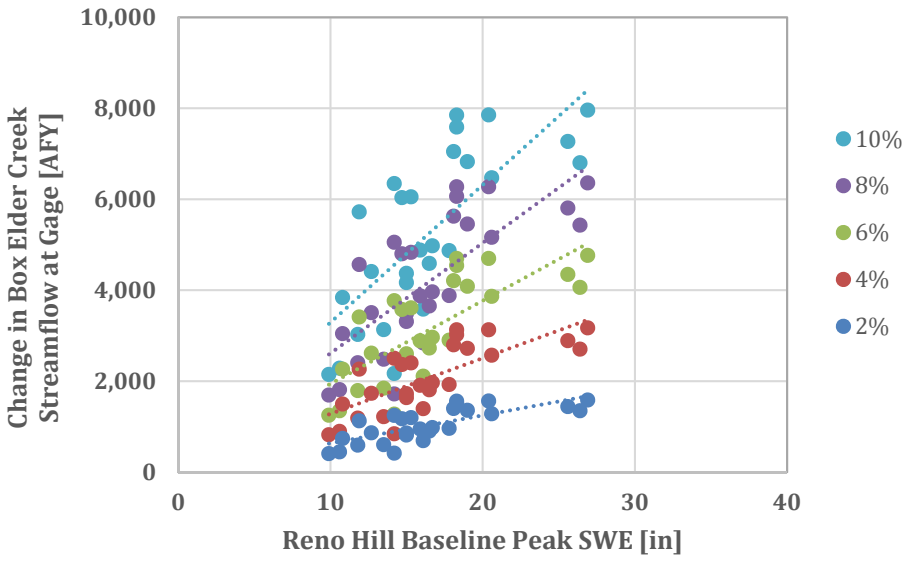

Figure 11.21 Model estimates of changes to streamflow (AFY) at the Box Elder USGS gage from cloud seeding as a function of change in: (upper) baseline total precipitation, (middle) baseline total snowfall, (lower) baseline peak SWE.

The largest increases in stream flow occur during those years when snowfall is greatest, in part, because the fractional increase in snow contribution is scaled based onto a larger baseline value. This scaling, however, is not constant. Instead, streamflow increases occur at a faster rate than does the change in basin-wide precipitation. The reason for this scaling effect is based on evapotranspiration demands in the basin. Wet years require less additional water to meet these demands, while dry years are more water limited and use additional snowmelt to help satisfy a portion of these demands. Lastly, systems with more groundwater influences appear to a slightly dampened response in streamflow gains compared to systems with limited or no estimated groundwater contributions. The dampened response produces slightly less gains on the annual basis but provides less variability about the mean response and thereby provides less uncertainty in possible gains. PRMS as a stand-alone program does not provide a physically based approach to groundwater flow and a more detailed investigation using NWT within the GSFLOW framework would need to be incorporated to make a more definitive assessment.

11.4.5 Comparison

The linear approach generally underestimated changes as compared with the limited modeling approach. In the case of Deer Creek Basin (Table 11.3), average values from the linear approach were 1247 to 6233 AFY with a minimum of 725 AFY and maximum of 12337 AFY. The limited model showed 1871 to 9515 AFY with a minimum of 795 AFY and maximum of 14713 (Table 11.9). The model shows average, minimum, and maximum changes of approximately 33%, 11%, and 16% more, respectively. In the case of Box Elder Creek Basin (Table 11.4), average values were 749 to 3743 AFY with a minimum of 435 AFY and maximum of 7410 AFY. The limited model showed 1036 to 5268 AFY with a minimum

of 404 AFY and maximum of 7960 AFY. The model shows average and maximum changes of approximately 28% and 7% more, respectively. The model shows minimum values approximately 5% lower than the linear regression. Reasons are unclear, and show the limitations of the linear model.

	Change	2%	4%	6%	8%	10%
Box Elder Creek	Average (AFY)	1328	2672	4030	5403	6790
	Minimum (AFY)	466	950	1452	1968	2502
	Maximum (AFY)	2114	4239	6369	8506	10654
	% Annual	4%	9%	13%	18%	22%
Deer Creek	Average (AFY)	1871	3759	5663	7582	9515
	Minimum (AFY)	795	1606	2440	3293	4164
	Maximum (AFY)	2921	5855	8796	11748	14713
	% Annual	4%	8%	12%	16%	21%

Table 11.9 Average, minimum, and maximum estimated changes for Box Elder Creek and Deer Creek basins streamflow from the limited modeling approach.

Since the linear approach is underestimating changes to streamflow compared to the hydrologic model, it possible that estimates for capture at Glendo reservoir may be higher. More insight might be gained from modeling the set of basins that were targeted in the linear approach.

12 Cost Estimates

The preliminary design for the Laramie Range Cloud Seeding Project includes 12 ground-based AgI generators and 7 LP dispensers (Fig 12.1).

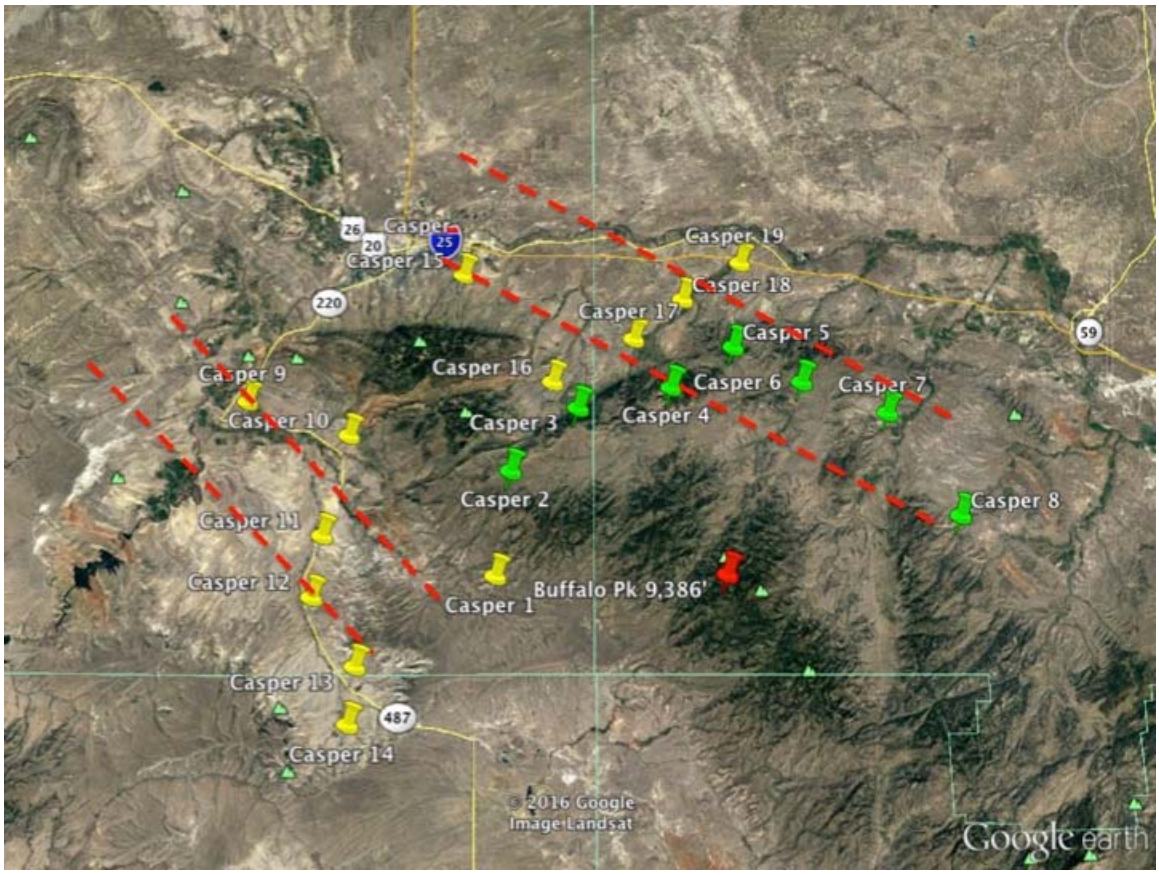

Figure 12.1 The preliminary design for generators and flight tracks. Yellow pins indicate ground-based AgI, green pins indicate liquid propane generator locations, and red dashed lines potential aircraft flight tracks.

DRI has been conducting operational cloud seeding programs and estimate program costs for more than five decades. The cost for a cloud seeding program includes the costs for all the hardware and equipment, consumables (AgI solution, propane, nitrogen, etc), shop and storage space costs, transportation, field equipment including snowmobiles and a truck, software and computers, as well as labor costs. The labor includes: the field technician's time, project management, daily 24/7 forecasting and operations, validation and evaluation, and report writing. We estimate that for a project of the size of the Laramie Range project that the fixed labor costs including shop rental fees are approximately $100,000. Figure 12.2 shows the 2015 costs for the DRI equipment and consumables package.

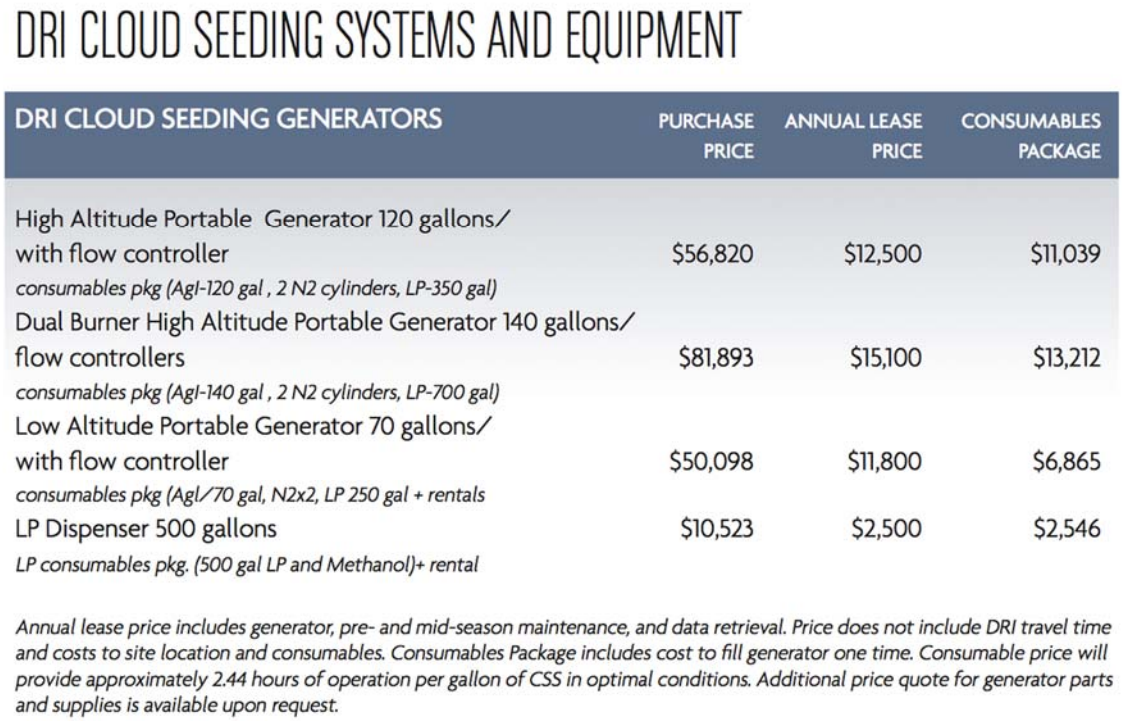

DRI CLOUD SEEDING SYSTEMS AND EQUIPMENT

DRI CLOUD SEEDING GENERATORS	PURCHASE PRICE	ANNUAL LEASE PRICE	CONSUMABLES PACKAGE
High Altitude Portable Generator 120 gallons/ with flow controller *consumables pkg (AgI-120 gal , 2 N2 cylinders, LP-350 gal)*	$56,820	$12,500	$11,039
Dual Burner High Altitude Portable Generator 140 gallons/ flow controllers *consumables pkg (AgI-140 gal , 2 N2 cylinders, LP-700 gal)*	$81,893	$15,100	$13,212
Low Altitude Portable Generator 70 gallons/ with flow controller *consumables pkg (AgI/70 gal, N2x2, LP 250 gal + rentals*	$50,098	$11,800	$6,865
LP Dispenser 500 gallons *LP consumables pkg. (500 gal LP and Methanol)+ rental*	$10,523	$2,500	$2,546

Annual lease price includes generator, pre- and mid-season maintenance, and data retrieval. Price does not include DRI travel time and costs to site location and consumables. Consumables Package includes cost to fill generator one time. Consumable price will provide approximately 2.44 hours of operation per gallon of CSS in optimal conditions. Additional price quote for generator parts and supplies is available upon request.

Figure 12.2 Hardware equipment and consumables cost.

The approximate hardware costs for leased ground-based generators sited in the field including all supplies, communications and a percentage of a weather station is listed in Table 12.1. Aircraft hourly costs were also included in the table.

Type of equipment	Costs per unit
Ground-based AgI generators	**$30,000**
Aircraft	**$1,000 (ferry to location), $2,000 (seeding time)**
Liquid Propane	**$15,000**

Table 12.1 Approximate unit costs for equipment for winter operations (does not include forecasting, operations, or reporting)

If the entire ground based design was implemented (12 AgI ground based generators and 7 LP generators) the project costs would be $565,000. If the number of AgI generators were to be reduced by half the costs for the project would be reduced to $385,000. If 50 hours of aircraft were desired the costs would be approximately $75,000.

The program can be scaled to any size by adding or subtracting the equipment costs from Table 12.1 from the original costs.

For example, the proposed initial year project should include just two-AgI generators placed in a Scenario 1 storm regime (NW flow). The sites Casper 1 and Casper 10 (see Fig 12.1) would be used for the initial year. The total cost for this initial project, including the initial set up, would be ~$150,000 depending on the costs of consumable project materials. This initial year, which would help create the necessary forecast and validation tools for the project could be evaluated and expanded or canceled beyond the initial year.

During the initial year of the project DRI recommends that the in-situ CB heights is measured to validate the feasibility of the LP sites (Casper 2 – 8), green pins in figure 12.1. If the cloud base heights are too high for much of the Scenario 2 storms the LP generators should not be used. This would reduce the project costs to $460,000.

13 Preliminary Cost Benefit Estimates

The results from the climatology (Task 3) and (Task 5) suggested that ground base AgI cloud seeding, LP cloud seeding, and AgI aircraft cloud seeding could all be conducted over the Laramie Range. We estimate that on average 25 to 40 hours of potential ground-based seeding per month is possible from the northwesterly flow cases of Scenario1 and 15 to 20 hours per month under the northeasterly flow regime of Scenario 2 (Fig. 13.1). In addition the model climatology suggested that 6% to 8% or more precipitation per year might be realized, on average, in the higher terrain when AgI cloud seeding conditions are present and even more when aircraft and LP seeding conditions are present.

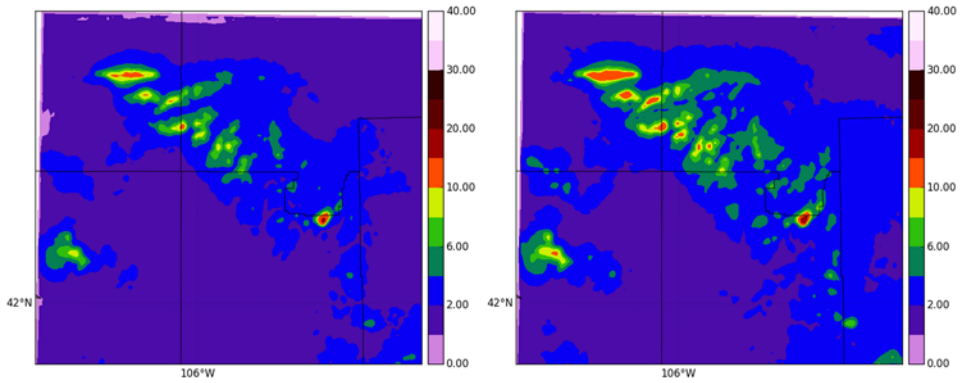

Figure 13.1. Total precipitation accumulated during 11 cold season periods (Nov-April) extending 2005-2015 total precipitation during CSP_{AgI} and $CSP_{propane}$ opportunities (in; bottom left and right panels, respectively).

The linear first order estimates of the additional precipitation reaching the North Platte River from assumed precipitation increases from an effective and well-designed cloud seeding in the Laramie Range are presented in Table 13.1. These estimates include basin runoff and cover a somewhat broader area than the cloud seeded region of the higher terrain. The much more detailed PRMS hydrologic model for Box Elder Creek also showed stream flow increases of this magnitude (see Task 11).

Inflow to Glendo (SWE increase in %)	2%	4%	6%	8%	10%
Average (AFY)	5,297	10,535	15,833	21,072	26,368
Minimum (AFY)	2,445	4,890	7,335	9,779	12,224
Maximum (AFY)	9,022	17,989	27,014	35,981	45,003

Table 13.1. Inflow values summed from all basins and the increases that may be captured in Glendo Reservoir.

If the entire ground based design was implemented (12 AgI ground based generators and 7 LP generators) the costs would be $565,000. If 50 hours of aircraft were desired the additional costs would be approximately $75,000.

The cost estimates as a function of runoff and project sizes are presented in Table 13.2. For a full program and a low estimate of only 2% increased runoff the project costs are over $100 per acre-ft. Using the results from the climatology it is estimated that a well targeted and operated project could produce an additional 16,000 to 20,000 acre feet of water on an annual average at between about $25 to $30 dollars and acre foot and perhaps as low as $20 per acre foot on a good year.

Increases in SWE	**2%**	**4%**	**6%**	**8%**	**10%**
Average Seeding Increases (AFY) at Glendo	5,297	10,535	15,833	21,072	26,368
Cost Acre-Ft (12 AgI+7 LP)	$106	$54	$36	$27	$21

Table 13.2 Cost benefit estimates at Glendo inflow as a function of increases in SWE in the Laramie Range.

For the smaller 2 generator project (only using Casper 1 and Casper 10) the SWE increases and cost estimates are calculated following the Huggins (2009) report on the Winter Park, CO cloud seeding project.

The estimate of the amount of SWE produced by seeding (W_s) during the Water Year is provided by multiplying the total expected time of generator operation for Scenario 2 storms (Table 3.2 - maximum 247 hours/year). The total generator time T_s is 247 hrs X 2 generators (T_s = 494 hours). Multiplying by the very conservative precipitation rate increase (P_s = 0.25 mm (0.01") per generator hour). This product is then multiplied by the area of effect (A_s = ~35 sq. miles), and then by seeding efficiency for the season (0.95 for a typical DRI project). To obtain the estimate in units of acre-feet the following conversions are also needed:

0.25 mm = 0.00328 ft.
1 sq. mile = 640 acres.

So, for the initial winter season the estimated snow water increase from seeding is:

W_s = 494 h x 0.25 mm/h x 0.00328 ft/mm x 35 sq mi x 640 acres/sq mi

W_s ≈ 9,073 acre-ft of SWE.

The cost for this SWE $150,000/9,073 acre-ft = $16.50/acre-ft.

14 Reports and Executive Summaries

This task requires preparing digital and paper copies of a final report and executive summary to be provided to the WWDC at the completion of this study. This report serves as the deliverable required for this task. An executive summary has also been written that summarizes the purpose, primary results, and recommendations from this study in a short document.

15 Report Presentations

Presentations on the study were provided at the technical advisory team (TAT) meeting held in Sheridan, WY on August 16, 2016. At this meeting DRI project principals, Frank McDonough, and John Mejia, presented information pertaining to preliminary study results and the atmospheric modeling assessment.
At the conclusion of the study, two public hearings were held pursuant to Wyoming Statute 41-2-114(b)(iii) on August 18, 2016 in Douglas and Wheatland, WY. The hearings were conducted in order to present the final results of the study, and accept public comment. During the course of the presentation, Mr. McDonough provided clarification and answered technical questions posed by the audience regarding the study results.

Verbal and written comments were accepted for the public record at each hearing. One substantive verbal comment was provided for the record. A summary of those concerns is provided in Appendix A. A total of three written comments were received prior to the close of the comment period and will also be included as part of the public record. The documents and comments from the public hearings are included in Appendix A.

Wyoming Statute 41-2-115(a) also requires that the WWDO identify whether or not any person, association or corporation engaged in private enterprise is capable of, and willing to construct, operate and maintain the proposed cloud seeding activities in lieu of the Office doing so. This statutory requirement was addressed at each public hearing, and no interested or capable parties were identified.

The documentation and comments from the public hearings are included in Appendix A.

16 Climatological Monitoring of the Study Area

16.1 Radiometer

A radiometer was installed in the Box Elder Creek area of the Laramie Range in early November 2015. This instrument, used to measure periods when supercooled liquid water clouds were present over the peaks of the range, operated almost continually until it was removed in early May.

Location: The location of the generator was (42.612951 N, -105.890519 W) (Fig 16.1), Will and Rachel Grant, 1976 Boxelder Rd, Glenrock, WY 82637 (Fig. 16.2). The site elevation is 2103 m (6,900-ft) MSL and the pointing angle (azimuth) is 180^{o}, toward the core of some of the highest elevations in the Range 15-km to the south (Fig 16.3). Two SNOTEL sites are within 20-km to the south of the radiometer and along the approximate radiometer azimuth.

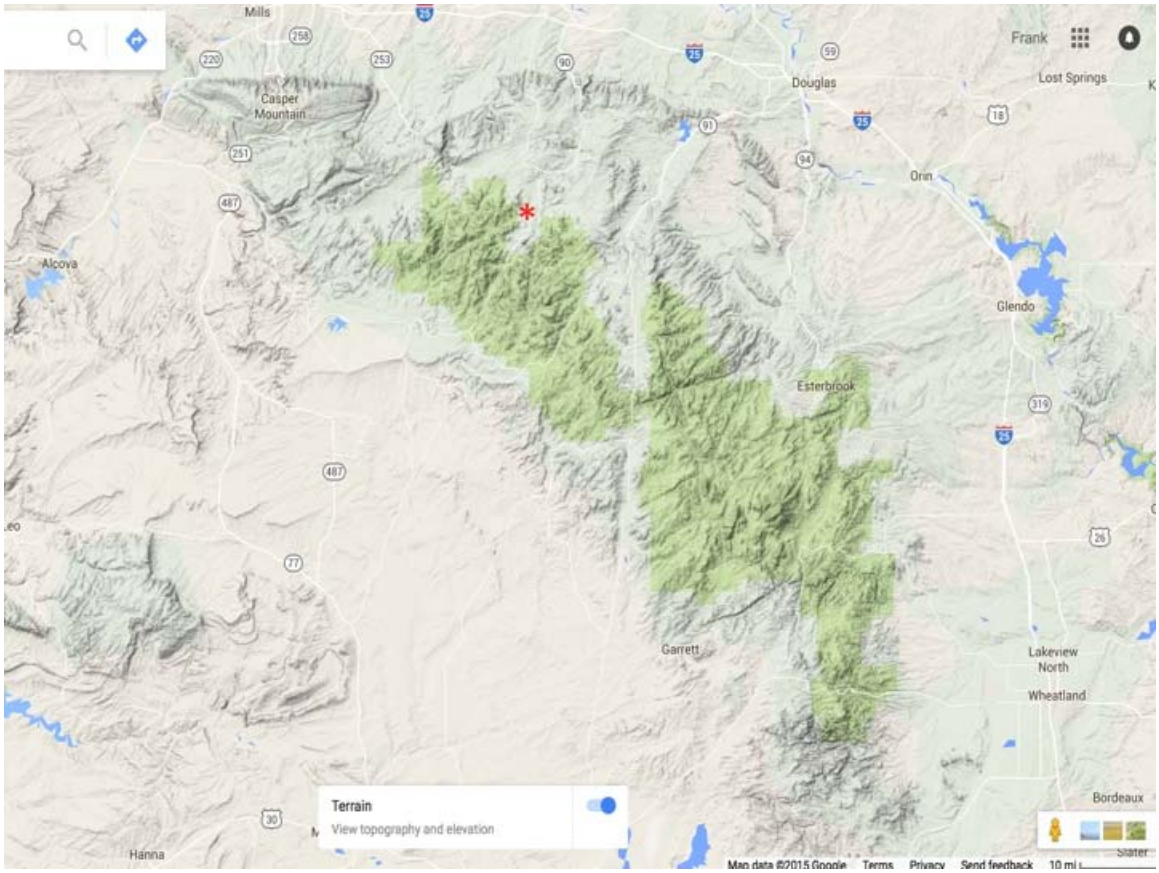

Figure16.1 The Laramie Range relief map with the radiometer site at the Grant Ranch in Boxelder Creek is identified by a red star.

Figure 16.2 The radiometer site (red star) at the Grant Ranch in Boxelder Creek. Dashed line depicts radiometer azimuth.

Figure 16.3 The radiometer site in Boxelder Creek at 6,900' MSL. Dotting line show the 180º azimuth pointing into the core of the Range above 9,000' MSL and 15-km to the south.

Installation: The radiometer was installed on 9 November 2015. Power for the radiometer and laptop is provided by the Grant's. The location is on the west side of an old barn on a raised platform (Fig. 16.4). The laptop was located inside the unheated barn. On 23 November an insulated box was built to house the laptop inside the barn. The heat from the laptop creates enough heat to keep the computer warm. Internet communications have not been successfully established yet, but the Grant's monitor the instrument as possible and report on it to the DRI team. TREC is tasked with a monthly visit to the instrument to grab data and assess the instrument.

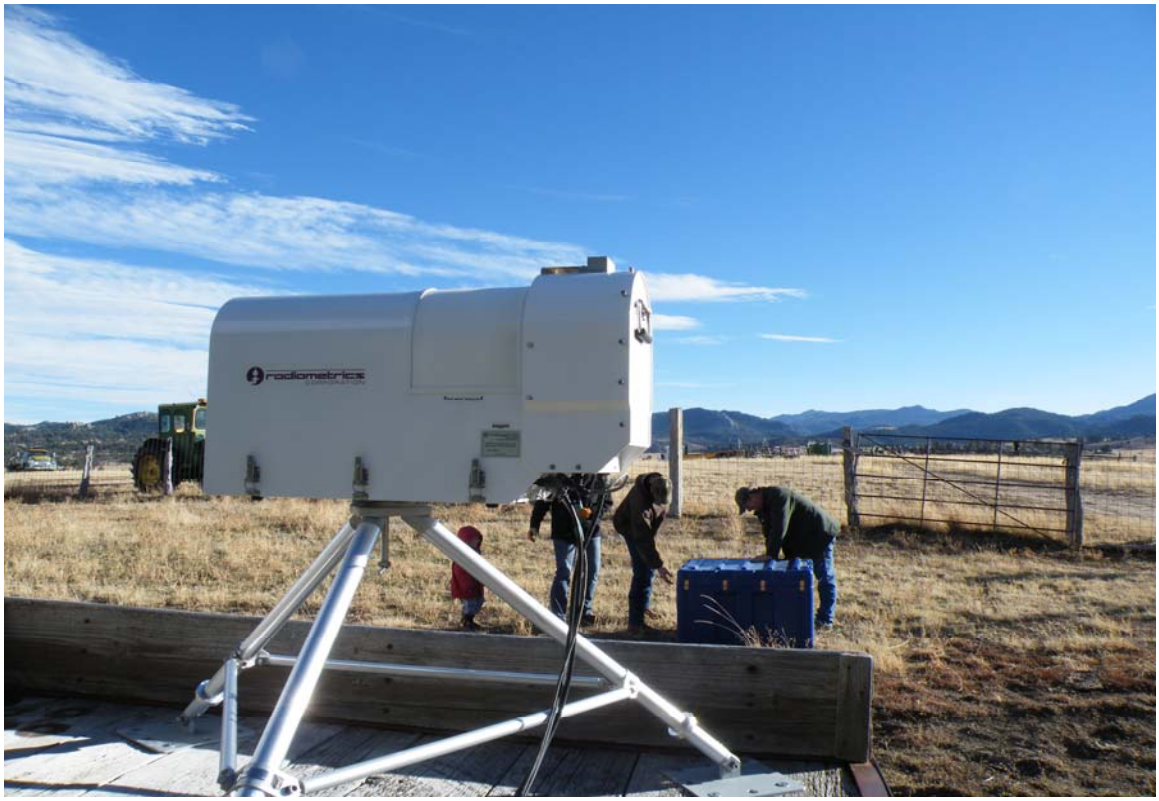

Figure 16.4 Radiometer sited at the Grant Ranch in Boxelder Creek. The high target peak area 15-km to the south are visible.

Figure 16.5 Radiometer view of the Buffalo Peak and Cherry Mountain area of the Laramie Range, 15-km south of the Grant Ranch.

Elevation scans: The software operating the radiometer is from NCAR. Five elevation angles plus a zenith angle scan are programmed into the radiometer – 8.1°, 12.15°, 15.3°, 30.15°, 45.0°. These angles are scanned every minute or so. Every 10-min, a black body calibration and a tipping curve are performed, which include the zenith scan (90°) with a water vapor profile as well as the liquid water path. Data files cover one entire day – 0000 UTC to 2355 UTC.

Results: The monthly time series of integrated liquid water for the winter (November 2015- May 2016) is presented in Figures 16.6 – 16.13. In November 2015 (Fig. 16.6) several periods when liquid water was observed by the radiometer. The maximum was early on November 17 when a cold front crossed the region. December 2016 there were several time periods when liquid water was observed in clouds during the first half of the month. A prolonged event occurred on December 15 on the cold side of a storm as it moved from northern Colorado towards the northern Great Plains. There were several periods of observed liquid water during January 2015. As an example, a departing low and cold front produced a prolonged period of observed liquid water on January 25. In February 2016 there were six events where the integrated liquid exceeded 2 mm. The event on February 16 occurred as a strong cloudy northwesterly flow cross the Laramie Range. In March 2016 there were only a few events, but the deep cyclonic upslope in later March suggested that up to 1 cm of integrated liquid water was in observed by the radiometer. In April, similar to March 2016 the integrated liquid water within the clouds was much higher than for

storms earlier in the winter. The warm cyclonic upslope storm on April 26 produced a large amount of liquid water within clouds.

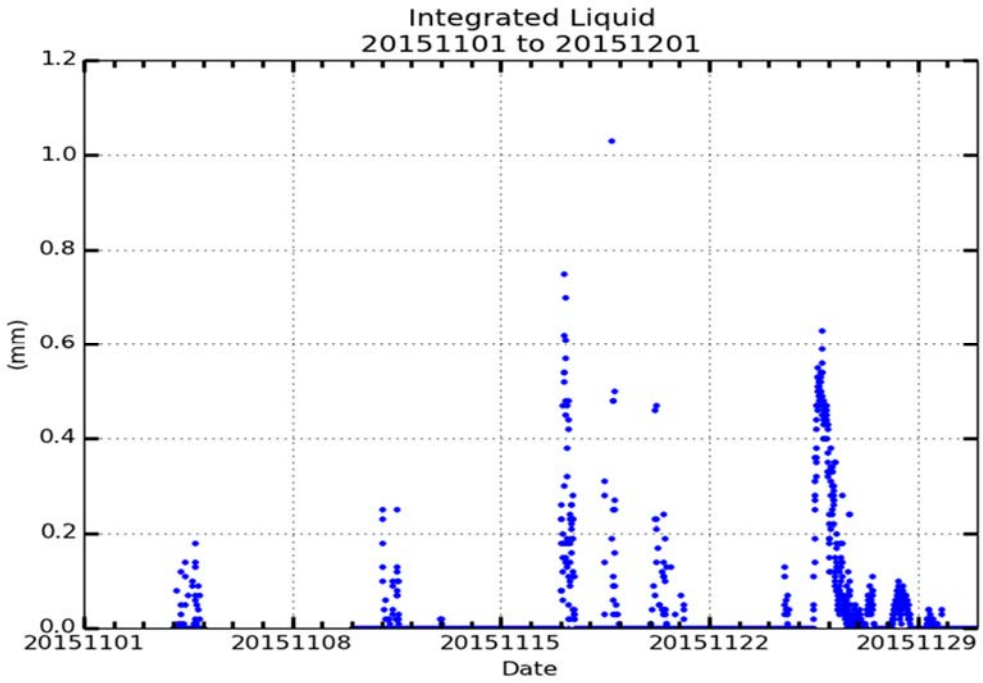

Figure 16.6 Radiometer observed integrated liquid water from the Box Elder location for November 2015.

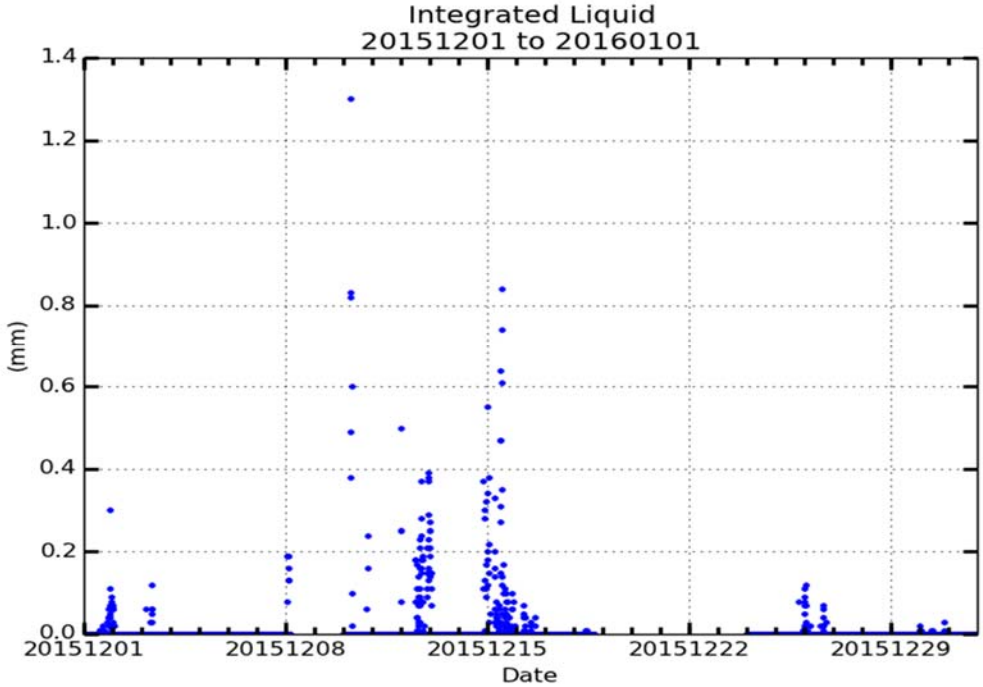

Figure 16.7 Radiometer observed integrated liquid water from the Box Elder location for December 2015.

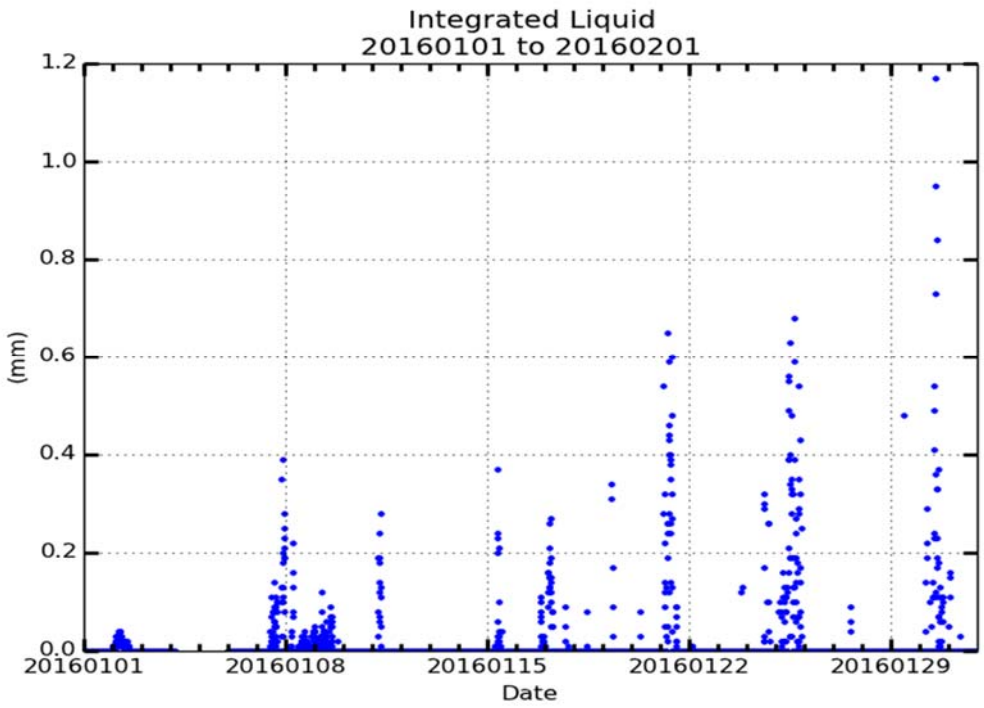

Figure 16.8 Radiometer observed integrated liquid water from the Box Elder location for January 2016.

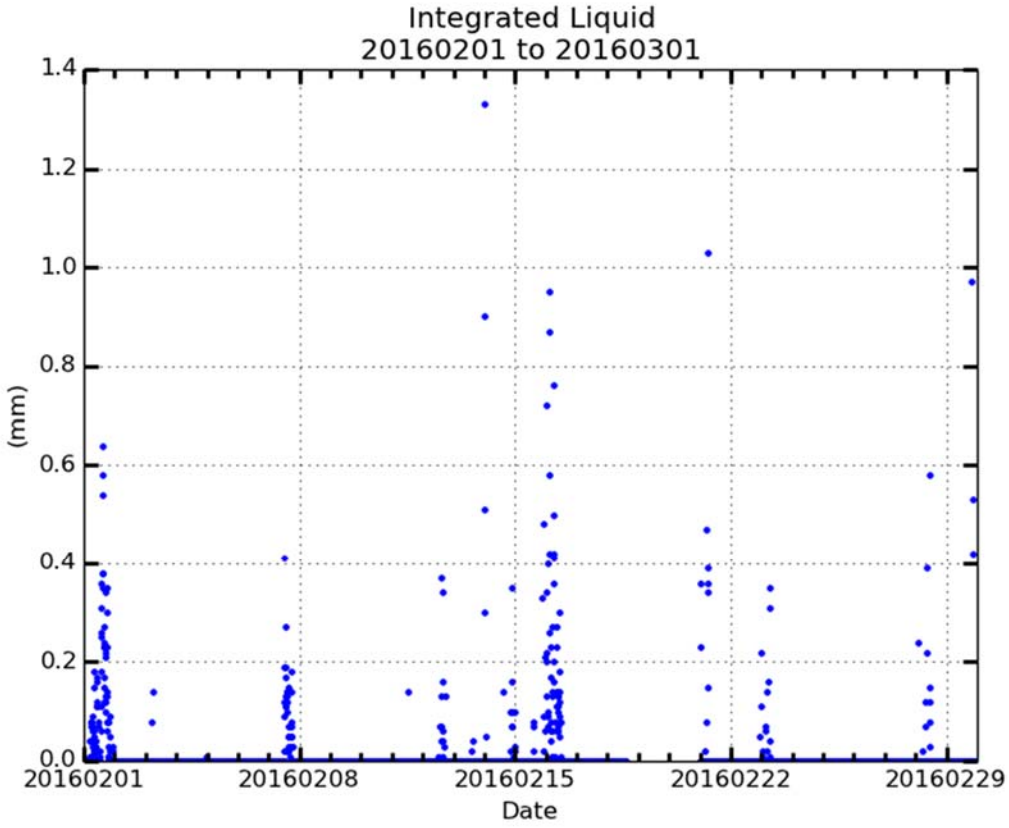

Figure 16.9 Radiometer observed integrated liquid water from the Box Elder location for February 2016.

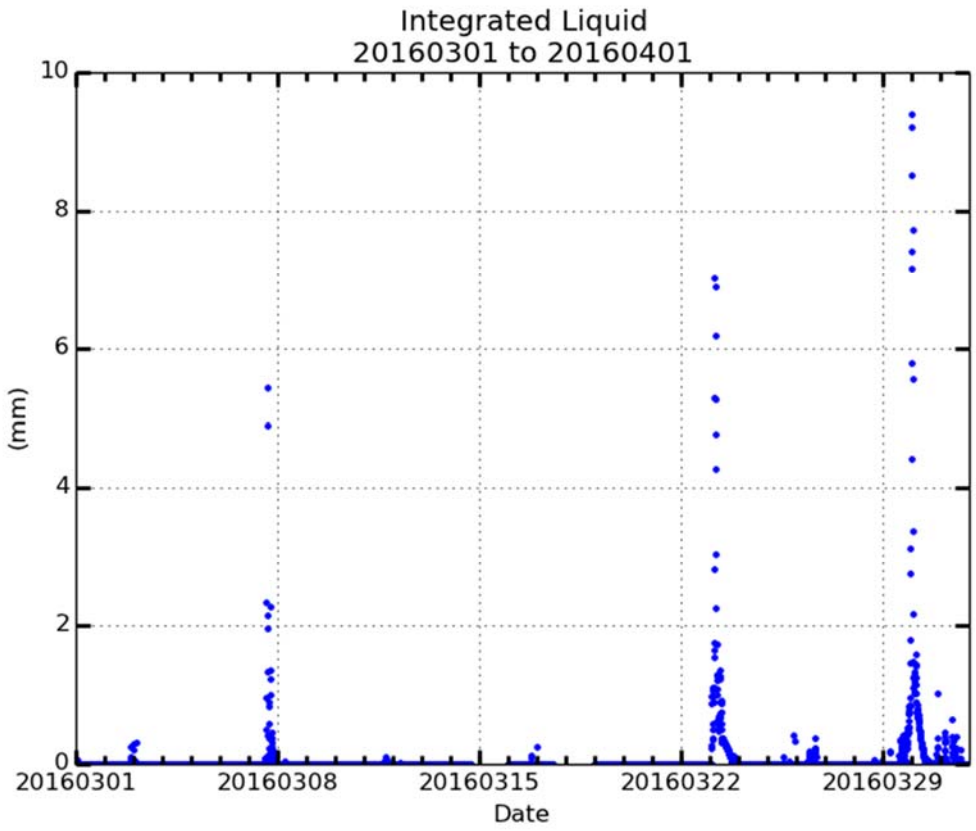

Figure 16.10 Radiometer observed integrated liquid water from the Box Elder location for March 2016.

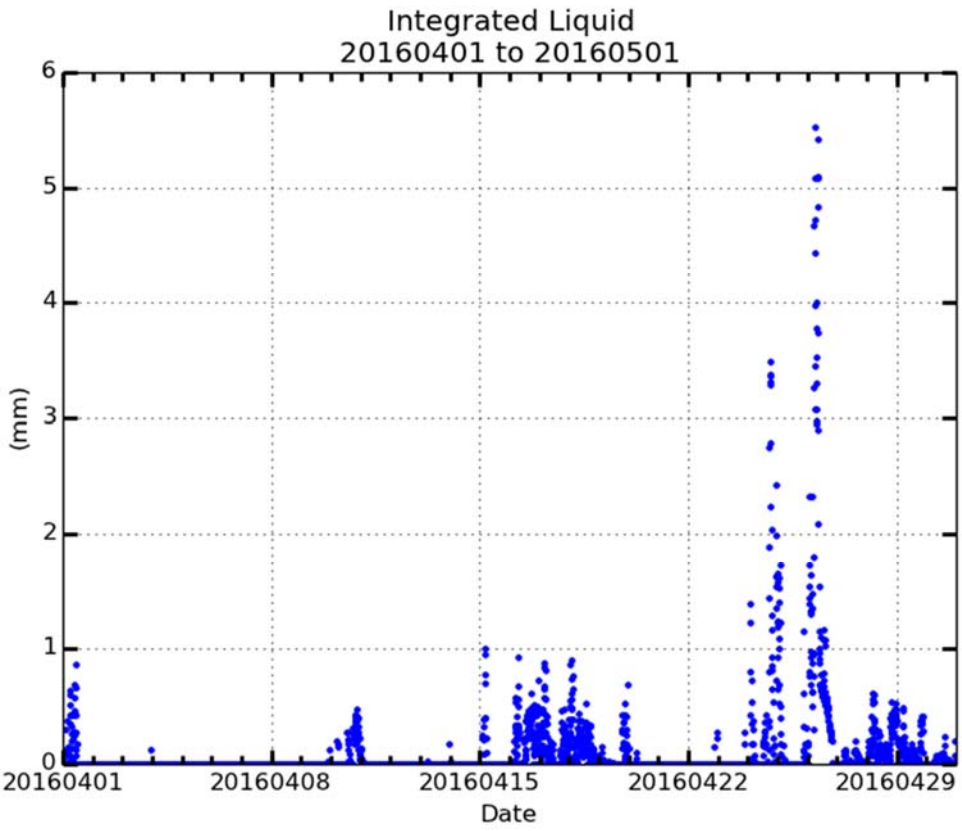

Figure 16.11 Radiometer observed integrated liquid water from the Box Elder location for April 2016.

16.2 Other Data Sets

A large observational data set was collected over the area over the winter season (Table 16.1).

Observational Data
Icing Pilot Report
Multi-channel GOES imagery
Nexrad Radar images (lowest tilt)
Surface Observations
NWS Soundings
Model Data
WRF Rapid Refresh Numerical Model

Table 16.1 Data sets collected over the Laramie Range for WY 2016

In addition daily cloud seeding forecasts were created and archived for the Laramie Range over the winter of 2015-2016 (and example is shown in Fig 16.6).

***Laramie Range: Jan 25, 2016 04 UTC**: A deep cloud layer resides over the Laramie Range. Cloud top temperatures are -55C and bases have risen to 11,000' MSL at this time. Temperatures at Reno Hill are -6C with ridge top winds from the north-northwest. 8" of fresh snow has fallen today with 0.7" of SWE. Some light icing was reported by aircraft at Casper 12,000' MSL at 2:40 UTC. Low-level radar coverage is poor, no echos observed across the area at this time. The forecast calls for the deep well-mixed cloud layer to remain over the area this evening and cloud bases may again drop below the mountain-top level, especially as cloud top temperatures warm. Cloud seeding may become possible by both ground based generators and aircraft flares from the northwest side of the range once the cloud bases drop below 9,000' MSL. Conditions should be closely monitored.*

Figure 16.6 Laramie Range forecast discussion for Jan 25, 2015.

17 References

Acharya, A., Piechota, T., Stephen, H., and Tootle G., 2011. Modeled streamflow response under cloud seeding in the North Platte River watershed. *J. Hydrology,* 409 (2011), 305–314.

American Meteorological Society, 1998. Planned and inadvertent weather modification. *Bull. Amer. Meteor. Soc*., 73. 331-337.

American Meteorological Society, 1998b. Scientific background for the AMS policy statement on planned and inadvertent weather modification. *Bull. Amer. Meteor. Soc*., 79, 2773–2778.

Bernstein, B.C, F. McDonough, M.K. Politovich, B.G. Brown, T.P. Ratvasky, D.R. Miller, C.A. Wolff, and G. Cunning, 2005. Current Icing Potential: Algorithm Description and Comparison with Aircraft Observations. *J. Appl Meteor*, 44, 969-986.

Bowden, J.H., C.G. Nolte, and T.L. Otte, 2013. Simulating the impact of the large-scale circulation on the 2-m temperature and precipitation climatology. *Climate Dynamics*, 40, 1903-1920.

Brands, S., J.M. Gutiérrez, S. Herrera, and A.S. Cofiño, 2012. On the Use of Reanalysis Data for Downscaling. *J. Climate*, 25, 2517–2526. doi:http://dx.doi.org/10.1175/JCLI-D-11-00251.1

Bullock, Jr., O.R., Alapaty, K., Herwehe, J.A., Mallard, M.S., Otte, T.L., Gilliam, R.C., Nolte, and C.G., 2014. An observation-based investigation of nudging in WRF for downscaling surface climate information to 12-km grid spacing. *J. Applied Meteorol. Clim.,* 53(1), 20-33.

Caldwell, P., H. Chin, D. Bader, and G. Bala, 2009. Evaluation of a WRF dynamical downscaling simulation over California. *Clim. Change*, 95(3–4), 499–521, doi:10.1007/s10584-009-9583-5.

Castro, C.L., R.A. Pielke Sr., and G. Leoncini, 2005. Dynamical downscaling: Assessment of value retained and added using the Regional Atmospheric Modeling System (RAMS). *J. Geophys. Res.,* 110, D05108, doi:10.1029/2004JD004721.

Cheng, W.Y.Y., and W.J. Steenburgh, 2005. Evaluation of surface sensible weather forecasts by the WRF and the Eta Models over the western United States. *Wea. Forecasting*, 20, 812–821.

Chin, H.N.S., Caldwell, P.M., and Bader, D.C., 2010. Preliminary study of California wintertime model wet bias. *Mon. Weather Rev.*, 138(9), 3556-3571.

Cotton W.R., and R.A. Pielke: “Human Impacts on Weather and Climate” 1995 ISBN 0-521-49929.

Daly, C., Neilson, R.P., and Phillips, D.L., 1994. A statistical-topographic model for mapping climatological precipitation over mountainous terrain. *J. Applied Meteorol.*, 33, 140–158.

DeFelice, T.P., J. Golden, D. Griffith, W. Woodley, D. Rosenfeld, D. Breed, M. Solak, and B. Boe, 2014. Extra area effects of cloud seeding - An updated assessment. *Atmos. Res.*, 135- 136, 193–203.

DeMott, P.J., et al., 2003. "Measurements of the concentration and composition of nuclei for cirrus formation." *Proceedings of the National Academy of Sciences* 100.25 (2003), 14655-14660.

Dixon, D., Boon, S., and Silins, U., 2014. Watershed-scale controls on snow accumulation in a small montane watershed, southwestern Alberta, Canada. *Hydrol. Process.*, 28, 1294–1306. doi: 10.1002/hyp.9667.

American Meteorological Society, 1998. Policy Statement: "Planned and Inadvertent Weather Modification," *Bull. Amer. Meteor. Soc.*, 79, 2771-78, December 1998.

Dorman, C.E., Mejia, J.F., and Koračin, D., 2013. Impact of US west coastline inhomogeneity and synoptic forcing on winds, wind stress, and wind stress curl during upwelling season. *J. Geophys. Res. Oceans,* 118(9), 4036-4051.

Dudhia, J., 1989. Numerical study of convection observed during the Winter Monsoon Experiment using a mesoscale two–dimensional model. *J. Atmos. Sci.*, 46, 3077–3107.

Eisler, R., 1996. Silver Hazards to Fish, Wildlife, and Invertebrates: A Synoptic Review, Contaminant Hazard Reviews, 32, Patuxent Wildlife Research Center, U.S. National Biological Service, Laurel, MD.

Epifanio, C.C., and D.R. Durran, 2001. 3-D effects in high drag state flows over long ridges. *J. Atmos. Sci.*, 58, 1051-1064.

Fernández-González, S., F. Valero, J.L. Sánchez, E. Gascón, L. López, E. García-Ortega, and A. Merino, 2015. Numerical simulations of snowfall events: Sensitivity analysis of physical parameterizations. *J. Geophys. Res. Atmos.,* 120, 10,130–10,148.

Frank, E.C., and Lee, R., 1966. Potential solar beam irradiation on slopes: U.S. Department of Agriculture, Forest Service Research Paper RM-18. 116. doi:10.1002/2015JD023793.

Gochis, D.J., Yu, W., and Yates, D.N., 2015. The WRF-Hydro model technical description and user's guide, version 3.0. NCAR Technical Document. 120 pg. http://www.ral.ucar.edu/projects/wrf_hydro/.

Grant, L.O., and P.W. Mielke, 1967: A randomized cloud seeding experiment at Climax, CO, 1960-65. Proc. Fifth Berkeley Symp. on Matematical Statistics and Probability, Vol. 5, University of California Press, 115-132.

Griffith D.A, D.P. Yorty, and S.D. Beall, 2014. Target/Control Analysis for Santa Barbara County's Operational Winter Cloud Seeding Program. *J. Wea Mod.,* 47.

Harbaugh AW., 2005. MODFLOW-2005, the U.S. Geological Survey modular groundwater model—the ground-water flow process, U.S. Geol. Survey Technical Methods, Book 6, Chap. A16.

Harris, E. R., 1981. Sierra Cooperative Pilot Project environmental assessment and finding of no significant impact. U. S. Dept. of Interior, Bureau of Reclamation, Office of Atmospheric Resources Research, Denver, Colo., 196 pp.

He, G. W., 2011. Anomalous scaling for Lagrangian velocity structure functions in fully developed turbulence. *Physical Review E*, 83(2), 025301.

Helsel, D.R., and R. M. Hirsch, 2002. Statistical Methods in Water Resources Techniques of Water Resources Investigations, Book 4, chapter A3. U.S. Geological Survey. 522 pp.

Henson, W.R., Medina, R.L., Mayers, C.J., Niwonger, R.G., and Regan, R.S., 2013. CRT – Cascade Routing Tool to define and visualize flow paths for grid-based watershed models: U.S. Geological Survey Techniques and Methods. 6-D2, 28 p.

Howell, W. E.,1977. Environmental impacts of precipitation management: Results and inferences from Project Skywater. *Bull. Amer. Meteor. Soc.,* 58, 488-501.

Hung-Neng S. Chin, Peter M. Caldwell, and David C. Bader, 2010: Preliminary Study of California Wintertime Model Wet Bias. *Mon. Wea. Rev.,*138, 3556–3571. doi: http://dx.doi.org/10.1175/2010MWR3409.1

Hunter, S. M., 2006: Potential water augmentation from cloud seeding in the Colorado River Basin, *J. Wea. Modification*, 38, 51, 57.

Janjic, Zavisa I., 1994. The Step–Mountain Eta Coordinate Model: Further developments of the convection, viscous sublayer, and turbulence closure schemes. *Mon. Wea. Rev.*, 122, 927–945.

Jensen, M.E., Rob, D.C.N, and Franzoy, C.E.,1969. Scheduling irrigations using climate-crop-soil data, National Conference on Water Resources Engineering of the American Society of Civil Engineers. New Orleans, LA. [Proceedings]. 20 pp.

Jin, J., and L. Wen, 2012. Evaluation of snowmelt simulation in the Weather Research and Forecasting model. *J. Geophys. Res.,* 117, D10110, doi:10.1029/2011JD016980.

Katragkou, E., García-Díez, M., Vautard, R., Sobolowski, S., Zanis, P., Alexandri, G., and Goergen, K., 2015. Regional climate hindcast simulations within EURO-CORDEX: evaluation of a WRF multi-physics ensemble. *Geosci. Model Development*, 8(3), 603-618.

Kelly C, McGuire K, Miniat C, and Vose J, 2016. Streamflow response to increasing precipitation extremes altered by forest management. *Geophys. Res. Letts*. 43(8), 3727–3736. DOI: 10.1002/2016GL068058.

Kennedy, A., Dong, X., Xi, B., Xie, S., Zhang, Y., and Chen, J., 2011. A comparison of MERRA and NARR reanalyses with the DOE ARM SGP data. *J. Climate,* 24, 4541–4557. doi:10.1175/2011JCLI3978.1.

Klein, D.A.,1978. Environmental Impacts of Artificial Ice Nucleating Agents, Colorado State University, Dowden, Hutchinson & Ross, Inc. Library of Congress Catalog Card Number, 78-7985.

Knoll, D.A., and Keyes, D.E., 2004. Jacobian-free Newton-Krylov methods: a survey of approaches and applications. *J. Computational Physics,* 193(2), 357-397.

Koracin at al., 2011. Regional Source Identification Using Lagrangian Stochastic Particle Dispersion and HYSPLIT Backward-Trajectory Models. *J. Air & Waste Manage. Assoc.*, 61, 660–672. DOI:10.3155/1047-3289.61.6.660.

Koracin, D., Panorska, A., Isakov, V., Touma, J. S., and Swall, J., 2007: A Statistical Approach for Estimating Uncertainty in Dispersion Modeling: An Example of Application in Southwestern USA. *Atmos. Environ.,* 41, 617-628.

Korolev A.W, and I.P. Mazin 2003. Supersaturation of Water Vapor in Clouds. *JAS,* 60, Dec 2003.

Leaf, C.F., and Brink, G.E., 1973. Hydrologic simulation model of Colorado subalpine forest. U.S. Department of Agriculture, Forest Service Research Paper RM-107. 23 pp.

Leavesley, G. H., Markstrom, S. L., Viger, R. J., and Hay, L. E., 2005, USGS Modular Modeling System (MMS) -- Precipitation-Runoff Modeling System (PRMS) MMS-PRMS: in Singh, V., and Frevert, D., eds., Watershed Models: Boca Raton, Fla., CRC Press, p. 159-177.

Leavesley, G.H., Lichty, R.W., Toutman, B.M and Saindon, L.G., 1983. Precipitation-runoff modeling system – User's Guide: U.S. Geological Survey Water Resources Investigations Report. 83-4238. 207 pp.

Leung L. Ruby, Yun Qian, and Xindi Bian, 2003. Hydroclimate of the Western United States Based on Observations and Regional Climate Simulation of 1981–2000. Part I: Seasonal Statistics. *J. Climate*, 16, 1892–1911.

Leung, L. R., and Y. Qian, 2003. The sensitivity of precipitation and snowpack simulations to model resolution via nesting in regions of complex terrain. *J. Hydrometeorol*., 4,1025–1043. doi:10.1175/1525-7541(2003)004<1025:TSOPAS>2.0.CO;2.

Li, X., Zhong, S., Bian, X., Heilman, W.E., Luo, Y., and Dong, W., 2010. Hydroclimate and variability in the Great Lakes region as derived from the North American Regional Reanalysis. *J. Geophys. Res.,* 115, D12104. doi:10.1029/2009JD012756.

Liang Xin-Zhong, Min Xu, Xing Yuan, Tiejun Ling, Hyun I. Choi, Feng Zhang, Ligang Chen, Shuyan Liu, Shenjian Su, Fengxue Qiao, Yuxiang He, Julian X. L. Wang, Kenneth Kunkel, E., Wei Gao, Everette Joseph, Vernon Morris, Tsann-Wang Yu, Jimy Dudhia, and John Michalakes, 2012. Regional Climate–Weather Research and Forecasting Model. *Bull. Amer. Meteor. Soc.,* 93, 1363–1387. doi: http://dx.doi.org/10.1175/BAMS-D-11-00180.1

Liang, X., D. P. Lettenmaier, E. F. Wood, and S. J. Burges, 1994. A Simple hydrologically Based Model of Land Surface Water and Energy Fluxes for GSMs, *J. Geophys. Res.*, 99(D7), 14,415-14,428.

Liou, K. N., Gu, Y., Leung, L. R., Lee, W. L., and Fovell, R. G., 2013. A WRF simulation of the impact of 3-D radiative transfer on surface hydrology over the Rocky Mountains and Sierra Nevada. *Atmos. Chem. Physics,* 13(23), 11709-11721.

Lo, J. C.-F., Z.-L. Yang, and R. A. Pielke Sr., 2008. Assessment of three dynamical climate downscaling methods using the Weather Research and Forecasting (WRF) model, *J. Geophys. Res.,* 113, D09112, doi:10.1029/2007JD009216.

Lowenthal, D.H., Watson, J.G., Koracin, D., Chen, L.-W.A., DuBois, D., Vellore, R., Kumar, N., Knipping, E.M., Wheeler, N., Craig, K., and Reid, S., 2010. Evaluation of Regional Scale Receptor Modeling. *J. Air & Waste Manage. Assoc.* 60, 26-42. doi: 10.3155/1047-3289.60.1.26.

Luria, M., Tanner, R.L., Valente, R.J., Bairai, S.T., Koracin, D., and Gertler, A.W., 2005. Local and Transported Pollution over San Diego, California. *Atmos. Environ*., 39, 6765-6776.

Manton, M.J., and L. Warren, 2011. A Confirmatory Snowfall Enhancement Project in the Snowy Mountains of Australia. Part II: Primay and Associate Analysis. *J. App. Meteor. Clim*., 50. July 2011.

Markstrom, S. L., Niswonger, R. G., Regan, R. S., Prudic, D. E., and Barlow, P. M., 2008. GSFLOW – Coupled Ground-Water and Surface-Water Flow Model Based on the Integration of the Precipitation-Runoff Modeling System (PRMS) and the Modular Ground-Water Flow Model (MODFLOW-2005): U.S. Geological Survey Techniques and Methods 6-D1, 240 pp.

Mass, C. F., D. Ovens, K. Westrick, and B. A. Colle, 2002. Does increasing horizontal resolution produce more skillful forecasts? *Bull. Amer. Meteor. Soc.,* 83, 407–430.

McAlpine, J.D., D.R. Koračin, D.P. Boyle, J.A. Gillies, and E.V. McDonald, 2010. Development of a rotorcraft dust-emission parameterization using a CFD model. *Environ. Fluid Mech*., 10, 691-710, doi:10.1007/s10652-010-9191-y.

McCarthy Mark P., P. W. Thorne, and H. A. Titchner, 2009. An Analysis of Tropospheric Humidity Trends from Radiosondes. *J. Climate*, 22, 5820–5838. doi: http://dx.doi.org/10.1175/2009JCLI2879.1

McEvoy, D. J., Mejia, J. F., and Huntington, J. L., 2014. Use of an observation network in the Great Basin to evaluate gridded climate data. *J. Hydrometeorol.*, 15(5), 1913-1931.

Mearns, L. O., et al., 2003: "Guidelines for use of climate scenarios developed from regional climate model experiments.", IPCC-TGCIA White paper, p38.

Mejia J., and D. Koracin, 2011: Numerical Weather Prediction and a Lagrangian Stochastic Simulation of Dispersion and Transport of Radiation Plume from Japan's Fukushima Nuclear Reactors Explosions. Effective Collaboration: Risk Communications and Data Sharing, Conference of Radiation Control Program Directors May 16, 2011, EPA, Center for Radiation Information and Outreach.

Mesinger, F., et al., 2006. North American regional reanalysis. *Bull. Am. Meteorol. Soc.,* 87, 343–360.

Meyer, J. D., Jin, J., & Wang, S. Y., 2012. Systematic patterns of the inconsistency between snow water equivalent and accumulated precipitation as reported by the Snowpack Telemetry Network. *J. Hydrometeorol.*, 13(6), 1970-1976.

Miguez-Macho, G., G. L. Stenchikov, and A. Robock, 2004. Spectral nudging to eliminate the effects of domain position and geometry in regional climate model simulations. *J. Geophys. Res.,* 109, D13104, doi:10.1029/2003JD004495.

Mielke, P.W., Jr., L.O. Grant, and C.F. Chappell, 1971. An independent replication of the Climax wintertime orographic seeding experiment. *J. Appl. Meteor.,* 10, 1198-1212.

Mlawer, Eli. J., Steven. J. Taubman, Patrick. D. Brown, M. J. Iacono, and S. A. Clough, 1997. Radiative transfer for inhomogeneous atmospheres: RRTM, a validated correlated–k model for the longwave. *J. Geophys. Res.*, 102, 16663–16682.

Mote, P. W., Allen, M. R., Jones, R. G., Li, S., Mera, R., Rupp, D. E., and Vickers, D., 2016. Superensemble regional climate modeling for the western United States. *Bull. Amer. Meteor. Soc*., 97(2), 203-215.

Niswonger, R.G., and Prudic, D.E., 2005. Documentation of the Streamflow-Routing (SFR2) Package to include unsatured flow beneath streams - a modification to the SFR1. U.S. Geological Survey Techniques and Methods. 6-A13. 62 pp.

Niswonger, R. G., Panday, S., and Ibaraki, M., 2011. MODFLOW-NWT, A Newton Formulation for MODFLOW-2005: U.S. Geological Survey Groundwater Resources Program, Techniques and Methods 6-A37, 44 pp.

Niu, G. Y., Yang, Z. L., Mitchell, K. E., Chen, F., Ek, M. B., Barlage, M., and Tewari, M., 2011: The community Noah land surface model with multiparameterization options (Noah-MP): 1. Model description and evaluation with local-scale measurements. *J. Geophys. Res. Atmospheres*, 116(D12).

Nygaard, J. E. Kristjánsson, and L. Makkonen, 2011. Prediction of in-cloud icing conditionsat ground level using the WRF model. *J. Applied Meteorol. Clim.*, 50(12): 2445-2459.

Omrani Hiba, P. Drobinski, and T. Dubos, 2015. Using nudging to improve global-regional dynamic consistency in limited-area climate modeling: What should we nudge?, *Climate Dynamics*, 44, 5-6, 1627.

O'Toole, Dr. Donal – professor, Dept Vet Sci Dr. Merl Raisbeck – professor, Dept Vet Sci January 23, 2010 Published in: *Wyoming Livestock Roundup*, Jan 2010.

Philipona R., A. Kräuchi, G. Romanens, G. Levrat, P. Ruppert, E. Brocard, P. Jeannet, D. Ruffieux, and B. Calpini, 2013. Solar and Thermal Radiation Errors on Upper-Air Radiosonde Temperature Measurements. *J. Atmos. Oceanic Technol.,* 30, 2382–2393. doi: http://dx.doi.org/10.1175/JTECH-D-13-00047.1

Prudic, D.E., Konikow, L.F., and Banta, E.R., 2004. A new Streamflow routing (SFR1) Package to simulate stream aquifer interactions with MODFLOW-2000. U.S. Geological Survey Open File Report. 2004-1043. 95 pp.

Rasmussen, R., Liu, C., Ikeda, K., Gochis, D., Yates, D., Chen, F., and Miller, K., 2011. High-resolution coupled climate runoff simulations of seasonal snowfall over Colorado: a process study of current and warmer climate. *J Climate*, 24(12), 3015-3048.

Regan, R.S., Niswonger, R.G., Markstrom, S.L., and Barlow, P.M., 2015. Documentation of a restart option for the U.S. Geological Survey coupled groundwater and surface-water flow (GSFLOW) model: U.S. Geological Survey Techniques and Methods, book 6, chap. D3, 19 p., http://dx.doi.org/10.3133/tm6D3.

Rife, D. L., and C. A. Davis, 2005. Verification of temporal variations in mesoscale numerical wind forecasts. *Mon. Wea. Rev.,* 133, 3368–3381.

Ritzman, J. M., Terry Deshler, Kyoko Ikeda, and Roy Rasmussen, 2015. Estimating the Fraction of Winter Orographic Precipitation Produced under Conditions Meeting the Seeding Criteria for the Wyoming Weather Modification Pilot Project*. J. Appl. Meteor. Climatol.,* 54, 1202–1215. doi: http://dx.doi.org/10.1175/JAMC-D-14-0163.1.

Rood S.B., Pan, J., Gill, K.M., Franks ,C.G., Samuelson, G.M., and Shepherd, A., 2008. Declining summer flows of Rocky Mountain rivers: changing seasonal hydrology and probable impacts on floodplain forests. *J. Hydrology,* 349: 397–410.

Rummukainen, M., 2010. State-of-the-art with Regional Climate Models. Wiley Interdisciplinary Reviews. *Clim. Change*, 82-96.

Silverman, N. L., M. P. Maneta, S.-H. Chen, and J. T. Harper, 2013. Dynamically downscaled winter precipitation over complex terrain of the Central Rockies of Western Montana, USA. *Water Resour. Res.,* 49, doi:10.1029/2012WR012874.

Silverman, B.A. 2009. An Evaluation of the San Joaquin Operational Cloud Seeding Program Using Monte Carlo Permutation Statistics. April 2009.

Silverman B.A., 2010. An evaluation of eleven operational cloud seeding programs in the watersheds of the Sierra Nevada Mountains. *Atmos. Res.,* 97(4). Sept 2010. 526 - 539.

Spero, T. L., M. J. Otte, J. H. Bowden, and C. G. Nolte., 2014. Improving the representation of clouds, radiation, and precipitation using spectral nudging in the Weather Research and Forecasting model. *J. Geophys. Res. Atmospheres* 119:10.1002/jgrd.v119.20, 11,682-11,694. Online publication date: 27-Oct-2014.

Stone, R.H., K. Smith-Miller, and P. Neeley, 1995. Mokelumne Watershed Lake Water and Sediment Silver Survey. Final Report to the Pacific Gas and Electric Company, Technical and Ecological Services, San Ramon, CA.

Stone, R.H., 2006. 2006 Mokelumne Watershed Lake Water and Sediment Survey. Final Report to the Pacific Gas and Electric Company, Technical and Ecological Services, San Ramon, CA.

Super, A. B., 1974. Silver iodide plume characteristics over the Bridger Mountain Range, Monana. *J. Appl. Meteor.*, 13, 62-70.

Super A. B., and J. A. Heimback Jr. Feasibility of Snowpack Enhancement from Colorado Winter Mountain Clouds: Emphasis on Supercooled Liquid Water and Seeding with Silver Iodide and Propane report submitted to CWCB.

Super, A. B. and J. A. Heimbach, 2005a. Randomized propane seeding experiment: Wasatch Plateau, Utah. *J. Wea. Modification*, 37, 35-66.

Swift, L.W., Jr., 1976. Algorithm for solar radiation on mountain slopes. *Water Resources Res.*, 12(1), 108-112.

Tewari, M., F. Chen, W. Wang, J. Dudhia, M. A. LeMone, K. Mitchell, M. Ek, G. Gayno, J. Wegiel, and R. H. Cuenca, 2004. Implementation and verification of the unified NOAH land surface model in the WRF model. 20th conference on weather analysis and forecasting. 16th conference on numerical weather prediction, pp. 11–15.

Thompson, G., P. R. Field, R. M. Rasmussen, and W. D. Hall, 2008. Explicit Forecasts of Winter Precipitation Using an Improved Bulk Microphysics Scheme. Part II: Implementation of a New Snow Parameterization. *Mon. Wea. Rev.*, 136, 5095–5115.

Thomson, D. J., 1987. Criteria for the selection of stochastic models of particle trajectories in turbulent flows. *J. Fluid Mech.*,180, 529–556.

Toth E, 2013. Catchment classification based on characterisation of streamflow and precipitation time series. *Hydrology Earth System Sci.*, 17, 1149–1159.

VanderKwaak, J. E., 1999, Numerical Simulation of Flow and Chemical Transport in Integrated Surface-Subsurface Hydrologic Systems: Ontario, Canada, University of Waterloo, Department of Earth Sciences, Ph.D. Dissertation, 217 pp.

Vonnegut, B., 1047. The Nucleation of Ice Formation by Silver Iodide. *J. Appl. Phy.*, 18(N7), July, 1947.

Von Storch, H., H. Langenberg, and F. Feser, 2000. A spectral nudging technique for 811 dynamical downscaling purposes. *Mon. Wea. Rev.,* 128, 3664–3673.

Walters C. K., J. A. Winkler, S. Husseini, R. Keeling, J. Nikolic, and S. Zhong, 2014. Low-Level Jets in the North American Regional Reanalysis (NARR): A Comparison with Rawinsonde Observations. *J. Appl. Meteor. Climatol.*, 53, 2093–2113. doi: http://dx.doi.org/10.1175/JAMC-D-13-0364.1.

Wang, W., Shaw, W. J., Seiple, T. E., Rishel, J. P., and Xie, Y., 2008. An evaluation of a diagnostic wind model (CALMET). *J. Applied Meteorol. Clim.,* 47(6), 1739-1756.

Warner, T. T., 2011. Quality assurance in atmospheric modeling. *Bull. Amer. Meteor. Soc*., 92(12), 1601.

Weinroth, E., Stockwell, W.R., Koracin, D., Kahyaoglu-Koracin, J., Luria, M., McCord, T., Podnar, D., and Gertler, A.W., 2008. A Hybrid Model for Ozone Forecasting. *Atmos. Environ*., 42, 7002-7012.

Weil, J., 2007. Linking a Lagrangian Particle Dispersion Model with Three-Dimensional Eulerian Wind Field Models. *JAMC*.
doi: http://dx.doi.org/10.1175/2007JAMC1764.1.

Williams, B. D., and J. A. Denholm, 2009. An assessment of the environmental toxicity of silver iodide – with reference to a cloud seeding trial in the Snowy Mountains of Australia. *J. Weather Mod.,* 41, 75-96.

Weather Modification Association, 2005. Weather Modification Association Capability Statement. http://www.weathermodification.org/capabilities.php.

Wolff C.A., and F. McDonoughm, 2010. A Comparison of the WRF Rapid Refresh and Rapid Update Cycle Numerical Model to Aircraft Icing Conditions. AMS 14th Conf. on Aviation Range and Aerospace Meteorology. Atlanta GA, 17-21 January 2010. (avail. online).

Xu, Haitao, Alain Pumir, and Eberhard Bodenschatz, 2016. Lagrangian view of time irreversibility of fluid turbulence. *Sci. China Physics: Mech. Astron.,* 59 (1), 1-9.

Xue, Y., Janjic, Z., Dudhia, J., Vasic, R., and De Sales, F., 2014. A review on regional dynamical downscaling in intraseasonal to seasonal simulation/prediction and major factors that affect downscaling ability. *Atmos. Res.*, 147, 68-85.

Yang, Y., M. Uddstrom, and M. Duncan, 2011. Effects of short spin-up periods on soil moisture simulation and thecauses over New Zealand, *J. Geophys. Res.,* 116, D24108, doi:10.1029/2011JD016121.

Yau, M.K., and Rodgers, R.R., 1989. "A Short Course in Cloud Physics", 1989. ISBN 0-7506-3215-1.

Zaidel, J., 2013. Discontinuous steady-state analytical solutions of the Boussinesq Equation and their numerical representation by MODFLOW. *Ground Water*, *Method Note*. doi: 10.1111/gwat.12019. pp 1-8.

Zhang, H., Pu, Z., and Zhang, X., 2013. Examination of errors in near-surface temperature and wind from WRF numerical simulations in regions of complex terrain. *Wea. Forecasting*, 28(3), 893-914.

Zhong, S., Li, X., Bian, X., Heilman, W.E., Leung, L. R., and Gustafson, W.I., 2012. Evaluation of regional climate simulations over the Great Lakes region driven by three global data sets. *J. Great Lakes Res.,* 38(2), 212-225.

18 Appendix A. Public Hearings and Comments

WYOMING WATER DEVELOPMENT COMMISSION

6920 Yellowtail Road, Cheyenne, WY 82002

Phone: (307) 777-7626
Fax: (307) 777-6819
http://wwdc.state.wy.us

Matthew H. Mead
Governor

Commissioners

Nick Bettas	Sheridan Little
Travis C. Brockie, I	William Resor
Karen Budd-Falen	Jeanette Sekan
Floyd Canfield	Rodney Wagner
David Evans	Todd Werbelow

Harry C. LaBonde, Jr., P.E.
Director

To: Katie Talbot

From: Jeni Cederle, Project Manager

CC: Hearing Record

Date: September 1, 2016

Re: Weather Modification, Laramie Range Siting and Design Study, Level II, August 18, 2016 Public Hearing

A public hearing was held on August 18, 2016 at the Converse County Courthouse, 107, N. 5th Street, Douglas, WY to present the draft study results and accept public comment concerning the Wyoming Water Development Commission's Weather Modification, Laramie Range Siting and Design, Level II Study. The hearing was declared open at 12:30 pm and closed at approximately 2:30 pm. Thirteen people attended the hearing (see enclosed Sign-in Sheet). The hearing notice was published three times in the state-wide Casper Star-Tribune newspaper. A recording of the hearing is available at the Water Development Office.

The public hearing was held pursuant to Wyoming Statute 41-2-114(b)(iii). During the course of the presentation, the consultant provided clarification and answered technical questions posed by the audience regarding the study results. No substantive verbal comments were received.

Written/email comments will be accepted and included as part of the public record if received by August 28, 2016. Two email comments were received prior to the close of the comment period and will be included as part of the public record. One written comment was received after the close of the comment period, and will not be included as part of the public record.

Comments to be included for the public record were received from:

Ms. Rachel Grant
1967 Boxelder, Rd.
Glenrock, WY 82637

1

Mr. Will Grant
Sno-Shoe Ranch, Inc.
1967 Boxelder Rd.
Glenrock, WY 82637

Comments received after the close of the comment period were received from:

Ms. Elsie Deininger
1761 Spring Canyon Rd.
Douglas, WY 82633

Enc.
Hearing Agenda
Hearing Script
Sign-in Sheet
Publication Affidavits
Comments Received for Public Record

WYOMING WATER DEVELOPMENT COMMISSION

6920 Yellowtail Road, Cheyenne, WY 82002

Phone: (307) 777-7626
Fax: (307) 777-6819
http://wwdc.state.wy.us

Matthew H. Mead
Governor

Commissioners

Nick Bettas	Sheridan Little
Travis C. Brockie, I	William Resor
Karen Budd-Falen	Jeanette Sekan
Floyd Canfield	Rodney Wagner
David Evans	Todd Werbelow

Harry C. LaBonde, Jr., P.E.
Director

To: Katie Talbot

From: Jeni Cederle, Project Manager

CC: Hearing Record

Date: September 1, 2016

Re: Weather Modification, Laramie Range Siting and Design Study, Level II, August 18, 2016 Public Hearing

A public hearing was held on August 18, 2016 at the Platte Valley Bank, 200 16th Street, Wheatland, WY to present the draft study results and accept public comment concerning the Wyoming Water Development Commission's Weather Modification, Laramie Range Siting and Design, Level II Study. The hearing was declared open at 6:30 pm and closed at approximately 8:31 pm. Nine people attended the hearing (see enclosed Sign-in Sheet). The hearing notice was published three times in the state-wide Casper Star-Tribune newspaper. A recording of the hearing is available at the Water Development Office.

The public hearing was held pursuant to Wyoming Statute 41-2-114(b)(iii). During the course of the presentation, the consultant provided clarification and answered technical questions posed by the audience regarding the study results. One substantive verbal comment was received at the hearing. Holly Kennedy, a representative of the Wyoming Farm Bureau Federation (WYFB), provided comment for the record. The WYFB comment is summarized below:

- The Farm Bureau would like to continue to be included in the process (kept up to date, mailings, public meetings etc.). Ms. Kennedy expressed that the Water Development Office had done a good job of keeping the WYFB included in the process thus far, and would like to see that outreach continue.
- The Farm Bureau (which consists of approximately 2,700 members) continues to support weather modification research; and maintains a reserved opinion regarding the implementation of weather modification operations.
- The Farm Bureau requests that coordination with the Forest Service grazing permit holders be instituted should an operational cloud seeding program be implemented in the Laramie Range. The WYFB requests that an operational cloud seeding program in the Laramie Range take into account permitted "on and

off" dates for the areas (elevations above 8,000 ft.) that would be affected by snow accumulation from the weather modification. The WYFB does not anticipate any conflicts, however would like confirmation that all livestock will be "off" the range during cloud seeding operations. If not, The WYFB would like to see coordination with the permittee to accommodate for any impacts to their operation.

Written/email comments will be accepted and included as part of the public record if received by August 28, 2016. One email comment was received prior to the close of the comment period and will be included as part of the public record.

Comments to be included for the public record were received from:

Mr. Donald Britton
Manager, Wheatland Irrigation District
30 West Frontage Rd.
Wheatland, WY 82201

Enc.
Hearing Agenda
Hearing Script
Sign-in Sheet
Publication Affidavits
Comments Received

You are invited to attend the Laramie Range
Weather Modification Feasibility Study
Draft Results Public Hearings

Thur., August 18, 2016 @ 12:30 pm
Community Room, Converse County Courthouse
107 N. 5th St., Douglas, WY

Thur., August 18, 2016 @ 6:30 pm
Platte Valley Bank, 200 16th St.
Wheatland, WY

Learn about the results of the cloud seeding feasibility study in the Laramie Range from representatives of the:
~ Desert Research Institute ~

Need more information?
Contact the Wyoming Water Development Office at:
(307) 777-7626 http://wwdc.state.wy.us/

Weather Modification Feasibility Study – Laramie Range
Draft Results Public Hearing

Converse County Courthouse, Community Room, Douglas, WY
Thursday, August 18, 2016 – 12:30 pm

Frank McDonough - Arlen Huggins - Ray DeLuna

1. **Introductory Comments**
2. **Geography and Snowfall in the Laramie Range**
3. **Cloud Seeding Climatology**
4. **Project Design**
5. **Environmental Considerations**
6. **Environmental Permitting**
7. **Potential Runoff**
8. **Cost Benefits**
9. **Answers to questions posed during the introductory meetings**
10. **Questions and Answers from Audience**
11. **Closing Remarks**

DRI
Desert Research Institute

Weather Modification Feasibility Study – Laramie Range
Draft Results Public Hearing

Platte Valley Bank, 200 16th St., Wheatland, WY
Thursday, August 18, 2016 – 6:30 pm

Frank McDonough - Arlen Huggins - Ray DeLuna

1. Introductory Comments
2. Geography and Snowfall in the Laramie Range
3. Cloud Seeding Climatology
4. Project Design
5. Environmental Considerations
6. Environmental Permitting
7. Potential Runoff
8. Cost Benefits
9. Answers to questions posed during the introductory meetings
10. Questions and Answers from Audience
11. Closing Remarks

TREC INC
Engineering & Environmental Management
A Woodard & Curran Company

WYOMING WATER DEVELOPMENT COMMISSION (WWDC) PUBLIC HEARING
LARAMIE RANGE WEATHER MODIFICATION FEASIBILITY STUDY PUBLIC HEARING

Date: August 18, 2016 *Meeting Location: Converse County Courthouse, Douglas, WY*

Name	Representing / Location	Email
Jeni Cederlee	WWDC CHEYENNE	Jeni.cederlee@wyo.gov
Barry Lawrence	WWDC CHEYENNE	Barry.Lawrence@wyo.gov
Arlen Huggins	DRI Reno, NV	huggins@dri.edu
Elsie Deininger	SW of Douglas	eldeininger@me.com
John Nelson	SW Douglas	jrn3676@outlook.com
Floyd Field	Self. Casper	FJField1496@Gmail.Com
Ray DeLuna	DRI Reno, NV	rdeluna@kiecorp.com
William & Rachel Grant	20 mi S of Glenrock	willandrachel@hotmail.com
Misty Hays	USFS - Douglas Ranger District	mahays@fs.fed.us
Cordie Lyon	USFS - Douglas Ranger dist.	clyon@fs.fed.us
Emilee Gibb	Wyo Livestock Roundup Casper	emilee@wylr.net
John Sullivan	Self Cold Springs Rd Douglas	
Jim Koehler	Douglas Bridge	jen@douglas-budget.com

Wyoming Water Development Office
6920 YELLOWTAIL ROAD TELEPHONE: (307) 777-7626 CHEYENNE, WY 82002

*** Proof of Publication ***

Casper Star-Tribune
P.O. Box 80, Casper, WY 82602-0080, ph 307-266-0500

AFFIDAVIT OF PUBLICATION

STATE OF WYOMING)
COUNTY OF NATRONA)

I, the undersigned, being a person in the employ of the Casper Star-Tribune, a newspaper published in CASPER, NATRONA COUNTY, WYOMING, and, knowing the facts herein set forth do so solemnly swear that a copy of the notice as per clipping attached was printed and published

Daily (Weekly)

In the regular and entire issue of said newspaper, and not in any supplement thereof, for 3 Consecutive Days (Weeks)

commencing with issue dated July 29, 2016
ending with issue dated August 12, 2016

Wyoming Water Development
6920 Yellowtail Rd.
Cheyenne, WY 82002

ORDER NUMBER 5741

Shawn M

Signed

Subscribed in my presence and sworn to before me this

16th day of August, 2016

Rebecca S. Harris

NOTARY PUBLIC
REBECCA S. HARRIS
STATE OF WYOMING
COUNTY OF NATRONA
My Commission Expires June 13, 2020

Public Hearing and draft report presentation on the: Laramie Range Weather Modification Feasibility Study

When: Thursday, August 18, 2016, 12:30 pm

Where: Converse County Courthouse, Community Room, 107 N. 5th St., Douglas, WY
AND

When: Thursday, August 18, 2016, 6:30 pm

Where: Platte Valley Bank, 200 16th St., Wheatland, WY

The Wyoming Water Development Commission will hold a public hearing to receive comments on the Laramie Range Weather Modification Feasibility Study. The Commission will also be seeking information as to whether the proposed project functions and services can be served by any person, association or corporation engaged in private enterprise. Representatives of the Water Development Commission will be present to explain the project and to record comments.
For further information contact:
Wyoming Water Development Office
6920 Yellowtail Road
Cheyenne, Wyoming 82002
307/777-7626
Published: July 29, August 5 & 12, 2016
Legal No: 5741

PUBLISHED ON: 07/29/2016, 08/05/2016, 08/12/2016

TOTAL AD COST:	228.76
FILED ON:	8/12/2016

*** Proof of Publication ***

Casper Star-Tribune
P.O. Box 80, Casper, WY 82602-0080, ph 307-266-0500

AFFIDAVIT OF PUBLICATION

STATE OF WYOMING)
COUNTY OF NATRONA)

I, the undersigned, being a person in the employ of the Casper Star-Tribune, a newspaper published in CASPER, NATRONA COUNTY, WYOMING, and, knowing the facts herein set forth do so solemnly swear that a copy of the notice as per clipping attached was printed and published

Daily (Weekly)

In the regular and entire issue of said newspaper, and not in any supplement thereof, for 3 Consecutive Days (Weeks)

commencing with issue dated July 29, 2016
ending with issue dated August 12, 2016

Wyoming Water Development
6920 Yellowtail Rd.
Cheyenne, WY 82002

ORDER NUMBER 5741

Shawn M

Signed

Subscribed in my presence and sworn to before me this

16th day of August, 2016

Rebecca S. Harris

NOTARY PUBLIC
REBECCA S. HARRIS
STATE OF WYOMING
COUNTY OF NATRONA
My Commission Expires June 13, 2020

Public Hearing and draft report presentation on the: Laramie Range Weather Modification Feasibility Study

When: Thursday, August 18, 2016, 12:30 pm

Where: Converse County Courthouse, Community Room, 107 N. 5th St., Douglas, WY
AND

When: Thursday, August 18, 2016, 6:30 pm

Where: Platte Valley Bank, 200 16th St., Wheatland, WY

The Wyoming Water Development Commission will hold a public hearing to receive comments on the Laramie Range Weather Modification Feasibility Study. The Commission will also be seeking information as to whether the proposed project functions and services can be served by any person, association or corporation engaged in private enterprise. Representatives of the Water Development Commission will be present to explain the project and to record comments.
For further information contact:
Wyoming Water Development Office
6920 Yellowtail Road
Cheyenne, Wyoming 82002
307/777-7626
Published: July 29, August 5 & 12, 2016
Legal No: 5741

PUBLISHED ON: 07/29/2016, 08/05/2016, 08/12/2016

TOTAL AD COST:	228.76
FILED ON:	8/12/2016

August 22, 2016

Rachel Grant

1967 Boxelder Rd.

Glenrock, WY 82637

RECEIVED

AUG 2 8 2016

WY WATER DEVELOPMENT COMMISSION

To whom it may concern,

I am writing concerning cloud seeding in the Northern Laramie Range Mountains. Our family ranch owns property and we live in the locations and elevations proposed for additional snowfall in this study. Most of the cloud seeding projects currently in operation in Wyoming are being done on public land. Public land might be used for grazing in the Summer months, but is not generally home to people or cattle in the winter. We live on and operate our ranch in the Northern Laramie Range year round; as do our ranching neighbors in the Boxelder and La Parele community.

We are opposed to any cloud seeding as we raise and winter cattle in this location. Any additional snow cover greatly increases the need to feed hay and the amount of hay fed. More snow in the Fall means the cattle cannot graze as long without supplemental feeding. It also greatly increases calving mortality when there is more snow cover. More snow cover in the Spring, and having snow longer causes the grass to start growing later and the soil warms up later, reducing grass and hay grown. We also have concerns that the very large resident elk herd will be forced to move their calving areas farther down out of the trees and into areas that would be in common with our calving beef cows, as we generally begin calving mid May and finish up by the end of June. This sharing of parturition areas is a huge brucellosis risk that has not been considered and could be a detriment not only to our ranch, but the entire state of Wyoming.

As ranchers we realize that it is a blessing to have more irrigation water. However, it is not equitable for the end user of the water to reap the benefits, while the costs and impacts of snowfall are borne by someone else.

At the August 18, 2016 meeting there were 'Seeding Protocols' that were mentioned. This checklist included the benchmark of whether snowpack had yet reached 150% of normal. If seeding occurs, would additional Snotel or similar sites be added for measuring? At what point do higher snowfall amounts constitute a new normal? It is not uncommon for us to currently have storms where 30 inches or more of snow falls. Would seeding then continue with little opportunity to mitigate damages from the last storm? There did not seem to be any protocols

that addressed this common occurrence and could make difficult ranch work like feeding and calving out cows catastrophic.

We realize that weather patterns do not vary if land is public or private, but often the impacts do. There are public roads in this area which the county tries to maintain year round. There is a rural school which four families currently attend. Even though the school district maintains a residence at the school location for the teacher, our children had over a week of snow days last year, mostly due to impassable roads. Beginning next year, our twelve year old daughter will need to be transported daily from the ranch to school in Glenrock as she will be too old to attend the rural school. Any additional snow and the drifting that accompanies it is costly and a burden.

Living in a more remote part of our state has its blessings and challenges. During the snowy season it is already difficult for our family to travel back and forth to town for necessities like groceries, in-town days for school, and medical care. We also believe that the ability for emergency services to respond to our location or to our neighbor's homes would be negatively impacted. We truly believe from the information presented to us concerning the Weather Modification Study, that even very small amounts of additional snow in our regular weather pattern would cause undue burden on our family and normal family life, our business, and livelihood.

As private property and business owners, we do not feel that it is right or even legal for the State of Wyoming to use our property and business as a storehouse for snow to benefit the downstream user. The state seems to feel that this Weather Modification Study/Project is just like the others in our state. That is simply not true. The Northern Laramie Range has vast areas of private land, where families make their year round homes and operate their ranch business. These mountains are not the public land storehouses of the western part of our state and treating them as such would be a mistake.

Sincerely,

Rachel Grant

WHEATLAND IRRIGATION DISTRICT
PO Box 727
30 West Frontage Road
Wheatland, WY 82201
Phone: (307) 322-2740 Fax: (307) 322-1749

Daniel Melcher Juan Reyes Marty Shepard Tyler Lauck Dave Olson

Donald D. Britton, Manager Kay Britton, Office Manager

Jeni Cederle
Project Manager

Jeni,

Thanks for inviting Daniel and me to you hearing on Weather Modification in the Laramie Mountain Range. The research company did an excellent presentation on logistic of on the ground and air operations.

I agree with their research on the Wind River Mountain Range and the North portion of the Laramie Mountain Range are most suitable for all the methods of cloud seeding but I feel the seeding in the Sierra Madres and the Elk Mountain sites have some potential to enhance runoff in Albany, Platte, Goshen and Laramie Counties.

It seemed to me that even stationary seeding equipment using propane would be feasible at times when conditions are sufficient to seed the weather systems that pass over. It could be a low cost operation by eliminating the use of airplanes and having stationary sites from Elk Mountain to the Wyoming/Colorado line. That, combined with the cloud seeding in Colorado over time could amount to a sizeable benefit to us and the State of Wyoming to supply our needs and the needs of water users downstream including water users in the Platte River System in Colorado and Nebraska.

I support continuing the practice of any and all methods to try to enhance our water supplies in Wyoming. Thank you to you and all the other members of the Wyoming Water Development Office that worked on the project.

Sincerely,

Donald D. Britton

Don Britton,
Manager,
Wheatland Irrigation District

August 22, 2016

Sno-Shoe Ranch, INC.

William Grant

1967 Boxelder Rd.

Glenrock, WY 82637

To whom it may concern,

I am writing concerning cloud seeding in the Northern Laramie Range Mountains. Our family ranch owns property and we live in the locations and elevations proposed for additional snowfall in this study. Most of the cloud seeding projects currently in operation in Wyoming are being done on public land. Public land might be used for grazing in the Summer months, but is not generally home to people or cattle in the winter. We live on and operate our ranch in the Northern Laramie Range year round; as do our ranching neighbors in the Boxelder and La Parele community.

We are opposed to any cloud seeding as we raise and winter cattle in this location. Any additional snow cover greatly increases the need to feed hay and the amount of hay fed. More snow in the Fall means the cattle cannot graze as long without supplemental feeding. It also greatly increases calving mortality when there is more snow cover. More snow cover in the Spring, and having snow longer causes the grass to start growing later and the soil warms up later, reducing grass and hay grown.

As ranchers we realize that it is a blessing to have more irrigation water. However, it is not equitable for the end user of the water to reap the benefits, while the costs and impacts of snowfall are borne by someone else.

Sno-Shoe Ranch hosted a radiometer weather instrument that was to be used in the Cloud Seeding Feasibility Study for the Northern Laramie Range. We hosted this instrument because we were concerned about the outcome of the study and were interested in data relevant to our location. At the time of the August 18, 2016 Public Hearing, this information had not yet been made available and was not presented at the hearing. We were disappointed that what was said to be an important part of this study was not available.

We realize that weather patterns do not vary if land is public or private, but often the impacts do. There are public roads in this area which the county tries to maintain year round. There is a rural school which four families currently attend. Any additional snow and the drifting that accompanies it is costly and a burden. It would be a taking by the state to impact our private property.

Sincerely,

William Grant

Sno-Shoe Ranch, INC.

19 Appendix B. Case Studies

1. Overview

Seven case studies were examined in depth in an effort to determine the multi-scale processes that could best contribute to an environment favorable for cloud seeding over the Laramie Mountains of southeastern Wyoming. The seven case studies were examined utilizing a spectrum of data sources including the following: radiosonde observations, North American Regional Reanalyses (NARR, ~32 km), North American Mesoscale (NAM) 12 km reanalyses, surface observations, radar observations, satellite observations including visible, infrared, microwave, and hyperspectral, as well as multiple simulated fields from the Weather Research and Forecasting (WRF) model, valid at 1 km horizontal resolution every thirty minutes for the seven 24-hour case study time periods. The simulated field which were employed included cloud water, cloud ice, vapor mixing ratio, horizontal winds, temperatures, and vertical velocities for the layer from 800-500 hPa analyzed in 50 hPa increments. From these, non-dimensional mountain height was also calculated for the 750-550 hPa layer. Additionally, soundings at three point locations were also generated, as well as vertical cross sections of potential temperature, relative humidity, and vertical motion along the axis of the Laramie range. The seven case studies, ranked in terms of their simulated total supercooled cloud water integrated over the entire 800-500 hPa depth and 47 (30-minute) time periods, were: 1) 1/14/2014, 2) 1/18/2006, 3) 2/28/14, 4) 12/29/05, 5)12/19/13, 6) 11/14/05, and 7) 12/15/2004. The layer where the most simulated supercooled cloud water was analyzed averaged over all seven case studies was 650-700 hPa which was also a region designated by the larger scale analyses as favorable for unstable lapse rate conditions and significant relative humidities (note Tables 1-4, Figures 1-2).

2. Large Scale Analyses

The larger scale analyses focused on 12-hourly radiosonde and 3-hourly NARR/NAM observations. Table 4 depicts the average sounding thermodynamic profiles for all seven case studies. The following key signals were ascertained for the period spanning each case study's 24 hours. Early on (in the first 12 hours) of the twenty-four hour cycle, lapse rates were most unstable between 800 and 500 hPa approaching and even exceeding moist neutrality thus indicating a katafront/upper-level downstream-tilting cold front structure which weakens and stabilizes in time. One could view this as a split front in which the upper-level cold pool is blocked less than the low-level cold pool and propagates faster equatorward as well as downstream relative to the low-level cold pool. Cooling builds downwards from top to bottom indicating that during the first 12 hours upper-level upward vertical motions/cold air advection prevail which are followed by, during the second 12 hours, progressively more lower-level upward vertical motions/cold air advection as the low-level accelerations catch up to the upper-level accelerations in the airflow. As the low-levels reach their coldest temperatures the upper-levels start to warm/stabilize during the second 12 hours. Thus a very unstable atmosphere evolves during the middle of the twenty-hour period which tends to stabilize towards the end of the twenty-four hour period.

For the remainder of this report we will focus on the differences between the most prolific supercooled cloud water case study and the least. Figures 3-7 inter compare the most prolific supercooled cloud water case study, i.e., 1/14/14 with the least prolific supercooled cloud water case study, i.e., 12/15/04. Based on these synoptic/meso-α scale observations the following key sequence of events were ascertained as being indicative of all of the seven case studies which varies in magnitude among the case studies, generally better organized and more intense in the most active supercooled cloud water case studies.

Early on during each of the case study days a double jet stream structure aloft is evident with a polar jet northern stream and coupled polar front amplifying across the northwestern U.S. One jet is amplifying meridionally to the north and west of Wyoming and a second jet remains quasi-zonal to the south in all the case studies and the strength of the jets is generally correlated with the supercooled cloud water available. This is evident when inter comparing these two case studies, i.e., 1/14/14 and 12/15/04. Most notable in Figures 3-4 is the difference between the two case studies in kinetic energy, cold air, and tilt over Wyoming during the baroclinic amplification of the trough. The active case exhibits a much stronger negatively-tilted northern branch of the polar jet and trough extending all the way to the Aleutian Islands. The least active case exhibits much weaker features and in general a more positive tilt to the Rossby wave system. Equatorward of this feature is a weaker polar jet southern stream transporting Pacific air which is already relatively mild and is being heated by downslope adiabatic compression as well as surface sensible heat flux over the Great Basin which sets up a leeside trough/low-level warm pool over Wyoming thereby blocking the low-level flow with large static stability/Brunt-Väisälä frequency with little moisture.

In time the northern stream amplifies/cools and propagates over the blocked warmer low-level flow coupling to the leeside baroclinic zone. This sequence of processes sets up cold air aloft and a polar northern branch jet streak exit region which contains ascending air accompanying a thermally-indirect ageostrophic circulation. This circulation strengthens the katafront/forward leaning cold front aloft, primarily in the jet's left exit region where upward vertical motions prevail. The result is unstable air/high relative humidity aloft representing an excellent environment for moist convection and low-level pressure rises along the barrier of the Laramie range. This upper-level momentum supports pressure rises generally parallel to the long axis of the Laramie Mountains resulting in the development of low-level barrier jets parallel to the multiple mountain barriers that lift low-level air both orographically/upslope and due to leeside barrier jet confluence. Note in Table 1 the very cold column with lapse rates generally near or even more unstable than moist neutrality. Note also Figures 5-7 which inter compare the meso-α/meso-β scale details of the most prolific supercooled cloud water case study (1/14/14) with the least (12/15/04). The larger magnitude wind values, stronger convergence, and more coherent long plume of moisture coupling back in time offshore to an atmospheric river southwest of Canada can be seen with the most prolific event. The least prolific event and the other five case studies represent a continuum in between (Figures 5-7). While the difference in specific humidity is not significant for these two case studies, i.e., 12/15/04 and 1/14/14, the cold air available for the prolific 1/14/14 case study is far more substantial and therefore able to create a more favorable environment for condensation even at these relatively coarse scales of motion (Figure 7).

These weaker meso-α/meso-β scale signals in the 12/15/04 case study are consistent with the very large synoptic scale features in Figures 3-4 for that case study.

3. Mesoscale Numerical Simulations

The 1 km WRF simulations provide information on the meso-β/meso-γ scale of motions near and over the Laramie Mountains. These data indicate sensitivity to the types of sub-synoptic scale circulations that produce significant supercooled cloud water in the 800-500 hPa layer. The WRF simulated cloud water in these layers was inter compared for the seven case studies by determining how many cutoff maxima were simulated in a given 50 hPa layer for each 30-minute time period. Simulated values greater than or equal to 0.2 g kg^{-1} were summed for each layer at each time period and multiplied by the number of maxima at a given time and layer (note Tables 1-3). These were integrated vertically for each time period over a 24-hour period for each case study. This enabled the ranking described earlier of most prolific to least prolific supercooled cloud water case study. The spatial distribution of clusters of these maxima over and surrounding the Laramie range can be seen depicted in Figure 8. Perhaps the most significant clusters from the point of largest magnitude values of integrated cloud water concentrated in a small region near or over the Laramie range are those located at: 1) ~42.5°N 106.0°W, 2) ~42.75°N 106.0-105.0°W, and 3) ~42.5°N 105.5-105.0°W, which basically flank the northwestern, northern, and northeastern sides of the range respectively. As can be seen in Figure 8, the sum of clusters maximizes in this region with the second most active sum of clusters near the Medicine Bow Range.

The mesoscale processes that focus regions of clusters and their inter case study variability must be related to vertical motions as well as moisture distribution and temperature. Large scale factors create an environment that leads to mesoscale terrain forcing which acts to focus small scale regions for ascending motions and condensation. Perhaps the most simple and general signal that could be used to understand mesoscale inter case study variability is the non-dimensional mountain height (M), or inverse Froude number (F):

$$\frac{1}{F} = M = \frac{NH}{U},$$

where N is the Brunt-Väisälä frequency:

$$N = \sqrt{\frac{g}{\theta}\frac{\partial\theta}{\partial z}},$$

H_m the adjusted mountain height, and U the mean wind that has a cross mountain component. These were derived from the WRF 1 km simulated Brunt-Väisälä frequency (N) using nine 25 hPa layers in the 750-550 hPa layer, average maximum elevation of the range (2900 meters for the target area - excludes Laramie Peak) minus the grid point terrain elevation for the adjusted mountain height, and mean wind velocity using the same nine layers within the 750-550 hPa layer as N. Epifanio and Durran (2001) clearly demonstrate that for a 3-dimensional mountain in which the asymmetry in length versus width is substantial, i.e., much longer length than width like the Laramie range, nonlinear effects often translate into flow deflection and columnar wave mode genesis when M is larger relative to smaller. Columnar waves represent upstream propagating waves that are transient and not anchored by local barrier jet effects. This means that flow separation

away from the terrain and wave genesis/breaking above and upstream from the terrain is favored for relatively large *M* values, and just the opposite for relatively small *M* values in which confluent flow near the barrier, as well as flow over the barrier, would be favored. Hence, the complex elongated three-dimensional terrain of the Laramie range would tend to sort out different modes of adjustment as a function of *N* (which is a function of $\partial\theta/\partial z$) and *U* embedded within the larger scale environment created by the larger scale jets and their accompanying baroclinic zones. Larger *N* and smaller *U* would favor deflection of flow as well as columnar mode/wave genesis, amplification, and breaking and smaller *N* and larger *U* would favor confluent flow close to the barrier as well as flow over the terrain. The latter environment is consistent with low wave drag and the former environment is consistent with high wave drag states, i.e., unstable versus stable environments.

This represents a spectrum of mountain blocking regimes that result in different patterns of ascending flow which has implications for patterns of condensation and supercooled cloud water. This difference would translate into strong large scale jets and low static stability (abundant deep cold air) creating stronger barrier parallel and confluent flow and weaker gravity waves above the terrain while the larger magnitude static stability and weaker wind regimes (less cold air) favoring more transient disturbances and weaker barrier jet confluence. Intuitively this would mean stronger ascent along the curved barriers particularly those interacting with upstream airflow during the more unstable case studies with stronger large scale jet forcing and more transient ascending features during weaker jets with less cold air. Thus slower moving and stronger ascent signals along the barrier at lower levels would be favored in much stronger jet/front systems at the larger scale and the opposite with more transient waves with less well-organized ascent at any one fixed location for weaker jet/front systems.

An example of this can be seen when we inter-compare the most and least prolific case studies on 1/14/14 and 12/15/04, respectively, in Figures 9-16. Figure 9 depicts the simulated soundings at 1200 UTC on the northwest side of the Laramie range near the active cloud water clusters at 42.5° N and 106.0° W. Evident are the higher wind velocities and lower static stability in the 1/14/14 case study compared to the 12/15/04 case study in Figure 9. The winds are twice as large in magnitude and lapse rate more than 50% greater (more unstable) in the 750-550 hPa layer in the 1/14/14 case compared to the 12/15/04 case. The impact on the non-dimensional mountain heights in the two cases is substantial, resulting values more than twice as large in the 12/15/04 case depicted at this time in Figure 10, particularly over the higher terrain. This significant difference in the two case studies forces the flow to adjust to the terrain in significantly different ways as described above in which the lower non-dimensional mountain heights in complex 3-dimensional terrain facilitate less intense blocking with air flowing over the barriers and weaker perturbation of the confluent flow than in the other case study, where much larger blocking results in the mountains diverting the flow facilitating transient upstream propagating waves and less barrier scale confluence.

The combination of this terrain blocking signal as well as wind direction, velocity, and larger scale pressure tendency across the region could influence the structure and variation of the kinematic fields responsible for vertical motions which could enhance the local relative humidity and condensational processes. Figure 11 depicts the 1 km simulated mean sea level pressure fields for both case studies at 1200 UTC and Figure 12

depicts the 3-hourly mean sea level pressure tendency between 1200 and 1500 UTC for both cases. The pressure fields reflect these differences in which the 1/14/14 case indicates a much more focused pressure gradient and pressure rise zone on the northwestern side of the Laramie Mountains, as well as in the valley west of the range, in contrast to the 12/15/04 case which has mostly high frequency gravity waves or narrow and smaller scale pressure perturbations oriented orthogonal to the Laramie range. These pressure field differences reflect the low-level (700 hPa) wind differences between the two cases depicted in Figure 12. The 1/14/14 case has a mountain-parallel/barrier jet oriented north-northwest – south-southeast west of the western slope of the Laramie range with substantial lateral shear on its eastern flank. This jet is very robust at 700 hPa relative to airflow anywhere else in the local region which establishes the seminal lateral shear zone in the local region. This confluent flow accompanying this jet also flank's the northern side of the Laramie range, as well as the eastern side.

The cloud water at 700 hPa in the 1/14/14 case is consistent with the ascent (Figures 14-16) flanking the northwest, northern, and northeastern slopes of the Laramie Mountains in between the northwestern slope lateral shear and northeastern slopes confluence accompanying flow veering. Even in the NARR winds depicted in Figures 5-6 the confluence of air in eastern Wyoming is much better defined relative to more amorphous diffluence in the same region when one inter compares 1/14/14 and 12/15/04. The 12/15/04 case study has weaker flow overall and virtually no western slope lateral shear or eastern slope confluence. The vertical motions in this case are all consistent with the pressure tendency fields in which the ascent is fragmented into waves orthogonal to the axis of the Laramie range. Unlike the 12/15/04 case, the 1/14/14 ascent fields tend to be less rapidly propagating and wrap around the predominantly northern slope zone. This difference also includes a lower level ascent maximum in the 1/14/14 case with the 12/15/04 case indicating much higher elevation vertical velocity maxima into the mid-troposphere as can be seen in Figures 15 and 16, which highlights a sequence of potential temperature (□), vertical velocity (*w*), and relative humidity vertical cross sections. The wetter air on the northern flank of the Laramie range in the 1/14/14 case study is apparent from these vertical cross sections. The 1/14/14 ascent fields tend to be more persistent at lower elevations, particularly on the northern flank of the mountains, thus creating adiabatic cooling closer to the moister "low-level" air below 650 hPa.

4. Summary and Conclusions

Seven case studies of significant orographic snowfall in the Laramie Mountains of southeastern Wyoming have been studied in an effort to understand the multi-scale processes that could create a favorable environment for supercooled cloud water. This involved employing analyses and other observations to diagnose the larger scale environment as well as mesoscale numerical simulations to diagnose the dynamics and thermodynamics responsible for generating supercooled cloud water in the local region.

The multi-scale analyses focused on inter comparing two case studies, one that produced the most and one that produced the least supercooled cloud water of the seven. The key layer for supercooled cloud water accumulation averaged over all seven case studies was between 650 and 700 hPa with the most prolific case study generating nearly 4 times the amount of cloud water as the least prolific case study (Tables 1-3, Figures 1-2). The ideal large scale features that created the most favorable environment for

supercooled cloud water development included a baroclinically unstable jet/front system accompanying northwesterly flow. Cold air in the left exit region of the upper jet overran warmer more stable air transported to the leeside of the Laramie range yielding early periods of decreasing static stability followed by stabilization later in the case study period. Moisture generally followed this jet in a plume originating off the coast of southwestern Alaska where it was associated with an offshore North Pacific atmospheric river.

The cold high momentum flow in the more active cloud water generating case study created a favorable terrain scale atmospheric structure for flow over the Laramie Mountains facilitating weak blocking and confluence zones with low-level ascent maxima that wrapped around the mountain range primarily on its northwestern, northern, and northeastern flanks. Vertical motions tied to these terrain features enhanced the larger scale cold air creating significant supercooled water in the most active case study. In the less active case study the larger non-dimensional mountain heights, generated by the higher stability and lower winds, created upstream propagating columnar modes and gravity waves with a higher level ascent but lower ascending values that reduced the available cloud water relative to the other case study. All of those factors play an important role in controlling the available supercooled cloud water for cloud seeding conditions in the Laramie Mountains of Wyoming. Clearly this small sample of case studies represents only a first pass climatology which may not tell the whole story. A much larger sample of case studies needs to be examined to validate the preliminary results presented here employing a very small sample of case studies.

LEVEL	# MAX	TOTAL [(CW+1)*10]	AVG [(CW+1)*10]	% OF #MAX	% OF [(CW+1)*10]
500MB	41	173	3.86	7	7.5
550MB	60	239	4.06	10.2	10.4
600MB	126	397	4.15	21.5	17.2
650MB	140	600	4.27	23.7	26
700MB	140	602	4.28	23.7	26
750MB	67	258	3.9	11.4	11.2
800MB	12	39	3.7	2.1	1.7
	586	***2308***	***4.02***	***~100***	***~100***

Table 1: Average values for all seven case studies of #MAX = number of cloud water maxima, TOTAL [(CW+1)*10] = total cloud water value in g kg^{-1} derived by multiplying number of maxima by the value of cloud water in each maxima, AVG [(CW+1)*10] = average cloud water value in g kg^{-1} , % of #MAX = percentage for each level of cloud water maxima and % of [(CW+1)*10] = percentage of each level of total cloud water. Key layer highlighted.

LEVEL	# MAX	TOTAL CW	AVG (CW+1.0)*10	% OF # MAX	% OF CW
500 MB	14	54	3.17	1.2	1.1
550 MB	103	418	3.85	8.7	8.5
600 MB	211	848	4.09	17.9	17.3
650 MB	305	1343	4.4	25.9	27.2
700 MB	322	1377	4.02	27.3	28.1
750 MB	212	817	4.06	17.9	16.5
800 MB	12	38	3.86	1	0.8
	1179	***4895***	***3.92***	***~100***	***~100***

Table 2: Same as Table 1 but for the most active cloud water generating case study on 1/14/14. Also included are the locations of clusters of cloud water maxima at each pressure level analyzed. Key layer highlighted.

LEVEL	# MAX	TOTAL CW	AVG (CW+1.0)*10	% OF #MAX	% OF CW
500MB	14	49	3.5	4.53	4.02
550MB	38	136	3.58	12.29	11.17
600MB	59	228	3.86	19.09	18.68
650MB	82	338	4.12	26.55	27.75
700MB	80	342	4.28	25.89	28.08
750MB	36	134	3.72	11.65	11
	309	***1218***	***3.91***	***100***	***100***

Table 3: Same as Table 2 but for the least active cloud water generating case study on 12/15/04.

Level (hPa, mb)	1200 UTC (T [°C])	1200 UTC (Γ [°C])	0000 UTC (T [°C])	0000 UTC (Γ [°C])	1200 UTC (T [C°])	1200 UTC (Γ [°C])
500	-23.3	-9.7	-26	-9.1	-23.1	-7.5
600	-13.6	-8.2	-16.9	-7.5	-15.6	-4.8
700	-5.4	-7	-9.4	-6	-10.8	-2.3
800	1.6		-3.4		-8.5	

Table 4: Riverton (RIW) Wyoming Average Thermodynamic sounding structures (temperatures and 100 hPa lapse rates), during 1200 UTC, 0000 UTC, 1200 UTC, of significant snowfall for all 7 case studies.

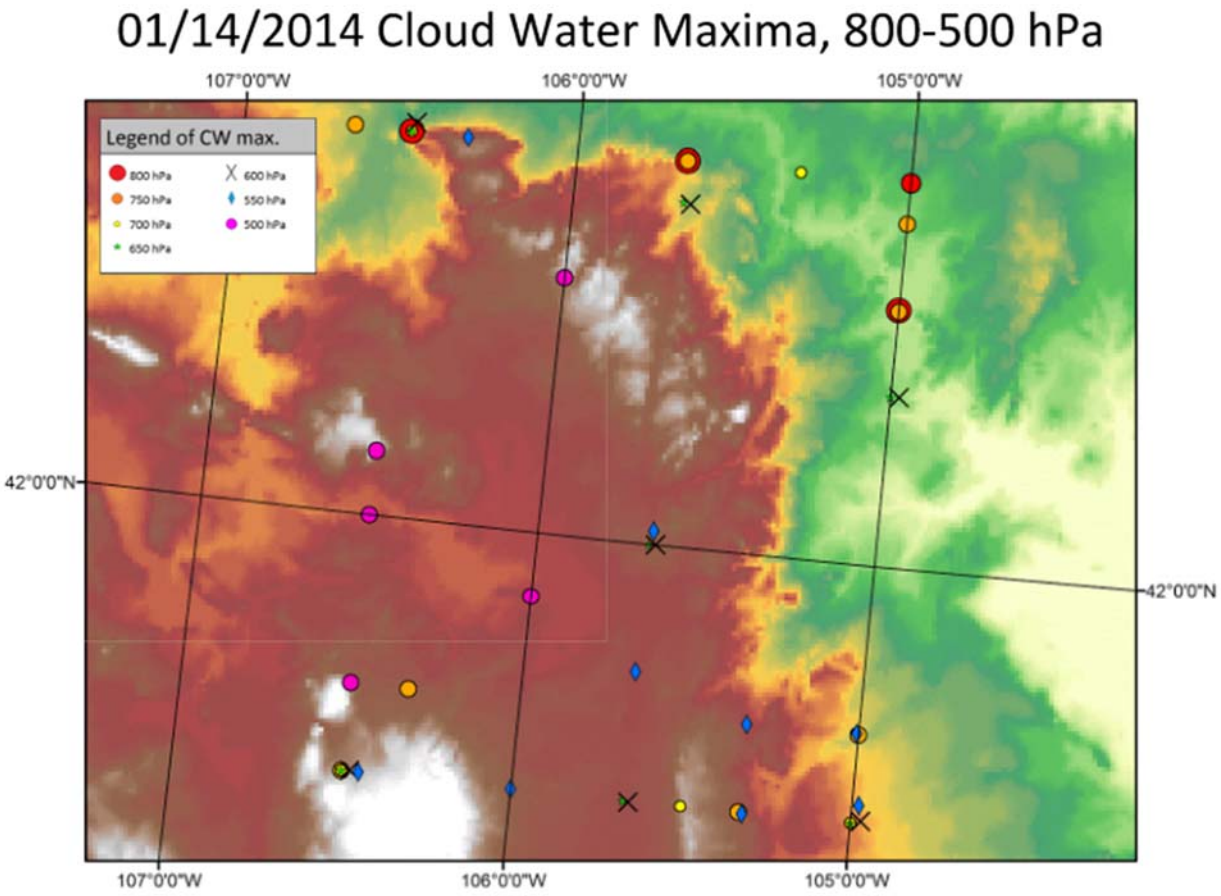

Figure 1: Locations of identified supercooled cloud water (CW) maxima between 800 and 500 hPa (identified every 50 hPa) from the most prolific CW producing case on 1/14/14.

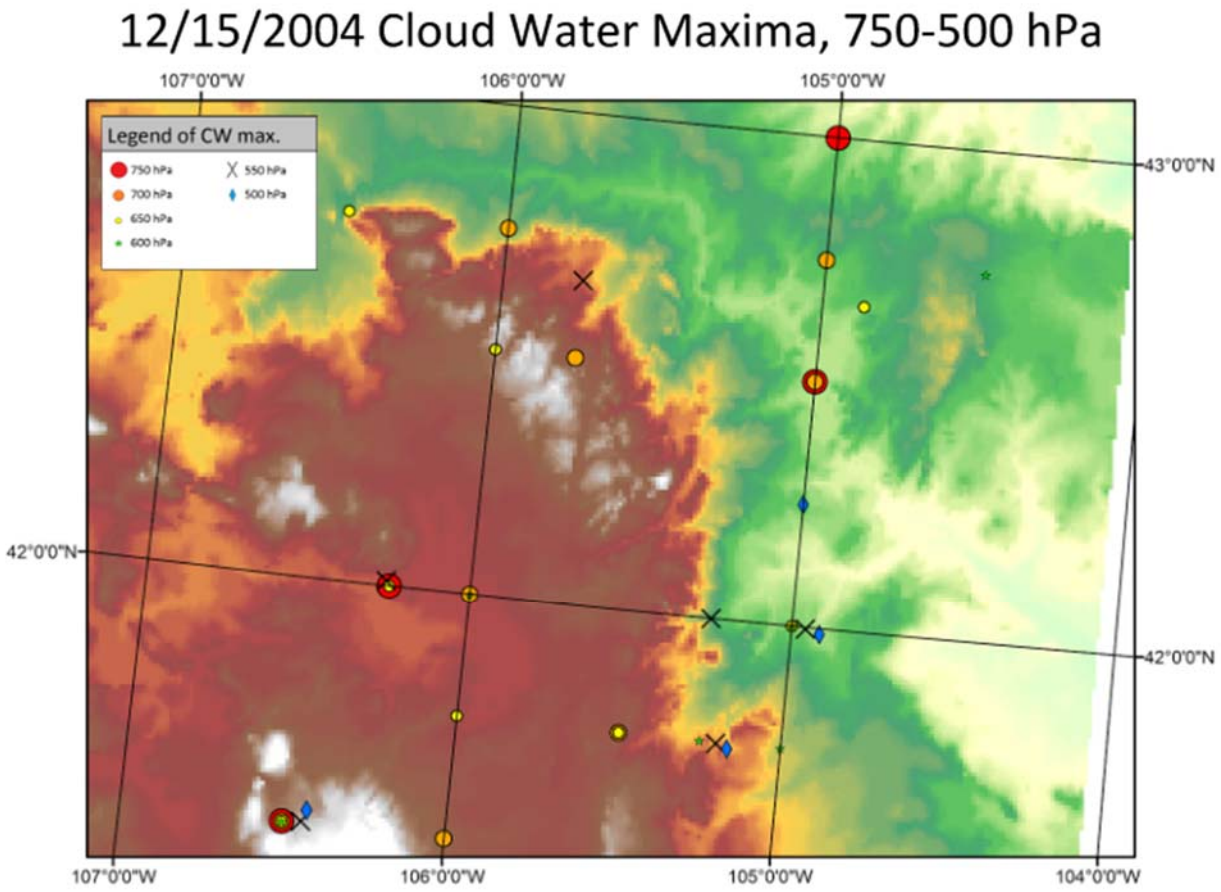

Figure 2: Locations of identified supercooled cloud water (CW) maxima between 750 and 500 hPa (identified every 50 hPa) from the least prolific CW producing case on 12/15/04.

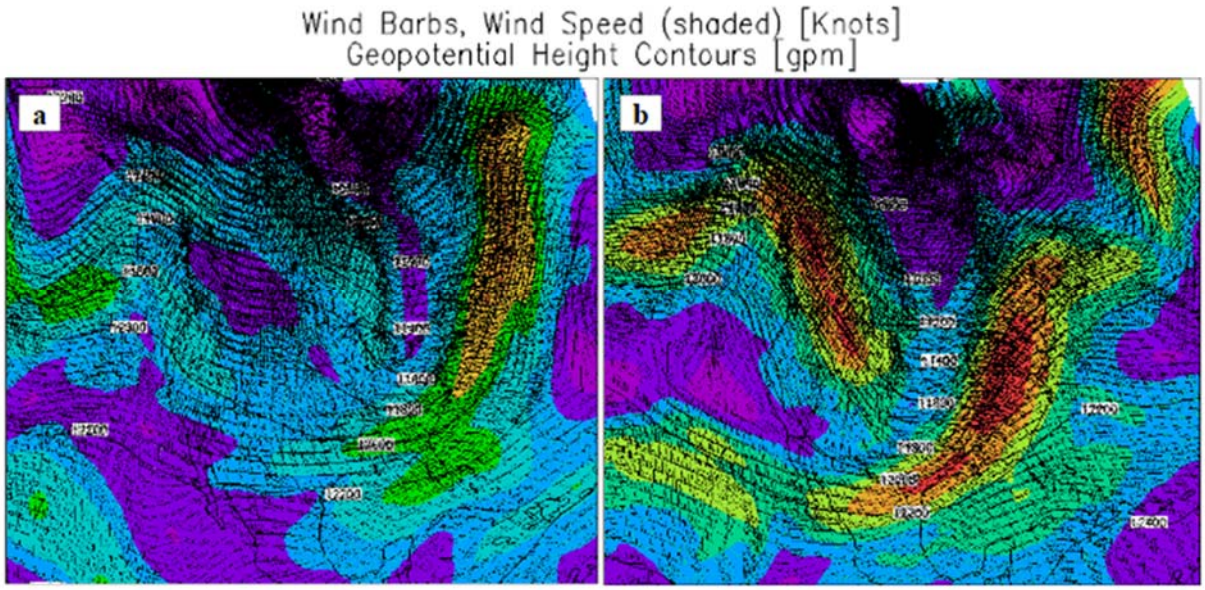

Figure 3: NARR 200 hPa wind barbs (kts), isotachs (kts), and isoheights (m) valid on **a)** 0600 UTC 12/15/04 and **b)** 0600 UTC 1/14/14.

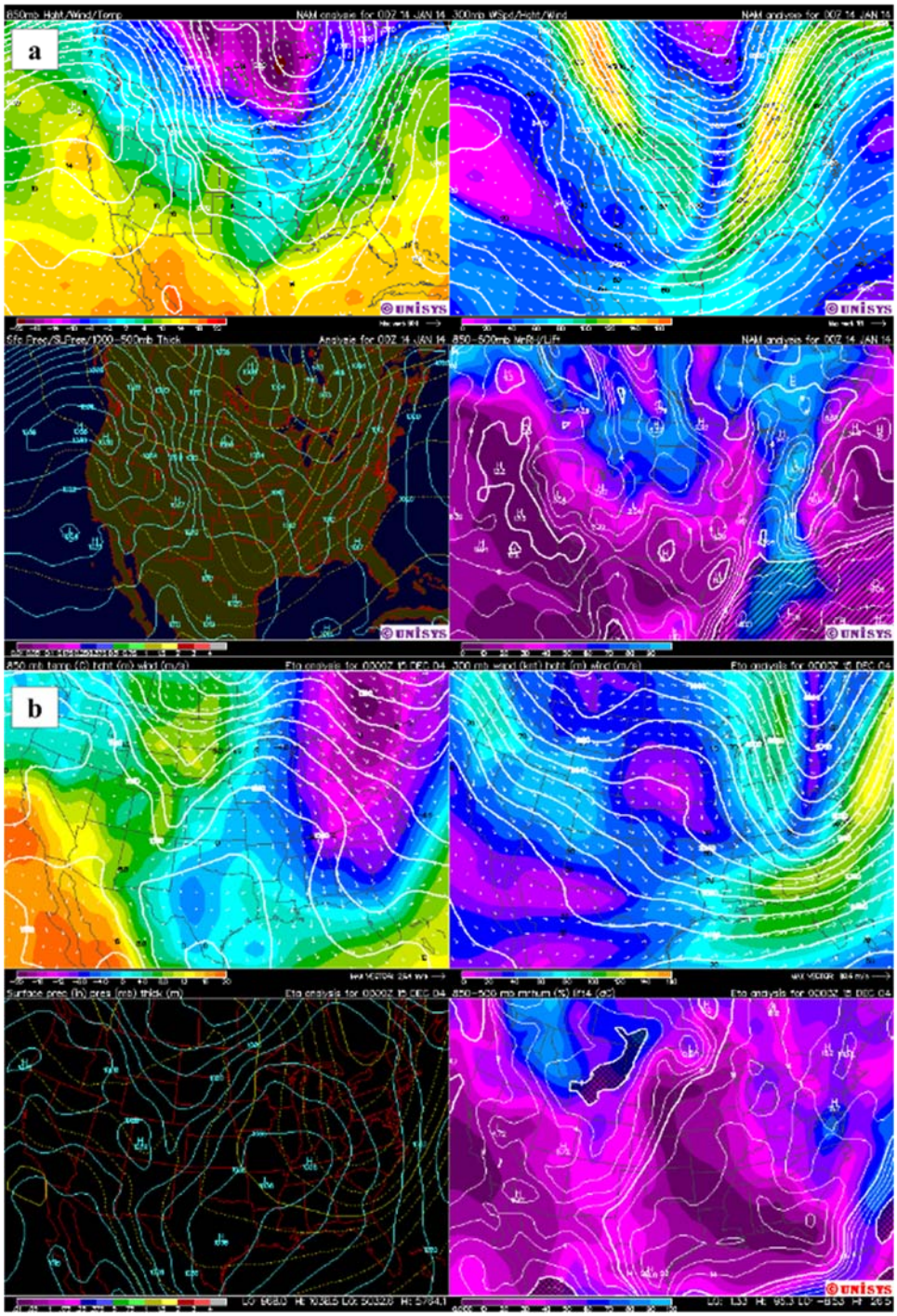

Figure 4: Four panel analyses from UNISYS of 850 hPa temperatures (°C),wind vectors (kts), and isoheights (m), 300 hPa wind vectors (kts), isotachs (kts), and isoheights (m), mean sea level pressure (hPa) and 1000-500 hPa thickness (m), and 850-500 hPa relative humidity (%) and lifted index (°C) valid at 0000 UTC **a)** 12/15/04 and **b)** 1/14/14.

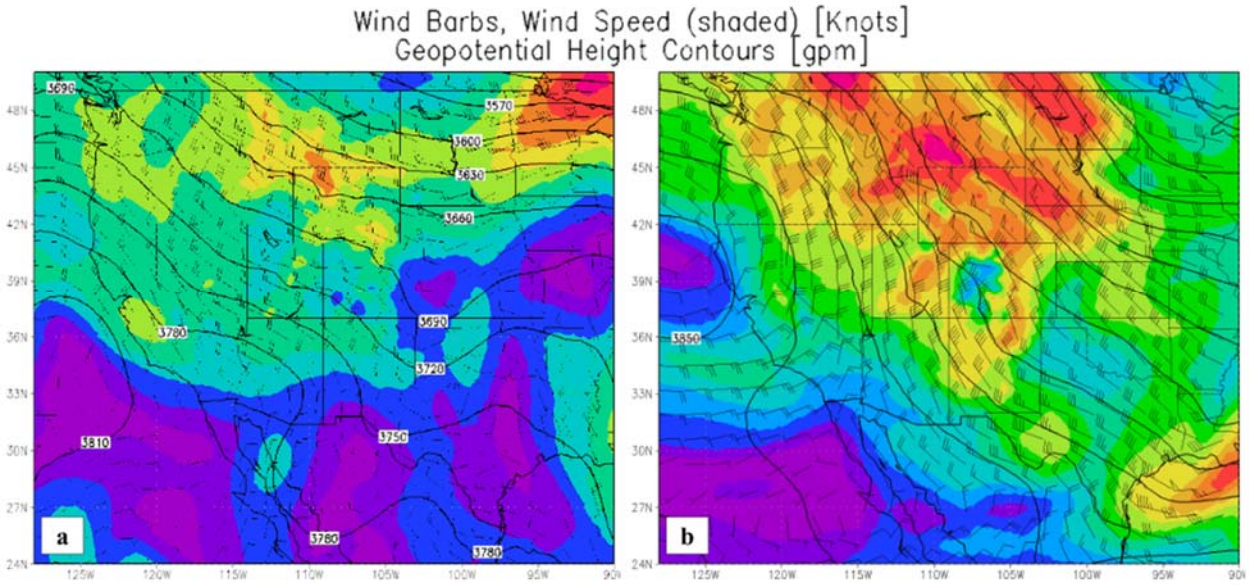

Figure 5: NARR 650 hPa wind barbs (kts), isotachs (kts), and isoheights (m) valid on **a)** 0600 UTC 12/15/04 and **b)** 0600 UTC 1/14/14.

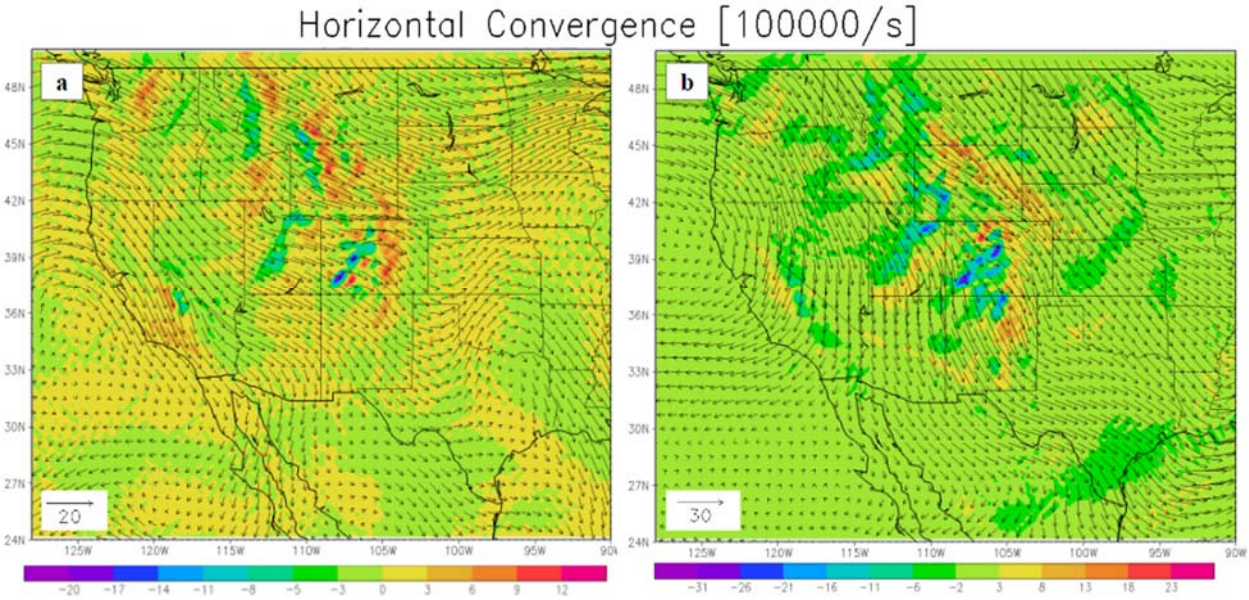

Figure 6: NARR 650 hPa wind barbs (kts) and velocity convergence ($s^{-1}x10^5$) valid on **a)** 0600 UTC 12/15/04 and **b)** 0600 UTC 1/14/14.

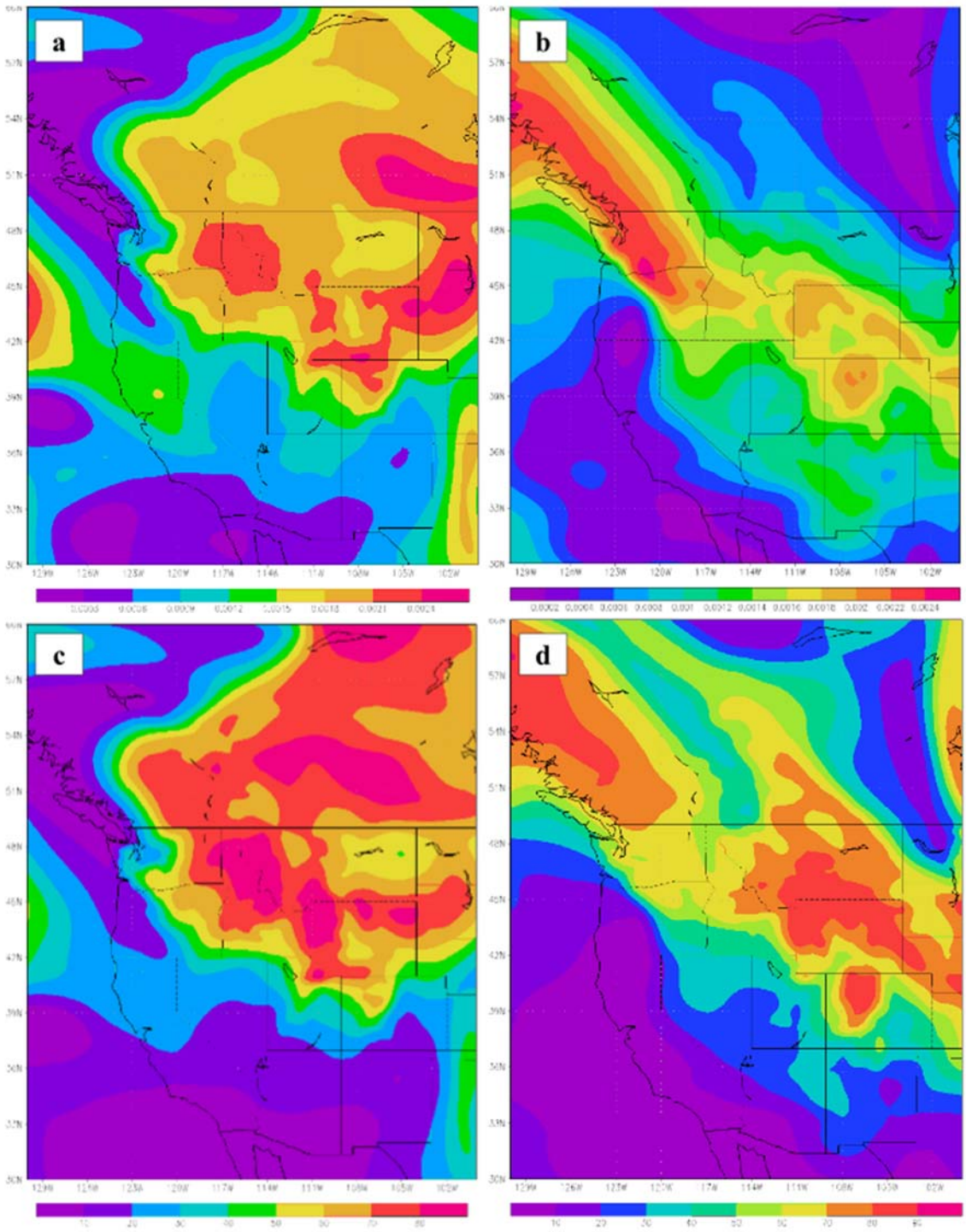

Figure 7: NARR specific humidity (g kg^{-1}) valid on **a)** 0600 UTC 12/15/04 and **b)** 0600 UTC 1/14/14, and NARR relative humidity (%) valid on **c)** 0600 UTC 12/15/04 and **d)** 0600 UTC 1/14/14.

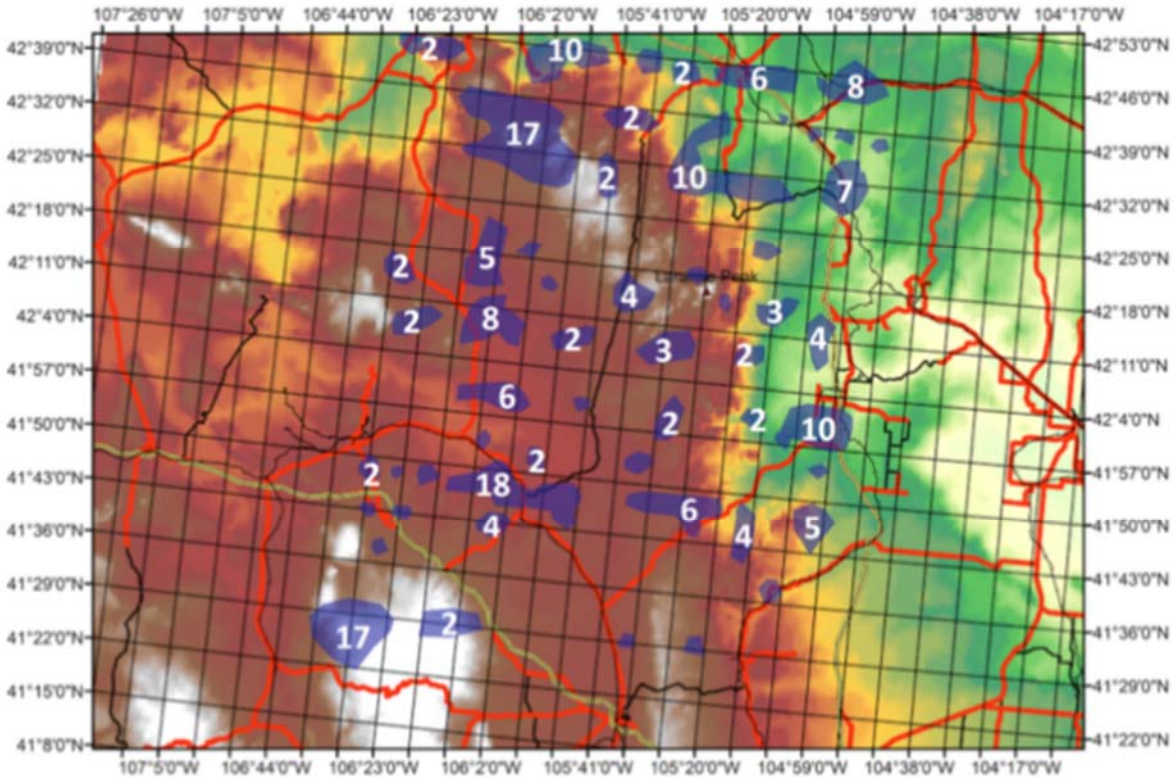

Figure 8: Clusters (blue polygons) of supercooled cloud water maxima from the seven case studies with the total number of clusters for all seven case studies in each of the locations labeled.

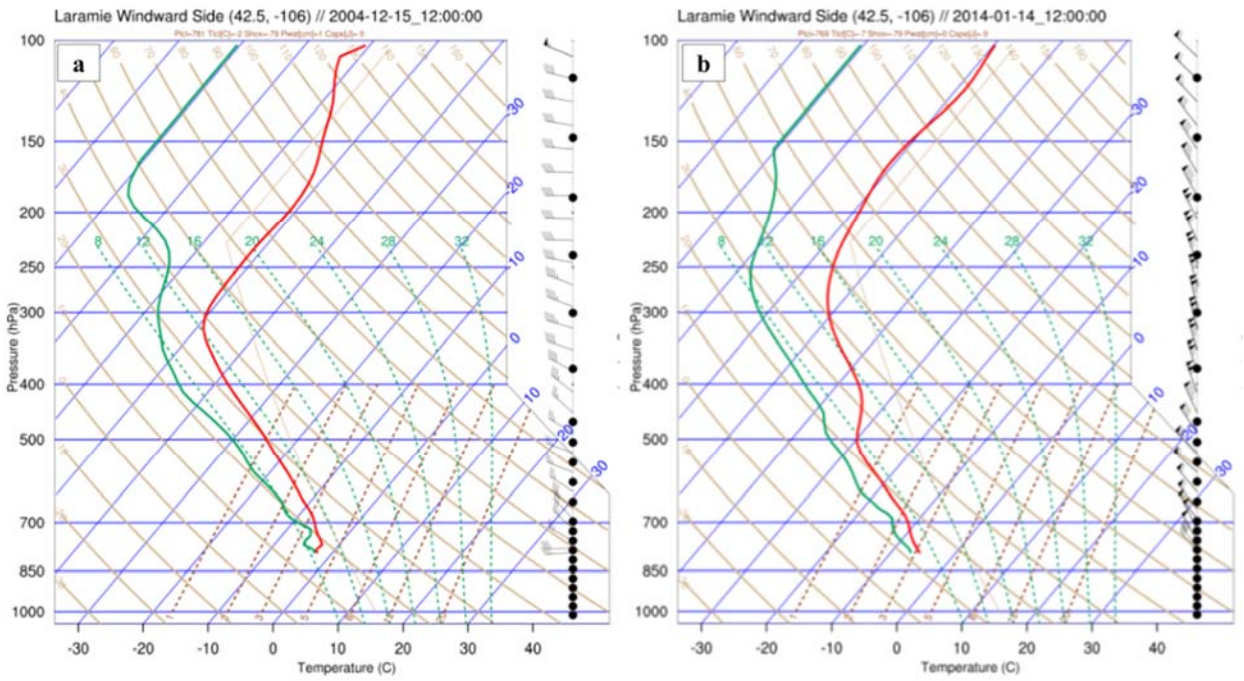

Figure 9: WRF 1 km simulated soundings at 42.5°N and 106.0°W valid on **a)** 1200 UTC 12/15/04 and **b)** 1200 UTC 1/14/14.

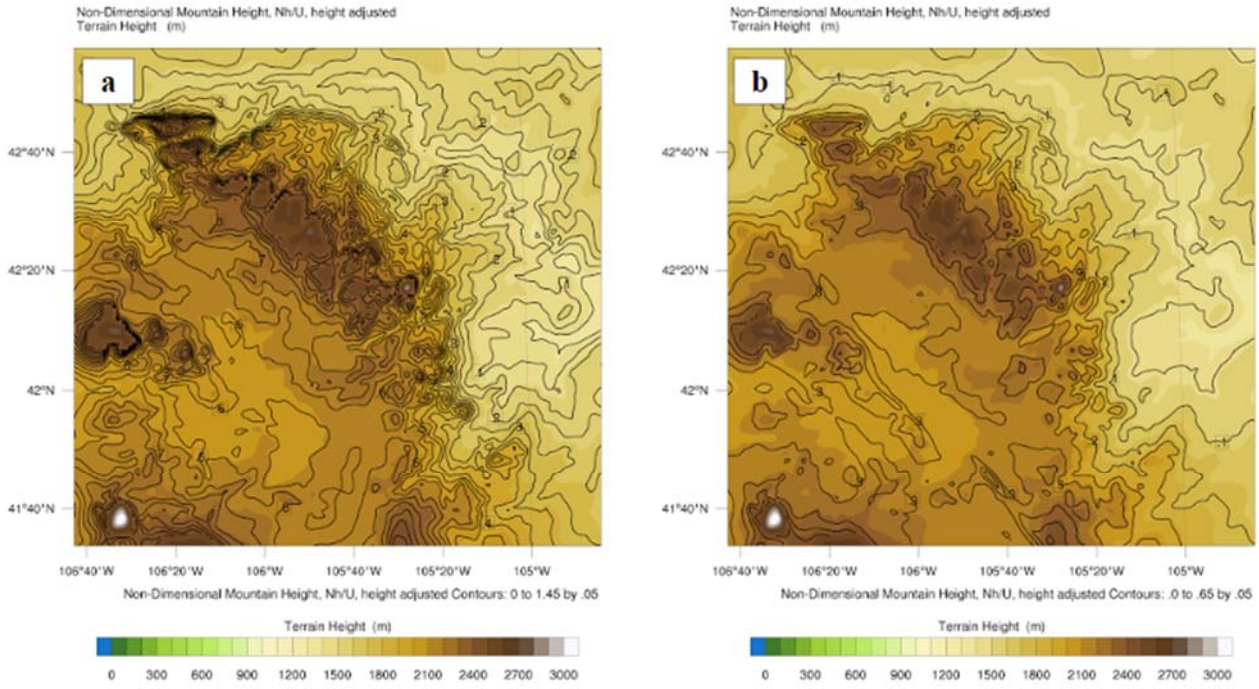

Figure 10: WRF 1 km simulated nondimensional mountain height ($M = NH_m/U$) valid on **a)** 1200 UTC 12/15/04 and **b)** 1200 UTC 1/14/14.

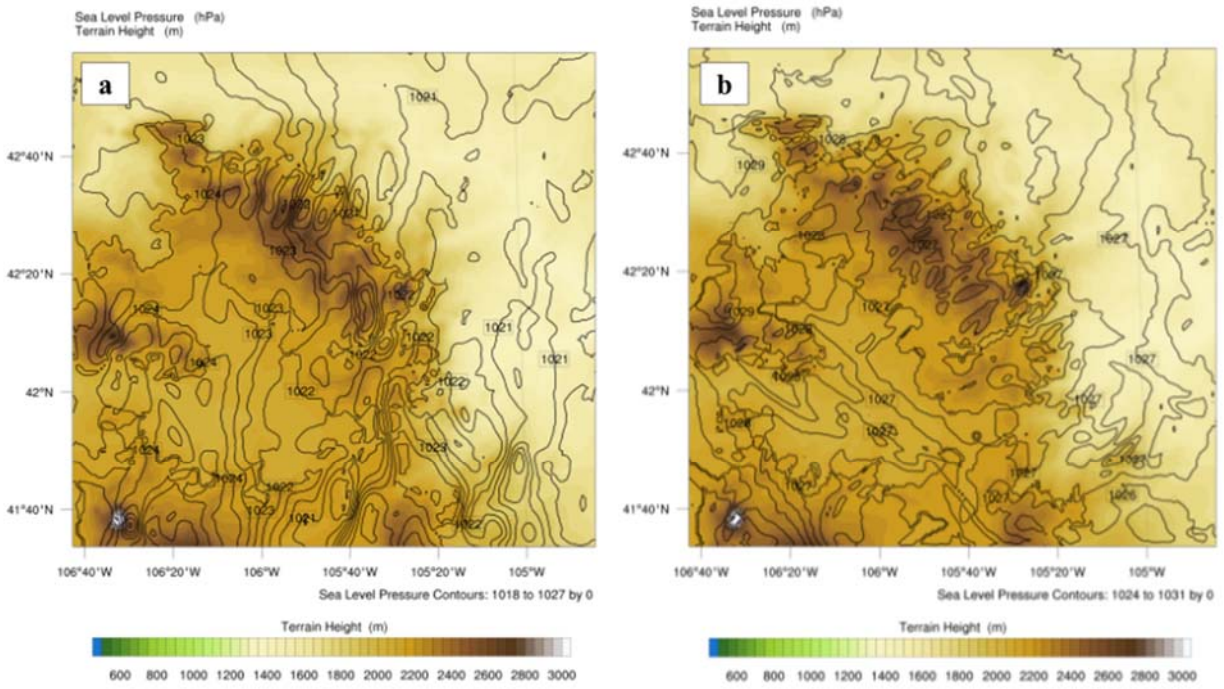

Figure 11: WRF 1 km simulated mean sea level pressure (hPa) valid on **a)** 1200 UTC 12/15/04 and **b)** 1200 UTC 1/14/14.

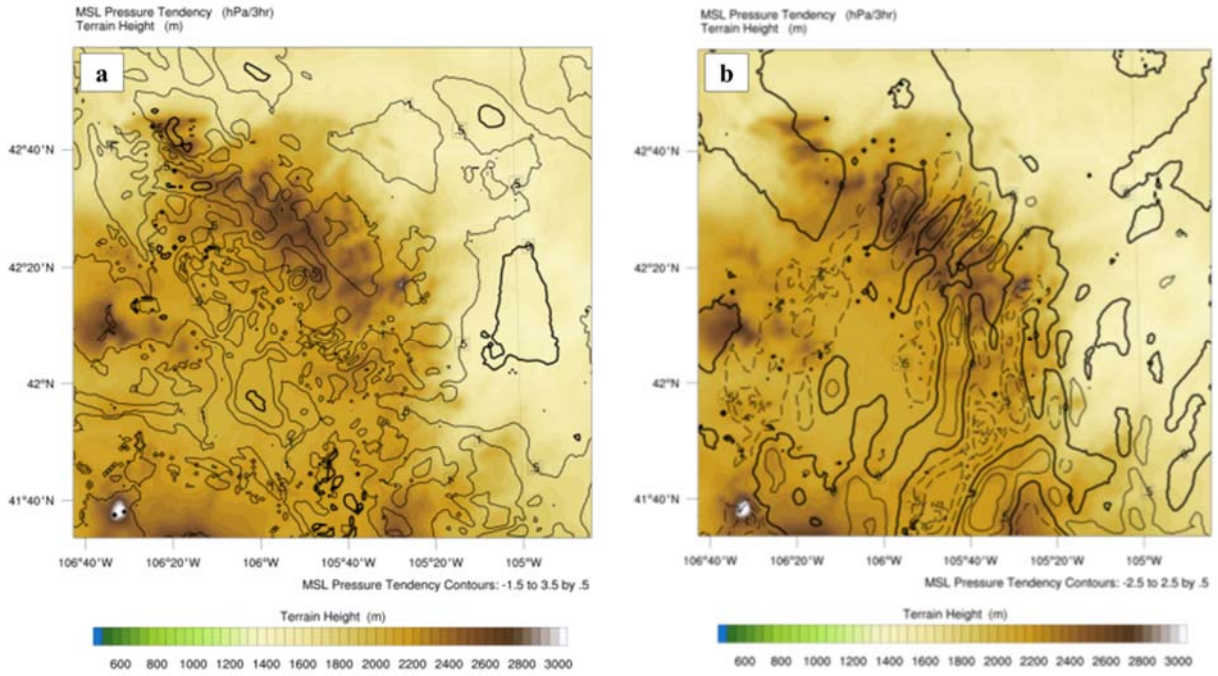

Figure 12: WRF 1 km simulated mean sea level pressure tendencies (hPa/3hr) valid from **a)** 1200-1500 UTC 12/15/04 and **b)** 1200-1500 UTC 1/14/14.

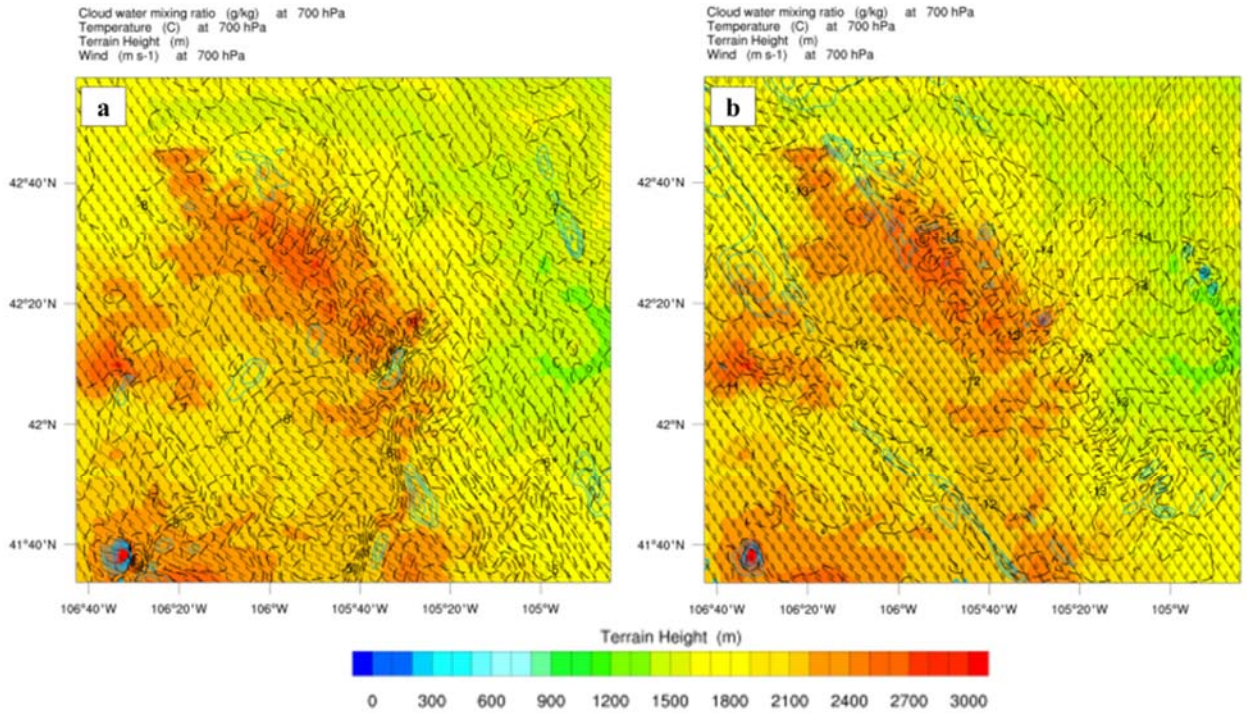

Figure 13: WRF 1 km simulated 700 hPa wind barbs (m s^{-1}), temperature (black lines in °C), and cloud water (light blue lines in g kg^{-1}) valid on **a)** 1200 UTC 12/15/04 and **b)** 1200 UTC 1/14/14.

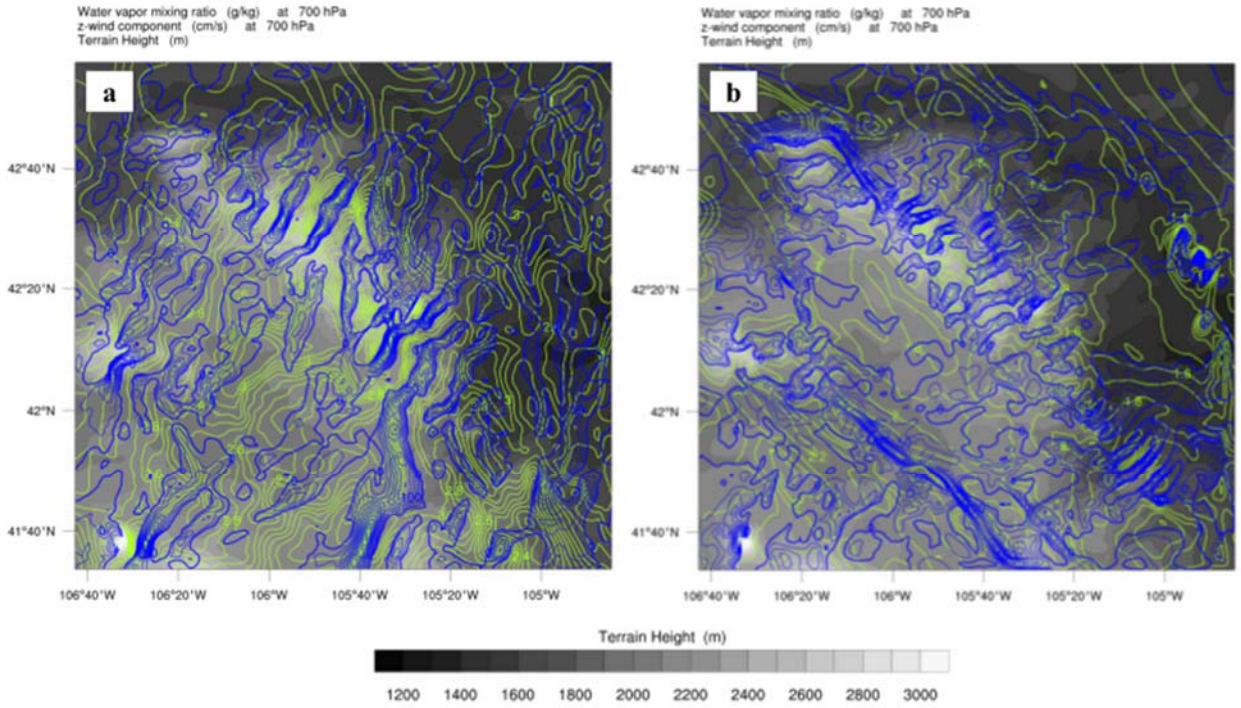

Figure 14: WRF 1 km simulated vertical motion (royal blue, cm s^{-1}) and mixing ratio (light green, g kg^{-1}) at 700 hPa valid on **a)** 1200 UTC 12/15/04 and **b)** 1200 UTC 1/14/14.

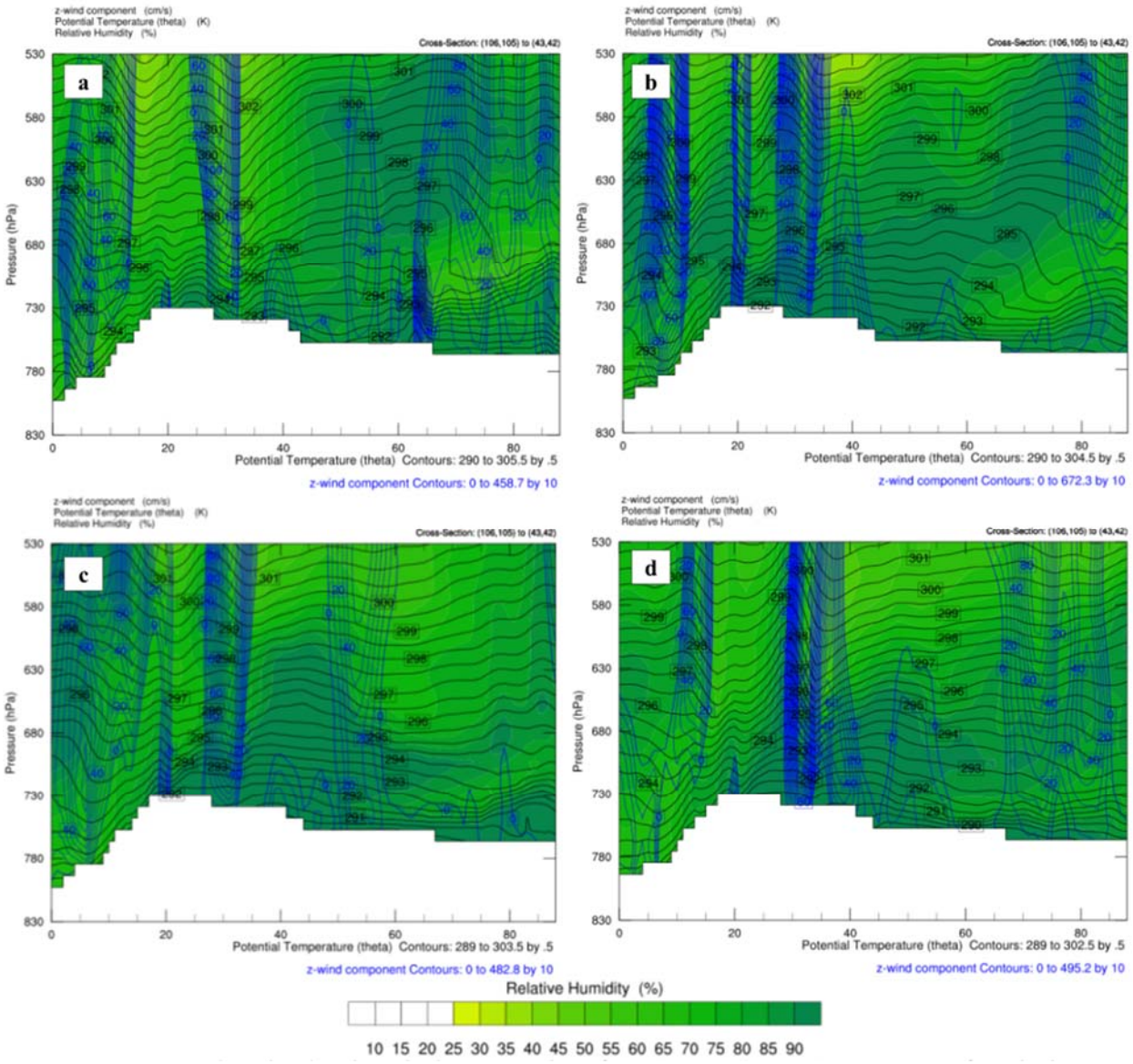

Figure 15: WRF 1 km simulated vertical cross sections from 43°N106°W – 42°N 105°W of vertical motion (royal blue, cm s^{-1}), potential temperature (black, K), and relative humidity (green filled contours in %) valid on 12/15/2004 at **a)** 0900 UTC, **b)** 1030 UTC, **c)** 1200 UTC and **d)** 1330 UTC.

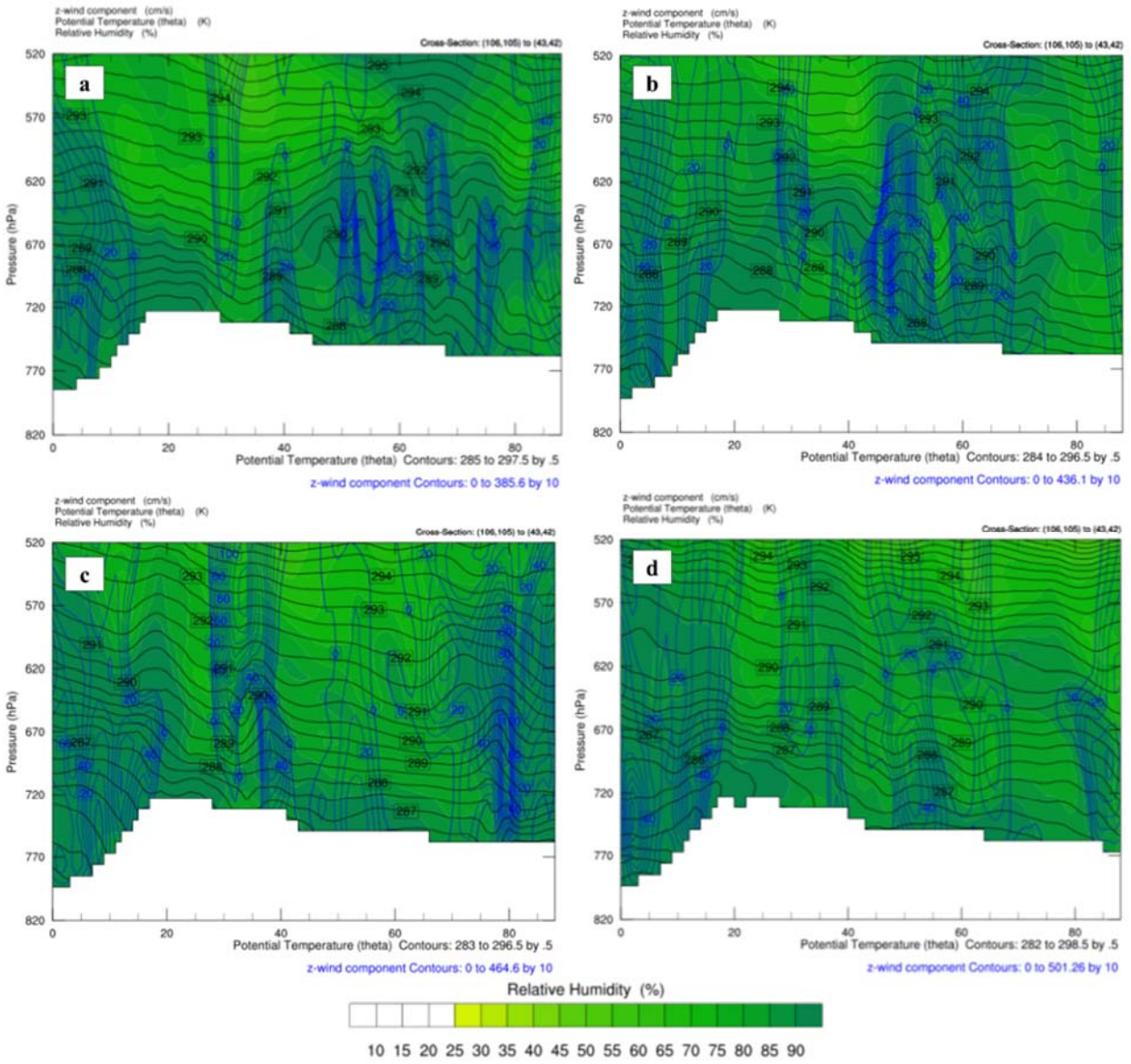

Figure 16: WRF 1 km simulated vertical cross sections from 43°N106°W – 42°N 105°W of vertical motion (royal blue, cm s^{-1}), potential temperature (black, K), and relative humidity (green filled contours in %) valid on 1/14/14 at **a)** 0900 UTC **b)** 1030 UTC, **c)** 1200 UTC, and **d)** 1330 UTC.

20 Appendix C. Table of Acronyms

DRI – Desert Research Institute
WWDC – Wyoming Water Development Commission
MSL – Mean sea level
NRCS - National Resources Conservation Services
SNOTEL – NRCS snow telemetry instrument and gauge
AgI – silver iodide
WWMPP - Wyoming Weather Modification Pilot Program
WRF - Weather Research and Forecast Model
SWE - snow water equivalent
SLW - supercooled liquid water
GOES - Geostationary Operational Environmental Satellite
PIREPs - icing pilot reports
SPC - Storm Prediction Center
hPa – hectoPascal
km – kilometer
m – meter
mi^2 – square miles
WRF-RAP - WRF-Rapid Refresh
WRF-NMM – WRF-North American Mesoscale
METAR - meteorological terminal aviation routine weather reports
CTT – cloud top temperature
IR – infra red
UTC - universal time coordinate
CB – cloud base height
AGL – above ground level
KCPR – Casper, WY METAR Station
KRWI – Riverton, WY radiosonde site
Kts – knots
N – north
E- east
W - west
NE – northeast
SW – southwest
NNW – west-northwest
LP – liquid propane
Hr – hour
F – froude number
RCM - Regional Climate Models
CSP - cloud seeding potential
LBC - lateral boundary conditions
NARR - North American Regional Reanalysis
Raob – radiosonde
PBL - planetary boundary layer

LSM – Land Surface Model
LSPDM - Lagrangian Stochastic Particle Dispersion Model
CIP - current icing product
RAWS - Remote Automated Weather Stations
NWS – National Weather Service
NEPA - National Environmental Policy Act
SPERP - Snowy Precipitation Enhancement Study
VIC - Variable Infiltration Capacity model,
WRF Hydro – WRF hydrology model
GSFLOW - Groundwater and Surface water Flow model
USGS - United States Geologic Survey
CFS - cubic feet per second
AYF – acre feet per year
ET- evapotranspiration
WM – weather modification
PET – potential evapotranspiration
PRMS - Precipitation-Runoff Modeling System
HRU - hydrologic response unit
MODFLOW NWT - groundwater flow model
UPW – Upstream Weighted
SRF2 - streamflow routing package
DEM - digital elevation model
SSURGO - Soils Survey Geographic Database
NSE - Nash-Sutcliffe Efficiency
TAT – technical advisory team